MODELLING THE NATURE AND CONSEQUENCES OF ACCIDENTAL RADIOACTIVE RELEASES TO THE ATMOSPHERE

Stuart John Strachan, B.A.

A Thesis submitted for the degrees of
Ph.D. to the University of London and D.I.C.

Nuclear Power Section,
Department of Mechanical Engineering,
Imperial College,
London, S.W.7.

November, 1979

Modelling the nature and consequences of accidental radioactive releases to the atmosphere.

S.J. Strachan

ABSTRACT□

Initially a review of methods used to model and assess consequences resulting from releases of radioactive fission products to the atmosphere is undertaken. Particular reference is made to a form of the CEGB code WEERIE (4,41). After appropriate modifications this code was the basis of dose predictions in this work. One aspect which has been significantly improved is the modelling of the depletion of airborne material. This improvement produced more realistic predictions of ground contamination which has led to the implementation of routines to estimate external exposures from this deposited activity. A range of notional MAGNOX and AGR accidents have been used to successfully demonstrate the improved abilities of these models. The recommendations of ICRP-26(3) are also considered in the discussion of these results. Properties of these notional releases have been studied in an attempt to identify diagnostic quantities which could be measured by emergency monitoring procedures.

Also included is a discussion of the accuracy of collective quantities calculated using various forms of 1971 UK census data. The range of notional AGR releases has been used to assess collective doses and associated risks for a real population distribution about a site. Further examples of collective quantities at sites in the UK are discussed in relation to site assessment. The concept of a "worst sector" as a critical population group at any given site is discussed. A method to model evacuation has been developed and a simple example is given with the associated reduction in collective doses.

□This work was supported by the NII but its results do not necessarily reflect the views of the NII.

ACKNOWLEDGEMENTS

I wish to acknowledge the support and valuable assistance received throughout the period of this work from the Nuclear Installations Inspectorate and its representatives. Also I wish to thank my supervisor, Dr. A.J.H. Goddard, and the many fellow students of Room 311, who over the last three years have always provided interesting debates (although not always relevant to academic research).

C O N T E N T S

		Page
Preface		1
Chapter 1.	Survey of methods	4
Section 1.1	Aims of codes	4
1.2	Review of WEERIE Models	5
1.2.1	Source of Activity	6
1.2.2	Dispersion in the Atmosphere	8
1.2.3	Depletion processes	9
1.2.4	Dose Evaluation	10
1.3	Application of results	12
1.3.1	Dose assessments and repercussions on siting	12
1.3.2	Emergency procedures	13
1.4	Use of Population Census data	14
1.5	Aims of this study	14
Chapter 2.	Incorporation of element dependent depletion processes	16
Section 2.1	Modelling deposition	16
2.1.1	General comments on deposition	16
2.1.2	Choice of element dependent dry deposition model	17
2.1.2.1	Limitations on modelling escape of activity	18
2.1.2.2	Limitations from deposition data	19
2.1.2.3	Plume Depletion Model	20
2.1.2.4	Computational Restrictions	20
2.2	Implementation of improved depletion model	24
2.2.1	Limitations of single and multi-group depletion models	26
2.2.2	Calculation of mean depletion	32
2.2.2.1	Derivation of analytic expressions	33
2.2.2.2	Application of depletion fractions	37
2.2.3	Extensions to other source depletion processes	40
2.3	Other features of plume dispersal	43
2.3.1	Changing downwind dispersion conditions	43

			Page
	2.3.2	Influences on dry deposition rates	44
	2.3.3	Change of Wind Direction	45
	2.3.4	Plume Rise	46
	2.3.5	Topographical Effects	46
	2.3.6	Resuspension of deposited material	47
	2.4	Examples of results from the improved models	47
	2.4.1	Comparison of 1 and 3 group depletion models	48
	2.4.2	Wash-out	52
	2.4.3	Change of meteorology	55
	2.4.3.1	Transition from stable to neutral conditions	55
	2.4.3.2	Reducing deposition velocities downwind	58
	2.5	Summary	61
Chapter 3	Estimation of external exposures from deposits		62
Section	3.1	Comments on the importance of contamination	62
	3.2	Estimation of gamma exposures from contamination	63
	3.2.1.	Source terms	64
	3.2.2	Local approximation to ground gamma exposure rate	66
	3.3	Weathering and roughness effects	73
	3.3.1	Ground Roughness	73
	3.3.2	Weathering Effects	75
	3.4	External beta exposures from contamination	76
	3.4.1	General comments	76
	3.4.2	Loevinger's formula for beta dose rates	79
	3.5	Examples of ground exposures	79
	3.5.1	Ground gamma rates 1 m. above deposit	80
	3.5.2	Ground beta rates 1 m. above deposit	85
	3.6	Summary and conclusions	89
Chapter 4	Comments on use of Population Data		90
Section	4.1	Type of information available	90
	4.2	Whole Site Assessment	92
	4.2.1	Definition of population distributions	92
	4.2.2	Irregular census units	95

			Page
	4.2.2.1	Mathematical representation of centroid data	95
	4.2.2.2	Accuracy of centroid data used with a continuous weighting function	97
	4.2.2.3	Accuracy of centroid data used with discrete weighting	101
	4.2.3	Properties of regular grid data	104
	4.2.4	Summary of use of data for whole site assessment	108
	4.3	Collective quantities in a sector	109
	4.4	Examples of real population distributions	111
	4.4.1	Comparison of ED to W/cp centroid data	112
	4.4.1.1	Site collective quantities	112
	4.4.1.2	Sector collective quantities	114
	4.4.2	Comparison of discrete and continuous weighting	117
	4.4.3	Properties of 1 km grid data	118
	4.5	Other uses of population data and conclusions	121
Chapter 5	A study of four notional AGR accidents		125
Section	5.1	Introduction	125
	5.1.1	Dose Equivalent Commitments	125
	5.1.2	ICRP Recommendations, a brief outline	126
	5.1.3	Application of ICRP 26 to WEERIE results	130
	5.2	Description of Notional AGR accidents	132
	5.2.1	Description of case 1	137
	5.2.2	Description of case 2	142
	5.2.3	Description of case 3	143
	5.2.4	Description of case 4	149
	5.3	Doses and exposures from notional AGR accidents	152
	5.3.1	Cloud doses from cases 1 and 2	154
	5.3.2	Exposures resulting from contamination predicted in cases 1 and 2	165
	5.3.3	Cloud doses from cases 3 and 4	176
	5.3.4	Exposures resulting from predicted contamination in cases 3 and 4	192
	5.4	Investigation of diagnostic predictions	209

	5.4.1	Gross decay counts from airborne activity	209
	5.4.2	Application of gamma exposure rate	215
	5.4.3	Ratios of beta to gamma energy deposition	221
	5.5	Summary and conclusions	224
Chapter 6	Collective dose commitments and site assessment		226
Section	6.1	Introduction	226
	6.2.	Potential effects of notional AGR accidents	227
	6.2.1	Comparison of accidents at one site	228
	6.2.2	Results of applying case 4 to real sites	238
	6.2.2.1	Collective 30^{o} sector doses out to 30 km	240
	6.2.2.2	Collective $22\frac{1}{2}^{o}$ sector doses to 100 km	252
	6.3	Site Assessment	259
	6.3.1	Comparison of weighted population about 8 sites	265
	6.3.2	Site and sector assessment extended to 100 km	272
	6.4	Definition of a trial "quality" factor	278
	6.5	Modelling and assessing an evacuation	287
	6.6	Summary and conclusions	292
Chapter 7	Conclusions and Suggestions for future work		293
Section	7.1	Conclusions	293
	7.2	Suggestions for future work	295
References			297
Appendix A	Method of estimating ground gamma exposure rate		301
Appendix B	Method of estimating ground beta exposure rate		324
Appendix C	Published papers		331

Contents (Continued) Location of figures

Figure	Chapter				
	2	3	4	5	6
.1	49	69	94	157	230
.2	49	69	102	157	232
.3	53	72	106	158	239
.4	56	81		158	241
.5	59	82		161	243
.6		82		161	244
.7		84		163	245
.8		86		163	246
.9		86		164	248
.10		88		167	249
.11				169	254
.12				170	261
.13				170	262
.14				172	262
.15				174	264
.16/31				177/199	285
.17/32				177/199	289
.18/33				178/200	
.19/34				178/201	
.20/35				180/203	
.21/36				180/203	
.22/37				182/204	
.23/38				184/206	
.24/39				184/206	
.25/40				185/208	
.26/41				187/223	
.27				189	
.28				189	
.29				193	
.30				193	

Contents (Continued) Location of tables.

Table	Chapter				
	2	3	4	5	6
.1	31	87	113	127,128,131	233
.2			113	134	237
.3			113/ 116	140	250
.4			116	140	251
.5			120	144	255
.6			120	144	258
.7			122	146	266
.8			122	148	268
.9			122	151	271
.10				151	273
.11				153	275
.12				153	277
.13				155	281
.14				155	283
.15				155	283
.16				191	286
.17				195	290
.18				197	
.19				207	
.20				211	
.21				213	
.22				217	
.23				219	
.24				225	

P R E F A C E

Early in the study of ionising radiations deleterious effects on the health of individuals were noticed. As the twentieth century progressed larger groups of people were exposed when radioactive materials and X-ray devices became more widely used medically and commercially. The concern generated by the characteristic effects on human beings due to excessive exposure to ionising radiation resulted in the foundation, in 1928, of the International Commission on Radiological Protection (ICRP).

A few years later the discovery of the neutron added a new source of radiation which proved to be the starting point for a large technology based on power produced by nuclear fission. The use of nuclear weapons on the two Japanese cities in 1945 and the continuing effects on the survivors made the understanding and control of radiations a more active field of study. During the 1950's the first steps were taken to the establishment of nuclear fuelled power generating plant. At the same time greater emphasis was placed on radiological safety for all practices involving the emission of ionising radiations, as reflected by an upsurge in the relevant literature, for example the publications of the ICRP.

The commercial use of nuclear energy to generate electricity has engendered the greatest concern among the general public in recent years (Flowers, 1976 (1)). Initially remote sites were used for reactors, but this imposes penalties in transmitting the electrical power as well as affecting construction and operational costs. As confidence in the safety standards applied to the design and operation of these systems has increased more densely populated sites have been accepted. In the UK the number of economically feasible remote sites is very limited so that the large scale development of nuclear power reactors necessitated the production of reactor types and associated siting criteria which permitted construction in quite close proximity to selected population centres. The accident in 1957 at the Windscale plutonium producing reactor resulted in a greater understanding of the problems to be dealt with at a site after an unplanned release has occurred in a gas cooled graphite moderated reactor. Equally important were the implications for reactor design, licensing and monitoring.

Controlled releases can be planned to minimise the risk to the surrounding population resulting from low level doses. Accidental releases could expose any or all areas about a site to doses arising from the plume and associated contamination of the ground. The collective dose commitments, the expected casualties (both early and latent) and the economic damage depend on the particular population about the site for the given nature and duration of a release and the local weather characteristics at that time. The Windscale incident confirmed the critical isotope for that particular reactor type as iodine-131, which has an affinity to the thyroid. Inhalation doses to the thyroid from this isotope formed the basis of subsequent UK siting criteria, where application of these limits necessitated estimates of nominal "risk" distributions associated with a particular reactor location (Gronow and Gausden, 1973 (2)). Future development plans were also taken into account during the selection and continuing inspection of a site.

Different reactor fuels and different accident sequences, as well as new reactor types, can affect the potential dose patterns about an installation sustaining damage. Computerised methods have been developed over the past two decades to cope with the large number of radioactive isotopes in a reactor and all the parameters describing an accidental release and subsequent dispersal in the environment. This has led to a wide range of experience in predicting consequences of activity in the atmosphere which can be incorporated in siting criteria and assessments which reflect many of the recent advances in this field of study. Probablistic representations of consequences from any accident can now be calculated and provide a method of more fully assessing risks from practices using radioactive materials.

Recently the ICRP has re-emphasised that risks from radiation in the nuclear energy industry should be minimised, but recognizing that some level of risk is accepted by the public and workers for any industry. Recommended maximum occupational and non-occupational exposure levels resulting from all stages in the nuclear fuel cycle have been published (ICRP 26, 1977 (3)). Radiological safety measures should ensure that these requirements are met and protective systems devised to ameliorate any extreme conditions. Particular practices may have different residual levels of risk, where the design of safeguards to achieve this low level of risk should be arrived at after a full assessment which might include a cost-

benefit optimization study if this is feasible.

The current work on predicting hazards within, say at most, 100 km of a site is based upon a modified form of the CEGB code WEERIE (Clarke 1974 (4)), which predicts releases from modelled reactor systems and the resulting doses after escape to and dispersion in the atmosphere. The only form of plume depletion used in the original code was a simple modelling of the effects of dry deposition, using one overall deposition velocity. As ground contamination is an important consequence of depositing activity released to the atmosphere, the appropriate sections of WEERIE have been improved and modified where practicable. Routines to estimate external gamma and beta exposures from the ground contamination have been developed to utilise the improvements. Also wet deposition processes and further modification to the atmospheric dispersion calculations can be made. The resulting ability to produce a wider range of dose and exposure estimates is finally applied to assessing the risks associated with particular nuclear reactor sites in the UK, using 1971 census data stored in a computer.

After a general survey of these topics in Chapter 1, the developments made in the methods employed in the computer code WEERIE are described in the next two chapters. The methods and expected uncertainties in the use of various forms of population census data are discussed in the fourth chapter. Results of applying the modified code to four notional AGR accidents are described in Chapter 5, while the methods for use in site assessment schemes are discussed with examples in the subsequent chapter. Finally the results of this work are summarised and suggestions for future studies are made.

CHAPTER ONE

Survey of methods to estimate radiological hazards from activity released to the atmosphere

Section 1.1 Aims of codes which assess the interactions of nuclear power installations with the environment

Many codes have been developed throughout the industrialised world to assess the diverse nature of the interactions of nuclear power installations with the environment. The primary sections of these codes can be categorised under the topics: terrestial and aquatic environmental transport; external and internal dosimetry and human dietary and behavioural factors.

The source term for activity entering the environment is another critical parameter, where a division can be made between routine and accidental releases. Exact values should be available for past routine releases so that a check can be made on any predicted doses to the surrounding population groups. These results can also be used as a guide to controlling future planned releases. Very few accidents have occurred in nuclear power installations which have led to the escape of activity from the site, so that most studies of these unplanned releases rely on the results of theoretical models describing a damaged reactor and properties of radioactive materials under these conditions.

Some codes only deal with one section of the complete history of activity, from the fission process to delivering a dose, and rely on input data from other codes. These can act as data generators for later stages in the overall calculations, or produce a standard set of values, such as the dose to an organ or tissue per unit inhaled activity of a given radionuclide.. A categorisation of 83 codes has been made in this form (Hoffman et al., 1977 (5)), where the quoted references also indicate the necessity of computerised methods in these assessments. This reflects the wide range of data needed at all stages of calculation in the codes which model the pathways of activity which lead to a dose or exposure. The radioactivity considered is primarily due to fission products, but contributions from heavy elements and activation products can also be considered in some codes (Kelly et al. 1977 (6)).

The scope of an inventory in a code can be designed to be flexible, so as to cope with many different sources of activity. To use this type of code experience must be gained in the appropriate fields so that the best available data is gathered. An alternative approach can be used where a code contains fixed libraries which cover a wide range of conditions, so a user identifies the critical sub-set of results in any given case. Similar options can be made available in environmental transport and dosimetry models. More basic choices, such as estimating routine or accidental releases, are usually made before a code is developed. Many important aspects of routine releases are beyond the scope of models dealing with potential accidents, where the short time scale of the latter is a major consideration in identifying the likely critical dose pathway.

The calculational methods used in any particular code can be related to steady state conditions, for continuous releases, or transitory concentrations as occurs in most accidents. Restrictions can be imposed on these models due to limitations of a computer system and support given to any particular research topic. In some circumstances this can mean that simple models can be preferred to more realistic but time-consuming schemes, provided the results are reasonably accurate. Another factor which is becoming more important is the confidence attached to particular assessment procedures((1), EPA review of WASH 1400 1976 (7), ICRP 29, 1979 (8)). Detailed criticism of codes by external bodies may be a method by which confidence can be demonstrated, rather than an internal assessment of accuracy, but this necessitates an expansion of published information.

The basis for deriving dose and exposure estimates in this work is the environmental assessment code WEERIE (Clarke 1973 (4)), originally developed by the CEGB to calculate airborne hazards from released fission products. A review of the models in this code is given in the next section.

Section 1.2 Review of WEERIE models

In the UK the CEGB and SSEB operate gas cooled graphite moderated nuclear power reactors (GCR's such as MAGNOX and AGR). The critical dose pathway for this category of reactor may be expected to be from airborne radioactivity. This led to the development

of WEERIE in a form primarily for assessing doses and exposures resulting from the plume of material in the atmosphere. In the USA, where practically only types of light water reactors (LWR's) are used, much effort has been put into developing codes to assess waterborne operational doses as well as potential atmospheric releases, reflecting some of the inherent differences between GCR's and LWR's. ((5), UNSCEAR 1977 (9)).

Two important aspects of the original version of WEERIE were the definition of source activity and atmospheric dispersion. Depletion of the plume by the creation of ground contamination was not considered in great detail. The evaluation of potential inhalation doses relied on a fixed library of past results from more specialised routines. These points are discussed in detail below.

Section 1.2.1 The source of activity in the atmosphere

When fissionable fuel is irradiated in a reactor core the by-products of the energy liberating mechanism are fission fragments which can be the major potential hazard from thermal reactors. Hazardous activation and corrosion products may also be generated in thermal reactors. Actinides and other heavy elements in irradiated highly enriched fast reactor fuel can pose potential risks. Routines have been developed to predict the accumulation of activity in a reactor.

For environmental analysis the accuracy required in estimating this core inventory is not as strict as for reactor physics studies. At the time WEERIE was developed the routine FISP, based on analytical formulae (Clarke 1972 (10)), was used to derive the activities of the major isotopes using burn-up and fuel rating data. Approximations had to be made for the fission yields produced by neutrons of a wide range of energies interacting with many fissionable isotopes. Time dependent fluxes could be used and allowances made for the hardening of the neutron spectrum with increasing burn-up. Although decay by neutron capture is modelled in FISP the production of radioisotopes by this pathway was not included in the basic library, where stable isotopes important in this effect were not dealt with by this early routine. The long lived iodine isotope I129 was not included in the original fission product library, as it was considered not to be of immediate

radiological significance in accident assessments. Some of these points are dealt with in Chapter five where reference is made to more modern routines, such as RICE (Nair, 1977 (11)), which can be used so that time dependent heavy element activities and corresponding fission products are calculated within one routine rather than separately as was necessary in previous work (Fitzpatrick 1974 (12)).

Once the core inventory has been estimated, after irradiation and possible cooling periods, the WEERIE code models the escape of this activity to the atmosphere. One problem with the analytical formulae used is that they become very complex by the end of a decay chain of six isotopes (Clarke 1973 (13)), and the effects of the finite length of numbers in a digital computer may become important. This model allows for varying rates of involvement of activity from the fuel, where a special case is made for bare fuel pins with ruptured cladding in an operating reactor. In the coolant circuit plate-out and subsequent resuspension of daughter products, after the parent has decayed, is modelled. One overall leakage rate is assumed from the containment system to the atmosphere, where any release can be diminished by appropriate filtration factors. Resuspension after decay of material trapped in the filters is assumed to occur by direct leakage to the atmosphere. This may not be valid in general for a wide range of isotopes which do not normally penetrate filters, as these would still have a finite distance to travel through the filters from the position where they were formed.

The leakage rate (λ) to the atmosphere was described originally as that from the coolant circuit. Alternatively this rate could be associated with two containments in series, say the coolant circuit (λ_1) and an outer containment (λ_2), giving an overall leakage rate, (1.1) $\lambda^* = \lambda_1.\lambda_2/(\lambda_1+\lambda_2)$. If the second containment is effectively open to the atmosphere the ratio $\lambda_2/(\lambda_2+\lambda_1)$ tends to unity and equation 1.1 reduces to the original case. In this second interpretation the filtration factors could represent the amount of material expected to be stopped by the combination of containments, besides the effects of plate-out in the coolant circuit.

A series of notional AGR accidents are described in Chapter five where some examples of the use of this model for prediction of released activity are given.

Section 1.2.2 Dispersion in the Atmosphere

A simple Gaussian plume model, for flat terrain, is used in WEERIE where the six Pasquill stability categories (A to F) are used in conjunction with a set of standard deviations derived from experimental results by Hillsmeier and Gifford (1962 (14) quoted in (13)). In such a model wind shear effects, due to the differences between the geostrophic and ground level wind velocities, are neglected, although these may be significant after material has dispersed throughout the atmospheric boundary layer. Also the effects of longitudinal spread of the plume are neglected as WEERIE deals with time integrated quantities such as inhalation dose commitments, external cloud exposures and ground contamination, A further assumption is that the vertical profile of a plume is unaffected by ground deposition under any conditions.

The original estimates derived from Pasquill's work (1961(15)) relied on the assumption that the visible edge of a plume of smoke corresponded to the 10% concentration limits of that plume. This scheme for estimating air concentrations at the ground for a ground level release, using the height and width of the plume, was expected to be accurate to within a factor of two for the following cases;

i. All stabilities, except extremes, for distances of travel of a few hundred metres in open country,
ii. Neutral to moderately unstable conditions, for distances of a few kilometres,
iii. Unstable conditions in the layer up to the first kilometre above ground with a marked inversion afterwards, for distances of travel of 10 km or more.

This assumes that a well defined wind direction occurs during each measurement period, and that the surface is not very rough (say z_o = 10 cms.). Inaccuracies of a greater extent can be expected in extreme conditions, such as stable low windspeed weather.

Most sets of gaussian dispersion parameters are derived from experiments at one site and a given height of release. Usually the implicit conditions imposed by the local terrain and source

height have to be met before an accuracy to within a factor of two can be expected. The averaging time for predictions can affect the expected accuracy, where longer time scales can be associated with smaller errors (Fryer and Kaiser, 1978 (16)).

The use of an empirical or semi-empirical gaussian model can allow predictions of ground level air concentrations of a reasonable degree of confidence under appropriate conditions, although the effects of wind-shear with height are normally neglected. No other simple model has obtained such acceptance as this gaussian scheme (Kaiser et al. 1976 (17)), Martin et al (1974) (18), Stallmann and Kamm 1973 (19)), where theoretical interpolations and extrapolations can also be made to predict the dispersion parameters required for a particular application (Smith 1973 (20)), allowing for ground roughness, insolation, sampling time, etc. This Gaussian plume method is limited to downwind ranges of less than about 100 km, while other systems have to be used for longer ranges. (ApSimon and Goddard 1977 (21), Maul 1977 (22), Scriven and Fisher 1975 (23)).

Section 1.2.3 Depletion Processes

As the primary aim of the original code WEERIE was to estimate air concentrations and associated doses the depletion model used was crude and acted as a process which could decrease cloud dosages rather than attempting to estimate ground contamination with an equal certainty.

The Gaussian dispersion model enables a source depletion model to be used, as described in Chapter two. Only one overall dry deposition velocity could be applied in the original depletion model, although the suggestion was made that wash-out could be included. This single overall dry deposition velocity cannot represent the properties of all isotopes in a mixed fission product release, particularly in the radiologically significant decay chains involving Te-I-Xe-Cs where physical and chemical properties change rapidly. Two examples of deposition properties for inert gas and halogen elements are described below.

The long lived radioactive inert gas krypton-85($t_{\frac{1}{2}}$=10.6 years) could become a significant waste product from the nuclear power industry. It has been recommended that the Windscale reprocessing plant has a facility to retain this isotope (Parker 1978 (25)). This gas is expected to suffer negligible depletion due to wash-out

or deposition through adsorption on aerosols, although it may deposit quite rapidly into a perfect sink at the ground before an equilibrium is produced between the ground and air concentrations (Tadmor 1973 (26)). The saturation of the soil by stable krypton can diminish the ground contamination, where the exchange process can effectively remove any radioactive krypton after the passage of the plume. This means that the net contamination of the ground by Kr-85 due to an accidental release may be negligible, but this may not be the case for longterm operational releases which build up a steady background level of this isotope in the atmosphere (Machta et al 1974 (27)). The isotope is expected to deliver external exposures and only insignificant inhalation doses (9).

Experiments have shown that elemental iodine deposits rapidly on vegetation, although organic forms are less readily assimilated and are associated with lower deposition velocities. Plant physiology is such that this iodine is transferred to the soil, giving an effective half-life for radioactive iodine-131 in vegetation of five days. The rate of transfer to the air from the soil is much slower so iodine-131 effectively decays with its intrinsic half-life of eight days once in the soil (Bolin, 1959 (28)). This transfer to the atmosphere from the soil means that there is negligible net deposition by stable iodine from the air to the soil. This behaviour can be further complicated by elemental iodine becoming associated with aerosols.

A detailed review of the results of the initial deposition process is undertaken in Chapter two with the intention of improving predictions of initial ground contamination. This should provide a more accurate description of the source terms for estimates of external exposures from deposited materials and crude assessments of potential food chains doses (8), where neither of these dose pathways are considered in the original version of the code WEERIE.

Section 1.2.4 Dose evaluation

Inhalation dose commitments are calculated in WEERIE for ten adult organs using a fixed set of dose commitments per curie inhaled for each fission product. The recommendations of ICRP 2 (1959 (29)) and the Task Group on Lung Dynamics (1966 (30)) were used in the original program SAURON (Clarke and Utting 1970 (31))

devised to evaluate these factors. One overall breathing rate is applied in this code where it is recommended that an average adult value is chosen.

Among the assumptions used to derive these dose factors are that all isotopes were considered insoluble when assessing the dose commitments to the lung and the four compartments of the gastro-intestinal tract, but for the bone, kidney, liver, thyroid and total body (i.e. all other organs and tissues not assessed separately) all isotopes were assumed to be soluble. This inconsistency will probably overestimate doses to individual organs, although no account is taken of radiation escaping from one organ which could deliver doses in other organs. Also different types of releases, which could be expected to have dissimilar physical and chemical properties, are given the same characteristics for delivering internal doses. This restricts the accuracy expected of the dose prediction model in different applications of WEERIE. Further details of these dose factors are discussed, and compared to other sets of values, at the start of Chapter five before estimates of dose commitments from a range of notional AGR releases are described.

One limitation of this set of dose factors is that differences due to age have not been made explicitly, although some account of this factor has been taken in deriving siting criteria (see review Shaw and Palabrica 1974 (32)). This may not be a serious deficiency given the comments in ICRP-26 on estimating risks from low doses of LET radiation. Hereditary effects cannot be assessed readily from the results of this code, as doses to reproductive organs are not given separately, only included in gross values for the "total body", but pessimistic assumptions can be made. This imposes restrictions on the detail in which consequences can be evaluated later in this study, although doses leading to somatic effects should be adequately covered.

Cloud beta doses and cloud gamma exposures are also calculated in WEERIE. The cloud beta dose is based on the infinite cloud approximation that all the energy absorbed in a given volume is equal to the amount of energy liberated in that volume. A similar assumption can be made to estimate gross gamma exposures but due to the penetrating nature of gamma rays this may not be

an adequate representation of a finite plume. Hence a numerical estimation procedure was included to cope with this effect. This routine also improved estimates of cloud gamma exposures outside the 10% plume limits, such as at large crosswind distances and below an elevated release. In later chapters some comparisons are made between these two cloud gamma estimates for plumes of mixed fission products.

The infinite medium build-up factor method used in the numerical estimate should represent the total gamma exposure reasonably well but cannot give the true spectrum of the photon flux at any given receptor. The true spectrum at a dose point from a monoenergetic source of photons would display the effects of compton scattering, photoelectric absorption and at higher energies pair production, bremstrhalung and other effects. This affects the detailed distribution of doses within a body, as modelled by a standard phantom in combination with a better description of photon transport processes. Even so simple and complicated methods can give gross estimates which may be quite close (Goddard et al 1979 (33)). No effects of any scattering and absorption properties of the ground are allowed for in these WEERIE routines estimating external doses and exposures from a cloud.

External exposure rates were not calculated from any ground contamination predicted by the original models in WEERIE. It was intended that this deficiency would be rectified in this work, once a routine was developed which could more realistically represent depletion processes. The methods for estimating these external exposures are described in Chapter three, Appendix A and B while some applications to notional reactor accidents are given in Chapter five.

Section 1.3 Application of results from WEERIE

The quantities estimated by WEERIE for a given release of fission products can be used in assessment of individual and collective doses, as well as aiding the development of emergency monitoring procedures.

Section 1.3.1 Dose assessments and repercussions on reactor sites

The doses calculated by WEERIE are intended to be estimates of individual doses, so can be directly compared to statutory limits

(e.g. adopted ICRP recommendations) and relevant Emergency Reference Levels (ERL's) (MRC 1975 (34)).

These exercises can give the expected dose patterns for each type of potential release from a nuclear reactor under different weather conditions. The effects of detailed safety measures can be assessed from these results and subsequently decisions may be taken to review specific design targets (Bell 1977 (35), Macdonald et al 1977 (36)). The activity which is allowed to be released during normal operational conditions can also be set for critical isotopes by the application of WEERIE. Overall safety assessments of reactor types could be undertaken using some of the results of this code, provided sufficient data was provided in an acceptable form for the constituent models.

Once these potential dose patterns have been derived collective doses can be assessed, as explained in Chapters four and six. There are many difficulties in the interpretation of collective doses as measures of absolute risk (ICRP 27 1977 (37), (6), Smith and Stather 1976 (38)). Some simple examples are given in Chapter six as an attempt to show qualitatively a few aspects of collective dose commitments.

Present siting criteria in the UK use population weighting functions which can define collective quantities. WEERIE can be used to define similar weighting functions, which are based on notional releases of mixed fission products rather than a nominal release of one isotope. The sensitivity of the derived collective quantities to changes in the weighting functions are discussed in Chapter six, where results of WEERIE calculations given in Chapter five are employed.

Section 1.3.2 Emergency procedures

If an accident were to occur emergency procedures would be put into operation. A large amount of information about the released activity would have to be gathered rapidly to aid the emergency controller.

The WEERIE models can provide advance estimates of quantities which could be measured in the field (36). External gamma exposures and beta doses from the cloud and ground are important, not only in assessing the magnitude of a release but also in locating the plume. Another quantity which can be measured immediately is the number of decays from a sample of airborne

activity. This sample would normally be taken for detailed analysis of the type of release. Predictions of these measurements for notional releases could be related to potential dose commitments delivered to specific organs and the desirability of any form of evacuation or other action. In some cases, such as gamma ray spectra, rapid measurements may be taken but no clear pattern might be discernable for several hours after a release starts, or after many kilometres travel downwind of the reactor, by which time serious health effects and economic damage may have been incurred (Tadmor, 1976 (39)).

Details of these predicted quantities for a series of releases from any particular reactor type could provide the data for specifying the capabilities of emergency monitoring systems at any site. Some of these applications are discussed at the end of Chapter five.

Section 1.4 Use of population census data

The second component in estimating collective doses is the representation of relevant population data. To apply the calculated collective quantities to siting criteria requires that real population distributions have to be considered.

Some crude estimates of collective dose commitments may be obtained using uniform population distributions within large regions (Martin et al 1974 (40), (8)) but this would not be adequate to show detailed differences between particular sites. Previous work has established, in a form suitable for use with computer programs, a population base from the full 1971 census (Fitzpatrick 1976 (4), Clarke et al 1976 (42)). A review of the expected errors in the use of these and other census data is given in Chapter four while some practical examples relating to siting criteria are given in Chapter six.

These methods can be used to study the application of current siting criteria and be extended to include other features which may be considered necessary in future site assessments, such as fatality, morbidity, loss of man-years, casualty rates and associated individual or collective risks.

Section 1.5 Aims of this study

One aim of this work was to improve the understanding of the consequences of reactor releases, using a range of notional AGR accidents modelled by the WEERIE code. In the light of these

releases limitations of the code could be studied.

As outlined above after a critical consideration of the models in this code the depletion routines were improved. This naturally led to the inclusion of routines to estimate external gamma exposures and beta doses from the modelled ground contamination. This added another facet to the prediction of consequences from mixed fission product releases, enabling some of the long term contamination problems to be described more accurately. The provision of these extra capabilities were essential to an investigation of diagnostic aspects of these releases.

A second aim was to continue a study of estimating potential collective doses and siting criteria in the UK. This consisted of further developments to the computerised population data handling facilities as well as using results from WEERIE to generate weighting functions for assessing collective doses. Limitations on the dispersion and depletion routines had to be considered when reviewing the generation of weighting functions. Some refinements to the dispersion and deposition routines in WEERIE were undertaken which could provide initial estimates of detailed effects which might influence future site assessments. The potential impact of accidents across international boundaries is not explicitly included in this work.

The methods used to extend the abilities of modelling radioactive releases to the atmosphere, and the resulting consequences are described in Chapters 2, 3, Appendix A and B. The results of this study of notional AGR releases are discussed in Chapter five. In Chapter four some considerations of modelling real population distributions are discussed. Chapter six contains an assessment of collective doses from the range of AGR notional accidents and the effects of modifications to current site assessment schemes.

C H A P T E R T W O

Incorporation of element dependent depletion processes and other aspects of plume dispersal into WEERIE

Section 2.1 Aspects of modelling deposition for mixed fission product releases

Changing the depletion model for radioactive material dispersing in the atmosphere requires detailed consideration of many aspects of the whole WEERIE code.

Section 2.1.1 General comments on deposition processes

Ground contamination results from the passage of a plume which includes depositing material, where the rate of formation of this deposition is directly proportional to the ground level air concentration.

The elements included in the fission product library of WEERIE include inert gases, alkali metals and a whole spectrum of other metals and non-metals. Hence a great range of physical characteristics can be expected when a mixture of fission products escapes to the atmosphere. This should be reflected by the models used to predict the dispersion and depletion of these radioisotopes.

Radioactive inert gases ejected to the lower atmosphere after an incident at a nuclear installation will not produce any significant ground contamination, as the soil is already saturated with stable inert gases (26). The exchange rates for inert gases between the atmosphere and the ground are low, while the unstable isotopes are usually only a minute portion of those particular elements normally found in the air. Both these effects reduce any radioactive inert gases trapped in the ground to negligible quantities.

A different situation arises for reactive elements, such as iodine and caesium. The deposition of this type of material can be described by the equation 2.1, so that the rate at which material accumulates on the ground (W) is proportional to the local air concentration (χ) and an effective deposition velocity (v).

(2.1) $W(x,y)\ (Ci(m^2.s)^{-1}) = v_g(m.s^{-1})*\chi(x,y,0)(Ci.m^{-3})$.

(Chamberlain 1953 (43)).

For very small particles, or vapours, gravitational settling is usually negligible but other processes produce a net flux of these materials to the ground where the gross effect is referred to as "dry deposition". Transfer of this material to the ground can be limited by the turbulent properties of the air in the immediate vicinity of the ground. Numerous elements, including caesium, zirconium and ruthenium, have been found to deposit on the ground at various rates depending on the elements' physical and chemical form and the type of surface acting as the sink for this atmospheric process.

In the original WEERIE program all elements were treated as having one common deposition velocity. This is clearly not a physically realistic assumption, as it creates contamination by inert gases and also does not allow for any differences in behaviour between the large number of non-gaseous fission products.

The most accurate method of modelling any deposition of these fission products would be to treat individually the deposition behaviour of all isotopes of every decay chain. Among the many reasons why this is not practicable are that available data are inadequate for this purpose and that doing these calculations would be prohibitive, even on a modern digital computer for 150 decay chains each of up to six isotopes, particularly when the results may not differ greatly from less complicated models. A consideration of the physical processes and the available data suggested a suitable compromise for a practical model, which is outlined below.

Section 2.1.2 Choice of grouped element dependent deposition model

There are several aspects of the general properties of dry deposition and the particular models in WEERIE which had to be considered when attempting to improve estimates of ground contamination from a mixed fission product release. These include the following:

i. Source term for released isotopes;
ii. The deposition process and its measurement;
iii. The plume depletion model;
iv. Computational limitations.

Although these factors are not wholly independent they constitute the major considerations in the final choice of an improved deposition model. Also the inclusion, if practicable, of wet deposition processes, in particular washout, was considered as another addition to improve the overall dispersion and depletion model.

Section 2.1.2.1 Limitations produced by modelling an escape of fission products.

In modelling the potential accidents of nuclear reactors which could lead to activity leaking to the atmosphere it is common practice to use element dependent release fractions to describe the escape from the fuel. Extended releases, for example where bare fuel operates in the reactor so that fission products migrate through the fuel directly to the coolant, may require more detailed isotope dependent data.

Element dependent properties such as plate-out, resuspension and filtration were also included in WEERIE in the modelling of radioisotopes being transported from the fuel to the release point in the atmosphere. Hence an element dependent representation of deposition in the atmosphere would be consistent with the earlier stages in the model for accidental releases. This represents a reduction in the data requirements from that for several hundred isotopes to that for just thirty seven fission product elements, including tritium from tertiary fission.

The source term for released activity relies greatly on the elemental release fractions from the fuel. Generally elements of one group in the periodic table are expected to have similar physical and chemical properties. Release fractions under various conditions are known only for a few potentially critical elements, while the remainder are grouped with one of these critical elements by reference to similarities in appropriate properties. Special conditions may alter the group a particular element is associated with, as occurs for the release fraction of ruthenium if it is expected to be either in elemental or oxide form (WASH1400 1974 (44)). This means that a further reduction in the amount of deposition data required could be expected due to grouping of elements with similar dry deposition characteristics.

Section 2.1.2.2 Limitations due to uncertainties in measurements of deposition

There are many uncertainties about the form of material which might escape from a reactor given any particular potential accident. Inert gases can be treated separately due to their special properties which are independent of a wide range of factors. Some uncertainties common in the deposition properties of most elements are exhibited by iodine.

Three forms of iodine can be expected to escape during an accident in a nuclear reactor, namely elemental, particulate and organic (primarily methyl iodide), each of which have different deposition characteristics. Elemental iodine is reported to have a relatively high deposition velocity compared to particulate forms, while methyl iodide has a much lower deposition rate. Aerosol particles of mixed constituent elements could be expected to have one typical deposition velocity provided chemically active species were not present in significant quantities.

A major problem in quantifying deposition rates is that experimenters find that sets of results under similar atmospheric conditions for one material, such as elemental iodine, and for a given surface, say grass, may have a factor of 2 to 40 between the extreme values determined (Hoffman 1977 (95)). Great caution has to be taken when using mean deposition velocities due to uncertainties in these rates, typically of up to a factor of three about the mean (See (8)). Any deposition velocity given to a group of elements should be at least a factor of, say, three different to that of any other group, to represent a significant difference in the group deposition characteristics.

Quite a severe limitation on the number of elemental deposition groups a model could deal with is imposed by the range of deposition velocities reported for radiologically significant depositing isotopes. Food chain doses and external exposures are the major pathways for deposited materials. Iodine and caesium are two elements with radiologically dominant isotopes for these processes, and so can form the basis for two deposition groups owing to the relatively strong deposition of iodine compared to caesium (Slade 1968 (45)). The inert gases can be represented as a non-depositing group, so giving a third group. A fourth group can be made available for special circumstances where an element, or group of elements, may be expected to require special treatment.

Section 2.1.2.3 Plume depletion model

Element dependent deposition implies that the depletion model has to cope with the effects of different deposition properties in one decay chain. This means that the radioactive decay and production process during downwind travel is coupled to the depletion process. In the case of a single overall deposition velocity in one decay chain depletion can be treated independently of radioactive decay along the chain (13).

The most significant radioisotopes occur in the chains which exhibit the greatest changes of deposition properties, namely Se-Br-Kr-Rb-Sr and Te-I-Xe-Cs-Ba. This reflects the importance which can be placed on improving the modelling of deposition processes. Up to four grouped element deposition velocities could adequately cover the relevant decay chains of these significant isotopes. Ruthenium is probably the only other element which may pose a contamination hazard in a wide range of potential accidents, but could be treated as depositing in a similar manner as caesium, strontium or other particulate forms.

Hence in principle up to four groups of element dependent deposition rates should be an adequate representation, but the computational implications have to be considered. This last point also applies to the inclusion of element dependent washout and other special features.

Section 2.1.2.4 Restrictions on deposition model due to computational limitations.

The uncertainties about deposition processes suggested that the advantages of a fast analytical model outweigh the potential accuracy of a more detailed scheme which would probably rely on expensive numerical solutions. As most sections of WEERIE use analytical functions this would also remain compatible with the aims for the original code, giving rapid but reasonably accurate predictions of consequences for a given set of parameters describing activity released to the atmosphere.

Due to the available core size on the Control Data Corporation computers at Imperial College the original version of WEERIE was converted to an overlay form (41), schematically portrayed in diagram 2.1. This structure did not require all the available

Diagram 2.1 Overlay Structure at Imperial College WEERIE program with unmodified depletion routines (Fitzpatrick (41))

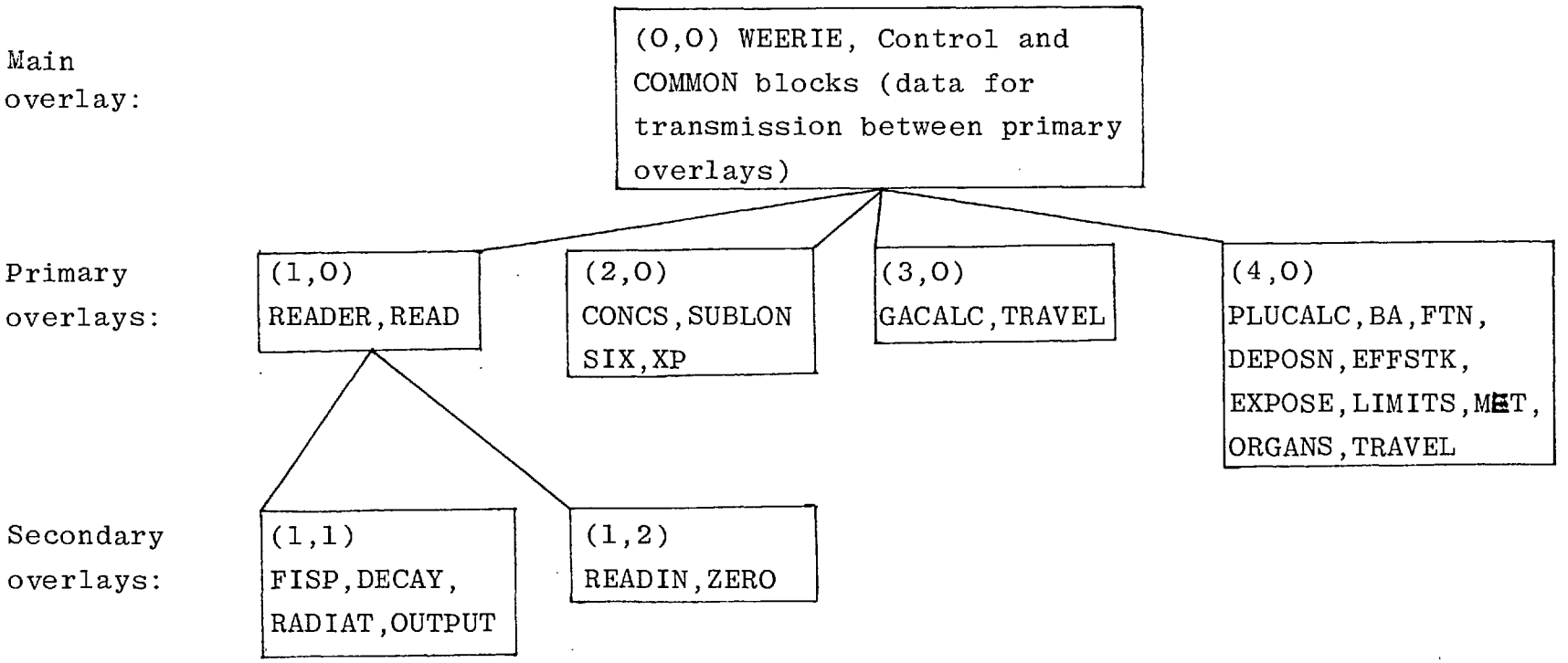

core space, so that the extra storage space required for the improved deposition model was accessible.

To reduce this increase in running costs some compensating improvements in the structure were undertaken. The overlay system described in diagram 2.1 meant that for a given step after an inventory and a release had been calculated the overlay (4,0) was used once if organ doses and contamination at one downwind point were required, where overlay (3,0) was used beforehand if an external cloud gamma exposure was to be estimated. To receive the next set of control data the overlay (1,2) had to be used, which involved the removal of overlay (4,0). If another exposure point was to be considered for the same release overlays (3,0) and (4,0) were recalled successively. The most time consuming section of this process was the recalculation of the gamma source array (GA) for all 428 entries in the isotope array in twelve energy groups at 16 downwind grid positions. This recalculation was not necessary if the meteorological and deposition parameters were not changed between consecutive exposure calculations, so this provided a valuable opportunity to economise time. Also time is wasted when an overlay is reintroduced into the core.

To reduce the time consumption of the dose calculation in the improved Imperial College version of WEERIE the overlay structure of diagram 2.2 was produced. In this version the array (GA) is only calculated if new meteorological or deposition conditions are presented. The dispersion, depletion and travel routines common to the estimation of external exposures, inhalation doses and other quantities are not removed from core when a new set of control data is read and the same release is used for consecutive exposure points. This structure also represents the coupling of the travel and depletion processes necessary for the grouped element depositional model, particularly when calculating the gamma source array (GA).

As can be seen from diagram 2.2 it has proved possible to incorporate extra features into this improved version of WEERIE to cope with washout, external ground gamma exposures and other quantities related to disintegrations in the cloud as a potential accident diagnostic tool. The details of the implementation of the improved depletion model and associated routines is described in the following sections where some examples of its use are also discussed.

Diagram 2.2 Modified Overlay Structure at Imperial College WEERIE with improved depletion routines underlined

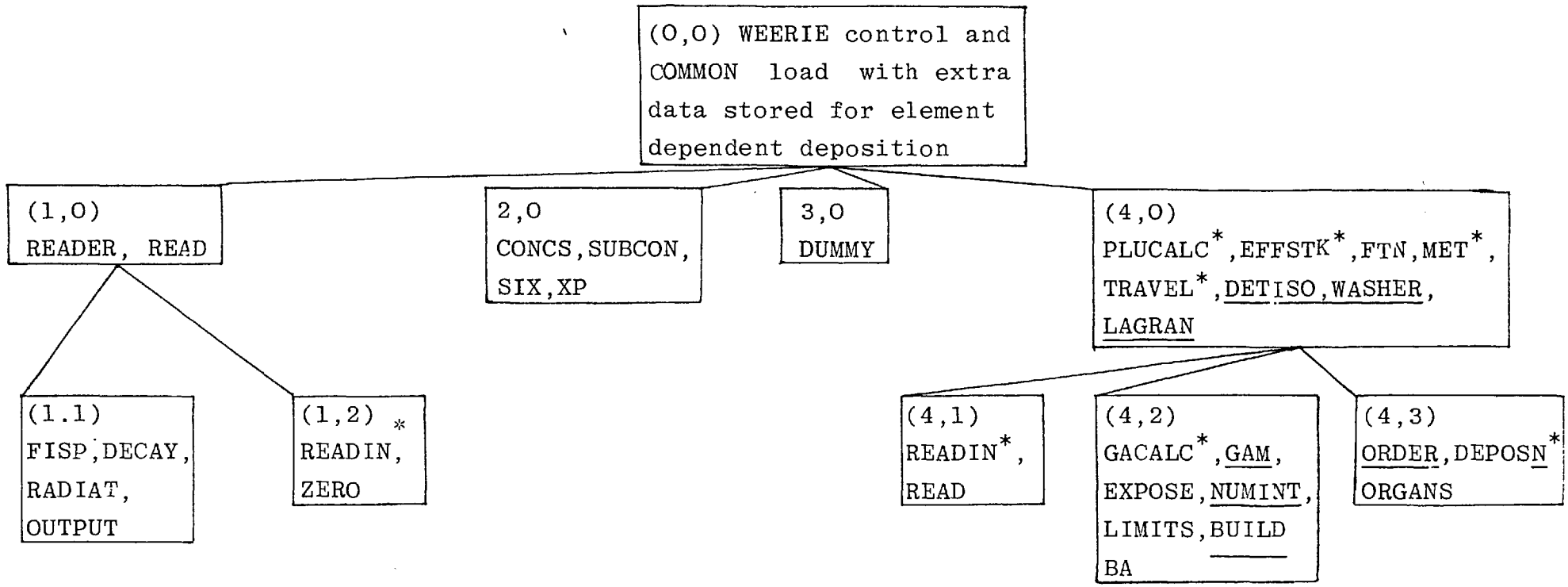

* original routines which needed modification

Section 2.2 Implementation of improved plume depletion model

When material is deposited on the ground this results in a reduction in downwind air concentrations. There are two basic approaches to modelling this process, which are usually referred to as source and surface depletion models.

The Gaussian plume model in WEERIE uses the simpler source depletion model. This assumes that the deposition process at ground level does not affect the vertical distribution of material. Hence the analytical form of the plume does not change with distance, only the effective source strength is reduced by the fraction of material which deposits by a given distance downwind. This depleted source term (Q^*) can be related to the downwind distance travelled (O to x) through the relationship (45),

$$(2.2)\quad Q^*/Q=\exp(-(2/\pi)^{\frac{1}{2}}.(v_g/\bar{u}).\int_O^x(\exp(-\tfrac{1}{2}(h/\sigma_z(p))^2)/\sigma_z(p))dp \quad , \text{ for}$$

constant deposition velocity (v_g), a mean windspeed $\bar{u}$, a source at height h and the vertical dispersion parameter $\sigma_z(x)$. In later examples in this work ground level sources are usually used, resulting in a simplification of equation 2.2. In general σ_z is not a simple function of downwind distance and is normally stored at 40 grid points from 1 metre to 100 km, so to evaluate equation 2.2 requires a numerical integration procedure (13). The air concentrations are now given by the equation 2,3,

$$(2.3)\quad X(x,y,z)= \frac{Q^*}{2\pi u\sigma_y\sigma_z} \cdot \exp(-\frac{1}{2}(\frac{y}{\sigma_y})^2) \cdot (\exp(-\frac{1}{2}(\frac{h-z}{\sigma_z})^2) + \exp(-\frac{1}{2}(\frac{h+z}{\sigma_z})^2)) \quad ,$$

and the ground level contamination (for time integrated air concentrations) by equation 2.4,

$$(2.4)\quad w(x,y)=v_g.\ \chi(x,y,O)\ Ci/m^2.$$

The limitation of this method is the assumption that the vertical distribution of material is unchanged by the dry deposition process at the ground. This requires that mixing throughout the plume occurs rapidly thus maintaining the amount of material depositing at the ground. This condition is not met when the meteorological conditions are stable, particularly when the deposition velocity is a large fraction of the friction velocity $(u_*)^*$, or of the rate of change of the vertical standard deviation σ_z.

Surface depletion models normally allow for deposition to occur at some reference height (z_r) close to the ground where appropriate parameters are still well defined. In these models the vertical distribution of airborne material is allowed to change as deposition continues, which is more realistic than the assumptions in the source depletion model. This requires greater complexity in modelling the vertical structure of the atmosphere and is reflected in greater computational costs.

Comparisons have been made between source and surface depletion models. For long travel times proportionately more released material in a surface depletion model is at a greater height than that predicted by a source depletion model with the same low level release height. Under these conditions a source depletion model tends to overestimate the ground level air concentration, typically where the vertical distribution profile is not expected to change significantly downwind. Hence the rate material is deposited onto the ground at large distances can be too great in source depletion models, eventually leading to a severe premature reduction of the total amount of material remaining in the atmosphere. Ground level air concentrations predicted by both methods, under neutral conditions have been found to agree to within 10% for travel times of 6 hours, 2 days and more than 10 days for deposition velocities of 3,1 and 0.3 0.3 $cm.s^{-1}$ respectively, before this long range deficiency of source depletion models becomes significant (Draxler and Elliot 1977 (46)). More complicated source depletion models have been developed to reduce the inadequacies of the original scheme (Horst 1977 (47)).

The source depletion model can be used for restricted ranges provided its limitations are recognised (Prahm and Berkowicz 1978 (48)). Depletion under stable conditions is the most limiting case, where the application of this simple model may not be of acceptable accuracy beyond about 20km for low windspeeds and a deposition velocity of about 1 cm/s. Consequences at greater downwind distances could be reasonably estimated for low deposition velocities and also for less stable atmospheric conditions.

---

*$u_* = (\tau/\ell)^{\frac{1}{2}}$ where τ =stress in air due to the difference between geostrophic and ground wind velocities and ℓ=atmospheric density. (24) (Footnote to page 24)

The limitations of a Gaussian dispersion model also affect the distance to which this simple dry deposition model can be applied. A single weather category is unlikely to last more than six hours at most, especially when diurnal variations are considered. Under low windspeed stable conditions the plume may only travel 15 km in two hours so that the restrictions of the source depletion model may not be the limiting factor in the calculation of air dosages. Generally the Gaussian plume model with source depletion is not used for dispersion beyond at most 50-100 km, which represents a distance by which many other influences have affected the plume outside of the considerations in simple models of atmospheric dispersion.

In the following sections some of the detailed problems which have to be dealt with in an element dependent deposition scheme are discussed.

Section 2.2.1 Limitations on single and multigroup dry deposition models

A single deposition velocity technique applied to all elements in a modelled mixed fission product release can employ the result given in equation 2.2 directly. This representation is of limited accuracy due to the observed differences in deposition behaviour for certain elements. For multigroup dry deposition rates equation 2.2 cannot be applied in its present form, as the deposition velocity (v_g) may change when a radioactive isotope decays in the plume and transmutes to a different element with new characteristics. Resuspension from the grounded material is not included in these models, where local doses and exposures should not be underestimated by this assumption.

When a single dry deposition rate is used for all isotopes in a decay chain the depletion fraction can be applied independently of the radioactive decay process. This is shown in the relationships below, where a source of parent (P_o) and daughter (D_o) material is released at x=0 and amounts P'_x and D'_x reach x metres downwind. The situation becomes more complicated as more isotopes in a decay chain are considered.

$$(2.5) \quad P'_x = Q_{1,0}^{x} \cdot f \cdot P_o$$

(2.6) $D'_x = Q_{1,O}^{x}(g.D_o + g'.(1-f).P_o)$, where $Q_{1,O}^{x}$ = source depletion fraction of material released at source reaching x metres downwind in single group model, (1-f)= fraction of parent to decay to daughter from O to x metres, and g,g'= fractions of source and plume produced daughter material to reach x metres downwind after decay.

If the plume produced daughter material is assumed to be created all at a distance x'(<x) while the deposition behaviour of parent (v_g^p) and daughter (v_g^d) material are different and, for the daughter, independent of the production route, a more accurate representation, in terms of source depletion fractions, can be given as below,

(2.7) $P_x^t = f.Q_{p,O}^{x}.P_o$, (2.8) $D_x^t = g.Q_{d,O}^{x}.D_o + g'.(1-f).(Q_{p,O}^{x'}.Q_{d,x'}^{x}).P_o$

where $Q_{i,a}^{b}$ = source depletion fraction for material i depositing from a to b. The determination of x' may pose difficulties but should give a reasonable estimate of the actual effect of deposition.

The expected fractional error for the parent and daughter airborne concentrations under given dispersion conditions can be represented as below, for the single group dry deposition model using the characteristics for either the daughter or parent nucleides.

(2.9) ($v_g^1 = v_g^d$) (a) $\left.\frac{\Delta\bar{\chi}}{\bar{\chi}}\right|_{d,x} = g'.(1-f).P_o.Q_{d,o}^{x}\left(1-\frac{Qp,o^{x'}}{Qd,o^{x}}\right)/D_x^t$

(b) $\left.\frac{\Delta\chi}{\chi}\right|_{p,x} = \frac{Qd,o^{x}}{Qp,o^{x}} - 1,$

(2.10) ($v_g^1 = v_g^p$)

(a) $\left.\frac{\Delta\chi}{\chi}\right|_{d,x} = \frac{g.D_o.(Q_{p,o}^{x} - Q_{d,o}^{x}) + g'.(1-f).P_o.Q_{p,o}^{x'}(Q_{p,x'}^{x} - Q_{d,x'}^{x})}{D_x^t}$

(b) $\left.\frac{\Delta\chi}{\chi}\right|_{p,x} = 0.$

In equation 2.9b, where the single group deposition model follows the behaviour of the daughter, the airborne parent material is overestimated if $v_g^d < v_g^p$, as for I-Xe, where this could be expected and the amount of daughter material is also overestimated through any contributions from the parent decaying in the plume. The degree of inaccuracy the single overall deposition model introduces in this case for both parent and daughter materials depends not only on the relative releases of these isotopes at the source but also differences in downwind decay and depletion. When the characteristic deposition rate of the parent is used in this single group model only the airborne concentrations of the daughter material are not accurately described.

The approximation of the one group model to a more realistic situation depends on the deposition velocity chosen for a given release and varies as the plume travels downwind due to the nature of radioactive decay. If a critical nuclide or element can be identified then its deposition behaviour can be used. For many types of releases several elements may be important in different dose pathways, so several runs would have to be made with an appropriate overall deposition velocity to cope with this situation.

Modelling processes giving the result of equation 2.8 by an element dependent source depletion model implies a coupling between decay and deposition not included in an overall single group deposition model. The process of radioactive decay is such that not all decays will occur at one downwind distance. To model exactly the continuous downwind production and deposition of daughter material would require a set of coupled differential equations to be solved by numerical methods. As mentioned earlier this could slow down calculations for an uncertain benefit in accuracy. An analytical approach which gives reasonable results is probably a better practical solution of this problem.

This could be done by assuming that any daughter material(i) produced during travel in the plume which reaches a given distance x downwind has travelled, on average, X_i metres. Assuming that this calculation is possible, as shown in the next section,

its accuracy can be estimated. The knowledge of X_i, and X' $(=x-X_i)$, enables the source depletion fractions $Q^{X_i}_{d,O}$, $Q^{iX'_i}_{p,O}$, Q^{x}_{d,X'_i} and Q^{x}_{p,X'_i} to be calculated from a set of Q*, where this can be done by routines in the original version of WEERIE provided storage is given for each set of Q*'s relating to a given group velocity (v^i_g).

In the routine TRAVEL which calculates the radioactive transmutation for isotopes reaching a given distance downwind, the contributions from an isotopes' precursors are separated from the decay of the amount of that isotope released from the source. The order of calculation in the decay chain proceeds from the parent and continues until the n^{th} daughter. Depletion for travel from O to x of the material released at the source can be made before this decay calculation is performed. During this decay calculation the allowance for depletion of material produced in the plume can be made. This does not allow for the fact that the parent material which decays does so before x metres and therefore does not experience the full depletion from O to x metres. This point will be taken up in more detail later. Reverting to the earlier example of a parent and one daughter the amounts of material left in the plume at x metres are, (2.11) $P'_x=f.Q^{x}_{p,O}.P_o$ and (2.12) $D'_x=g.Q^{x}_{d,O}.D_o+g'.(1-f).Q^{x}_{p,O}.Q^{x}_{d,x'}.P_o$. In the special case of one overall deposition velocity the term $Q^{x}_{d,x'}$ can be omitted. For any cases where all the precursors of a given isotope, i, had the same deposition velocity as that of this isotope the one group equations could then be used. The estimated error of this element dependent source depletion model can be given in the form below,

$$(2.13)\quad (v^p_g \neq v^d_g)\quad (a)\quad \left(\frac{\Delta\chi}{\chi}\right)_{d,n} = \frac{g'.(1-f).Po.Q^{x'}_{p,O}.Q^{x}_{d,x'}.(Q^{x}_{p,x'}-1)}{D^T_x}$$

$$(b)\quad \left(\frac{\Delta\chi}{\chi}\right)_{p,x} = O.$$

This approximation (2.13b), suggests that the parent nuclide, which can be interpreted as one with negligible contributions from any precursors decaying in the plume, should have its behaviour as accurately represented as the source depletion model permits.

There are some special cases relating to the accuracy of this estimate, as given in equation 2.13(a). For this element dependent model if the parent is non-depositing (v_g^p)=0, such as the inert gases krypton and xenon, then $Q_{p,a}^{b}$=1 identically, so that the error of airborne daughter activity is minimised, unlike the case where the single overall deposition model is used. Another case where the element dependent model is an improvement occurs for short lived daughters, relative to travel time and the half life of its parent,so that x' roughly equals x and the source depletion term ($Q_{p,x'}^{x}$) is almost unity, as for Kr88/Rb88.

The relative merits of the two models can be assessed approximately by the ratio of equations 2.13 and 2.9, giving 2.14, where the difference only is in the treatment of the in plume produced daughter material.

$$(2.14)\ (v_g^l = v_g^d \neq v_g^p)\ (a)\ \frac{\frac{\Delta X}{X}\ \text{E.D.D.}}{\frac{\Delta X}{X}\ \text{l.G.D}} = \frac{(Q_{p,x'}^{x}-1)}{d,x\left(\frac{(Q_{d,o}^{x'}-1)}{(Q_{p,o}^{x'})}\right)},\quad (b)\ \frac{\frac{\Delta X}{X}\ \text{E.D.D}}{\frac{\Delta X}{X}\ \text{l.G.D.}} = 0.$$
$$p,n$$

This clearly shows that the element dependent deposition (EDD) scheme always estimates the parent air concentrations better than the one group deposition (1GD) model, for different parent and daughter deposition rates. Equation 2.14(a) also shows that the accuracy of the original model's daughter contributions arising from the parent decaying in the plume depends on the relative deposition of parent and daughter while the improved model's only drawback is slightly underestimating this contribution, but this can be circumvented as shown below. Another case is that of a non-depositing daughter, e.g. I-Xe, where the right hand side of 2.14(a) becomes the ratio 2.15 ($Q_{p,x'}^{x}$-1): ($Q_{p,x'}^{x}/Q_{p,o}^{x}$ -1). Hence where $Q_{p,o}^{x} << Q_{p,x'}^{x}$, such as for large x and reasonably large x' when the parent deposits quite rapidly, the parent's contribution to the air borne daughter material is more accurate in an element dependent source depletion model.

Table 2.1 Example of importance of element dependent deposition

Model	Source depletion Q_a^b in category F conditions			amount of I132 (atoms)			
	a km	b km	Q_a^b	I132 from Te132 decays in plume	I132 from source	Total I132 air	Total I132 (relative ground)
At source	0	0	1	0	6.6(17)[β]	6.6(17)	(-)
No deposition	0	20	1	4.7(17)	2.8(17)	7.5(17)	(0)
Ideal source depletion model							
(v_g(Te)	0	11.3	0.538)				
v_g(I)	11.3	20	0.488	1.2(17)	-	-	-
	0	20	0.041	-	0.11(17)	1.3(17)	(1.6)
Single deposition model							
$v_g^I \doteq v_g^I$	0	20	0.041	0.19(17)	0.11(17)	0.3(17)	(0.36)
$v_g^I = v_g^{Te}$	0	20	0.455	2.1(17)	1.2(17)	3.3(17)	(0.99)
Application of equation 2.12							
(v_g^{Te}	0	20	0.455)				
(v_g^T as for ideal model)				1.0(17)	0.11(17)	1.1(17)	(1.3)

[β] e.g. 1.2(3) = 1200

A simple numerical example is given in table 2.1 for the Tel32/I132 decay chain, where the isotopes have half lives of 78 hrs and 2.2.hrs respectively. The total quantities released result from a notional MAGNOX single channel meltout depressurisation accident, extending over a period of about an hour. This example shows that the use of a deposition velocity of 1 $cm.s^{-1}$ in a source depletion model under Pasquill category F conditions should be limited to about 20 km. Under these conditions the original single overall dry deposition velocity scheme has to be used with caution as an order of magnitude change in the predicted air concentration can be produced by a factor of four change in the deposition rate. The improved element dependent source depletion model estimate is much closer to the value which could be reasonably expected when using a source depletion model. In this case once a value of x' has been calculated a correction factor of $1/Q_{p,x'}^{x}$ can be made to the sole daughter material produced in the plume, so nullifying the underestimate of the element dependent model as expressed in equations 2.12 and 2.13.a.

The steady state between decays of Tel32/I132 was disturbed by the accident sequence and is in the process of being re-established while the material travels downwind with no dry deposition. This steady state is again disrupted by modelling the different deposition rates of this parent-daughter pair. Another point of interest is that the different depletion models predict a smaller range of ground contamination by I132 than that seen in the cloud concentrations. Both the interpretations of the one group deposition model are lower than the element dependent estimate, although I132 ground contamination is not radiologically significant due to its short half-life.

The mean distance travelled by I132 isotopes produced in the plume which at least reach 20 km downwind of the source has been calculated by the methods discussed in the following section.

Section 2.2.2 Calculation of the mean depletion of isotopes produced during travel downwind

To use a source depletion model in the context of element dependent dry deposition velocities account must be taken of the

effects of radioactive decay producing new radioisotopes as material travels downwind. In the decay chains in WEERIE up to six isotopes are present, so that some daughter material can be produced by a complicated pathway as the plume disperses. This process is dealt with below, where an anlaytic expression is determined for the principle parameter: the mean distance travelled ($X_{n,m}$) in the plume by the nth isotope produced by its precursor the m^{th} isotope of that decay chain.

Section 2.2.2.1 Derivation of an analytic expression for the mean travel distance ($X_{n,m}$)

The radioactive decay process for an isotope n can be represented as having a mean decay rate λ such that the fraction of the material n left after a time t is given by,

(2.16) $N(t)/N(O)=\exp(-\lambda t)$. The number decaying in any infinitesimal interval t to t+dt can be given by (2.17) $dN=-\lambda.N(t).dt$. The major property of the radioactive decay process is statistical in nature. The decay of any single nuclide cannot be accurately predicted, only a probability of decay can be calculated given the characteristics of that type of nuclide.

The probability of a nuclide (i) decaying between t and t+dt can be given as,

(2.18) $P_i(t)dt=\lambda_i.\exp(-\lambda_i t).dt.$

This expression can be used for the chain of isotopes which lead from the parent isotope m to the final daughter isotope n. Assuming that isotope m exists at $t_m=O$ and decays at $t^d_m=t^I_{m+1}$ where t^I_{m+1} is the time at which isotope m+1 is created this notation can be carried through so that isotope n is created at $t^I_n=t^d_{n-1}$. For the calculation required here the probability of isotope n existing at least to some time t has to be evaluated allowing for the sequence of decays arising from the precursors m,m+1 .....,n-1.

The probability of isotope m+1 decaying in a time from $t_{m+1}=t^I_{m+1}(=t^d_m)$ to $t_{m+1}=t^I_{m+2}$, after decay by the mth isotope, is given by

(2.19) $$P_{m+1}(t_{m+1},\lambda_{m+1})dt_{m+1}=P_m(t_m,\lambda m)dt_m.\exp(-\lambda_{m+1}(t^d_{m+1}-t^d_m)).\lambda_{m+1}dt_{m+1}$$

$$=\exp(-t^d_m(\lambda_m-\lambda_{m+1})).\exp(-\lambda_{m+1}t^d_{m+1}).\lambda_m\lambda_{m+1}dt_m dt_{m+1}.$$

Hence the probability of isotope n being created by a time $t_n=t^d_{n-1}$ is given by,

(2.20) $P(t_m,t_{m+1},\ldots,n,m)dt_m\ldots.dt_{n-1}$

$= \exp(-t^d_m(\lambda_m-\lambda_{m+1})).\exp(-t^d_{m+1}(\lambda_{m+1}-\lambda_{m+2}))\ldots.\exp(-t^d_{n-1}\lambda_{n-1}).$

$\lambda_m\ldots.\lambda_{n-1}dt_m..dt_{n-1}$

The probability of isotope n existing from time t^d_{n-1} to at least time t is given by

(2.21) $N(t,t^d_{n-1})=\exp(-\lambda_n(t-t^d_{n-1}))$. The resultant probability for isotope n being produced, by decay from isotope m from a time $t_m=0$, and still existing at a time $t_n=t$ is given in equation 2.22, removing the superscripts,

(2.22) $P(t_m,t_{m+1},\ldots.,t_{n-1},t_{n,m})dt_m\ \ldots.\ dt_{n-1}$

$= e^{-t_m(\lambda_m-\lambda_{m+1})}.e^{-t_{m+1}(\lambda_{m+1}-\lambda_{m+2})}\ \ldots..e^{-t_{n-1}(\lambda_{n-1}-\lambda_n)}$

$e^{-\lambda_n t}.\lambda_m\ldots.\lambda_{n-1}.dt_m\ldots.\ dt_{n-1}$

This can be used to calculate the mean period ($T_{n,m}$) for atoms of the n^{th} isotope which are produced by decays from isotope m and still exist at a time t after the initial release of isotope m. The expression for $T_{n,m}$ is given below where the ith isotope can exist from t=0 until $t_i=t_{i+1}$ when that isotope i decays, where isotope n-1 can decay up to a time $t_{n-1}=t$ to produce isotope n.

(2.23) $$Tn,m=\frac{\int_{t_{m=0}}^{t_m=t_{m+1}}\ldots\int_{t_{n-1}=0}^{t_{n-1}=t}P(t_m,\ldots.,t_{n-1},t,n,m).(t-t_{n-1})dt_m..dt_{n-}}{\int_{t_{m=0}}^{t_{m+1}}\ldots\int_{t_{n-1}=0}^{t}P(t_m,\ldots.t_{n-1},t,n,m)dt_m\ldots.dt_{n-1}}$$

This can be evaluated analytically, but becomes progressively more complicated as the number of isotopes between n and m increases. One property of these $T_{n,m}$ is that if isotope m is extremely short lived then the condition below can be expected to hold, (2.24) as $\lambda_m \to \infty$ then $T_{n,m} \to T_{n,m+1}$ and $T_{n,n-1} \to t$ as $\lambda_{n-1} \to \infty$. This can be observed in the formulae below for $T_{n,n-1}$, $T_{n,n-2}$ and $T_{n,n-3}$.

(2.25) (a) $$T_{n,n-1} = (t.D_{n,n-1})/(1-e^{-tD_{n,n-1}}) - 1)/D_{n,n-1}$$

(b) $$T_{n,n-2} = \frac{t.D_{n-1,n-2} - \frac{(1-e^{-tD_{n,n-1}})}{(D_{n,n-1})^2} + \frac{(1-e^{-tD_{n,n-2}})}{(D_{n,n-2})^2}}{D_{n,n-1}.D_{n,n-2}}$$

$$\frac{}{\left(\frac{1-e^{-tD_{n,n-1}}}{D_{n,n-1}}\right) - \left(\frac{1-e^{-tD_{n,n-2}}}{D_{n.n-2}}\right)}$$

(c) $$T_{n,n-3} = A/B$$

$$A = \frac{D_{n-2,n-3}}{D_{n-1,n-2}.D_{n-1,n-3}.D_{,n,n-1}}\left(t-\left(\frac{1-e^{-tD_{n,n-1}}}{D_{n,n-1}}\right)\right)$$

$$-t\left(\frac{1}{D_{n-1,n-2}D_{n,n-2}} - \frac{1}{D_{n-1,n-3}.D_{n,n-3}}\right)$$

$$+\left(\frac{1-e^{-tD_{n,n-2}}}{D_{n-1,n-2}.(D_{n,n-2})^2}\right) - \left(\frac{1-e^{-tD_{n,n-3}}}{D_{n-1,n-3}(D_{n,n-3})^2}\right)$$

$$B = \frac{D_{n-2,n-3}(1-e^{-tD_{n,n-1}})}{D_{n-1,n-2}.D_{n-1,n-3}.D_{n,n-1}} - \frac{(1-e^{-tD_{n,n-2}})}{D_{n-1,n-2}.D_{n,n-2}} + \frac{(1-e^{-tD_{n,n-3}})}{D_{n-1,n-3}.D_{n,n-3}}$$

where (2.25) (d) $D_{n,m} = \lambda_m - \lambda_n = -D_{m,n}$

When the condition, (2.26) $tD_{n,m} \rightarrow 0$, applies for all precursors m, then the result (2.27) $T_{n,m} \rightarrow t/(n-m+1)$ is found for the three formulae above, 2.25 a,b and c, being determined by the (n-m+1)th order terms in the expanded exponential. This limiting result can be expected by a simple consideration of the integrals in 2.23 for the case where all λ_m equal λ_n in the portion of the decay chain from m to n, or by expanding the exponentials.

The above time parameter t can be taken directly from the routine TRAVEL where it is essential for the calculation of radioactive decay. To use the results of 2.25 to calculate the source depletion fraction $Q^x_{X_{n,m}}$ for isotope n this time parametrization has to be converted to one of distance. For a constant uniform windspeed ($\bar{u}$) the transformation is quite simple and takes the form: (2.28) $t=x/\bar{u}$, so values of $X_{n,m}$ can be derived after the appropriate substitutions in equations 2.25 (i.e. $tD_{n,m}=xD^*_{n,m}$ where $D^*_{n,m}=(\lambda_m-\lambda_n)/\bar{u}$, etc.) or directly as, (2.29) $X_{n,m}=\bar{u}.T_{n,m}$.

The time parametrization is more flexible than that of distance, as can be seen when the uniform windspeed changes (to $\bar{u}_c$) at a distance x_c downwind, corresponding to a change of meteorological conditions. This distance relates to a time $t_c=x_c/\bar{u}$ so that the transformation from time to distance now becomes,

(2.30) (a) $t = \begin{cases} (x/\bar{u} & \text{for } x<x_c \\ (t_c+(x-x_c)/\bar{u}_c & \text{for } x>x_c \end{cases}$ (b) $x = \begin{cases} \bar{u}t & \text{for } t<t_c \\ \bar{u}t_c+\bar{u}_c.(t-t_c) & \text{for } t>t_c \end{cases}$

If equation 2.23 were to be evaluated in terms of downwind distance the integration would become even more complicated when there is a change of windspeed. This problem does not arise in a time parametrization, as the windspeed does not enter the calculation of $T_{n,m}$: only when the depletion fraction is calculated is the windspeed involved.

This model approximates the effect of depletion on the mean distance travelled by the in plume produced daughter material. An attempt could be made to reduce the extent of any systematic effect by treating dry deposition as another "decay mode" of

the activity. The differential form of the source depletion fraction (2.2) is

(2.31) $dQ/Q = -(2/\pi)^{\frac{1}{2}}.(v_g/\bar{u}).\exp(-\frac{1}{2}(h/\sigma_z(x))^2).(dx/\sigma_z(x))$,

which can be rewritten in the form of 2.17 as

(2.32) $dQ=-\lambda^*.Q(t).dt$ where $\lambda^*=(2/\pi)^{\frac{1}{2}}.\ v_{g/\sigma_z(t)}\ .e^{-\frac{1}{2}\left(\frac{h}{\sigma_z}\right)^2}$.

Hence the total removal rate of material from the plume can be written as (2.33) $dN=-(\lambda+\lambda^*).N(t).dt$. Employing this equation in an attempt to solve equation 2.23 would require complicated numerical analysis, dependent on the particular meteorological conditions being modelled. The decay 'constant' λ^* does not produce any daughter material but changes from one isotope to the next will affect the amount remaining in the plume. This approach would be more appropriate in a very detailed model of transportation of radioactivity throughout the whole environment.

Limiting the scope of this aspect of the depletion model to the assumptions described earlier should still produce adequate estimates of downwind air concentrations and ground contamination within the overall limitations of the dispersion and depletion scheme.

Section 2.2.2.2 Application of depletion fractions to in-plume produced material

A problem has to be met when the amount of daughter material is produced by in-plume decays of several parent isotopes $P_m, P_{m+1}\ldots\ldots, P_{n-1}$ released from the source, rather than one. The total amount of daughter material produced in this manner in the plume is:

(2.34) $D'_n=D^m_n+D^{m+1}_n+\ldots.+D^{n-1}_n$, where each contribution D^i_n has a different depletion history, represented by the factor $Q^x_{X_{n,i}}$, for the decay sequence from the ith to the nth isotope. In the routine TRAVEL only the quantity D'_n is explicitly represented in the calculations, so some mean depletion fraction $\bar{Q}^x_{X_n}$ has to be evaluated in the form:

(2.35) $$\bar{Q}^{x}_{X_n} = \left(\sum_{i=m}^{n-1} a_i.Q_{X'_{n,i}}\right)/\left(\sum_{i=m}^{n-1} a_i\right).$$

A simplifying assumption can be made to equation 2.35 by limiting the number of precursors considered to the earliest which could contribute more than 1 in 10^4 of the nth isotope nuclides. This number was chosen as being adequate to represent the major contributions to any isotope. Also it was found that this cut-off value did not require any decay sequences involving more than four isotopes. For a notional MAGNOX depressurisation accident only these three functions in equation 2.25a, b and c, were needed. Subsequent experience also showed this to cope with a range of notional AGR releases.

There are several cases where the resultant depletion factor in 2.35 is independent of the weighting functions (a_i). Potentially the most important of these occurs for a parent nuclide with a single unstable daughter, e.g. Csl37/Bal37^m, Tel32/Il32, Rul06/Rhl06, Rul03/Rhl03^m and Kr88/Rb88. In this case only one decay sequence is required so that $\bar{Q}^x_{X'_n} = Q^x_{X'_{n,n-1}}$ (or $\bar{X}_n = X_{n,n-1}$), as the weighting function a_{n-1} identically cancels on the right-hand side of equation 2.35. Where the effective parent is explicitly defined, as in this case, the correction for the parent not travelling the distance from $X'_{n,n-1}$ to x can be made. In more complicated cases an approximation would have to be made if the major precursors each had different deposition velocities, although the parent-single daughter correction should cope with some of this effect, as the calculation proceeds along each decay chain.

A second case is where the daughter is non-depositing, such as the inert gases krypton and xenon. Here, as $v_g=0$, all the source depletion fractions are identically unity, including $\bar{Q}^x_{X'_n}$. A similar effect is produced when the daughter isotope, n, has a half life (τ_n) which is very short compared to its precursors and the time of travel (t). In this third case all $X'_{n,m}=x-b.\bar{u}.\tau_n$ due to this short half life of isotope n, where b is of order unity. This is when τ_n is so small that the source depletion fractions $Q^x_{X'_n}$ are approximately unity, with no significant dependence on the weighting functions a_i.

The primary decay chains which require the application of a mean depletion fraction from equation 2.35 involve metastable states of isotopes, particularly those of the element tellurium. This occurs in the region of the elements Te-I-Xe, where dry deposition behaviour could be expected to vary greatly along one decay chain and radiologically significant isotopes are concerned. The most sensitive isotopes to this weighting process would be those of xenon, such as $Xe131^m$, $Xe133^m$, Xe133 and Xe135, but if non-depositing behaviour is assumed for this element the weighting process is only effective through its influence on the precursors, not directly on the xenon isotopes depletion fraction, as explained above. The next most sensitive isotopes are those of iodine, in particular I131. Due to this isotope's eight day half life the contributions from its shorter lived precursors are typically only of order 1 in 10^3 at short distances so the effects of this source depletion model are not of great importance. The decay chain with A=133 is very complicated and gives several decay sequences where the daughter contributions from $Te133^m$ and Te133 could provide over 10% of the final $I133^m$ and I133 airborne activities.

The weighting functions a_i should be related to the amount of isotope i which can decay and so provide a contribution to isotope n by x metres downwind. This will depend primarily on the quantity P_i of the isotope i released at the source. The decay rates of the isotopes from i to n-1 could also be brought into the weighting function as below, using the result of equation 2.16,

(2.36) $a_i = P_i . F$, possibly with F = 1 no allowance for rate of decay, nominal decay .

$$\text{or } F = \prod_{j=i}^{n-1} \left(1 - \exp\left(-\lambda_j . t/_{(n-m)}\right)\right)$$

Under Pasquill-Smith category C dispersion conditions, with $\bar{u}=5$ m.s^{-1}, there is no significant difference (to 5 S.F.) between the ground contamination within 30km downwind of a notional MAGNOX depressurisation accident from the two forms of this factor F. For the same release under Pasquill category F conditions only ten isotopes are affected by amounts ranging up to 1% for particular decay sequences involving metastable

states by a distance of 30 km downwind, where the source depletion model may not be accurate for these stable conditions. The gross cloud gamma exposure under these conditions is not altered by more than 1 in 10^5, showing the insensitivity of radiologically significant isotopes to changes in this weighting scheme. This suggests that the mean value of the source depletion fraction ($\overline{Q}^{X}_{X'_n}$) is dominated by a single precursor on the occasions when equation 2.35 has to be applied.

To test this supposition a weighted average value of the mean distance travelled by the in-plume produced daughter material was used, in the form below,

$$(2.37)\quad \overline{X}_n = \left(\sum_{i=m}^{n-1} a_i.Xn,i\right)/\left(\sum_{i=m}^{n-1} a_i\right), \text{ with } a_i=1.P_i.$$

It was found, under both category C and F dispersion conditions. that only the concentrations of the limited number of isotopes affected previously by a change in the weights a_i were affected by this modification of the source depletion model. The differences arising from the use of $\overline{X}_n$ and $\overline{Q}^{X}_{X'_n}$ were found to be alike but less than those resulting from the change in weighting function through the factor F of equation 2.36. This upholds the supposition that downwind production of a given isotope in any decay chain in WEERIE is normally dominated by one precursor.

Having incorporated this element dependent dry deposition model into WEERIE and improved estimates of downwind hazards further depletion processes can be modelled which were not included in the original code.

Section 2.2.3 Extensions of source depletion method to other depletion processes

Another major depletion process is that due to the behaviour of water in the atmosphere, where the effects can be more important, under some circumstances, than those of dry deposition. The wet depletion processes can be divided into washout and rain-out, as well as more restricted categories for fog, hail, sleet and snow. A simple distinction between washout and rain-out is that in the former precipitation falls through the plume while in the latter the precipitation occurs due to the presence of airborne material. In rain-out the ionising properties of

radioactive material could have a significant influence on the processes involved. Hence washout could be expected to be represented more simply than rain-out, as is the case (see (45)).

The results of washout can be estimated by a method compatible with the source depletion model used for dry deposition. Rain is assumed to fall through the whole effective depth and width of the plume and uniformly remove material at a fixed fractional rate $\Lambda(s^{-1})$. This process is less likely to change the vertical distribution of airborne material than dry deposition, so this assumption is again made but is expected to be more realistic. The rate of loss of material from the plume at a given distance x downwind can be expressed as (2.37) $dQ(x)= -\Lambda(\int_0^{\infty} \chi\ (x,z)dz)dx$, where infinite limits are used to represent the process affecting the whole plume, $\chi\ (x,z)$ is the crosswind integrated concentration and Q(x) is the depleted source strength by this distance assuming rain to have fallen during the whole travel period of the plume to this position. Once the integral is evaluated this equation reduces to, (2.38) $dQ/Q=\Lambda dx/\bar{u}$. For a constant windspeed and washout rate this produces the source depletion fraction (2.39) $Q_{w,0}^{t(=x/\bar{u})}= \exp(-\Lambda . t)$, independent of the plume dispersion parameters.

The ground deposit formed by this washout process can be represented as, (2.40)

$$\omega_w(x,y)= \frac{\Lambda . Q'(x) . e^{-\frac{1}{2}(\frac{y}{\sigma_y})^2}}{(2\pi)^{\frac{1}{2}} . \bar{u} . \sigma y(x)} \qquad \text{(see (45))}$$

For a ground level release (h=0) this can be written in the form, (2.41) $\omega_w(x,y)=v_w . \chi\ (x,y,0)$ where $v_w=(\pi/2)^{\frac{1}{2}}\Lambda . \sigma_z\ m.s^{-1}$. A set of Q_w at the same downwind distances as Q* for dry deposition can be evaluated and stored for a given value of the washout coefficient and a set of v_w calculated for the specific dispersion parameters. The use of this v_w allows a ready calculation of ground contamination by using $v_{gc}=v_g+v_w$.

The value assigned to the washout coefficient depends on many factors including the rate of rainfall (R mm/hr), the spectrum of raindrop sizes and the spectrum of airborne material as well as a whole range of physical and chemical characteristics. Gross washout coefficients for aerosol particles, with low dry deposition velocities (e.g. $v_g < 3\ cm.s^{-1}$), have been given in the

form, (2.41) $\Lambda\ (s^{-1})=a.R\alpha$, where a is a constant and typically α lies between $\frac{1}{2}$ and 1. Washout coefficients of the order $10^{-4}\ s^{-1}$ have been observed for aerosols in light rainfall, where long term averages are typically below this value. The type of rainfall can be important where very fine raindrops can more efficiently scavenge some aerosols from the atmosphere than rainstorms with large raindrops. The washout of submicron aerosols is particularly sensitive to many parameters, so empirical results may provide a better guide to the consequences of this washout process for airborne radioactive effluents than idealised theoretical models.

Washout has been found to be an element dependent process, as the chemical activity and the physical solubility of materials (aerosols, vapours and gases) are important with respect to precipitation. Bromine has a high reaction rate with water and has a correspondingly high washout coefficient while the lower reaction rate of iodine is reflected in a much lower washout rate (45). The inert gases, krypton and xenon, which do not react with water could be expected to have very low washout coefficients. Hence if the element dependent deposition model is used with zero deposition velocity for the inert gases, this condition can be used as a signal to prevent the washout model being applied to isotopes of krypton and xenon.

Another feature which the washout model can include is the ability to only allow the portion of the plume from x=0 to $x_R=\bar{u}t_R$ to be affected by this depletion process. Beyond the distance x_R there is no further washout so the source depletion fraction is (2.42) $Q_{w,0}^{x>x_R}=\exp(-\Lambda t_R)$. More complicated sequences of washout superimposed at different distances downwind could be programmed into the model if these were to be considered of importance given the limitations of the overall gaussian dispersion model.

Several factors have been neglected from this model due to the problems of any simple attempt to quantify such effects as:

i. Run-off of rainwater on the ground (important in urban areas)(Slinn, 1978(49))

ii. Evaporation of gases precipitated to the ground (45)

iii. Mixed releases of material, heat and water vapour (particularly in conditions suitable for condensation)

iv. Possible interactions between washout and dry deposition (these are assumed to be independent in this model).

A few other features which could be introduced into WEERIE's dispersion model are described in the next section, after which some examples of the modifications are given.

Section 2.3 Other features of plume dispersal

Some influences on dispersion and depletion of a plume and the resulting hazards were not modelled in the original version of WEERIE. A few of these will be briefly discussed below, including:

Changes of dispersion conditions downwind of the source;
Influences on dry deposition rates;
Changes of wind direction as plume travels downwind;
Plume rise;
Recirculation of air and topographical effects;
Resuspension of deposited material.

Section 2.3.1 Changing dispersion conditions downwind of the source

The most important effect on the dispersion of a release with a short timescale can be the change-over from day to night conditions in the diurnal cycle.

Night-time dispersion conditions tend to be stable and so not very dispersive. When dawn comes there is usually a period of vigorous increase in the height of the mixing layer, corresponding to unstable conditions, before daytime dispersion conditions evolve, often neutral in temperate latitudes. Other air movements can cause a change of dispersion conditions for a plume in the atmosphere. Smith has derived a set of gaussian dispersion parameters which can allow for some of these effects given the initial time of release and relevant meteorological data. Detailed models of the atmospheric boundary layer flow can better predict dispersion but at great expense compared to a simple gaussian model.

A simple change of dispersion conditions can be included in the WEERIE model provided some curde assumptions are made. At the downwind travel distance, x_c, the weather is assumed to instantaneously change from condition M to M' with windspeeds of u and u' respectively. The time and distance relationships are

given by equations 2.30a and b, so that the dispersion parameters and source depletion fractions can be related to the travel and depletion routines parametrized in time (t). The dispersion parameters have been crudely matched at x_c such that,

(2.43) $$\sigma(x) = \sigma^{M}_{y/z}(x) \quad \text{for } x<x_c$$

(y or z) $$\sigma^{M}_{y/z}(x_c) + \sigma^{M'}_{y/z}(x) - \sigma^{M'}_{y/z}(x_c) \quad \text{for } x>x_c.$$

In the real atmosphere a transition period would exist rather than this modelled sudden changeover. As the dispersion parameters are stored at a fixed set of downwind distances (x^i_g) the Lagrangian interpolation routine used to evaluate these values at any particular distance will tend to round off this sudden changeover, unless x_c coincides with one of these fixed points.

Although this could crudely model the fumigation of a plume at dawn the distance already travelled by this time may imply gross inaccuracies in the predicted air concentrations due to the limitations of the source depletion model, as discussed earlier. For site analysis only short range dispersion would often be considered under many conditions so this changeover of conditions may not be of major significance to any use of WEERIE to provide results for collective dose estimates. Applications of this feature should be used more as a tool for general qualitative results rather than in any attempt for quantitative values, as more accurate deposition models could be used in conjunction with better, but more expensive, dispersion models.

Section 2.3.2. Influences on dry deposition rates

For the submicron diameter aerosol particles expected to be released as a result of postulated accidents in nuclear reactors, their dry deposition rates can be limited by atmospheric turbulence. Hence different dispersion conditions could influence the dry deposition rates. Greater turbulence is often associated with greater windspeeds for a given dispersion category.

Due to the characteristically large spread of results about mean dry deposition velocities it has been difficult to find any significant correlations with dispersion conditions or windspeeds.

Nevertheless a factor (GFACV) has been incorporated into the model detailed in the previous section and is a direct multiplier to all grouped dry deposition velocities beyond the changeover distance x_c, so (2.44) $v_g^{i'} = \begin{cases} v_g^i & x < x_c \\ v_g^i . GFACV & x > x_c \end{cases}$. The limitations of the source depletion model should be noted when using this factor, as well as the inherent uncertainties associated with dry deposition rates and the gaussian dispersion formulae.

Other effects can be simulated by this factor in conjunction with the change of dispersion conditions modelled in the earlier section. For example if a depositing isotope were assumed to be of two distinct physical forms with different dry deposition rates then a value of x_c could be specified but with the same dispersion conditions at all distances. This distance would then be chosen with the assumption that the majority of the quickly depositing material, at a rate v_g^c, had been removed at an average rate $v_g^a (< v_g^c)$ and the remaining material had a lower deposition velocity $v_g^b (= GFACV . v_g^c)$. This could be applied to a mixture of elemental iodine and the more inert methyl iodide. Also there is evidence to suggest that this effect could be a reasonable representation of the behaviour of aerosols in the atmosphere (Whitby 1976 (50)). This reflects the unstable nature of some small aerosols in the atmosphere, where a more stable region can exist beyond about 20km downwind travel, which is at the limit of the source depletion model in stable conditions. Another condition where this particular use of the model could apply is where the plume is assumed to cross from land to sea, where stabler air could exist over the water but the depletion rate might increase due to properties of the water which enhance deposition.

Detailed knowledge of the physical form of a plume's contents and the path it takes would be needed for this feature to be employed, particularly the relevant deposition data.

Section 2.3.3 Change of wind direction

The gaussian model used in WEERIE assumes a linear path for the plume dispersing downwind. This is unlikely to occur in the real atmosphere, due to the nature of the dispersion process as well as topographical features on the land.

External cloud gamma exposure estimates relative to the plume

axis could be affected after a sufficient travel time. Local beta exposures and inhalation doses would still have the same distribution about the plume axis given a gaussian model. The greatest effect would be in the collective dose commitment estimates, when the dose - distance relationship is applied to a population distribution. The concept of a worst sector would have to be modified from that proposed by Gronow and Gausden (1973(2)).

The radius of curvature of a path could be very large compared to the scale of tens of kilometres over which this gaussian plume model can be applied. Meandering of a plume in stable conditions might be modelled at short distances but short time averages would probably be required. These considerations lead into aspects of dispersion modelling which are still subjects for basic research in atmospheric physics.

Section 2.3.4 Plume rise

Much work has been done on estimating plume rise due to such parameters of the released material as upward momentum, sensible heat content and for large radioactive releases self-heating due to decay processes.

Simple models, as in WEERIE, allow an effective height of release to be given to the plume. More complicated models not only predict the path of the plume under different conditions but also the amount of mixing due to the plume rise process as well as the different properties of the atmosphere above the ground (Briggs (51), Russo et al 1977(52)).

The effect of plume rise is to remove high doses from the short range characteristics of a release, see equation 2.3 (45). The total number of latent casualties for a given release of radionuclides will generally not be greatly affected by this process, but it can be a critical factor in estimating early fatalities (44), (6).

As explained earlier the dispersion parameters used in WEERIE are most relevant to ground level releases and cannot be applied as accurately to dispersion higher in the atmospheric boundary layer, as would be required in plume rise models.

Section 2.3.5 Topographical effects

Topography has a localised effect on dispersion so cannot be

readily modelled in any general dispersion scheme without a loss of accuracy, especially for one as simple as the gaussian model (Schriber et al. 1979 (94)). Local measurements of dispersion would implicitly contain effects particular to one site, but are difficult to obtain and of limited use elsewhere.

Large scale features can influence the flow of material systematically but this would generally be at a scale beyond the scope of the model used in this code. Recirculation of material in a large valley, or fjord, can be an important limitation on dispersion in the atmosphere over some averaging times. Another special effect which could be observed under stable conditions is a plume splitting when it meets a hill penetrating the level of the plume. The plume remains on one level and eventually recombines downwind of the peak, after sufficient lateral dispersion.

These effects have not been incorporated in this code's dispersion model.

Section 2.3.6 Resuspension of deposited material

The element dependent deposition model described earlier assumes that there is no resuspension of deposited material while the plume travels downwind. This is not a valid assumption as both radioactive decay and normal wind action can resuspend material into the atmosphere. In a short time period after the plume has created a deposit resuspended material could be assumed to travel down the same track as the plume. Once a sufficient delay occurs to allow a change of wind direction or dispersion conditions, before resuspension, the problem is immediately complicated.

Neglecting resuspension generally could often give a pessimistic estimate of hazards in the track of a plume as regards deposited activity. Some of the problems of relocation of deposited material are discussed in chapter 3.

Section 2.4 Some simple examples of the use of the improved dispersion and depletion routines in WEERIE

The effects of an element dependent depletion model on the potential doses and exposures will be varied. The most obvious feature of this model is the improvement of the ground contamination estimate, given the limitations of the gaussian plume model associated with a source depletion scheme. Where a single isotope or element dominates the inhalation dose given to a single organ, such as iodine to the thyroid, any special deposition prop-

erties assumed for that element will be reflected directly in that organ's dose commitment. Quantities involving a wide selection of elements, such as external gamma ray exposures, will generally follow any trend given to the majority of elements.

The distances to which the source depletion and the gaussian plume models are valid depend strongly on the meterological conditions assumed. This combined with radioactive decay of isotopes limits some of the effects which can be modelled. Also in choosing conditions to demonstrate the capabilities of the improved depletion and dispersion models the extent of deposition has to be considered. For low deposition velocities, out to a range of a few tens of kilometres, depletion is greatest under stable low-windspeed conditions and becomes insignificant for very unstable conditions. A limited range of conditions are considered in these examples, including high-windspeed neutral and slightly unstable conditions, which are quite common in the UK. In addition stable category F conditions are used as an example where severe depletion occurs even with low deposition velocities.

The remaining sections of this chapter will display some of these features for the improved depletion and dispersion models.

Section 2.4.1 Comparisons of a single overall deposition velocity to a 3 group element dependent model

The example given in this section uses a notional MAGNOX single channel melt-out accident as the source of a mixed fission product release (Macdonald (61,83), Strachan and Goddard 1978(60)). The deposition velocities used in the grouped element dependent model are halogens, v_g=1.2 cm.s^{-1}; inert gases v_g=0 and all other elements are assumed to be in an aerosol form with v_g= 0.3 cm.s^{-1}. For the single overall depletion model this characteristic aerosol deposition velocity is assumed, so a balancing effect could be expected for ground contamination between the halogens and the inert gases relative to the three group model. Time integrated air concentrations are calculated by WEERIE so expressing contamination in curies per unit area.

Two dispersion conditons are considered, namely slightly unstable Pasquill-Smith category C ($\bar{u}$=5m.s^{-1}) and stable Pasquill category F. Dry deposition within 30km of the source does not rapidly remove material from the plume under the former conditon, whereas the latter stable condition exhibits much greater deplet-

Fig. 2.1 Ratio of 3 to 1 group dry deposition predictions for notional MAGNOX release (stable conditions)

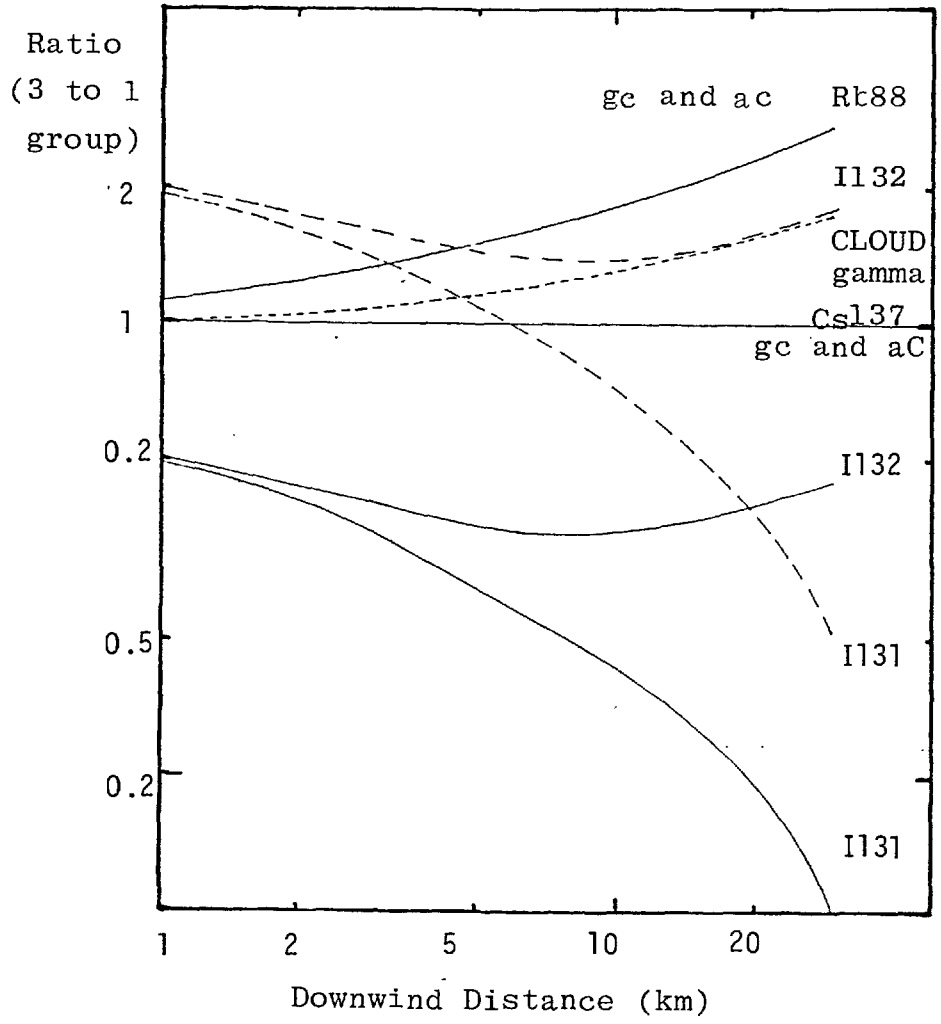

Fig. 2.2 Ratio of 3 to 1 group dry deposition predictions for notional MAGNOX release (slightly unstable conditions)

ac: air concentration (——)

gc: ground contamination(-----)

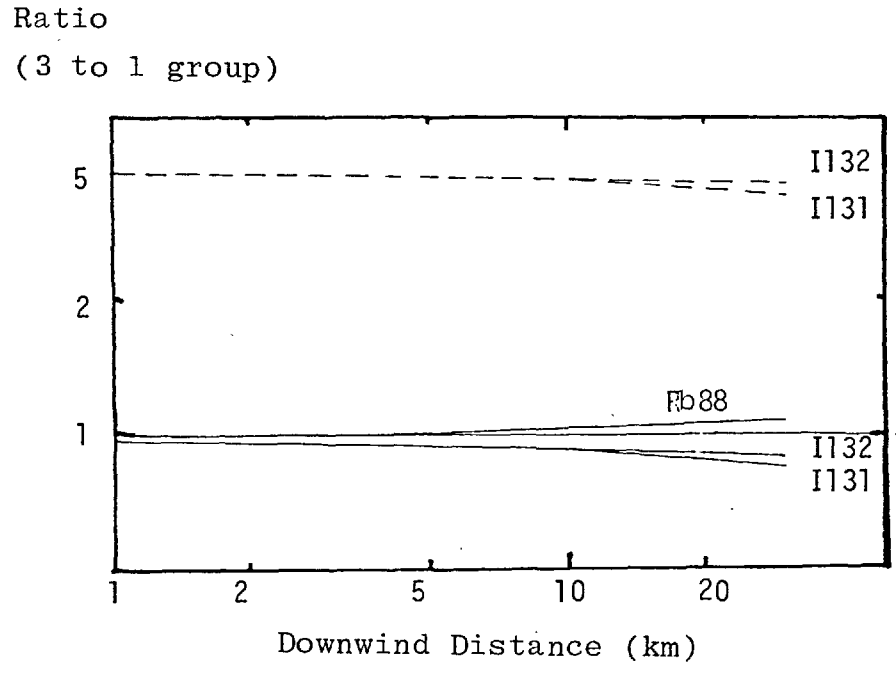

ion. Appropriate short time scale lateral dispersion is assumed for the released material in both sets of dispersion parameters.

Figure 2.1 displays the ratios of the predictions of the three and one group models of the ground contamination under stable (F) dispersion conditions for the isotopes Rb88, I131, I132 and Cs137. For the case of a long lived isotope, Cs137, which has no significant precursors and is given the same deposition rate in both models, this ratio is always unity. The ratio of air concentrations at ground level can be deduced by extracting the appropriate deposition velocities in both models from the ground contamination ratios. The ground level air concentration for Cs137 is again unity at all distances. Hence lung and bone inhalation doses are not sensitive to the differences in these models, as the isotopes significant to these organs, Sr, Ru, Cs etc., are treated identically. Krypton-88, an inert gas, is given zero deposition velocity in the three group model so that it experiences no depletion, but this is not the case when using a single overall deposition velocity. As a result in the one group model both the ground level air concentration and ground contamination of rubidium-88 ($t_{\frac{1}{2}}$=18 mins.), the short-lived daughter of Kr88, are progressively underestimated as the material travels downwind. This could affect estimates of doses to the stomach, small intestine and lung, as well as contributions to the external cloud gamma exposures at relatively high emission energies.

In the three group model iodine isotopes are given a high deposition velocity. I131 has few contributions from precursors so it is rapidly depleted in the three group model relative to the one group model. In the three group model the I131 ground contamination levels are still higher 5km downwind of the source, even though over 70% more I131 has been removed from the plume than in the one group model. I132 ($t_{\frac{1}{2}}$=2.2hrs.) shows a more complicated behaviour, due to having a continuing downwind contribution from Te132 decaying in the plume. I132 air concentrations are initially lower and decreasing in the three group model, relative to the one group model, as the amount of this isotope released at the source is still dominant in the plume. However beyond ten kilometres the I132 produced from Te132 decays in the plume progressively become dominant, so that the I132 reaching these greater distances by this decay sequence does not

experience such a great depletion. Eventually a steady state would be attained below the level of the one group model's air concentration for I132, but under these stable conditions it is probably beyond the useful range of the source depletion model. Even though the I132 air concentration is reduced by this three group model, relative to the one group model, the ground contamination is still greater at all distances. When this three group model is used in place of the original one group model these two effects on iodine isotopes reduce the thyroid inhalation doses at all distances, but can increase ground contamination at short distances for I131 and larger distances for I132.

Also shown in figure 2.1 is the ratio of the on-axis numerical estimate of the cloud gamma exposure from the three and one group models. This averages over all the elements in the plume as all contribute some gamma activity. Due to the whole inert gas inventory of the MAGNOX channel being released in this notional accident, and only 10% of the halogen activity, the three group model's assumed non-depositing behaviour for the inert gases more than compensates for the rapid depletion of the prolific gamma emitting iodine isotopes, relative to the results of the one group deposition model. If the iodine release fraction is reduced to 1% the cloud gamma exposure is decreased by about 40%, showing the importance of any treatment of iodine isotopes in the plume.

The complementary curves are shown in figure 2.2 for the higher windspeed slightly unstable Pasquill-Smith dispersion conditions which are not very conducive to rapid depletion of the plume material. This is evidenced by the ground level air concentration curve for I131, where, even with the higher three group iodine depletion rate, this quantity is within 15% of the single group value within 30km of the source. The greater iodine deposition velocity in the three group model is reflected by the high values of the ratios for both I131 and I132 ground contamination. These are almost equal to the ratio of the iodine deposition velocity in both models, $v_g^3(I)/v_g^1 = 4$. The effects of krypton deposition in the one group model are again reflected in the behaviour of rubidium-88, but this difference does not exceed 6% by 30 km. As before the estimates for isotopes with no precursors and with aerosol deposition characteristics do not differ between the two deposition models. Hence it can be expected that both dry deposition models will give similar inhalation dose

commitment predictions within this range of 30km under slightly unstable dispersion conditions.

The ratio of numerical cloud gamma exposure estimates does not deviate from unity by more than 0.4% up to 30, however it goes through a minimum at about 4 km under these conditions. No great emphasis should be placed on such small differences, as these effects are of no significance when the inaccuracy of the numerical estimate under most conditions could be 10% for a given plume geometry.

The effects of different uses of the element dependent dry deposition model on external exposures from the material on the ground are considered in the next chapter, where these differences could be expected to be greater than these found for the cloud gamma exposure.

Section 2.4.2 Simple example of washout

The initial release of a wide range of fission products from a notional AGR major depressurisation melt-out accident is used to demonstrate the effects of washout, at a rate of $10^{-4}(s^{-1})$. The rainfall is assumed to cut-off at x_R=43.2km(t_R=0.1 days). A set of dispersion parameters is used to represent slightly unstable Pasquill-Smith category C weather. An inversion at z_i= 1000 metres is assumed to exist, where this is crudely modelled by restricting the vertical dispersion parameter to less than $z_i/2.142$, which represents the 10% limit of the plume not penetrating the inversion. As dry deposition under these conditions is not excessive this assumed long range behaviour of the vertical dispersion coefficients should not unduly deplete the plume (Draxler and Elliot). Both washout and dry deposition is assumed to occur for distances less than x_R and only the latter beyond this distance, without any change of the deposition velocities.

Figure 2.3 shows the results of washout combined with dry deposition relative to those for dry deposition only under the conditions described above. The lung and thyroid inhalation dose commitment ratios both show progressive depletion of the airborne material as washout continues to x_R. A feature of this three group depletion model is that as the inert gases are assumed to be non-depositing, with respect to dry deposition, they are also assumed not to be washed out by rainfall. These inert gases do not contribute significantly to inhalation doses, so the curve in figure 2.3 shows the effects of washout reducing airborne concentrations of depositing isotopes and also inhalation doses,

Figure 2.3 Ratios of results from 3 group dry deposition models, with element dependent washout for first 2.4 hours of downwind travel, for a notional AGR depressurisation release under slightly unstable conditions with an inversion relative to dry case.

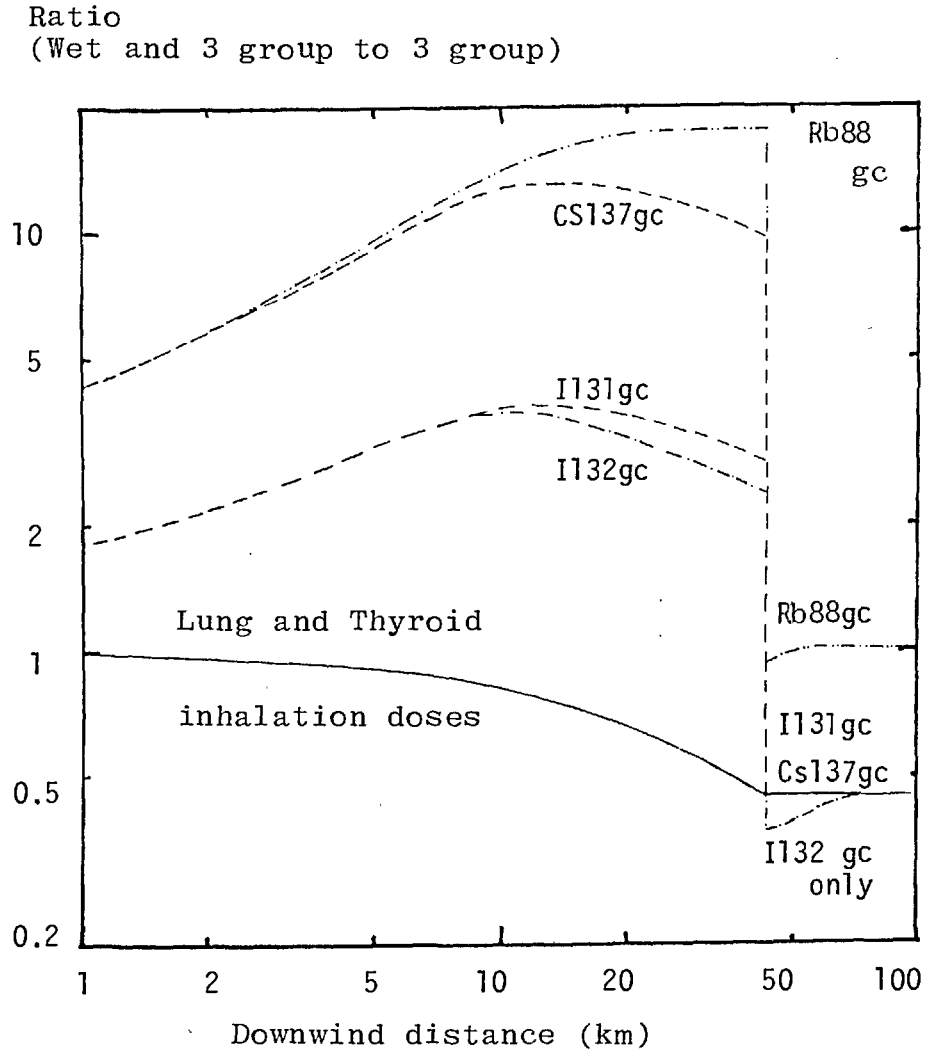

eventually by 55%. After washout stops the ratio of these two cases is constant as the same dry deposition behaviour is postulated. This shows that, as expected from equation 2.37, the effect of washout is very dependent on the effective depth of the plume.

Also shown in figure 2.3 are the relative ground contamination curves for these two depletion cases. This shows more explicitly the dependence of the effective washout velocity on the height of the plume, as expected from equation 2.41. The relative contamination depends to a first approximation on the ratio, (2.45) $(v_w+v_g).Q_w:v_g$, so for small v_g the effects of v_w increasing are relatively greater, as displayed by the ratios for Rb88 and Cs137(v_g=0.3 $cm.s^{-1}$) compared to those for I131 and I132 (v_g=1.2 $cm.s^{-1}$). Once the upper boundary of the plume approaches the inversion layer detailed differences between these isotopes are observed.

Rubidium-88 reaches a steady state, as its presence in the plume by 20km is due almost exclusively to decays of krypton-88 which is not depleted by this three group model. Here the short lived daughter isotope will be travelling a fixed mean distance $X_{n,n-1}$, so if the vertical dispersion parameter does not vary with distance both v_w and $Q^x_{X_{n,n-1}}$ will also be constant for this Kr88/Rb88 decay chain. Beyond x_R the Rb88 concentrations return to that with no washout, with a slight undershoot immediately after washout ceases and the dry deposition steady state is produced. The ratio of unity is produced by the washout in the elemental dependent model not affecting the inert gas krypton-88, which is the sole source of rubidium-88 in this distance range.

Caesium-137, having no significant precursors, is subject to the total depletion from the source, so once the plume stops dispersing vertically v_w is constant but $Q_{w,\bar{U}}^{x}$ continues to decrease. This produces a maximum in the ratio of the washout and dry deposition combined ground contamination relative to the dry deposition case for Cs137. After the rain ceases the Cs137 ground contamination ratio becomes a constant, at the same level as for the inhalation doses, reflecting the extra depletion produced by washout.

Ground contamination by I131 can be expected to show the same type of behaviour as that of Cs137. This is observed in

figure 2.3, but at a lower relative value due to the dry deposition velocity for iodine being four times that of caesium in the element dependent dry deposition model. The behaviour of I132 shows the effect of washout on both the material produced by in-plume decay of Te132 and that originally released at the source. With a half life of 2.2 hours I132 can be expected to travel on average about 40km under these conditions. The I132 contribution from in-plume decay of the already depleted Te132 will be further depleted by the appropriate factor for the travel distance $X_{n,n-1}$. Here the difference between I131 and I132 ratios reflects a neglection of the correction for too much Te132 depletion (see Table 2.1). Once the depletion due to rainfall ceases the two cases revert to the same overall depletion scheme, but the ratios again reflect the net loss by washout, as for Cs137. Again an undershoot occurs with I132, but this is greater than that observed for Rb88 due to the longer lived I132 retaining the depletion effects of washout to a greater distance beyond that at which the rain ceases.

This example has shown some of the detailed effects which could occur when a plume of mixed fission products experiences uniform washout.

Section 2.4.3 Examples of the change of meteorology feature

Two cases are discussed in this section where the notional MAGNOX single channel melt-out on depressurisation accident again supplies the source of plume material. The first case demonstrates the effects of going from a stable, low windspeed condition to a higher windspeed neutral flow at a downwind distance x_c. In the second example the same stable conditions are used throughout but the deposition rate is decreased beyond x_c.

The reference set of consequences used to derive the ratios in both cases assumes short time scale stable dispersion parameters as used in section 2.4.1. Prolonged lateral dispersion parameters (Beattie and Bryant, 1970(53)) are used for both the complex conditions. This enables the effects of different lateral dispersion parameters to be displayed simply at distances before x_c.

Section 2.4.3.1 Transition from stable to neutral dispersion conditions

In this example the neutral dispersion conditions, with a

Figure 2.4 Ratio of results for a MAGNOX release using element dependent dry deposition for prolonged dispersion with a transition from stable to neutral conditions 3.6km downwind (with a change of deposition velocities), relative to dispersal in a short time-scale under stable conditions.

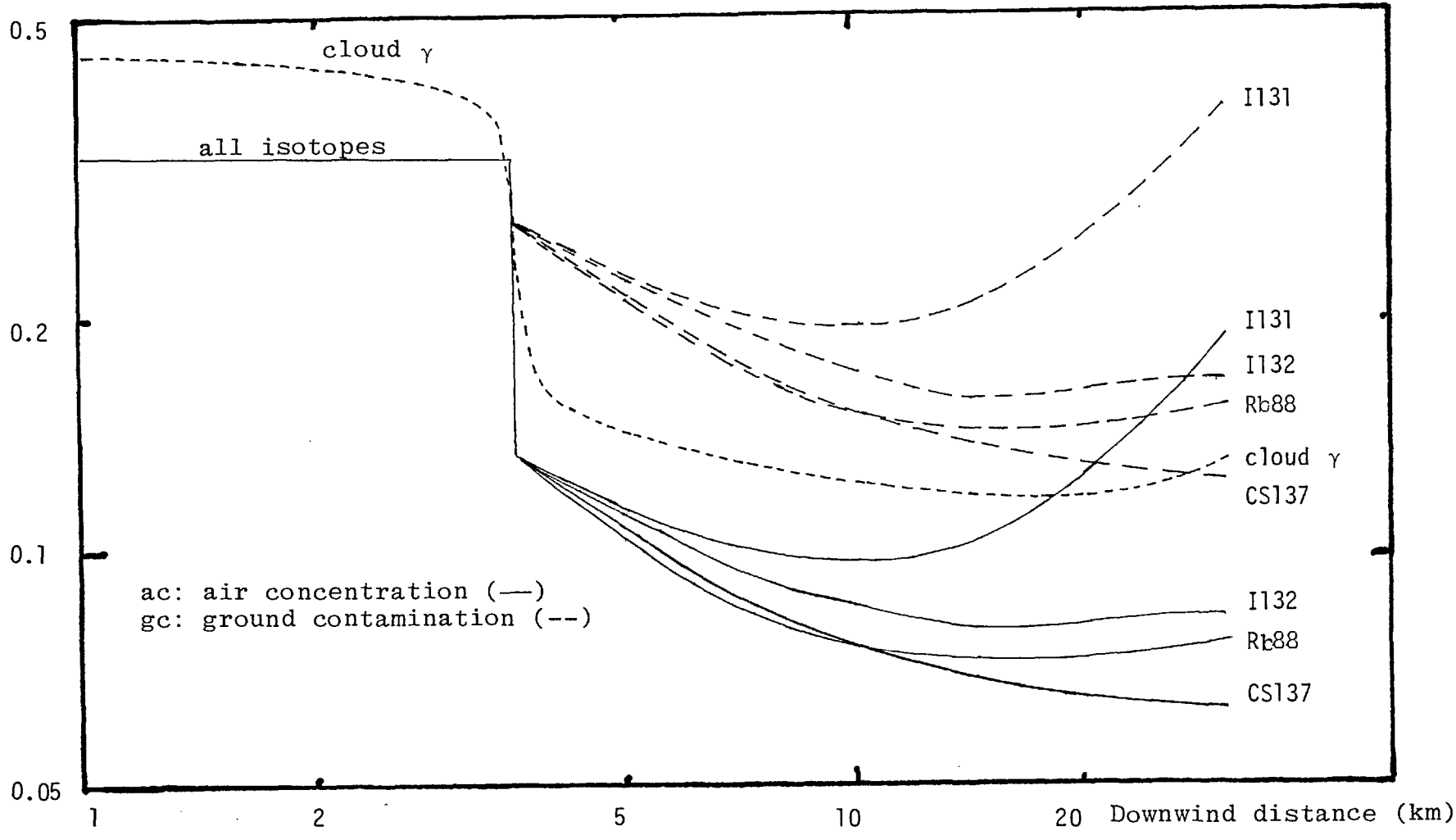

mean windspeed of 5 $m.s^{-1}$, are assumed to start at 3.6 km. Before this, stable conditions with a mean windspeed of 2 $m.s^{-1}$ are assumed to exist for half an hour. At all downwind distances prolonged (Pasquill category C) lateral dispersion parameters are assumed, where these broaden the plume by about a factor of three compared to the short time scale conditions. A change of deposition rates is also assumed to occur beyond x_c and this is represented by a value of GFACV=2 corresponding notionally to the increased turbulence.

Figure 2.4 portrays some of the quantities of this complex situation relative to that of short time scale dispersion. Before the transition only the effects of different lateral dispersion parameters are observed. All the isotopic ground and air contaminations are reduced to about 33% of the values in the narrower plume, which would be reflected in any inhalation doses in this limited downwind range. The numerical estimate of the cloud gamma exposure is closer to that of the narrower plume, being greater than 40% before the influence of the meteorological transition. This reflects the extended range from which the cloud gamma exposure can be delivered.

At the transition point the cloud gamma exposure does not show as sharp a change as the air concentrations. The more dispersed plume in this second region leads to a ratio of about 0.12 between 10 km and 20 km. This factor reflects the increase in the mean windspeed and the vertical dispersion parameters after the transition. The greater windspeed has the effect of extending the physical range of the radioactive material in the plume, so that by a given distance, beyond x_c, less decay has occurred than in the reference case. The neutral conditions are also less conducive to deposition than the stable conditions, although the GFACV value of two lessens this difference. This explains why ratios for I131 ground and air contaminations experience an upturn beyond 15 km, where depletion under the stable reference conditions is very severe. The contribution of iodine isotopes generally to the cloud gamma exposure is also evidenced by the upturn in the ratio of this quantity towards 30 km. I132 also experiences an increase in this range, though less marked than I131 as the relative differences of depletion on its low deposition rate parent Te132 are smaller between the two conditions than for iodine isotopes released at the source.

The ratios for Rb88, the short lived daughter of Kr88, are found to follow a similar trend to that of I132 but without the complications of a parent with depositing characteristcs. Only the ratios of Cs137 in figure 2.4 continually decrease in the neutral flow. This isotope does not have any significant precursors, so the doubled deposition velocity offsets the relative reduction in the depletion fraction produced by the increases in vertical mixing and the mean windspeed.

The neutral dispersion conditions beyond x_c could be extended beyond 30 km, but the reference case, of stable dispersion conditions, used to derive these ratios is probably not a reasonable representation of long range behaviour. This limited comparison has still shown some of the important features of a type of fumigation which could be of practical use in estimating consequences from mixed fission product releases.

Section 2.4.3.2 Reducing deposition velocities downwind of a release

In this example the stable low windspeed conditions, with prolonged time scale lateral dispersion parameters, are assumed to continue beyond the transition point 5 km downwind but the deposition velocities are reduced by the factor GFACV=0.2. The source depletion fractions produced by dry deposition in the first 5 km are given below for the two non-zero rates used, $Q_0^5(v_g=1.2$ cm.s$^{-1})=0.178$ and $Q_0^5(v_g=0.3$ cm.s$^{-1})=0.648$.
This shows the important effect of plume depletion in normal stable conditions. A significant change of mean deposition behaviour might be expected under these conditions especially for any elements existing in several different physical and chemical forms.

The ratios of several characteristics of this particular example, relative to the stable short time scale conditions used in section 2.4.1 are given in figure 2.5. The initial portion of the curves are the same as before the transition in the corresponding curves in figure 2.4. After this distance x_c the air concentrations of depositing radionuclides can be expected to show a relative increase, due to the reduction of the deposition rates. This would be reflected by correspondingly greater predicted dose commitments in WEERIE. However the postulated decrease in deposition rates may mean that this material is less

Figure 2.5 Ratio of results for a MAGNOX release using an element dependent dry deposition model for prolonged dispersion, allowing for a change of deposition velocities 5 km downwind, relative to short time scale dispersion under stable conditions.

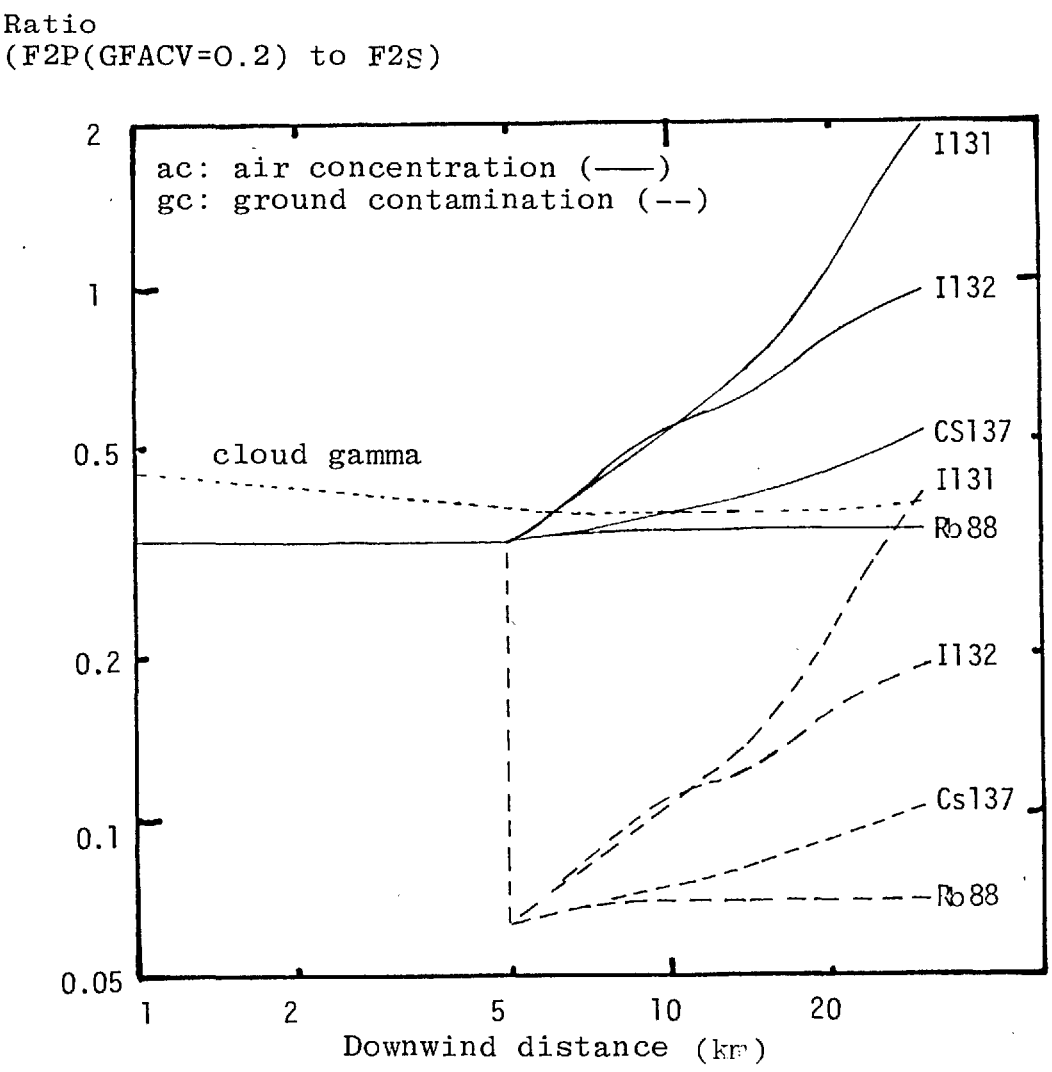

effectively trapped in the lungs and the dose patterns in the human body could be affected. It could be necessary to use a different set of dose per inhaled activity factors for materials with significantly different deposition properties, but this may not be justified given the expected accuracy of a gaussian dispersion model and other aspects of modelling radioactive releases.

Returning to figure 2.5 the greatest relative increase in air concentrations can be expected for the iodine isotopes and I131 in particular, given the properties of its precursors as described earlier. For I131 cloud dosage a factor of almost seven increase is produced by the lower deposition velocity between 5km and 30km. The I131 relative ground contamination is immediately reduced at the transition by GFACV but by 30km is above the relative level at x_c due to the comparative lack of depletion. A similar effect is produced for I132 ratios, but to a lesser extent due to the significant contributions by in-plume decays of Te132. The relative differences in the depletion of Te132 are less than those of I131 due to the lower deposition velocity given to tellurium in the element dependent deposition model. These increases help to reverse the decrease in the numerical estimate of the cloud gamma exposure due to the differences in the lateral dispersion parameters.

In the case of Cs137 the relative difference due to the decrease in deposition velocity beyond the transition is less than for iodine isotopes, due to a lower deposition velocity producing proportionately less depletion. The relative reduction in the ground contamination would be reflected in a decrease of the long term external gamma exposures, but this topic is better dealt with in the next chapter.

Rubidium-88 air concentrations show the least relative change from the particular use of this change of meteorology and the GFACV value. Again the non-depositing characteristics assumed for this isotope's main precursor, Kr88, are important. The slight change is due to the lower deposition rate of Rb88 producing a small percentage change in the relative value of $Q^{x}_{X',\ n,n-1}$ which is close to unity due to the short half life (18 minutes) of this daughter isotope. There is a small transition region between 5 km and 10 km before the mean steady state arises, where Rb88 could be expected to travel about 2 km on average before decaying.

This particular example under stable conditions highlights possible effects due to the nature of the plume material changing with downwind travel.

Section 2.5 Summary of improvements to the depletion routines in the WEERIE code

The incorporation of a grouped element dependent deposition model allows a more accurate description of ground contamination to be made, within the limitations of the gaussian plume dispersion model and the source depletion scheme. The improvements also result in better estimates of airborne concentrations and related consequences. The model enables detailed effects of the depletion process on daughter nuclides to be observed. Additional meteorological features, of which washout is potentially the most important, can allow a wider ranger of accident consequences to be modelled. Although some of these new features may be a crude representation of the real atmospheric processes their use should give valuable experience in attempts to quantify particular situations. The greatest uncertainty in any depletion model, for a given dispersion shceme, is still the values allocated to dry and wet deposition rates.

Having produced an improved set of dispersion and depletion models the significant consequences of ground contamination can be more fully studied. The next chapter deals with the application of methods to estimate external gamma and beta exposures from this contamination.

C H A P T E R T H R E E

Estimation of external exposures from deposited fission products

Section 3.1 Some general comments on the importance of ground contamination

Ground contamination has been recognized as one of the major consequences of an accident in a nuclear reactor which leads to radioactivity dispersing in the atmosphere (A.E.O. 1957 (54), (44)).

This has led to the fixing, in the UK, of Derived Emergency Reference Levels (DERL's) for ground contaminated by several radioisotopes (Baverstock and Vennart 1976 (55)). Complicated models have been developed to estimate doses resulting from contaminated foodstuffs. This problem involves many factors beyond the dispersion of material in the atmosphere (8). The only reference made to potential food-chain doses will be in terms of the appropriate DERL's for the UK.

Direct external exposures from radioactive ground contamination have been shown to be significant in producing early fatalities in major postulated accidents, under a restricted range of conditions((44), (6), McGrath et al. 1977 (56)). Long-term exposure rates result from any deposited nuclides which have half-lives of many years. The original form of the WEERIE code did not contain routines to estimate these direct exposures. With the improved depletion and dispersion routines, described in Chapter two, an adequate source term for these calculations is now available.

A consideration of the properties of beta and gamma radiations can aid in the selection and development of appropriate routines to estimate exposures from the deposited material. The short range of low energy beta rays in dry air, at STP, suggests that these exposures could be accurately estimated from the contamination in the immediate vicinity of the point of interest. Gamma rays of most energies have much larger ranges in air than beta rays, typically of order 100 metres, so that a large portion of the ground deposit probably has to be considered in any reasonable estimate of these gamma exposures. This would involve integrating contributions from a source, derived from a gaussian plume, varying in strength in two

dimensions, so that a numerical routine would be required to cope with this problem.

In WEERIE cloud gamma exposures are calculated from grouped gamma ray energies with energy deposition build-up factors. The total exposure is summed over gross contributions from point sources distributed within the plume rather than any more detailed method explicitly modelling energy degradation of photons after scattering processes from corresponding sample points. The gamma exposures from ground deposits can be expected to be greatly influenced by the scattering and absorption properties of the ground, whereas this effect is not always so significant in the case of cloud exposures. To make full use of the data already stored in WEERIE a similar type of estimate can be used for these ground gamma exposures.

Other schemes are available (Chapter 7 of (45), chapter 4 of Jaeger 1968 (57)) but have limitations. For example the estimates due to Gamertsfeller (quoted in (45)) model the cross-wind gaussian distribution but do not allow for changes of dispersion parameters with downwind distance. Also a crude estimate of the effects of the ground has been made in this particular method, where half the emitted photons, at all positions relative to the receptor, are assumed to be lost in the ground, so neglecting the effects of scattering out of the ground. In addition this method would require a large storage space for essential extra information, in the form of the values of integrals. A discussion of the advantages and disadvantages of a point source build-up model is given in the appropriate sections of Appendix A and this chapter.

Section 3.2 Estimation of gamma exposures from ground contamination

As a first step in the development of a numerical routine to estimate ground gamma exposures the case of an infinite uniform deposit on a smooth plane is considered, as discussed in Appendix A. The routine derived from these basic considerations has to be converted to a form suitable for the calculations required in WEERIE.

The original WEERIE code had routines which predicted, numerically, the exposure due to the passing cloud of radionuclides. A numerical estimate of ground gamma exposure rates can utilise some of the routines within the original WEERIE provded appropriate modifications are made. These modifications, and their implications on the use of computer resources, are discussed in the following paragraphs.

Section 3.2.1 Source terms for the gamma calculations

Numerical gamma calculations require the source of photons to be determined for every cell of a sampling grid which models the distribution of the deposited material. In WEERIE the amounts of released isotopes are stored in an array, P(150,6), and the gamma ray source spectrum is modelled in twelve energy groups proposed by Sidebotham (see Appendix A)(58), so leading to a source term, S(12), at any given point summed over many hundred isotopes for each energy group.

The above procedure was recognized as being too expensive to be repeated for every point source in a numerical cloud gamma calculation (13). This led to the formation of a grid of sixteen downwind source terms which were only affected by travel, and in the modified model also by depletion. Interpolation between two of these travel grid points could be used to define the source term for each energy group at any given downwind distance x.

The downwind travel grid positions were defined as having travel times, (3.1) $t_n=e((n-1).0.72)$ seconds, leading to positions, (3.2) $x_n=\bar{u}.e((n-1).0.72)$ metres. For a windspeed of $2m.s^{-1}$ the sixteenth grid point was about 100km downwind, at the limit of the paramet-risation of the gaussian dispersion model in WEERIE. At greater windspeeds these grid points were separated by greater distances than at low windspeeds and also the last point was beyond the limit of the dispersion model. To correct this situation, and reduce errors in the interpolation of the gamma source strengths, the travel grid points were redefined as (3.3) $t_n=e((n-1).Dt)$ seconds and (3.4) $x_n=\bar{u}.t_n$ where $Dt=(\ln(100000.0/\bar{u}))/15.0$. This locates all the source gamma travel grid points within the region where the dispersion model is explicitly defined.

Once this source term has been found for a given plume sample point, x metres downwind, the appropriate dispersion factor can be applied for lateral and vertical dispersion. This value is then used in a gaussian quadrature procedure to estimate the cloud gamma exposure. Up to N^3 sample points (N_{max}=9) can be used in this three dimensional integration. For on-axis points (y=0) all N^3 points are located on one side of the plume to increase accuracy: the result being multiplied by two, using the symmetry of the ideal plume.

To calculate the ground gamma exposure the only further modification needed to the routine defining the travel grid for source terms in each energy group is that the effective deposition velocity has to be applied to represent the ground contamination. Afterwards the appropriate dispersion factor can be applied, as before, to produce the source term assumed to represent a particular cartesian grid cell in the numerical routine for estimating the ground gamma exposure rate.

Some calculational advantages can be taken from the cartesian integration grid with one axis parallel to that of the plume. In this method for ground gamma calculations all the crosswind grid cells at one downwind distance have the same source term interpolated from the travel grid values. For all these crosswind cells the point source strengths can be derived by applying the gaussian function for one value of each of the lateral and vertical dispersion parameters. A polar coordinate system centred on the receptor would have cells each with different downwind distances, requiring the source strengths and dispersion factors to be recalculated many hundred times more than for the cartesian grid (see Appendix A). This saving in the number of interpolations is of order (n^2-n), where n is the number of cell divisions on one cartesian axis, and n=28 for the complete square cartesian grid.

Again symmetry of the deposit left by the plume can be used to simplify the calculations. For off-axis points the full 28x28 grid is used. When the receptor point is in the vertical plane including the axis of the plume only one half of the plume deposit needs to be integrated over to derive the total exposure rate. As the routine should give reasonably accurate results

for half the grid, 28x14 (downwind by crosswind), a saving in time can be produced for this ground gamma calculation, rather than the increase in accuracy chosen by the authors of WEERIE for the numerical cloud gamma estimate.

The general accuracy of this routine when representing the deposit from a gaussian plume depends on the relationship between the characteristic dimensions of the plume and that of the grid. The routine will lose some of its accuracy as the dispersion parameters decrease to less than the size of the grid cell dimensions. This applies to receptor points close to the source of a ground level release where the dispersion parameters are smallest, particularly if no building entrainment is modelled (which effectively broadens the plume) or stable conditions are assumed. As the smallest grid cells close to the receptor have dimensions of only several metres any error from this effect should not extend to any great distance along the axis of the plume, at most a few hundred metres under stable conditions for a ground level release.

Another situation where the accuracy of the model is reduced occurs for a receptor point well removed from the axis of a plume which is narrow compared to the cell dimensions at the extreme of the cartesian grid. The plume would be effectively represented as a line with a source strength depending on downwind distance. Systematic underestimation could occur if only one line of large grid cells covered the width of the plume, where the point sources at the cell mid-points would not generally coincide with the peak of the ground contamination. Again this effect would be most noticeable very close to a point ground level release of radioactivity.

Some method must be provided by which these conditions can be recognized without requiring detailed inspection of the numerical ground gamma calculation. As with the cloud gamma calculations this can be achieved by using an approximation based on the local activity. The method employed is described in the following section.

Section 3.2.2 Local approximation to the ground gamma exposure rate

The simplest exposure rate approximation relying only on local contamination levels is to assume these deposits extend

uniformly over an infinite smooth plane. This ignores all plume dependencies beyond those determining the local contamination. Using a Monte Carlo method French (1965 (59)) tabulated the direct and scattered dose rates from uniform gamma emitting sources (1 photon per cm^2 per second) on a smooth infinite plane for source photon energies ranging from 0.1MeV to 3.5MeV. Simple interpolation could be used to derive the results appropriate to the Sidebotham energies within this range. To derive values for the three Sidebotham groups with mean photon energies higher than 3.5MeV a more complicated procedure was undertaken.

Each of the tabulated sets of direct and total exposure rates per unit uniform surface contamination has been approxmated by a fitted function, for E>0.25 MeV, of the form below:
(3.5) $\dot{D}(E)=C+B(A.\exp(-E')+(1-A).\exp(-E'))$, where E'=E-0.25 MeV and the values were normalised to the direct rate for source photons at E=0.25 MeV. This process enabled values of the exposure rate for source photons of high energies to be estimated and crosschecked against the results of an extrapolation of the graphs of direct and scattered flux, where this checking process can also be applied to lower energies. The difference between the sum of the estimated direct and scattered rates and that of the estimated total rate was less than 3% at all energies. This compares favourably with the error of about 10% associated with the basic set of values, derived by French, so no significant uncertainty was introduced by this procedure to extend the range of values.

These results due to French are for a receptor three feet above the uniformly contaminated ground, while the numerical routine uses one which is a metre above the ground. A correction factor for this effect was calculated at energies of 1.25 MeV and 0.67 MeV by the numerical routine with an appropriate modification. As the difference between both these factors was negligible it was assumed that no significant error would be introduced to total exposure rates from a mixed fission product deposit by applying this value to all the values at the twelve Sidebotham kernal energies.

Once the local gamma source term (GA(x,y,E)) at the point of interest (x,y) has been calculated these values derived from those of French (FR(E)), for the exposure rates from an infinite uniform smooth plane of contamination, can be applied to produce an estimate of this effect of local contamination. Hence a local value of the ground gamma exposure rate has been defined as (3.6) $G(x,y)=\phi(x,y)\sum_{i=1}^{12} GA(x,y,E_i).FR(E_i)$,

where $\phi(x,y)$ is the appropriate dispersion factor.

When the result of the numerical ground gamma routine in WEERIE deviates markedly from this local estimate the detailed distribution of material may have to be considered. Some examples are given in the following paragraphs.

Section 3.2.3 Comparison of numerical and local ground gamma exposure rate estimates

The MAGNOX release (Strachan and Goddard 1979 (60)) is used, as in Chapter two, to provide some simple examples of gross ground gamma estimates in this section. A three group element dependent deposition model is used, as before, where inert gases are not deposited from the plume while halogens are preferentially deposited relative to all other depositing elements.

Figure 3.1 shows the total ground gamma exposure rate forty hours after the formation of the deposit when this notional release was assumed to disperse under Pasquill-Smith category C weather conditions. The effects of building entrainment can be observed in both estimates up to about 200 metres from the source. Broadening of the plume at these short distances helps to reduce the difference between the local and numerical estimates, which does not exceed a factor of two beyond a few tens of metres. Another factor which tends to reduce this difference is that there are fewer high energy gamma emitters after progressively longer cooling periods, as these usually have relatively short half lives. This means that only the low energy photons contribute to the total exposure rate, where these have shorter mean free paths in air than, say, 3 MeV photons. Thus the low energy photons delivering an exposure at the given point of

Figure 3.1

Total ground gamma exposure rate from deposit 40 hours after formation due to notional MAGNOX release (slightly unstable conditions)

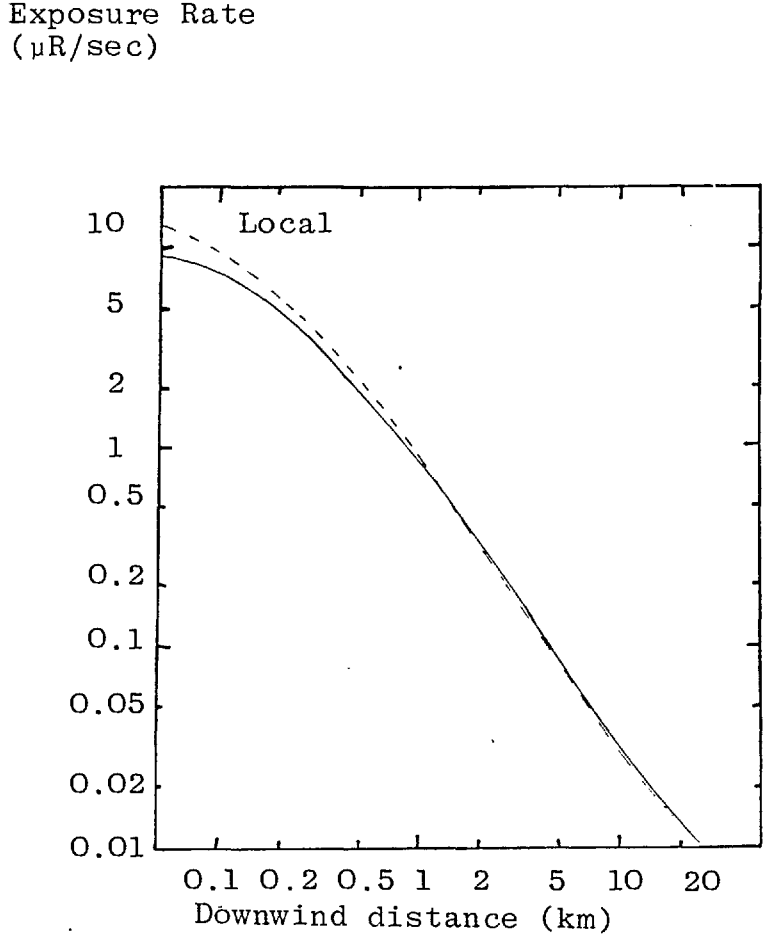

Figure 3.2

Initial total ground gamma exposure rate from deposit due to notional MAGNOX release (stable conditions)

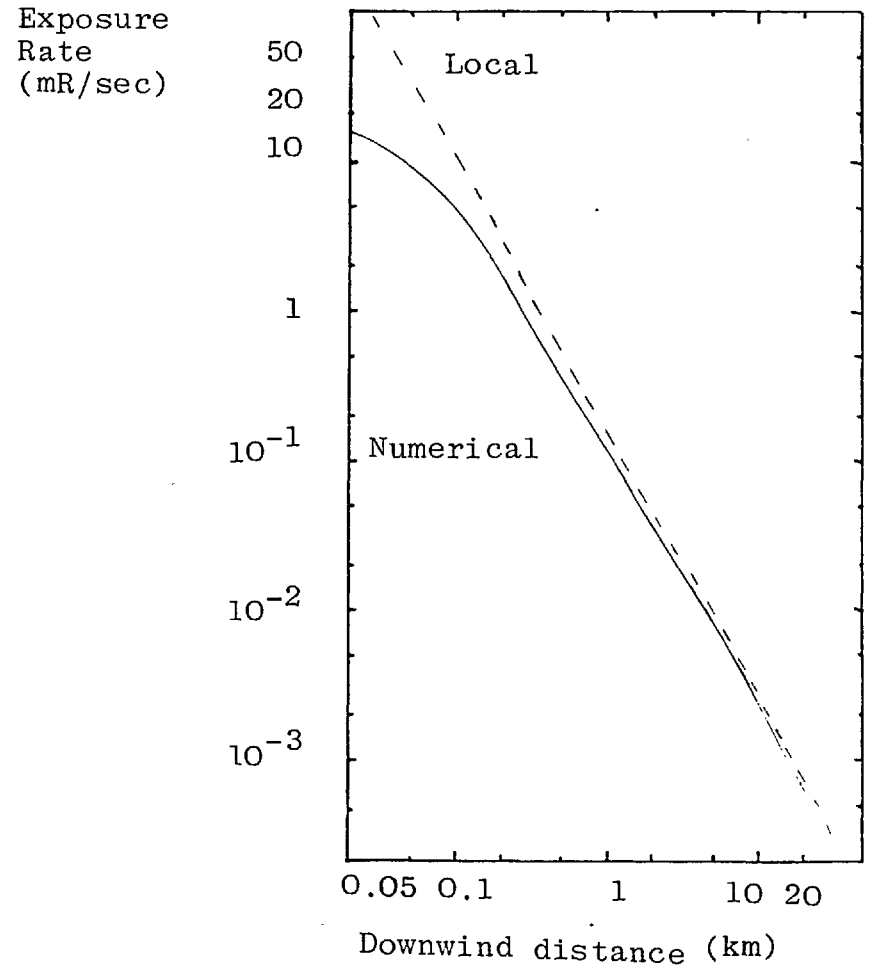

interest originate from a restricted area within the deposit. Within this area, which is smaller than for high energy photons, the contamination won't differ greatly from that at the exposure point so this should lessen any difference between the local and numerical estimates. Due to the large number of gamma emitting isotopes in the release the effect of high energy photon emitters is not of overriding importance as half the initial exposure rate is due to source photons of less than 1 MeV and the long term rate is due primarily to 0.66 MeV photons from $Cs137/Ba137^{m}$.

Using the same released activities but dispersing under stable Pasquill category F, low windspeed conditions the initial ground gamma exposure rate estimates on the axis of the plume can be plotted, as in figure 3.2. As can be observed from the local estimate of the ground gamma exposure rate no building entrainment has been assumed for this point source release at ground level. Even so the finite size of the plume is such that a difference of a factor of ten exists between the estimates at short ranges of a few tens of metres. A factor of two difference extends to over one hundred metres while agreement to within 10% is not reached until about 3 km, where the lateral dispersion parameter is about ninety metres. These short range differences emphasize the restricted size of the deposit which limits the total ground gamma exposure rates.

The total rate, on-axis 1 km downwind, has a contribution of 70% resulting from the first four energy groups (up to 1.28 MeV) and 90% by the first five groups (up to 1.88 MeV). About 45% of the total exposure rate comes from the third and fourth energy groups, spanning the range from 0.64MeV to 1.28MeV. This range coincides with the two energies at which the ground correction factors were available (see Appendix A), so a large portion of this exposure rate from mixed fission products is due to source photons of energies where these factors should be most appropriate.

It has been found that the on-axis cloud gamma numerical and local exposure estimates show greater differences than the corresponding ground gamma exposure rate estimates for a given release. This reflects the more restricted geometry of the

receptor one metre above a plane source of gamma rays rather than the much larger solid angles subtended at the receptor from volume sources contributing to cloud gamma exposures. When the plume has small dimensions the numerical cloud gamma estimates lose proportionately more critical source points than the numerical ground gamma exposures, so the former results are more sensitive to photons escaping from the finite plume. Examples of cloud gamma results are also given later in Chapter five, as well as in references (13), Macdonald et al 1973 (61) and (60).

The crosswind distribution of deposited material from a gaussian plume also results in differences between the local and numerical ground gamma exposure rate estimates. An example is given in figure 3.3 for slightly unstable dispersion conditions one kilometre downwind where the lateral dispersion parameter is 78 metres. Both estimates are in close agreement within the 10% limit of the deposit at this downwind distance but the trend of the numerical estimate is to be greater than that proportional to the local contamination. Within a couple of mean free paths of this 10% "boundary" the local estimate falls off rapidly with the gaussian distribution of ground contamination, while the numerical estimate shows a less rapid decline. Due to the limitations of the numerical sampling grid the exposure rates more than two mean free paths from the plume boundary may not be as well represented as at smaller crosswind distances, and become progressively less accurate out to four mean free paths.

This again shows that the ground gamma exposure is quite dependent on the local ground contamination, as expressed by the closeness of both estimates within the 10% plume limits. The numerical routine can be used to estimate the ground gamma exposure rates in the vicinity of the plume deposit, where dispersion is quite rapid so the limitations of this routine may not be critical in any study of this effect. The differences between the two crosswind estimates of external exposures at all downwind distances may be more significant, for irradiation of the public, than those for on-axis exposure rates at short distances which could be within a typical boundary fence or exclusion area.

Figure 3.3

Crosswind dependence of total ground gamma exposure rate, 40 hours after formation one kilometre, from deposit due to notional MAGNOX release (slightly unstable conditions)

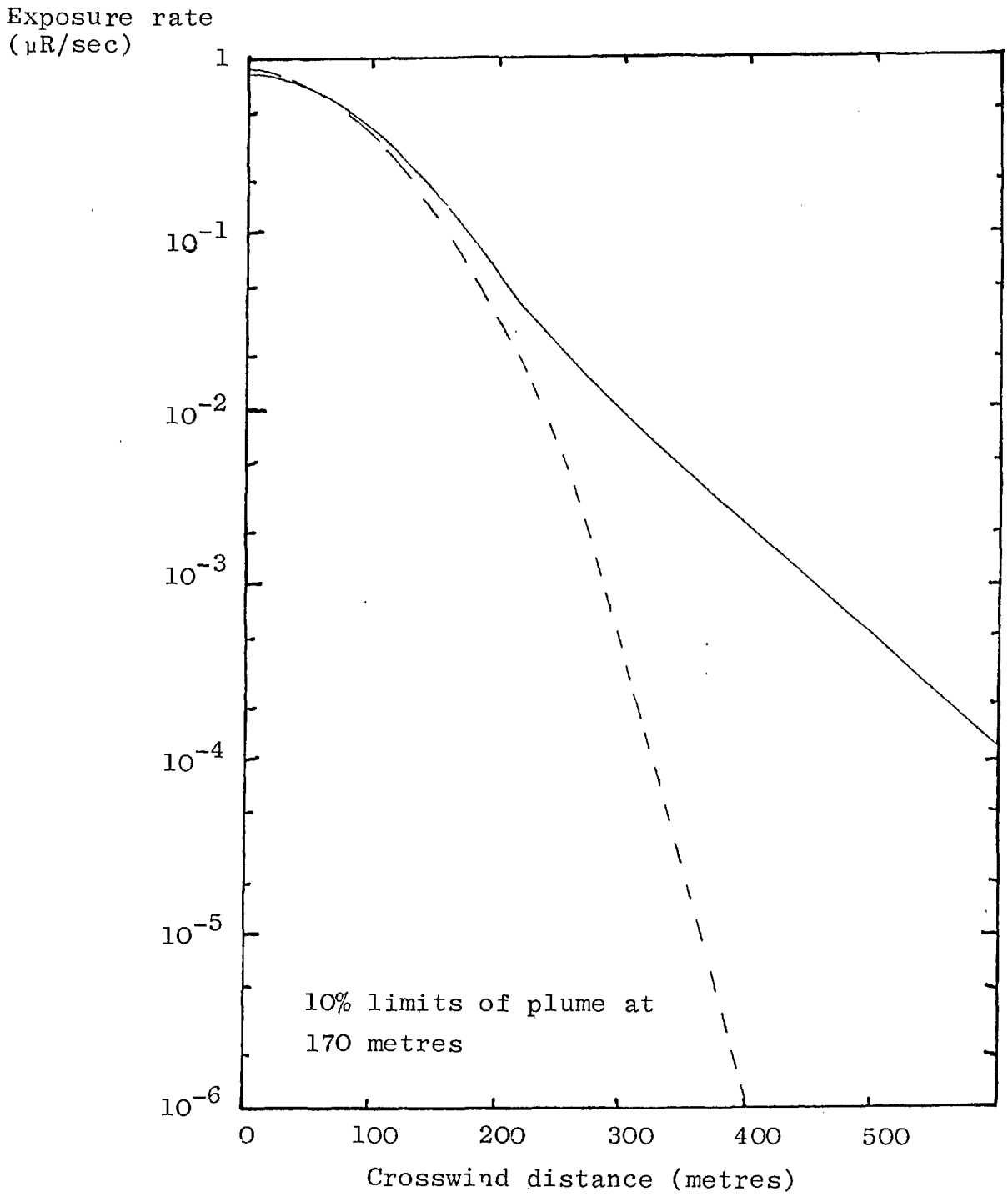

One of the effects of ageing the deposited material has been noted in this section but there are other potentially greater influences acting on this material in the real world. These are discussed briefly in the following section.

Section 3.3 Weathering and roughness effects on ground gamma exposure rates

Both weathering and ground roughness can reduce the exposure rates from contaminated land relative to estimates assuming smooth plane static deposits. Ground roughness is a simpler problem than weathering, as described in the next two sections.

Section 3.3.1 Ground roughness

The numerical routine developed for estimating ground gamma exposure rates assumes that the ground-air interface is smooth. For most land this is not the case, so any contamination of these areas would produce exposure rates different to these idealised estimates.

An important characteristic of a land area for ground gamma exposures is the roughness of the surface. Any gamma rays emitted from material in small depressions are least attenuated, or scattered, when travelling away from the main body of the ground, for a solid angle less than that for the smooth plane (2πster radians). This can further restrict the range at which ground contamination can significantly contribute to direct exposures, particularly where the receptor is close to the ground (Huddleston et al 1965 (62)). Rough ground can be expected to reduce the overall exposure rate from contaminated ground, due to the effective shielding by the roughness elements, where this will also affect the spectrum of incident photons at the receptor.

In this configuration the source no longer occupies a plane but has expanded to a volume source where the material will generally have a non-uniform distribution within each roughness element. This different type of source would require much more detailed analysis to enable an accurate estimate of the exposure rate from the gamma emitting contamination to be made. Local soil, vegetation and terrain would be important in producing a three dimensional source.

The results from a smooth plane model can be modified to approximate the effects of ground roughness on the total ground gamma exposure rate. Two methods of achieving this approximation have been considered ((62), Corbett 1977 (63)).

The simpler assumption to allow for ground roughness is to apply an overall reduction factor (R_g). This can modify directly the final results of a smooth plane estimated exposure rate, for one source energy or all energies. For an effective infinite uniform rough plane source of monoenergetic gamma emitting material this factor can range from 0.3 to 0.8. A typical value of 0.5 could be used to represent the effects of rough ground. The gamma spectrum from a mixed fission procut deposit tends to have a mean energy of about 1 MeV so the above factors could be applied without any great errors. Where the amount of deposited material varies rapidly in a short distance a different factor may be necessary, dependent on the particular spatial relationship between the deposit, the ground roughness and the exposure point.

Another method to modify the results of a smooth plane estimate is to insert an extra layer of air (of thickness d metres) between the surface sources and the receptor point. This attempts to model the additional absorption and scattering produced by a rough surface. The basic equations described in Appendix A are altered, as the slant distance from the point source to the receptor becomes,

(3.7) $r_n=(\rho_n^2+(1+d)^2)^{\frac{1}{2}}$ metres, so changing the contributions from all grid cells. The ground correction factors could also be altered to match the new height of the receptor. As the recommended values of the extra thickness of air are in a range about 14m, corresponding to rough desert terrain ((62),(57) after Clifford (64)), the receptor remains within 0.2 mean free paths of the surface, so that no changes in the cartesian grid would be required if this method was implemented.

This effect could be used to take account of conditions in the locality of a site for assessing these external exposure rates, or just as a general reduction factor. The interactions of gamma rays with buildings and other artifacts is another topic

which is important in estimating the consequences of contamination, but is a separate field of study for civil defence purposes (57).

Section 3.3.2 Weathering effects

The weathering experienced by radioactive contamination in the terrestial environment is a much broader scientific problem than the effects of ground roughness on ground gamma exposure rates. Many processes produce the effects of weathering including:

i) Resuspension of deposited material;
ii) Soil erosion processes;
iii) Leaching from the soil;
iv) Seasonal biological activity in the soil.

The chemical nature of the deposited isotopes can be a critical factor for the rate at which weathering occurs. Caesium-137 contamination from fall-out has been studied (Bryant 1966 (65)) and curves showing the weathering effects have been produced (Griffiths et al 1978 (66)). Generally a rapid decline in the external gamma exposure rate occurs in the first few years to about 30% of the original value, after which a much slower decrease occurs over several decades. This is produced by this radioisotope being removed from the locality of the deposit and being redistributed within the top soil layers. After about two years the remaining Cs-137 tends to become fixed in the soil, producing a steady level of external exposure. Formulae have been devised to model these effects on external exposures, where no significant differences were found between soils contaminated by Cs137 in carbonate form ((67) quoted in (63)).

The redistribution of activity to below the surface will provide extra shielding to individuals close to the contamination. Again, as for the effects of ground roughness, a volume source would be required to more accurately describe external exposures after the effects of weathering. Many other dose pathways are affected by weathering, in particular food chain doses, inhalation doses from resuspended activity (potentially important for decontamination work (Anspaugh et al 1975 (68), (6)) and those arising from waterborne activity. Any simple

weathering model reducing the deposited activity to match the lessening of external exposures with time could be misleading if other dose pathways were also considered which were dependent on this contamination.

To model the effects of weathering would introduce many considerations beyond the scope of the aim to develop a code which can describe the immediate impact of activity released to the atmosphere. Neglecting weathering would result in the external exposure rates being pessimistically large in the region about the deposit. For this reason the external exposures from deposits of mixed fission products are not studied here beyond one year's ageing, where these should be treated as gross upper limits by the end of this period.

Section 3.4 External beta exposures from ground contamination

The short range of beta particles in air allows a dose rate from ground contamination to be calculated solely from a knowledge of the local beta sources. The scattering and absorption mechanisms for the charged beta particles are very different from those of uncharged high energy photons. Some general comments on beta doses will be made explaining the choice of one particular method suitable for WEERIE, where this specific method is described in greater detail in Appendix B.

Section 3.4.1 General comments on external beta doses

The nuclear decay process by which beta particles are emitted from nuclides can produce an electron or a positron, depending on the characteristics of the decay scheme. These charged particles are the same as, or the antiparticles of, those electrons bound to atoms which produce the main scattering effects when beta rays lose energy in normal matter.

Monoenergetic beta particles tend to have one range in a given homogeneous medium. Most of the initial energy is lost in the first half of the range. In later stages of the slowing down process the beta particles can have very erratic paths due to scattering with atomic electrons of equal mass. This results in "straggling" being observed close to the end of the range of beta rays.

As beta particles initially deposit energy quite rapidly emitters external to a body can be expected to produce primarily a surface dose. The human skin can vary in thickness from 3 mg/cm^2 to 100 mg/cm^2 over the whole body. For beta particles of energy about 1 MeV these thick regions can provide a large degree of shielding for internal organs and tissues. Clothing can provide a significant shielding effect from external beta emitters, but its contamination can cause problems.

High energy beta particles, of more than say 10 MeV, have much larger ranges in air, 10's of metres, than 1 MeV electrons which penetrate about one metre. These high energy particles lose energy primarily by Bremsstrahlung, so extending the range over which beta decay energy is deposited. This effect starts to become important for beta energies of at least 3 MeV (Enge. 1966 (69), Cross 1968 (70)), so tends to impose an upper limit for many attempts to describe energy deposition by nuclear beta rays. The application of these methods to doses received from fission product beta decays is not unduly restricted, because it is rare for long lived isotopes, of at least a few days half life, to have beta decay energies above this limit.

The transport of monoenergetic, monodirectional electrons in one homogeneous medium was theoretically described by Spencer (1955) (71) using a moments method combined with asymptotic properties to describe deep penetration. The electrons were not assumed to cross any boundaries in this study. Comparison of these theoretical results to experiment showed good agreement up to energies of about 2 MeV, although at very low energies the predictions are also expected not to be very accurate. Straggling effects can pose problems for this method at large penetrations (see Zerby and Keller 1967 (72)).

When fission products decay by either allowed or forbidden beta transitions normally three particles result, namely the nucleus, the beta particle and a neutrino. The nucleus has a recoil energy which is lost rapidly in a very short distance but its electron structure is excited, due to the change of nuclear charge, so it can produce X-rays. These X-rays can deposit significant energy within the range of the beta particles, so adding to the external doses. This effect can cause

some difficulties when making detailed measurements of beta rays' energy deposition. The neutrino effectively does not interact with matter in a distance as small as the range of beta rays, so can be neglected from dose assessments, but as it is a third particle it shares the decay energy and conserves both linear and angular momentum. This results in the beta particles from this decay process having a continuous range of energy from zero to a maximum, E_o. The probability distribution of electrons having a particular measured energy within this range is dependent on the type of nuclear transition occurring (69).

To represent the energy deposition for the whole beta particle energy spectrum from nuclear beta decays in terms of a set of values for monoenergetic electrons would require an integration procedure. A detailed mesh of energies would have to be used to produce results of acceptable accuracy. Extensive interpolation of Spencer's tabulated results would be required to obtain good integrals over each beta spectrum (70). To duplicate the moments method would require a significant expenditure of calculational time.

As beta particles from fission products are expected to produce doses primarily to the skin, where this tissue is not very sensitive to this LET irradiation, the detail necessary to apply Spencer's work may not be justified in the WEERIE code. Methods have been developed to predict beta energy deposition in media with less detailed information requirements. Differences have been noted for energy deposition between gases and solids as well as for different source geometries, such as plane and point (Loevinger 1956 (73), Cross 1967 (74), 1969 (75)), although these differences were not great and occurred mainly at short ranges.

The particular case of a uniform, infinite, smooth plane source of beta emitters depositing energy in dry air has been considered by Loevinger (1955 (76), 1956 (73)). This can be applied to the beta dose rate one metre above a deposit of mixed fission products. Details of this method, along with a discussion of its limitations, are given in Appendix B. A few brief comments on the results derived from this method follow in the next section.

Section 3.4.2 Use of Loevinger's formula for beta dose rates

Loevinger derived empirical formulae for dose rates from point beta sources and extended these to deal with plane sources. These latter results can be applied for external ground beta dose rate estimates in the modified WEERIE code, as only the mean beta decay energy and the height of the receptor above the plane need to be specified (see Appendix B). The former quantities are already in a library of this code, for cloud beta dose estimates, and the latter parameter can be fixed for one metre of dry air at STP.

This metre of air severely attenuates beta rays with initial peak energies below 0.5 MeV, which covers a wide range of fission products. This effect is not modelled in cloud beta dose estimates, so beta to gamma ratios from deposited material measured one metre above the ground may show detailed differences to corresponding ratios for estimates of external doses and exposures from the cloud.

This scheme uses one effective attenuation coefficient for the whole beta spectrum of a given nuclide. This assumption is only a good approximation for peak beta energies in the range 0.5 MeV to 5 MeV and where energy deposition occurs in a light (low Z) medium. The ground air interface and the significant beta ray emitters among the fission products in this application of Loevinger's formula fall within the range of validity.

The comments of a previous section in this chapter on the effects of ground roughness and weathering are of importance to ground beta external dose rates. The ground roughness effects could be very significant for these short range beta rays. Hence the results of this method should only be used as an indication of general levels of external beta dose rates from fission products deposited on the ground in the track of a plume.

Section 3.5 Examples of external ground exposures in the modified models of WEERIE

This section will display some of the differences produced by using a three group or one group dry deposition model. The MAGNOX release is again the source term for the airborne material.

Section 3.5.1 Ground gamma exposure rates one metre above the deposit

The dry deposition velocities used in this section are the same as in section 2.4.1 for the one and three group depletion models. Some general points can be made before detailed examples are given.

The majority of the released activity is assumed to be in aerosol form, so has the same treatment in both deposition models. Caesium-137 falls into this category so the long term external ground gamma exposure rates predicted by both models is the same. Hence any differences due to the three group model, enhancing halogen contamination and modelling non-deposition of inert gases, relative to the single overall group model, at short downwind distances under all weather conditions, will only be observed for times characteristic of those isotopes which contribute significantly to external ground gamma exposures. The radioactive decay process can be such that the two models diverge for short cooling times, of several days (60).

The greatest differences between the two models can be expected for stable low windspeed conditions. Figure 3.4 gives the distance dependence of the on-axis total initial ground gamma exposure rate for both models under these conditions. This shows that the simple one group model overestimates this exposure rate by 25% 1 km and 30 km downwind and by more than 33% at intermediate distances. Many factors determine this net difference where the particular deposition velocities, elemental release fractions and dispersion conditions are critical. Under these conditions the enhanced halogen deposition in the three group model does not compensate for the different treatment of inert gas deposition in the one group model.

Greater differences are observed in the exposure rates due to individual energy group sources. The initial grouped on-axis gamma exposure rate is shown in figures 3.5 and 3.6, accumulating with each higher energy group source, from the deposit at 1 km and 20 km downwind, respectively, under stable conditions. At one kilometre downwind the one group model has a much larger low energy exposure rate than the three group model, due to isotopes of xenon in the deposit. For the three gamma ray groups centred on energies from 0.76 MeV up to 1.55 MeV the three group model shows the effects of enhanced iodine deposition velocities,

Figure 3.4

Initial ground gamma exposure rates from notional MAGNOX release under stable conditions using single and element dependent dry deposition models.

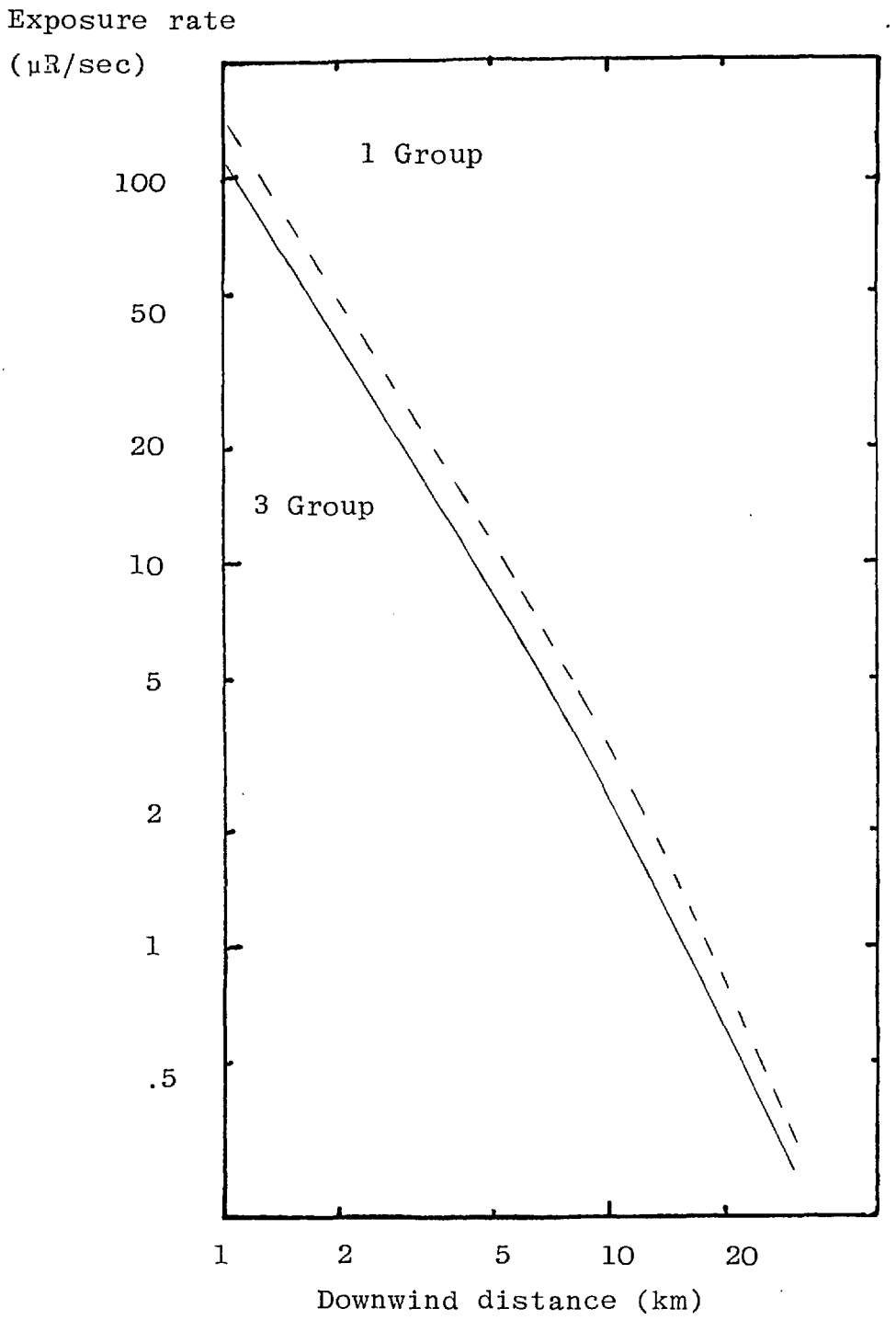

Figure 3.5

Single and three group deposition model predictions of initial ground gamma exposure rate accumulating with source photon energy groups for notional MAGNOX release 1 km downwind (stable conditions)

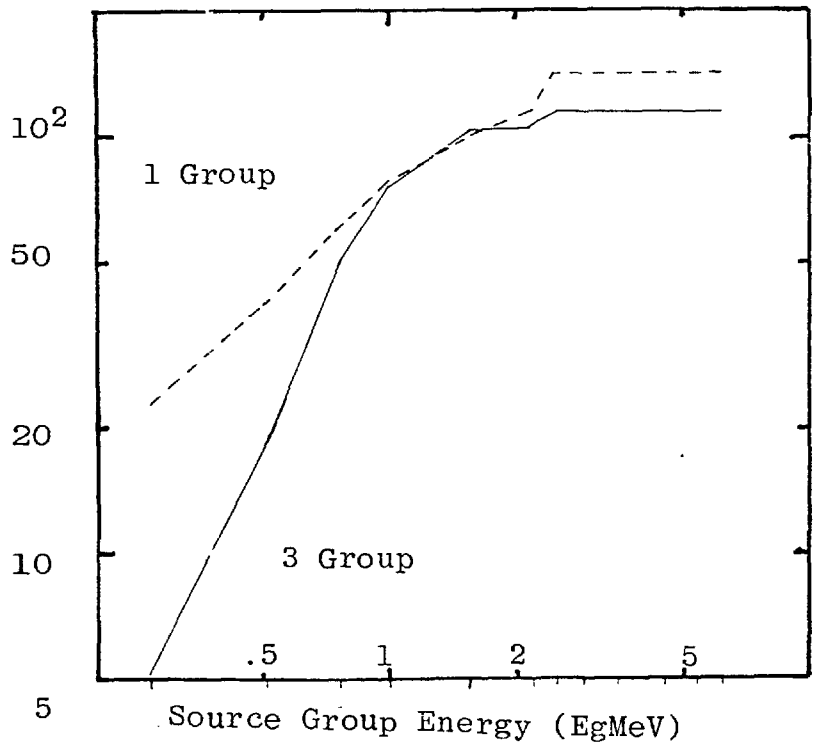

Figure 3.6

Single and three group deposition model predictions of initial ground gamma spectral exposure rate accumulating with source photon energy groups for notional MAGNOX release 20 km downwind (stable conditions)

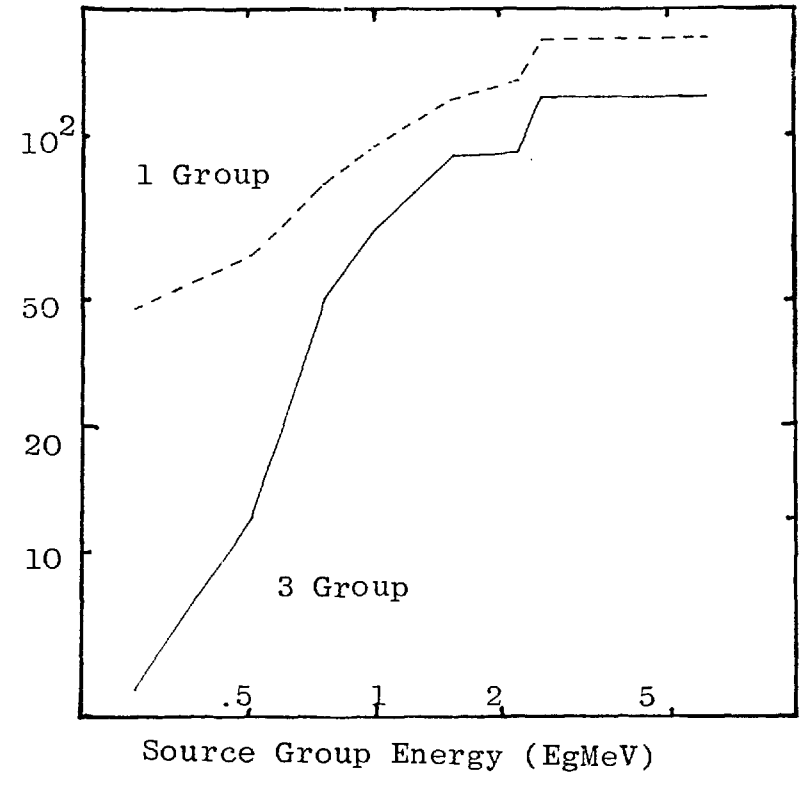

such that both models have very similar total exposure rates for energies up to about 1.0 MeV to 1.55 MeV. Higher energies again show the effects of inert gases depositing, primarily the isotope krypton-88, in the one group model.

Figure 3.6, for the ground gamma exposure rate 20 km downwind, shows curves of a similar form but the three group model is lower relative to the one group deposition model, due to the severe depletion of the rapidly depositing iodine isotopes which emit gamma rays significantly in the range 0.62 MeV to 1.88 MeV. Due to the non-deposition of Kr-88 in the three group model there is still a large contribution to the initial ground gamma exposure rate at 2.5 MeV from the short lived depositing daughter rubidium-88. This high energy peak in the initial source exposure spectrum will diminish with a half life of the decaying principal isotope, Kr88($t_{\frac{1}{2}}$=172 mins) for the one group model and Rb88($t_{\frac{1}{2}}$=18 mins) for the three group model, where there is a common background contribution from caesium-138 ($t_{\frac{1}{2}}$=33 mins). Although the size of this high energy contribution may not be critical for doses it could be used to guide diagnostic measurements attempting to identify a particular type of release.

Slightly unstable Pasquill-Smith category C dispersion conditions can lead to different relative values of the initial ground gamma exposure rate predicted by the two deposition models, where significant changes are also produced when the halogen release fraction is reduced from 10% to 1% (60). Figure 3.7 shows the initial on-axis ground gamma exposure rates under these more dispersive conditions.

As these high windspeed conditions, category C, do not produce any severe depletion from the plume, even for the enhanced iodine deposition velocities, the relative differences between the two models is constant. Here the three group deposition model predicts an initial ground gamma exposure rate about 25% greater than that from the one group deposition model. The importance of different dispersion conditions on depletion can be observed by this difference being opposite to that found under stable conditions (see figure 3.4). Under these slightly unstable conditions the depletion is so limited that the enhanced iodine deposition velocities more than compensate for

Figure 3.7

Initial ground gamma exposure rate from deposit downwind of ground level notional MAGNOX release (slightly unstable conditions)

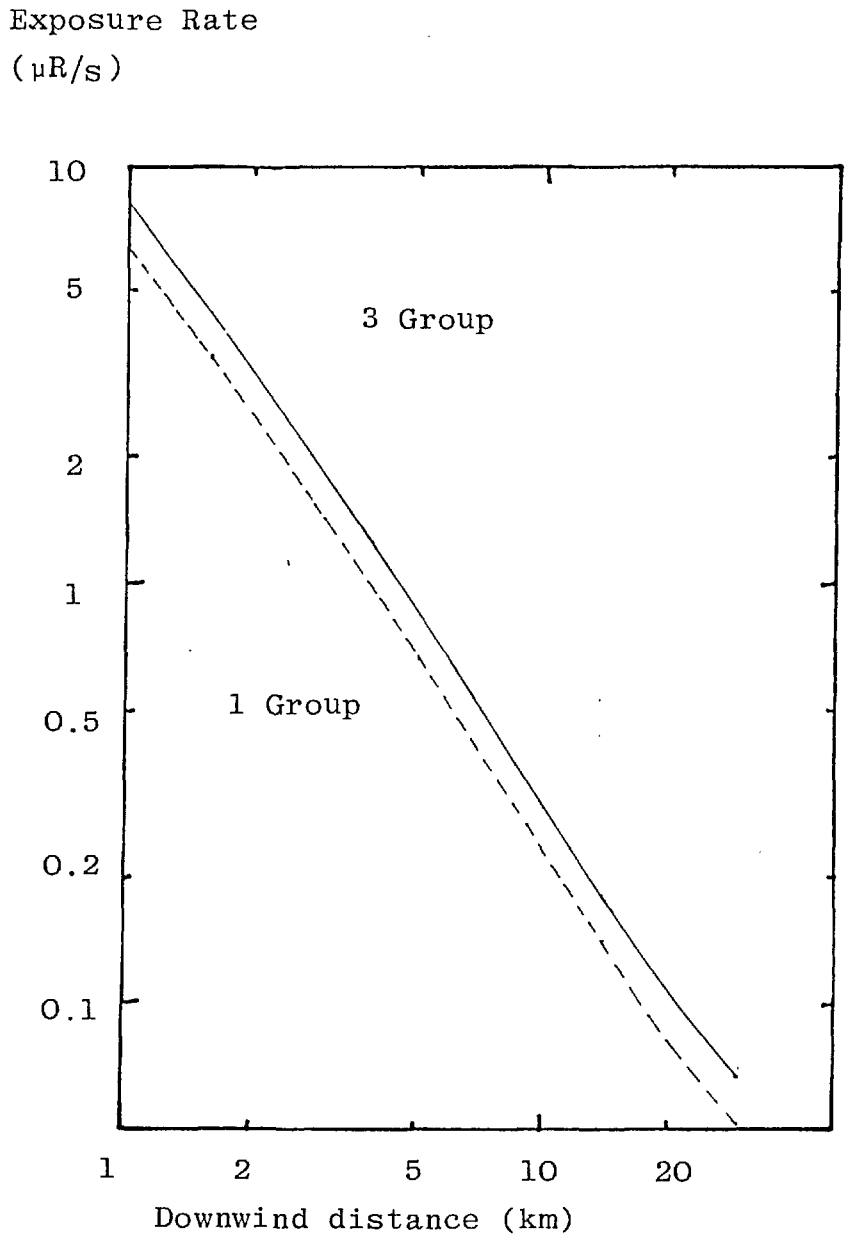

the negligible contamination in the element dependent deposition model by inert gases.

These two depletion models predict different ground contaminations and ground gamma exposure rates, so the total ground gamma exposure delivered by each deposit will differ for a given period depending on the type of release. The differences are in the treatment of inert gases and halogens, where the most significant gamma emitters in these groups decay within a month. After these particular isotopes have decayed both models will predict effectively the same long term exposure contributions, where these are derived from such elements as caesium and ruthenium which are not affected by the differences in the two models.

Section 3.5.2 Ground beta dose rates one metre above the deposit

Gross ground beta dose rates are discussed in this section, as details of the energy spectrum could not be described simply owing to the overlapping of the continuous beta spectra of the many isotopes involved in this MAGNOX release.

Long term ground beta dose rates, after attenuation by one metre in air, are the same in both dry deposition models as these are determined primarily by rhodium-106, the short lived daughter of ruthenium-106($t_{\frac{1}{2}}$=369 days). Shorter lived beta emitters which have relatively large beta decay energies include some isotopes of iodine, tellurium and caesium. The very long lived beta emitters, krypton-85 and tritium, have low decay energies, so neither make contributions when either dry deposition model is used in these examples.

The initial on-axis ground beta dose rates are shown in figure 3.8 for both deposition models, assuming the release occurs under stable low windspeed conditions. These curves show a relative difference dissimilar to the corresponding curves for the initial ground gamma exposure rate, shown in figure 3.4. In the case of initial ground beta dose rates the alkali metal isotopes Rb88 and Cs138 are both important contributors. A single overall deposition velocity approximately halves the inert gas concentrations by 30 km, where this affects the in-plume decays to these two isotopes as shown in Table 3.1. By ten kilometres downwind in the element dependent depletion model these effects exceed the ground beta contributions by inert

Figure 3.8

Single and three group dry deposition model predictions of initial on-axis ground gamma beta dose rate in air for a notional MAGNOX release (stable conditions).

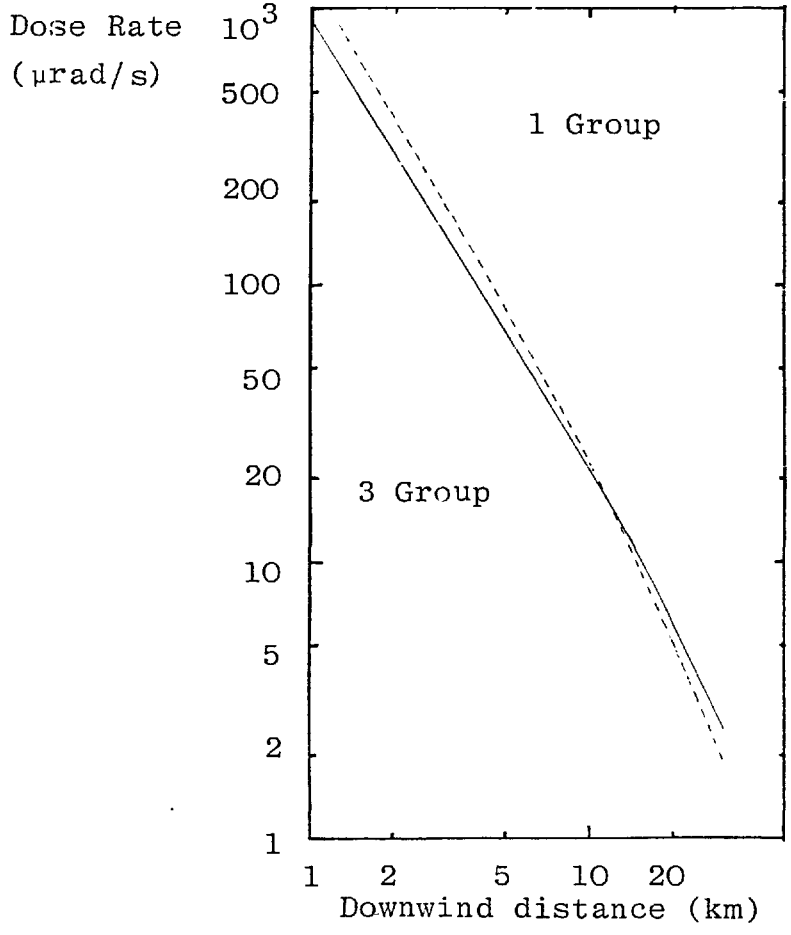

Figure 3.9

Single and three group dry deposition model predictions of initial on-axis ground beta dose rate in air for a notional MAGNOX release (slightly unstable conditions).

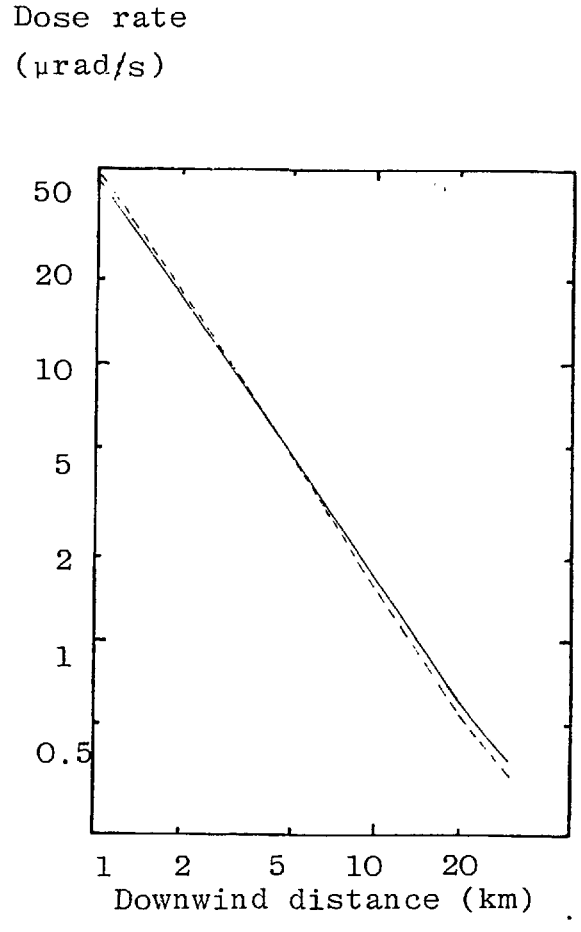

Table 3.1 Ratio of predicted ground contamination by the three group model relative to the one overall group depletion model.

Downwind distance (km)	RATIOS (3 group to 1 group)	
	Rubidium-88	Caesium-138
1	1.10	1.07
30	2.47	1.38

gases in the one group dry deposition model, so this total dose rate exceeds the predicted initial dose rate of the one group deposition model. A deficit of about 40% at short distances is reversed to a surplus of about 20% beyond 20 km. At these larger distances any iodine contributions are not significant in the three group deposition model due to the rapid depletion assumed for these isotopes.

The corresponding curves for dispersion under slightly unstable conditions are shown in figure 3.9. In this case depletion is only a minor effect within a few tens of kilometres, so that the initial ground contamination by Rb88 and Cs138 are not very dependent on the model used. Even so the trends of these two gross curves again show the influence of non-depositing behaviour assumed for inert gases in the three group model although the relative difference of about 10% by 30 km is probably similar to the uncertainties of using the Loevinger beta dose rate formula for a plane source of mixed fission products.

The gross ground beta dose rate predicted by each deposition model has a different dependence on the ageing time of the contamination, due to the different constituent isotopes. Figure 3.10 shows this effect for the MAGNOX release under slightly unstable conditions at an on-axis receptor point one kilometre downwind of the source. At short times after the deposit is formed the inert gases in the single overall depletion model increase the rate above that from the deposit of the three group model. This contribution starts to diminish and after seven hours does not compensate for the enhanced iodine contamination's beta decay energy in the three group deposition model. Finally after more than 30 days all iodine isotopes

Figure 3.10 Effects of radioactive decay on predicted on-axis ground beta dose rate from single and three group dry deposition models, 1 km downwind of a notional MAGNOX release (slightly unstable conditions)

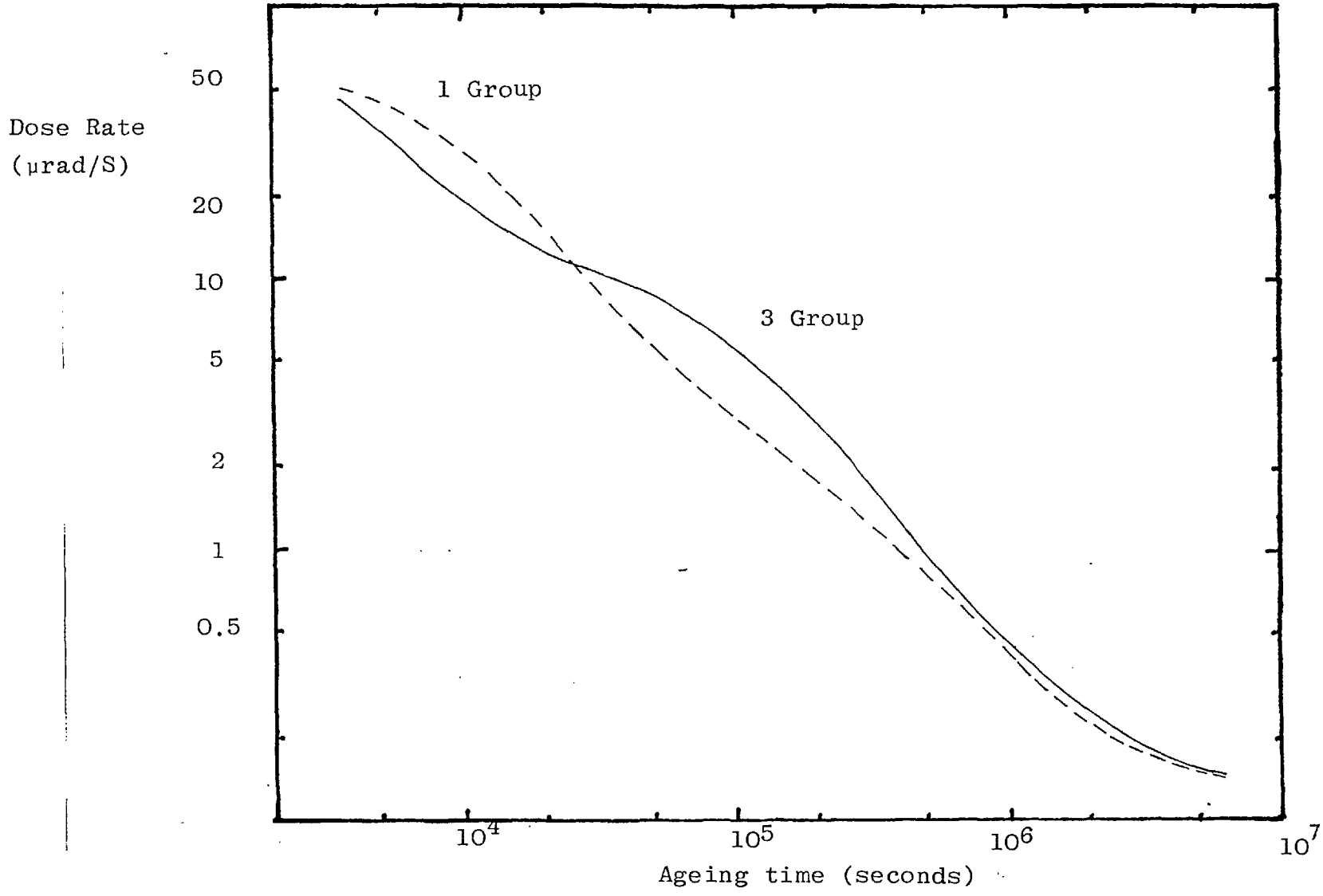

have decayed, so the ground beta rates predicted by both models come into close agreement, as foreseen earlier in this section. After 35 days the three group depletion model predicts a total beta dose one metre above the deposit which is over 30% greater than the estimate derived from the one group deposition model. This contrasts with the differences between the early behaviour predicted by the two models, where the one group model estimates the beta dose rate after a few hours as being more than 25% in excess of that derived from the element dependent deposition model.

This emphasises that the use of different deposition models can have significant effects on the external exposure rates from ground contamination, which can change as the deposit ages, where a factor of two difference was observed in figure 3.10 after about a day.

Section 3.6 Summary and conclusions

It has proved possible to incorporate routines into the modified version of WEERIE to provide estimates of external ground gamma exposure and ground beta dose rates from the contamination modelled by the element dependent depletion scheme. This enables comparisons to be made to the corresponding cloud estimates. Further the decay process in the deposit enables more features of the improved dispersion and depletion routines to be observed.

The ground gamma calculations are performed in more detail than those for the beta estimates as external gamma exposures are usually radiologically more significant. Examples of these potential exposure routes will be given in Chapter five for a range of notional AGR accidents. The next chapter will deal with some of the problems of applying these potential doses and exposures in calculating collective quantities for real population distributions.

CHAPTER FOUR

COMMENTS ON THE USE OF THE POPULATION DATA FROM THE U.K. 1971 CENSUS

This chapter contains a brief description of the uses of census data in the assessment of population distributions about nuclear installations, or other sites. Attention will be given to the probable inaccuracies which can be associated with particular uses of this population data.

Section 4.1 Type of information available

The Office of Population Censuses and Surveys (OPCS) control the basic population data derived from the 1971 census in the UK. The information for Northern Ireland was compiled separately from that for England, Scotland and Wales. Also such islands as the Isle of Man and the Channel Islands were not included in data processed by OPCS.

The information provided by OPCS can be based on 100% or 10% samples. For the purposes of site assessment, or collective dose estimates, population totals can be used with appropriate factors for the separate groups about a site. The population totals are derived from a 100% sample of the basic units of a census. These units are the enumeration districts (ED's) which are areas covered by one census enumerator. ED boundaries are chosen by local authorities to aid planning and other decisions. The boundaries are usually easily recognised landmarks and define an area which does not normally encompass more than about 280 households in England and Wales. Hence the ED can have a very irregular shape and its size in rural and urban areas can be quite different. Often special ED's are defined for residential hospitals, prisons and bases of the armed forces, where these have no explicit boundaries.

Together many ED's comprise a Ward or Civil Parish (W/CP) in England and Wales and the latter units are listed within each Local Authority (LA), which was generally a county for the 1971 census. In Scotland there was a different local government structure and a lower general overall population level, where both these factors led to ED's of large physical size compared to those in England and Wales.

This population data has been converted by the OPCS into square grid cells in units of side 100km, 10km, 1km and 100 metres, as defined by the National Grid (NG), although the 100 metre data are not available for all parts of the country. The regular grid data produced by this method has different characteristics to those of the irregular ED or W/CP data. In an attempt to produce computer printed character maps of population distributions rectangular grids were defined from the W/CP and the 1 km data with sides in the same ratio as line-printer characters (41), (42).

Population totals refer to residents under the headings of private males, private females, non-private males and non-private females. The total number of households are also included in the data referred to as persons male, female and households (PMFH). From these subdivisions of the population gross totals of all residents in each census district can be derived. This information could often be adequate for assessing collective doses and associated risks (ICRP 26). More detailed assessments could be made by using the different dose-sensitivities of males and females. In a very detailed study a 10% sample of the census data might be used to represent the distribution of ages in a population about a given site. It may only be justified to use this specialised information for critical communities or other selected groups once a critical dose pathway has been found (ICRP 26, 27, 29).

The form of the census data is such that it lends itself to one particular mode of calculation of collective quantities. The gross population total for each ED and W/CP is provided along with the eight figure national grid reference of the weighted population centroid (to the SW corner of a 100 metre square). Hence integer arithmetic can be used on a digital computer to identify exactly the location of a census unit, which corresponds to a delta function representing the population regardless of the particular ED or W/CP boundaries and internal distribution of people. Similar information is provided for the regular grid forms of the population census data. An estimate of the accuracy of this use of the data is given in later sections of this chapter.

Population movements could be considered in site assessment. Both occupational movement beyond the boundaries of a census unit and net migration since the preceding census is available. The latter covers long term changes of residential population which could be updated each year with reasonable accuracy, in areas adjacent to a site, provided sufficient effort was devoted to this task. The former point is part of the more difficult problem of dealing with transient populations. This can be a very site dependent effect and could be critical during the peak season of a major holiday resort or during a large festival in one town. At present these short term transient populations have to be considered separately from residential populations (see chapter 6).

Residential census data is the prime source of population information for site assessments and its use will be discussed in detail in the following sections.

Section 4.2 Use of population data in the assessment of a whole site

Two population groups can be identified for each site, namely the surrounding population and a critical subset of this population. This section will deal with problems associated with using census data to assess the complete population distribution in all directions about a site. The problems associated with calculations involving a critical group through the use of a worst sector technique will be dealt with in a subsequent section.

Section 4.2.1 Definition of population distributions

As remarked earlier the population census data represents all the population for a unit as residing at one point: the population centroid of that area (ED or W/CP). The form of this data is such that population densities cannot be so readily used. This means that the relevant population distribution (P), where the site is taken as the origin of a cartesian coordinate system (x,y), can be represented by,

(4.1) $P(x,y)=\sum_{i=1}^{N} P_i . \delta(x-x_i, y-y_i)$, assuming there are N population centroids within the region (A) to be assessed and

(4.2) $\int_A \delta(x-x_i, y-y_i)dx.dy =$ 1 if A includes (x_i, y_i)
0 if A excludes (x_i, y_i).

Similar expressions can be given when a plane polar coordinate system is used.

Any collective quantity (Q) resulting from a weighting or dose function (W) for an area A in all directions about the site can be represented as;

(4.3) (a) $Q(A) = \int_{A} \sum_{i=1}^{N} W(x,y).P_i.\delta(x-x_i, y-y_i).dx.dy$, which reduces to

(4.3) (b) $Q(r_n) = \sum_{i=1}^{N} W(x_i, y_i).P_i = \sum_{i=1}^{N} Q_i$, for an area A where $x_i^2+y_i^2<r_n^2$. In the real world each term Q_i in the summation of equation 4.3.b would be better represented as below:

(4.4) $Q_i' = \sum_{j=1}^{N} P_{ij}.W(x_i+dx_j, y_i+dy_j)$, where dx_j and dy_j represent the distribution of population within the ith census area for the internal elements (P_{ij}) of the population P_i such that equation 4.5 holds, see figure 4.1. (4.5) $P_i = \sum_{j=1}^{NJ} P_{ij}$. The greatest detail of the physical distribution of the population group would be achieved when all P_{ij} were unity. If a detailed weighting function (W^{lk}) was to be used, depending on a gender l and an age group k of the population, then the total population in the ith area would have to be considered as:

(4.6) $P_i = \sum_{j=1}^{N^j} \left(\sum_{l=1}^{N^l} \sum_{k=1}^{N^k} P_{ij}^{lk}\right) = \sum_{l=1}^{N^l} \sum_{k=1}^{N^k} P_i^{lk}$

The corresponding elements of the collective quantity Q_i would be represented by:

(4.7) $Q_i = \sum_{l=1}^{N^l} \sum_{k=1}^{N^k} W(x_i, y_i).P_i^{lk}$, substituting equation 4.6 into equation 4.3(b). Further detailed breakdowns for particular organ dose commitments can be described (UNSCEAR, 1977).

The elements in the equations 4.3 and 4.7 are implicitly averaged over the ith census unit. The following discussion is to assess the accuracy associated with these terms when used in computer based routines which calculate collective quantities from the 1971 census data. Two classes of population data are used namely irregularly shaped ED and W/CP units and regular grid cells.

Figure 4.1 Diagram of the scatter of population elements of an irregular census unit about the weighted centroid

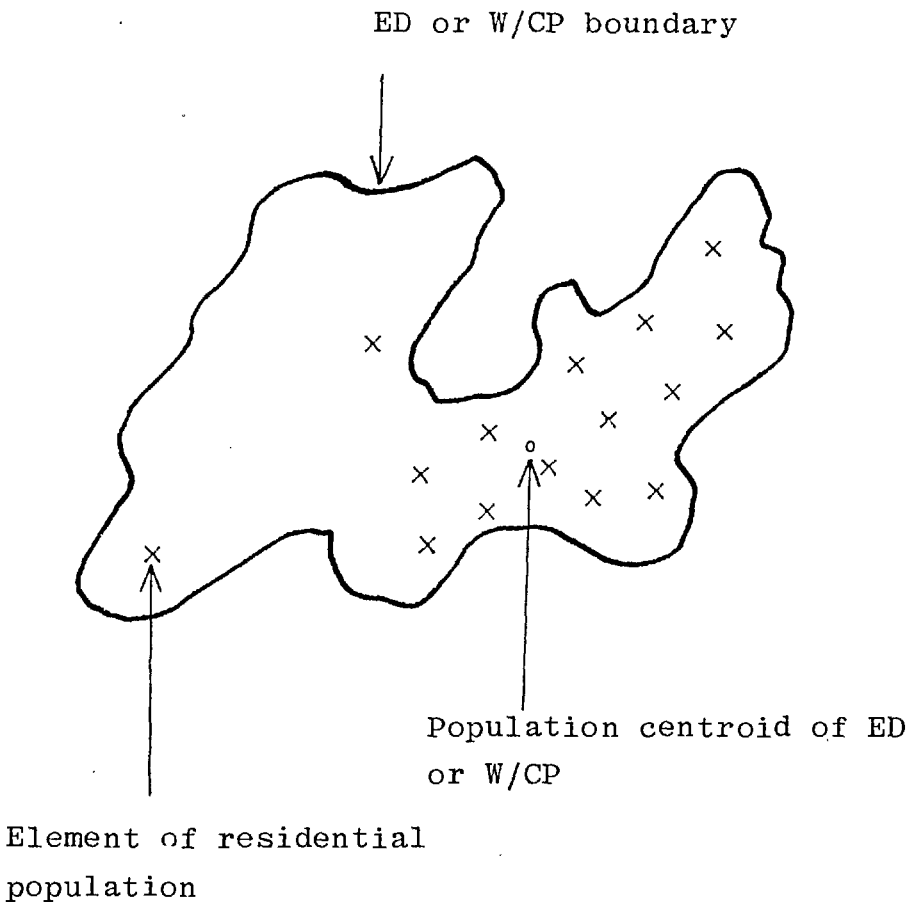

Section 4.2.2 Properties of irregular census units

The two census units, ED's and W/CP's, both represent irregular areas depending solely on local features. The internal distribution of population within one of these areas could affect a collective quantity, particularly where the weighting function varies rapidly with distance. Before discussing this aspect of the accuracy of population data a few points can be made about the total population figures.

As mentioned earlier any transient population groups have to be considered separately, so this census data should provide the best available estimate of the residential population. The OPCS does not release the exact results for population totals in ED's or W/CP's, but uses a process called "Barnardisation" to ensure the "confidentiality" of this data. Barnardisation consists of adding +1, 0 or -1 to the population of an ED or a W/CP which contains more than 25 people or 8 households. This means that the total population of all the ED's in one W/CP may not equal that from the W/CP data, but over a large sample the deviation should average to zero. Hence there is a fractional error associated with each census district with a typical magnitude of order: (4.8) $|\varepsilon_i^B| = |1/P_i|$ for $P_i > 25$ and 0 for $P_i < 25$, where (4.9) $\sum_{\text{all } i} \varepsilon_i^B = 0$ for each set of population data (ED or W/CP).

The error associated with Barnardisation in any one census district is at the very most 4%, where this would probably only occur in a sparsely populated rural area. Collective quantities would be insensitive to this process as people from many census units would normally be considered. Effectively the zero deviation result expressed in equation 4.9 would apply to most estimates of collective quantities.

Section 4.2.2.1 Mathematical representation of population centroid census data

The distribution of population within one area was represented by equations 4.4 and 4.5. The population centroids can be formally defined as:

(4.10) (a) $x_i = (\sum_{j=1}^{N^j} (x_i+dx_j).P_{ij})/P_i$

(b) $y_i = (\sum_{j=1}^{N^j} (y_i+dy_j).P_{ij})/P_i$. This leads to the following relationship for the internal deviations $(dx_j.dy_j)$ of the elements of population making up the ith census district group with the relevant centroid (x_i,y_i):

(4.11) (a) $\sum_{j=1}^{N^j} dx_j.P_{ij}=0$, (b) $\sum_{j=1}^{N^j} dy_j.P_{ij}=0$.

These conditions can be related to the collective quantities (Q_i') in equation 4.4 when the weighting function is expanded about the centroid (x_i,y_i), giving:

(4.12) $Q_i'=\Sigma_{j=1}^{N^j} P_{ij}.(W(x_i,y_i) + dx_j.\frac{\partial W}{\partial x}|_{x_i,y_i} + dy_j.\frac{\partial W}{\partial y}|_{x_i,y_i} + O(dx^2))$.

This assumes that the variables x and y are independent and that all relevant derivatives of the function (W) are continuous and finite in the region of the ith census district. The latter condition is readily satisfied by selection of a suitable weighting fucntion, particularly one which represents physical behaviour of a pollutant dispersing in the atmosphere. The independence of the variables x and y can be assumed, although there may be relationships between the quantities dx_j and dy_j due to the nature of human society (e.g. streets).

Lumping the terms of second or higher order as $O(dx^2)$ enables equation 4.12 to be rewritten as 4.13, as values of W and its derivatives are only required at the centroid (x_i,y_i).

(4.13) $Q_i'=W_i.\sum_{j=1}^{N^j} P_{ij} + \frac{\partial W}{\partial x}|_i \sum_{j=1}^{N^j} P_{ij}.dx_j + \frac{\partial W}{\partial y}|_i \sum_{j=1}^{N^j} P_{ij}.dy_j + O(dx^2)$.

Substituting from equations 4.11, 4.5 and 4.3 for values in 4.13 gives the equation:

(4.14) $Q_i'=Q_i+O(dx^2)$, showing that where the function W can be expanded in this manner the error in the ith area's collective quantity is of second order in the deviations of the actual population distribution about its centroid.

The second order terms can be evaluated in plane polar coordinates (r,ϕ) in the form:

$$(4.15)\quad O(dr_j^2)=\sum_{j=1}^{N^j}\frac{P_{ij}}{Z}\left(r_i dr_j d\phi_j\cdot\left(\frac{\partial}{\partial r}\frac{1}{r}\frac{\partial W}{\partial \phi}\Big|_{r_{i,i}} + \frac{1}{r_i}\frac{\partial}{\partial \phi}\frac{\partial W}{\partial r}\Big|_{r_i,\phi_i}\right)\right.$$

$$\left. + r_i^2\, d\phi_j^2\cdot\frac{1}{r_i^2}\frac{\partial^2 W}{\partial \phi^2}\Big|_{r_i,\phi_i} + dr_j^2\cdot\frac{\partial^2 W}{\partial r^2}\Big|_{r_i,\phi_i}\right)$$

Some weighting functions will have no azimuthal dependence in a given sector which encloses all the ith census area. In this case the derivative $\frac{\partial}{\partial \phi}$ is equivalent to a zero operator on the weighting function, so the error term of 4.15 and 4.14 reduces to just,

$$(4.16)\quad O(dr_j^2) = \sum_{j=1}^{N^j}\frac{P_{ij}}{2}\, dr_j^2\cdot\frac{\partial^2 W}{\partial r^2}\Big|_{r_i}$$

If (4.17) $W(r)=A/r^p$, where p is between zero and two for most weighting functions associated with doses related to atmospheric dispersal of radionuclides, then:

$$(4.18)\quad O(dr_j^2)=W(r_i)\cdot\sum_{j=1}^{N^j} P_{ij}\cdot\frac{p(p+1)}{2}\cdot(dr_j/r_i)^2=Q_i(\overline{dr}_j^2/r_i^2),$$

where $p(p+1)/2$ is of order unity. Hence the error, which in this case is always an overestimate, in a collective quantity using a weighting function of this form (equation 4.17) is proportional to the ratio of the mean square deviation ($\overline{dr}_j^2$) of the ith population about its centroid to the square of the separation of this centroid from the site (r_i^2).

Section 4.2.2.2 Limitations on accuracy of centroid data using continuous weighting function

A discussion of the results of the last section applied to the ED and W/CP census data follows. This information is used for whole site populations, extending in all directions from the site as the centre of the weighting function.

In many applications the weighting function is not given any dependence on direction from the site (Gronow and Gausden (2)), so the error term in equation 4.18 might be observed. This means that the mean square deviation of the internal population distribution about the census unit's centroid is the immediate source of error. An estimate of this value can be obtained from

considering a circular population unit with a uniform distribution out to a boundary a_i metres distance from its centroid, so (4.19) $\overline{dr_i^2}=\frac{1}{2}(a_i)^2$. This gives the fractional error in the collective quantity approximately as (4.20) $f(Q_i)=\frac{1}{2}(a_i/r_i)^2$.

As the W/CP data consists of a total of n ED units, typically about ten, the error in collective quantities derived from this data can be expected to be generally larger than that using ED data for the same assessment. Through this effect, for a given population distribution, any collective doses calculated with W/CP data would be expected to be generally greater than that using ED data.

Each set of census units can be crudely divided into urban and rural categories (Fitzpatrick (41)). The rural ED's can typically span several kilometres, so a typical deviation ($a_i(ED_r)$) could be 1 km. Urban ED's may just consist of a few streets so that the deviation could be as low as 200 metres. The corresponding W/CP error terms will typically be greater by a factor of about $n^{\frac{1}{2}}$ (i.e. about 3).

A minimum deviation of about 70 metres is introduced by the fact that the population centroid is placed at a corner of a 100 metre square in the national grid. This will affect the validity of conditions 4.11 which allow an exact cancellation of the first order term in the expansion of the weighting function, in equation 4.12. This error can be expressed as

$$(4.21)\quad O(\text{centroid})= -p.(W(r_i)/r_i).\sum_{j=1}^{n^j} P_{ij}.(dr_j+\varepsilon_j) = -p.(W(r_i)/r_i).\sum_{j=1}^{N^j} P_{ij}.\varepsilon_j = -Q_i.\bar{\varepsilon}_i/r_i.$$

Although this cancellation will no longer be exact the result should still be small as the centroid minimises any deviations and only a small perturbation ($\bar{\varepsilon}_i$) from this true centroid has been made. A maximum fractional error can be estimated for all ε_j=+0.07 kilometres, so giving an error of order 7% at 1 km and 0.7% at 10 km. For many centroids in a given assessment area this effect should become negligible.

From the typical sizes of the census units the distances by which a given accuracy is achieved for collective dose

estimates can be derived. These results are shown in Table 4.1 for accuracies of 10% and 1%. The random interaction of the centroid being slightly misplaced and the second order error in using population centroids mean that the ED data could be expected to be accurate to at least 10% within about 4 kilometre in rural areas and about one kilometre for urban areas.

As only a few semi-urban sites, with an effective exclusion radius of 1 km, have been used for some AGR designs ED data should cope reasonably with estimating real collective quantities at all distances, although the ED data may have to be subdivided close to a site in low density population areas. Collective doses based on W/CP data can be expected to agree with ED based results beyond about 3 km and 10 km for urban and rural areas respectively. The advantage of using W/CP data is that few units need to be evaluated to cover quite large population sub-groups, so a saving in computational time can be made over methods using ED results at larger ranges.

Normally a collective quantity for a site assessment is required within a given radius r_n. This final delimeter will cut across many census unit boundaries. Some populations centroids will be included which represent areas not fully within the assessment area while others will be excluded even though they represent people within this circular boundary. This effect can be expected to be random in nature and ideally result in no net error being introduced to the collective quantity. An estimate of the size of this error can be made where the number of census units cutting the boundary can be represented as (4.22) $N^c=2\pi r_n(f_r/d_r+f_u/d_u)=N^c_r+N^c_u$, where d_r, d_u are the typical diameters of rural and urban units where the total of each type occupy respectively the fractions f_r and f_u of the boundary. The fraction of this boundary occupied by the sea (f_s) results in the identity, (4.23) $1=f_r+f_u+f_s$. Using the values of deviations a_i to give a diameter $d_i(=2^{3/2}.a_i)$ this gives the following approximate relationships for ED's and W/CP's respectively (assuming $f_r=f_u=\frac{1}{2}$) ;

(4.24) (a) $N^c_{ED} = 6.5 \, . \, r_n$, (b) $N^c_{WCP} = 2.4 \, r_n$.

An outer boundary could typically be 30 km for site assessment by either population set, or possibly 100 km in some

circumstances where primarily W/CP data would be used. Hence of order 100 population centroid areas would cross this boundary. This fairly large number of samples might be expected from statistical theory (Maisel) to have a mean deviation proportional to the square root of this number. For an estimate of the fractional error produced by this effect the total number of centroids (N^T) in the area has to be known, say where (4.25) $N^t = \pi . r_n^2 (f_r/d_r^2 + f_u/d_u^2)$. Substituting in approximate values for ED's or W/CP's gives

(4.26) (a) $N^T_{ED} = 40 . r_n^2$ (b) $N^T_{WCP} = 4 . r_n^2$.

By the outer radius (r_n) the weighting function ($W(r_n)$) will be below the mean individual weighting value W, so that the maximum fractional error for this cut-off effect, assuming each census unit to contain approximately the same number of people, is of order: (4.27) (a) $f(Q_{ED}) = (W(r_n)/W) . (1/(7 . r_n))$,

(b) $f(Q_{WCP}) = (W(r_n)/W) . (1/(2 . r_n))$.

More typical values could be closer in the following,
(4.28) (a) $f(Q_{ED}) = (W(r_n)/W) . (1/(20 . r_n^{3/2}))$,

(b) $f(Q_{WCP}) = (W(r_n)/W) . (1/(3 . r_n^{3/2}))$. As the ratio of $W(r_n)/W$ may be less than one tenth the likely errors from this cut-off effect should not be significant, being less than 1% for results using W/CP data out to 30 km.

For many purposes the collective site quantities at distances $r_i (< r_n)$ are also required. The above analysis can be applied to these fractional errors in collective values ($Q(r_i)$). This can impose quite large errors when populations close to a site are considered. Under these conditions few people are present within a radius r_i, if this is small, so the ratio $W(r_i)/W$ may be taken pessimistically as unity. This can result in 10% errors in collective quantities within about 1 km and 5 km for ED and W/CP data respectively. In rural areas this effect can be expected to be greater than in urban areas, as there are fewer centroids representing the rural area so proportionately more will cut a given boundary than in urban areas.

This cut-off effect can be just as, or even more, severe than the errors expected due to the use of centroid data when the population group involved is close to the site. The ED data should still be reasonably accurate by a few kilometres. As this last effect has a radial dependence of $r^{-\alpha}$, where α, say, is in the range 1 to 1.5, this random error in the results using W/CP population data can still be important out to 10 km in rural areas.

These three factors affecting the accuracy of using population centroid data while evaluating collective site quantities, using a continuous weighting function, within a radius r_n of the site suggest that ED data is preferable in all cases for its accuracy, and is essential for rural areas within at least 10 kms of the site. The next sub-section applies some of these considerations to the case where discrete weighting function for radial delimeters r_i and r_{i+1} are used with these centroid census data.

Section 4.2.2.3 Accuracy of centroid data used with discrete weighting functions

A simple discrete site weighting function can be defined as having a uniform value (W_i) for any population unit between the radial distances r_{i-1} and r_i in all directions about the site, see Figure 4.2. This would produce a collective quantity for each annular region which would only be equal to that from a corresponding continuous weighting function if

(4.29) $W_i \cdot \sum_{\text{all } k} P_{ik} = \sum_{\text{all } k} W(r_{ik}) \cdot P_{ik}$ for $r_{i-1} < r_{ik} < r_i$. Hence the accuracy of this method will depend on how well the discrete weighting function is chosen to represent the mean dose to the population groups in each annulus.

The accuracy of this method would improve as more annular elements were taken, so that the discrete weighting function did not deviate significantly from a corresponding continuous weighting function. The particular population distribution in each annulus could also affect the accuracy of this method. An overestimate would be obtained if the population was mainly at the outer boundary (r_i), while an underestimate would occur when most people reside close to the inner boundary (r_{i-1}).

Figure 4.2 Diagram of whole site and single sector annular zones

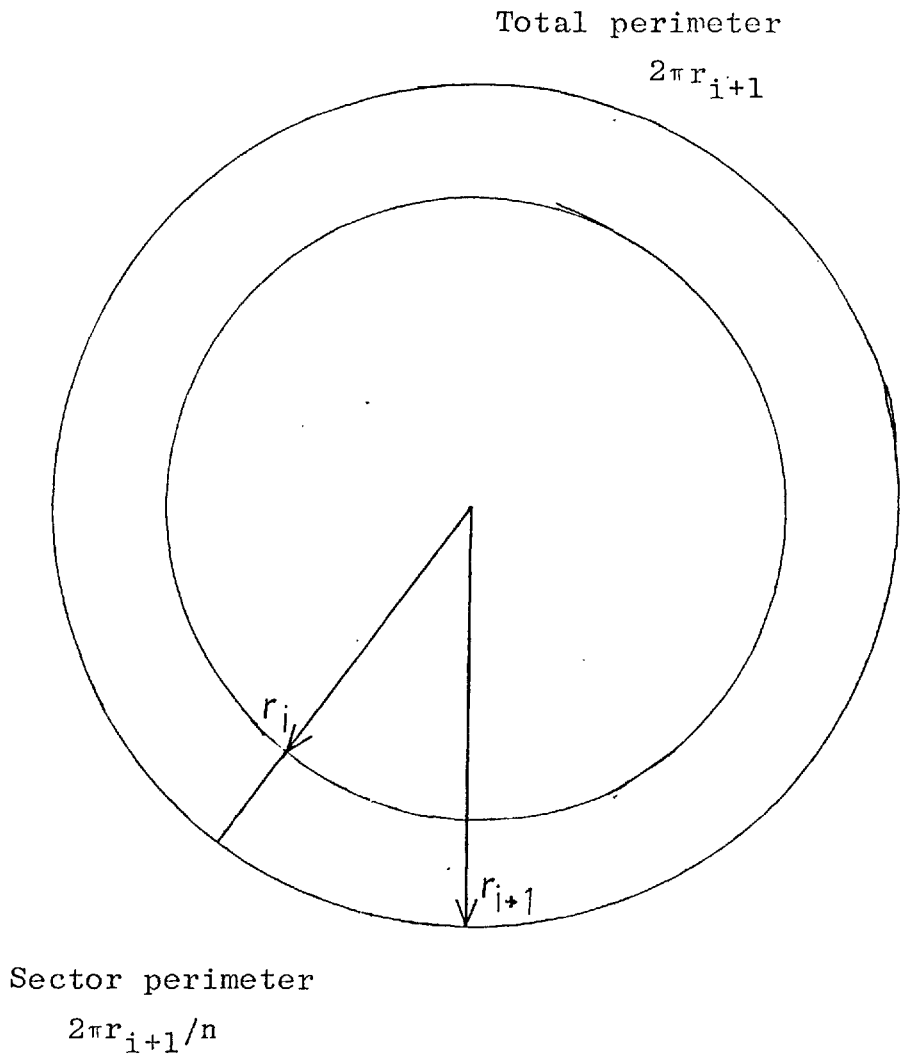

Provided the annulus was large enough sufficient units could be included so that the averaging procedure implicit in equation 4.29 usually occurred. This might be achieved by defining the discrete and continuous functions using equation 4.30: $W_i=W(\bar{r}_i)$ where $\bar{r}_i=(r_i+r_{i-1})/2$ say. This suggests a compromise has to be reached when choosing values of r_i.

Due to the independence of the discrete weighting function with respect to radial distance from the site within the ith region there is no systematic error due to the distribution of population about the centroid for a census unit. This means that the only internal inaccuracy of collective quantities derived from a discrete weighting function results from how the census units cut the annular boundaries. As described in the previous section the likely size of this error will depend on the dimensions of census units and the distances of the boundaries from the site.

An estimate of this cut-off error in this form of collective quantity calculation can be expressed as below, allowing for different mean sizes and populations of census units in each region by using the term α_i, accumulating out to a distance r_n;

(4.31) $dQ(r_n)= \sum_{i=1}^{n}(W_i-W_{i+1}).r_i.\alpha_i.\phi_i + W_n.r_n.\alpha_n.\phi_n$, where ϕ_i represents the random nature of this effect and, say, lies in the range +1 to -1. The total collective quantity can be defined as below:

(4.32) $Q(r_n)=\sum_{i=1}^{n}W_i.\beta_i.(r_i^2-r_{i-1}^2)$, where β_i allows for differences in census units between each area. Assuming that the typical fractional error can be given by that for the critical ith annulus then,

(4.33) $f(Q)=((W_i-W_{i+1})/W_i).(\alpha_i/\beta_i).\phi_i.r_i/((r_i+r_{i-1})(r_i-r_{i-1})$, where $r_o=0$. Using an average value of α_i/β_i of 1/7 and 1/2 for ED and W/CP data respectively (see equations 4.27 a, b) and that the discrete weighting functions decrease by a factor of about 2 (Gronow and Gausden...) then equation 4.33 can be evaluated as;

(4.34) (a) $f^c(Q_{ED}) =\phi_i.r_i/(14.(r_i^2-r_{i-1}^2))$,

(b) $f^c(Q_{WCP})=\phi_i.r_i/(4.(r_i^2-r_{i-1}^2))$.

If a critical group is in the 2km to 3km annulus from a site the error introduced to the discrete collective quantity could be about 4% and 15% for ED and W/CP population data respectively. Although there are fewer sources of internal error when using a discrete weighting function there could be severe cut-off inaccuracies induced compared to the results from a continuous weighting function. These could be of order 25% or more within 2 km of a site if a factor of two existed between consecutive values of a discrete weighting function. The larger the annuli are the less likely extreme discrepancies would be to occur, but this would be offset by an increase in the deviation of the discrete function from its corresponding continuous function. Experience would have to be gained to obtain a balance of these two effects so enabling a discrete weighting procedure to give reasonable agreement with a potentially more accurate continuous weighting scheme to evaluate collective quantities.

Section 4.2.3 Properties of regular grid census data

There are two main differences between the regular grid and the ED or W/CP sets of population data. As noted earlier ED and W/CP units can be very irregular, so it is difficult to assess exactly which portion of these units are cut by a given boundary. The second difference is that the regular grid data only gives the total population within that cell, not its population centroid as given by ED and W/CP data.

The advantages of using a population centroid with a continuous weighting function were that errors were of second order in the census units' internal population distribution and that these errors should not cause an underestimate of collective quantities. When the regular grid data is used the population centroid can, on average, be expected to coincide with the area centroid. The mid-point (x_i^m, y_i^m) of the ith regular grid cell can then be used as an approximate centroid. This gives a collective quantity defined as:

$$(4.35) \quad Q^m = \sum_{\text{all } i} P_i . W(x_i^m, y_i^m) = \sum_{\text{all } i} Q_i^m \quad .$$

A more accurate description of the ith cell's population distribution would give:

(4.36) $Q'^{m}_{i} = \Sigma_{\text{all } j} P_{ij}.W(x^{m}_{i}+\varepsilon_{j}, y^{m}_{i}+\varepsilon'_{j})$.

Expanding this in a manner corresponding to equation 4.13 gives:

(4.37) $Q'^{m}_{i}=W(x^{m}_{i},y^{m}_{i}).\Sigma_{\text{all } j}P_{ij} + \frac{\partial W}{\partial x}\Sigma_{\text{all } j}\varepsilon_{j}.P_{ij}+ \frac{\partial W}{\partial y}\Sigma_{\text{all } j}\varepsilon'_{j}P_{ij}+O(\varepsilon^{2})$

In any particular cell the first order terms will not cancel if the population centroid is not at the mid-point of that square cell. Converting equation 4.37 to plane polar coordinates (r,ϕ) and assuming, as before, an inverse power law for the weighting function (see equation 4.17), which is independent of the azimuthal angle (ϕ), gives:

(4.38) $Q'^{m}_{i}=Q^{m}_{i} -W(r^{m}_{i}).(p/r^{m}_{i}).\Sigma_{\text{all } j}dr_{i}P_{ij} +O(dr^{2}_{j})$, where dr_j can be a positive or negative distance from the cell's mid-point for the element of population P_{ij}.

A mean error term can be defined as:

(4.39) $dQ_{i}=-pQ^{m}_{i} .(\overline{dr}_{i}/r^{m}_{i})$,

where $\overline{dr}_i$ represents the separation of the population centroid from the mid-point of the cell (see Figure 4.3). Hence a first approximation to the overall error expected in the collective quantity for N regular grid cells can be given as:

(4.40) $dQ=-p\Sigma_{i=1}^{N} Q^{m}_{i} .(dr_{i}/r^{m}_{i})$, where p is of order unity. For a large sample the following condition could be expected to hold: $\Sigma_{i=1}^{N}\overline{dr}_{i}=0$. This has been confirmed using a sample of 100 metre square grid data, with entries in 538 one kilometre cells about Heysham and Bradwell. The mean easterly ($dE=\Sigma dx/538$) and northerly ($dN=\Sigma dy/538$) net deviations of the population centroids from the mid point of a cell were such that $(dN^{2}+dE^{2})^{\frac{1}{2}}$ = 21 metres (to 2 SF's). The population weighted mean separation of the population centroid from the centre of the 1 km square cell was found to be 170 metres (to 2 SF's) for this sample.

The factor in equation 4.40 (i.e. Q^{m}_{i}/r^{m}_{i}) may affect this averaging process, although it is unlikely to be correlated with the cell deviations ($\overline{dr}_i$).

A pessimistic estimate of this error term can be made assuming $\overline{dr}_{i}=(2/3).a/2$, where a is the side of the square cell.

Figure 4.3 Diagram of whole site and single sector annular zones.

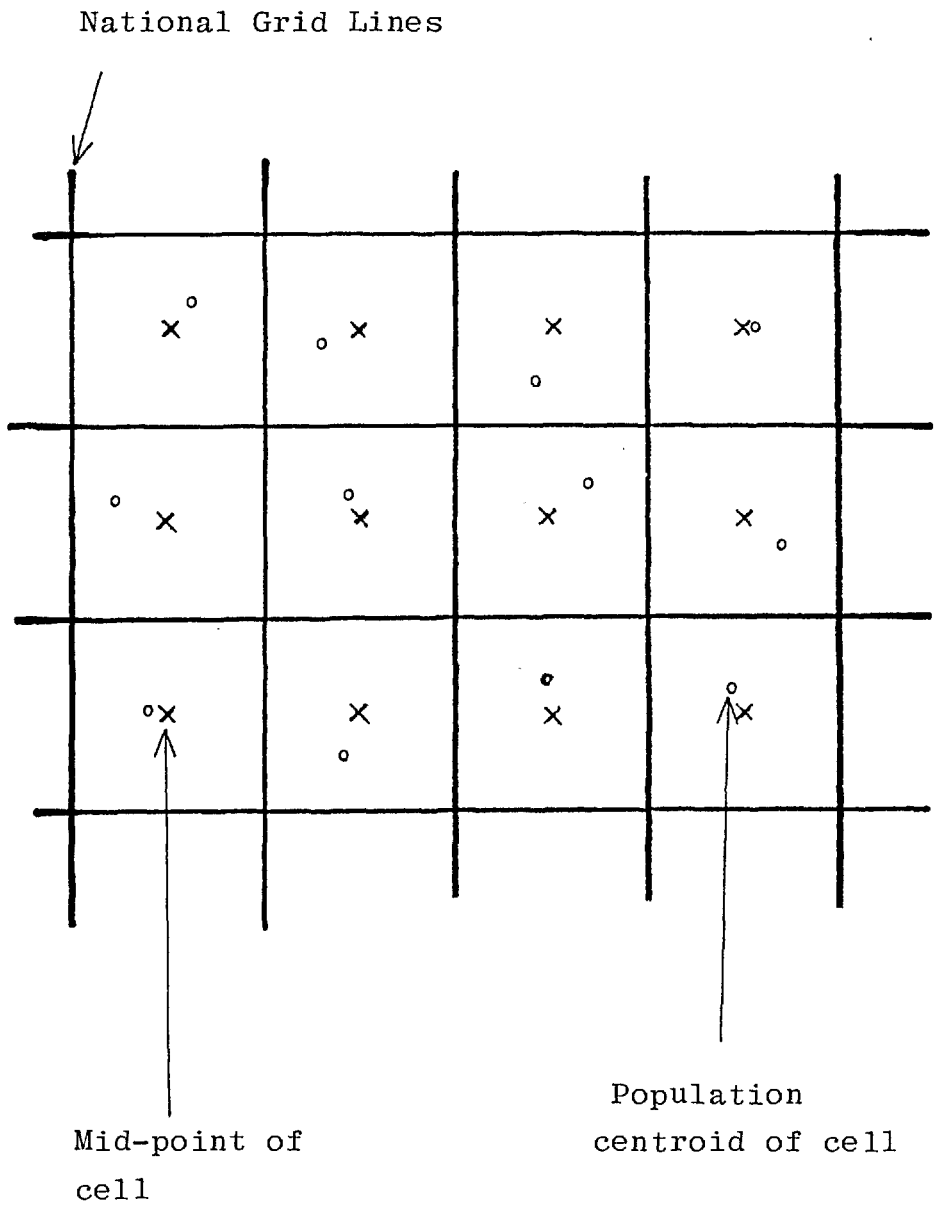

For 10 kilometre data a fractional error of approximately 10% might be expected in a range about 35 km from a site. The more detailed one kilometre grid data could have a 10% error occurring typically about 3 km to 5 km from the site, comparable to ED and W/CP resolution of population.

The 100 metre square grid poses a different problem as the mid-point of one cell cannot be accurately located when using standard national grid references. These coordinates would locate the effective mid-point of the cell for collective dose assessments at a corner of that 100 metre cell. As the source of a release and the track of the resultant plume of activity is unlikely to be known to within one hundred metres in the event of an accident, it would probably not be worthwhile trying to use more accurate population coordinates than these standard national grid references.

This means that the population of a 100 metre square cell will always be misplaced, say at the south-west corner, $\overline{r'}$, rather than the mid-point, $\overline{r}$, relative to an origin. The deviation (da) from the cell's mid-point induced by this relocation can be expressed as:

(4.41) $da=(a/2^{\frac{1}{2}}).\sin(135-(\alpha/2+\phi))/\sin(90+\alpha/2)$, where α is the angle between $\overline{r}$ and $\overline{r'}$ and a = 100 metres. Where the radial distance is large compared to 100 metres the angle α is negligible, so equation 4.41 becomes: (say ϕ is related to north).

(4.42) $da=(a/2).\sin(45+\phi)/\sin(45)$. Given a population distribution with point symmetry, or symmetry about one axis through the site at a given radial distance, this systematic error will cancel when all 360^{o} of the whole site population are included in a collective dose estimate.

At any given cell the maximum fractional error for the 100 metre data can be given as:

(4.43) $f(Q)=da/r=0.07/r$ where r is in kilometres. Hence this 100 metre data should be of reasonable accuracy even at an AGR exclusion boundary of one kilometre. This has better resolution than ED data in rural areas close to a site.

The effects of cutting off a calculation for a collective quantity at some distance r_k will produce errors in a similar manner to those expected for irregular census units. Owing to the regular nature of the grid units considered in this section these errors in any one portion of the outer boundary could be of the same sign, although the effects would cancel for a uniform population along the whole boundary.

The number of square cells, of side a kilometres, crossing the boundary r kilometres distant from a site is of order $2\pi r/(\gamma.a)$, where γ is of order unity and represents the average length of the boundary within one cell, say $\gamma=1$. At this distance let a fraction, such as $\frac{1}{4}$, of this number of units be cut by the boundary so that about half their population, at a density of α' per cell, is erroneously included. This produces an extra collective contribution of:
(4.44) $dQ=\pi r\alpha'W(r)/(4a)$. The total collective quantity within this radius can be given approximately as (4.45) $Q=\pi\alpha\overline{W}.(a/r)^2$, for an average cell population density of α with a mean weight of W. Considering one kilometre square grid data (a=1 km) the fractional error is (4.46) $dQ/Q=(1/(4r)).(\alpha'.W(r))/(\alpha.\overline{W})$. The value of $\alpha'Wr(r)/(\alpha.\overline{W})$ should be less than unity when the critical group in the weighted population is at a distance less than the outer boundary (r). This result can also be interpreted for use with discrete weighting functions.

Comparison of the result in equation 4.46 with corresponding results for ED's and W/CP's show that 1 km grid data should typically exhibit smaller inaccuracies than rural or possibly even urban W/CP's. Urban ED's should still enable more accurate estimates of collective quantities to be made than this 1 km data. In the case of rural ED's the 1 km grid data may be more accurate than this irregular form of centroid data, although the deviation of the regular cell's population centroid from its mid-point would tend to limit the accuracy at short distances from the site.

Section 4.2.4 Summary of use of population data for whole site assessment

Continuous weighting functions combined with population centroid data can be used for estimating collective quantities

to reasonable accuracies, where the intrinsic error tends to be an overestimate proportional to the ratio of the mean square deviation of the population about the centroid in a census unit to the square of the centroid's separation from the site centre. When regular square grid data is used in place of centroid data the corresponding inaccuracies are proportional to a first order ratio of a deviation of population about the point representing the position of cell and the distance of this point from the site. Census data can be chosen which should enable reasonable estimates of these collective quantities to be made. Some of these discrepancies can be expected to roughly cancel for regular grids when collective quantities over a whole site are calcualted.

Often the collective dose within a circular region centred on the site is required. This produces an additional error due to the boundaries of the population units not coinciding with the boundary of the region being assessed. When this circular boundary is close to a site it may produce "cut-off" errors larger than those intrinsic in the methods used to represent these population distributions.

Discrete weighting functions may be used to provide estimates of whole site collective quantities with accuracies similar to those for continuous functions provided optimum annular bands are chosen. Even so a fixed scheme for the use of discrete weighting functions may fail to give a reasonable estimate for certain population distributions, so this method should not be used in isolation (see chapter 6).

The population distributed in a sector can also be considered as a critical group for a single release of activity, as a whole site population can for a series of releases. The next section briefly deals with some aspects of calculating sector collective quantities which differ from those for a whole site.

Section 4.3 Collective quantities in a sector

The same basic calculational methods can be used to estimate sector collective doses as those for a whole site (equations 4.1 to 4.7), but different boundaries limit the extent of the calculation. Hence the only major difference in expected errors will be due to cut-off effects at these boundaries. These may be important in defining a worst sector.

A sector of angular width $2\pi/n$, with a given radius r, shares one nth portion of the circular boundary used for the collective site quantity for the same outer radius. There are also boundaries in the form of two radii from this portion of the circular boundary to the site centre. This gives the ratio of the sector to site perimeters as (4.47) B(sector)/B(site)= $1/\pi+1/n$ while the areas are in the ratio
(4.48) A(sector)/A(site)=1/n.

If the crude assumption is made that all the units which cut these sector boundaries produce a similar contribution to the error, these two factors can be used to convert the expected fractional errors for a whole site to an estimate of these for a sector. This can be done as below:
(4.49) $f(Qsector)/f(site)=B_{se}/B_{si} \cdot (A_{si}/A_{se}) = n/\pi+1$.
This reflects the greatgr perimeter of a sector for a given area, but the increase in number of census units cutting this perimeter of a sector relevant to the whole site may enable a better averaging of gains and losses to occur for the sector.

Typically the angular widths of sectors are similar to those subtended by plumes for prolonged dispersion times, such as 30^{o} or $22\frac{1}{2}^{o}$, where n becomes 12 and 16 respectively. This suggests that uncertainties in sector collective quantities can be about five times those in site quantities for the same outer radius of the assessment area. Hence the use of small census units, which intrinsically enable site quantities to be the most accurately estimated, should be used for the assessment of a sector. W/CP data would be quite inaccurate within 10 km while rural ED data may be poor within 5 km of a site. The regular 1 km grid data would be of a similar accuracy as typical ED data about a nuclear power plant, but could be readily supplemented at short ranges by more accurate 100 metre grid data, if these are available.

One restriction on these cut-off errors for a set of n sectors is that the sum of all the errors produced by the radii cutting the census unit boundaries should be zero. This will affect the result in equation 4.49 when n is small (say 4 or less), but such large sectors would probably only be used for crude calculations (ICRP29).

When this grid has a fixed orientation a worst sector can only be defined to an angular accuracy of $\frac{1}{2}.(2\pi/n)$. Also the magnitude of the worst sector collective quantity may be underestimated by up to a factor of two. A worst fixed sector is unlikely to coincide with the true worst sector, so use of a fixed grid should only be used to identify a broad region to be studied in more detail.

When a worst sector is being searched for, using real population data, the minimum required angular accuracy ($d\phi$) can be crudely estimated as the ratio of the population unit's characteristic dimension (d) to the outer radius (r_n) of the assessment area: (4.50) $d\phi=d/r_n$ radians. For a radius of 30 km and a characteristic dimension of about 1 km, typical of ED or 1 km grid data, this angular accuracy requirement is about two degrees. A critical group may be at smaller distances, but the size of units would also be smaller as this would generally be a large community with smaller ED's. This should also be similar to the agreement between these two data sets when predicting a worst sector for a site. W/CP data typically consists of physically larger units so any worst sector defined by this means could disagree with an ED estimate by a margin of up to about six degrees at this range. Better resolution could be expected from all these data sets if the outer radius was extended to say 100 km.

Section 4.4 Examples of the use of real population distributions

This section includes the presentation of some numerical examples dealing with the accuracy of various population data sets given a fixed weighting function.

The weighting function used is that published by the NII (Gronow and Gausden) for an AGR with a prestressed concrete pressure vessel, and is derived from inhalation dose commitments resulting from a nominal release of activity to the atmosphere. This was originally defined as a discrete weighting function, for radial distances out to 20 miles (32 km), but has been redefined for metric boundaries out to 30 km. Interpolation between these new discrete values enables a corresponding continuous function to be defined. These functions are independent of the orientation of the line separating a population unit and the site being assessed.

The relative accuracies of the two types of population centroid data, ED and W/CP, are compared for both whole site and sector assessments. The effects of using discrete and interpolated functions are also considered. Further some limited samples of 1 km grid data, at a semi-urban site and a remote site, are used to display some properties of regular grid representations of population distributions.

Section 4.4.1 Comparison of ED to W/CP population centroid data

The two data sets, ED and W/CP, represent the major source of information about population distributions used during this period of study. It has been found that adequate accuracy was obtained with W/CP data beyond 30 km. ED data has been exclusively used within 30 km of a site, so comparisons between these two population centroid systems is limited by the range after which it is inefficient to use ED's.

The comparisons are split between site and sector assessments, making use of results for eleven sites in the UK.

Section 4.4.1.1 Site collective quantities derived from ED and W/CP data

The continuous form of the weighting function is used for the comparison of site weighted population values made in this section.

At each site the ratio of the collective site quantity up to a given distance using the W/CP population distribution to the corresponding result derived from ED data was determined. No corrections had been made to either set of population data in any attempt to correct for the real distribution of residents about any given centroid. This means that some population units may lie pessimistically close to the centres of some sites. In chapter six an example is given of a correction for this effect. The W/CP data are normally such that centroids closest to a site are further removed than the closest ED centroids, particularly for rural sites.

Having produced this set of ratios from W/CP and ED results, the mean value (R) for eleven sites can be calculated at each radial distance. These are shown in table 4.2 along with the relative mean deviation (dR), at these intermediate distances, of

Table 4.1 Distances for intrinsic errors in population centroid data

Type of site	Error	Radius typical of given intrinsic error (km.)	
		ED's	W/CP's
Urban	10%	0.6	2
	1%	2	6
Rural	10%	3	9
	1%	10	30

Table 4.2 Comparison of site collectuve results for W/CP and ED population data using a continuous function (averaged over 11 sites)

Outer radial distance from site (r km)	Mean ratio of collective values (R) W/CP to ED	Relative mean deviation(dR/R) about the value R	r.(dR/R)
2	0.92	1.14	2.10
3	1.20	0.54	1.95
5	0.85	0.36	1.80
8	0.99	0.11	0.88
12	0.97	0.050	0.60
16	0.98	0.044	0.70
30	0.99	0.018	0.54

Table 4.3a Comparison of sector collective results for W/CP and ED data using a discrete function (averaged over 11 sites

Outer radial distance from site (r km)	Mean ratio of collective values (R) W/CP to ED	Relative mean deviation (dR/R) about the value R
3	1.51	0.42
5	0.91	0.67
8	0.92	0.43
12	1.01	0.20
16	1.01	0.19
30	1.01	0.12
(30 (interpolated function)	0.99	0.12)

W/CP results from the corresponding ED values. Within eight kilometres of a site the W/CP results can deviate from the ED values by large amounts, where the discrepancies are likely to increase closer to a site. From 8 km to 30 km the mean site values of both data sets are in good agreement. The relative mean deviation at each of these distances decline with increasing separation from a site, to about 2% by 30 km which is similar to the results given by equation 4.27(b).

Also shown in table 4.2 are the values of the relative mean deviation multiplied by the radial distance (r) of the appropriate boundary. From the preceding sections these deviations, away from the immediate vicinity of a site, can be expected to have a $1/r$ dependence, due to the errors primarily resulting from the cut-off effects of the assessment boundary crossing the census units' boundaries. In this sample of eleven sites this dependence may hold roughly for the results beyond 8 km. At these large distances the ED data could be taken as the true result, so this allows the deviations to be interpreted as absolute errors for the W/CP values. Closer to a site the irregular results produced by both sets of centroid data do not lead to any firm conclusions, although the mean deviations at 2 km and 3 km fit, marginally better, a $1/r^2$ dependence, but this may not be significant.

This has shown that collective site quantities calculated from ED population data are not reproduced accurately by using W/CP data within about ten kilometres of a site. Further from a site, except possibly at very remote sites with a sparse population distribution, these two data sets have comparable accuracies when whole site quantities are estimated.

Section 4.4.1.2 ED and W/CP derived results for sectors

In this section the worst sector at each site is derived for both sets of centroid data, using a discrete $22\frac{1}{2}^\circ$ sector weighting function. Both the angular accuracy of these methods and the agreement of the total collective sector quantities can be assessed. The effects of a discrete weighting function also have to be considered as only cut-off errors should be observed rather than deviations from a centroid.

The procedure used to determine a worst sector at a site for either population set could locate this worst sector to the nearest $\frac{1}{2}^{o}$. From the earlier discussion an angular resolution of about 2^{o} could be expected (equation 4.50) for results dominated by contributions out to 30 km from a site. It was found that each worst $22\frac{1}{2}^{o}$ sector at each site given by the two data sets, agreed to within $3\frac{1}{2}^{o}$: the mean angular deviation was about 2^{o} for the eleven sites, which is in agreement with the expected angular resolution. Only two semi-urban sites were included in this sample so no significant difference between rural and urban census units could be determined. In these worst sector assessments the urban areas within 30 km will tend to be dominant so similar angular resolution might be expected for any sites with several large towns within the assessment area.

The ratios of the mean total sector quantities at various downwind distances for W/CP to ED results are displayed in table 4.3(a), along with the relative mean deviations at these radial distances from the site. Comparatively large deviations between the results for the $22\frac{1}{2}^{o}$ sectors occur within about 10 km of a site, due to the different cut-off and intrinsic errors for the two data sets. These only reduce to about 10% in the final region from 16 km to 30 km, where a similar deviation is found for the total sector values using a continuous weighting function.

The simple cut-off error form, of 1/r or that of equation 4.33, cannot be expected to be observed as readily as for a whole site, due to the effects of the radial boundaries to the sectors having errors at all distances out to a given radius (r). When these two sets of discretely weighted populations are considered a $1/(r_i+r_{i-1})$ dependence seems to be observed in the mean deviations of the W/CP results relative to those of the ED's. In table 4.3(b) this approximate relationship can be observed to hold for separations from a site of at least 5 km better than a $1/r_i$ or a $r_i/(r_i^2-r_{i-1}^2)$ relationship, where the last reduces to $1/(r_i+r_{i-1})$ if (r_i-r_{i-1}) is proportional to r_i.

Table 4.3b Distance dependence of mean deviations about discrete sector collective results from W/CP data relative to ED data

Outer radius from site (r_i km)	$r_i.(dR/R)$	$(r_i+r_{i-1}).(dR/R)$	$((r_i^2-r_{i-1}^2)/r_i).(dR/R)$
3	1.3	2.1	0.70
5	3.4	5.4	2.1
8	3.4	5.6	2.1
12	2.4	4.0	1.3
16	3.0	5.3	1.3
30	3.6	5.5	2.6
(30(continuous function)	3.6	5.5	2.6)

Table 4.4 Mean ratios of whole site results using W/CP data with discrete and continuous weighting functions (averaged over 16 sites)

Outer radius from site (r km)	Mean ratio of collective values (R) discrete to continuous weights	Mean deviation (dR/R) relative to the value R
5	0.99	0.11
8	1.01	0.079
12	1.00	0.059
16	1.00	0.047
30	1.00	0.043

A further property of these $22\frac{1}{2}^{\circ}$ sector collective quantities can be seen in tables 4.2 and 4.3a: the ratio of the mean deviations for $22\frac{1}{2}^{\circ}$ sectors to the corresponding whole site values. It was suggested, in equation 4.49, that this ratio could range up to about six for sectors of angular width $22\frac{1}{2}^{\circ}$, where this appears to hold for this sample, allowing for the comments made in the preceding paragraph. The values calculated for these eleven sites do show that sector collective quantities are less accurately estimated than site values, although at short distances the discrepancies between ED and W/CP data sets are more important sources of inaccuracy.

The two sets of centroid data can be used to effectively identify the same worst sector at a site, by a given distance r_n. If the critical group of residents within this area is within about 10 km of the site large differences between the ED and W/CP sector collective doses could be expected. Generally these collective quantities for a sector tend to be less accurately estimated than whole site characteristics.

Section 4.4.2 Comparison of discrete and continuous weighting functions

Atmospheric dispersion is a physically continuous process, so the only advantage of using a discrete weighting function to describe consequences resulting directly from this dose pathway is a simplification of the procedures for calculating a collective dose commitment. In this section the results of this discrete weighting function are compared to those obtained using a continuous function.

Table 4.4 displays the mean ratios of the discrete to continuous whole site results, for distances out to 30 km, using W/CP centroid data for sixteen sites. This shows that on average the results from the discrete function agree very well with those of the continuous function at distances of at least 5 km from the site. This represents the balancing effect of population being distributed within an annulus so that condition 4.29 is satisfied for these NII functions.

The relative mean deviations quoted in table 4.4 show that there is a spread of results between the discrete and continuous

functions. These are of order 10% at five kilometres and decrease to a level below about 5% beyond twelve kilometres. Hence for whole site assessment the discrete weighting functions can give results equivalent to those derived by continuous weighting functions.

The worst $22\frac{1}{2}^{\circ}$ sectors defined by discretely weighting the population can also be compared to the use of the corresponding continuous weighting function. For eleven sites the mean ratios for these differently weighted sector results, by 30 km, using ED and W/CP data sets were 1.04 and 1.07 respectively, with corresponding mean deviations of 0.058 and 0.10. This shows a slight, but probably not significant, tendency for the discrete method to overestimate the sector collective dose. Again the W/CP data are less accurate than the ED data, as reflected by the factor of almost two between the mean deviations. These two values of the mean deviation of the ratios of discrete to continuous results are less significant than the intrinsic ED to W/CP differences for the sector values, as given in table 4.3a.

In this section the discrete weighting functions have been shown to be equivalent to those of the continuous weighting function for estimating both site and sector collective quantities at ranges from about 5 km to 30 km. Both methods will still be included in the collective dose assessment routines to provide a check on this agreement for all sites.

Section 4.4.3 Properties of the one kilometre grid data

A limited sample of 1 km grid data was obtained to assess its usefulness compared to the ED and W/CP 1971 census centroid data. This extended to at least 16 km from a semi-urban site and 12 km from a rural site. Convenient direct comparisons between the regular and irregular census units are only made for whole site quantities.

Given the full 1 km data of the UK, with over one hundred thousand entries, this could be more conveniently stored in blocks associated with 10 km national grid squares. Similarly 100 metre data could be categorised by the 1 km grid. This method would allow rapid selection of large blocks of data rather than a prolonged search for many smaller units, as necessary with the irregular ED and W/CP data.

One advantage of the OPCS 1 km grid system is that the population for large rural ED's (and W/CP's even more so) is broken into smaller units. This effectively moves people away from major communities closer to their real locations, and is most evident close to a rural site. In the rural example the closest ED centroid is over 1.5 km from the site, while a 1 km grid cell's mid-point is less than 0.5 km distant. Even for the semi-urban site the 1 km data allows for a small community within 2 km of the site which the ED data includes in a more distant centroid. The resolution provided by 100 metre grid data would be better than that of this 1 km data but ED files could be edited to provide an equivalent accuracy.

The ratios of collective site quantities derived by 1 km grid data relative to W/CP and ED data at these two sites are given in table 4.5, where a continuous weighting function is used in all cases. As expected the rural W/CP and ED results are not in good agreement with the 1 km data, although this significantly improves by about 10 km. No W/CP centroids lie within 5 km of this rural site, so this greatly exaggerates these differences. For the semi-urban site both the ED and W/CP centroid data are in effectively good agreement with 1 km grid data, taking into account the typical mean deviations given in table 4.2.

The effects of discrete and continuous weighting functions can be observed for these particular sites using ratios of resulting site collective quantities derived from 1 km grid data. These results are given in table 4.6 for the semi-urban and rural sites. The discrete function tends to overestimate this collective site quantity, but probably not significantly. Good agreement, apparently to a couple of percent, is obtained between these two weighting systems at both sites by 12 km.

An alternative method of assessing the accuracy of 1 km grid data would be to allow an effective site centre to be chosen randomly within 0.5 km of the true centre of the site. This has been done for the semi-urban site where twenty three points were selected. The mean fractional deviations derived from the two sets of discrete and interpolated collective site values are given in table 4.7, at various distances from the

Table 4.5 Comparison of collective site results between 1 km grid data and the ED and W/CP centroid data for two particular sites (continuous weighting function)

Outer radius (in km)	Rural site		Semi-urban site	
	Q(1km Data) / Q(W/CP)	Q(1km Data) / Q(ED)	Q(1km Data) / Q(W/CP)	Q(1km Data) / Q(ED)
2	-	3.03	-	-
3	-	3.31	0.75	1.05
5	-	2.00	0.98	0.89
8	1.29	1.23	1.08	1.06
12	1.31	1.15	1.04	1.00
16	NA	NA	1.01	1.01

Table 4.6 Comparison of discrete and continuous weighting functions for site collective results using 1 km grid data at two sites

Outer radius (in km)	Ratio of discrete collective site value to corresponding continuous result	
	Semi-urban site	Rural site
0.5	-	1.08
1	-	1.15
2	1.07	1.15
3	1.11	1.15
5	1.07	1.10
8	1.07	1.03
12	1.02	1.02
16	1.01	NA

site. At short ranges there are differences due to the limited population distribution not changing its discretely weighted value as much as that for the continuously weighting function for this range of effective site centres. These results indicate the size of errors likely to exist in the values derived for collective site calculations for the particular site coordinates.

The ratio of the discrete to continuous semi-urban site's results from this sampling procedure is given in table 4.8. This shows much better agreement at short ranges than would be expected from the mean deviations given in table 4.7. Also given in table 4.8 are the ratios for these derived mean discretely and continuously weighted quantities relative to those corresponding to the actual site coordinates. These show more variation than just the change from discrete to interpolated functions. This difference between the results for the particular site and the mean of the points about this real site is smaller than the mean deviations given in table 4.7.

A comparison can be made between the mean result of this sampling procedure and the ED and W/CP results for the actual site coordinates, for the continuous weighting function. This is given in table 4.9 and shows the three sets of values to be in close agreement beyond 5 km from the site. These results are similar to those of table 4.5, where the W/CP data is still most divergent close to the site.

The properties of one kilometre grid data are such to give an accuracy equivalent to that of ED centroid data, where urban areas are critical, but could give more accurate estimates close to rural sites than these unedited centroid data.

Section 4.5 Other uses of population data and concluding remarks

There are several methods by which doses can be delivered to groups within the population for both planned and unplanned releases. These include:

Inhalation doses and external doses from airborne activity;

External doses from ground deposits;

Food chain doses;

Table 4.7 Relative mean deviations produced by the sampling procedure on 1 km grid data whole site results at a semi-urban site

Outer radius (r km)	Relative mean deviation (dR/R)	
	Continuous weights	Discrete weights
2	0.353	0.256
3	0.460	0.381
5	0.268	0.247
8	0.046	0.052
12	0.032	0.035
16	0.018	0.020

Table 4.8 Comparison of mean site values from the sample procedure with 1 km grid data to the particular site values

Outer radius (r km)	Ratio of collective site results at the semi-urban site		
	$\frac{Q(\text{sample, discrete})}{Q(\text{sample, continuous})}$	$\frac{Q(\text{sample, discrete})}{Q(\text{site, discrete})}$	$\frac{Q(\text{sample, continuous})}{Q(\text{site, continuous})}$
2	1.06	0.98	0.99
3	1.04	0.77	0.82
5	1.04	1.03	1.06
8	1.04	0.94	0.96
12	1.00	0.99	1.01
16	1.00	0.99	1.00

Table 4.9 Comparison of continuous site collective values for the mean of the 1 km grid sampling procedure to the centroid data for the site coordinates

Outer radius (r km)	Ratio of collective continuous site results (semi-urban site)	
	$\frac{Q(\text{sample})}{Q(\text{ED})}$	$\frac{Q(\text{sample})}{Q(\text{W/CP})}$
3	0.86	0.62
5	0.94	1.04
8	1.02	1.04
12	1.01	1.05
16	1.01	1.01

Water-borne contamination;

External doses from activity during transport.

The first two of these can be estimated using residential populations and simple weighting functions derived from atmospheric dispersal formulae, as described earlier in this chapter. Both food chain and waterborne dose pathways may involve concentrating mechanisms in the environment which means that a totally different type of weighting function may be needed (ICRP 29). Lastly estimating the population dose from transporting radioactive substances may require more detailed information than that available with purely residential census data. Also the distance dependence of doses from a transportation flask could be very different to that associated with atmospheric dispersal of radionuclides. (See Macdonald and Mairs, 1978(97)).

These different methods of delivering collective doses will have different characteristic errors associated with the use of real population distributions. Both food chain and waterborne pathways may have very large margins of error on the expected doses from either routine or accidental releases, possibly an order of magnitude above and below a mean value. Hence it may not be necessary to use population distribution data as detailed as described in the bulk of this chapter, although age, diet and gender distributions may be more significant. Where atmospheric dispersal is the direct dose pathway what is considered an accurate air concentration may be in error by a factor of two (Pasquill). This means that it should be adequate if the population distribution is represented in such a way that would give possible errors only of order 10%. Doses from a transport flask may be very accurately known under routine conditions, so the limit on the accuracy of these collective dose estimates could be the information about other road or rail users along the transport route. In unplanned stationary conditions this might revert to an assessment of airborne activity.

Direct inhalation dose commitments from radionuclides released to the atmosphere are used to define the current UK siting criteria, reflecting the critical acute dose pathway for potential accidental releases from nuclear power reactors. Hence the use of the population centroid data described in this

chapter should be of adequate accuracy to investigate this type of collective dose assessment and associated implications for siting policy.

CHAPTER FIVE

A STUDY OF FOUR NOTIONAL AGR ACCIDENTS

Section 5.1 Introduction

In this chapter a series of four notional AGR accidents are described. A range of release conditions are covered so that resulting time integrated air concentrations can be used to characterise each type of release. These notional releases are modelled upon the effects of :

1. Simple failure of the cladding to 20 pins on a major depressurisation incident;
2. More prolonged heating and clad failure of 20 pins following the same depressurisation;
3. Single channel melt-out without a breach of the pressure circuit (e.g. a blockage);
4. Single channel melt-out accompanying a major depressurisation incident ("incredible" but theoretically possible).

Cases 1 and 2 represent two different ranges for releases of volatile isotopes which are "free" between the fuel and cladding. Cases 3 and 4 enable a comparison of the consequences of prolonged releases with filtration to those of a short time scale release for a similar escape pattern from the fuel in a single channel. Before dealing with the results of these notional accidents some aspects of dose calculations will be reviewed. The calculation of doses in WEERIE and the implications of the recommendations in ICRP 26 are discussed.

Section 5.1.1 Dose Equivalent Commitments

Inhalation dose commitments in WEERIE are estimated by applying a rem/Ci (inhaled) factor (F) to the product of the time integrated air concentration (X) and an average breathing rate (B), as in equation 5.1.

(5.1) $D(\text{of organ } k)=F_{i,j,k}*X_{i,j}(x,y,z)*B$, for isotope (i,j).

These organ sensitivity factors were calculated by a biological model SAURON (31). Doses from insoluble activity have been calculated for the lung and the four compartments of the gastro-intestinal tract. Soluble isotopes give doses to bone, kidney, liver, thyroid and "total body", where the last includes blood, muscles and other organs and tissues not mentioned individually. In this model radiation escaping from one organ or tissue is

CHAPTER FIVE

A STUDY OF FOUR NOTIONAL AGR ACCIDENTS

Section 5.1 Introduction

In this chapter a series of four notional AGR accidents are described. A range of release conditions are covered so that resulting time integrated air concentrations can be used to characterise each type of release. These notional releases are modelled upon the effects of :

1. Simple failure of the cladding to 20 pins on a major depressurisation incident;
2. More prolonged heating and clad failure of 20 pins following the same depressurisation;
3. Single channel melt-out without a breach of the pressure circuit (e.g. a blockage);
4. Single channel melt-out accompanying a major depressurisation incident.

Cases 1 and 2 represent two different ranges for releases of volatile isotopes which are "free" between the fuel and cladding. Cases 3 and 4 enable a comparison of the consequences of prolonged releases with filtration to those of a short time scale release for a similar escape pattern from the fuel in a single channel. Before dealing with the results of these notional accidents some aspects of dose calculations will be reviewed. The calculation of doses in WEERIE and the implications of the recommendations in ICRP 26 are discussed.

Section 5.1.1 Dose Equivalent Commitments

Inhalation dose commitments in WEERIE are estimated by applying a rem/Ci (inhaled) factor (F) to the product of the time integrated air concentration (X) and an average breathing rate (B), as in equation 5.1.

(5.1) $D(\text{of organ } k)=F_{i,j,k}*X_{i,j}(x,y,z)*B$, for isotope (i,j).

These organ sensitivity factors were calculated by a biological model SAURON (31). Doses from insoluble activity have been calculated for the lung and the four compartments of the gastro-intestinal tract. Soluble isotopes give doses to bone, kidney, liver, thyroid and "total body", where the last includes blood, muscles and other organs and tissues not mentioned individually. In this model radiation escaping from one organ or tissue is

not accounted for in doses to any other part of the body.

A more recent evaluation of these factors, for fission products from a fast reactor, (6), using the latest ICRP recommendations, produced values (F) which included the irradiation dose delivered to a single organ by the fractions of a given isotope in other parts of the body. Table 5.1a displays, for some radiologically significant isotopes, the rem/Ci(inhaled) values for the lung, thyroid and bone with the SAURON "total body" factors included as a separate listing. Also included in this table are corresponding factors used in the Reactor Safety Study (41) for a series of LWR releases.

The same models have been used in both the CEGB and NRPB Studies for the lung (30) and the gastrointestinal tract (Eve, 1966 (85)). The lung dose commitment factors would be expected to be the most alike, but there are order of magnitude differences for isotopes such as Sr89, Sr90, Cs134, Cs137 and Ba140 due to different assumptions about transportation within the model. More wide ranging differences can be expected to exist for organs, such as the bone and thyroid, where the dose pathways are more extended from the initial inhalation of activity. These three sets of dose commitment factors, in table 5.1(a) are intended to represent reasonable estimates, but show significant differences in some possibly critical organ sensitivities. The WEERIE values used in this present study might cause appreciable overestimation of the dose delivered by some isotopes in particular organs:

a, Lung- Sr89,Sr90,Cs134,Cs137 and Ba140;
b, Bone- Ce144,Sr89,Sr90 and Y91;
c, Thyroid; I134(but is significantly underestimated for Te132 and $Te131^{m}$).

Section 5.1.2 ICRP Recommendations, a Brief outline

In ICRP 26 the concept of dose equivalents (Ht) has been formalised as,

(5.2) Ht=organ(t) dose equivalent
=Q*Dt*N, where Dt=absorbed dose in organ t,
N=1 (at present),
Q= quality factor of the radiation producing Dt.

Table 5.1(a) Life-time integrated dose commitments (rem/Ci(inhaled)) (Clarke and Utting, Kelly et al., WASH1400)

Isotope	LUNG		
	Sauron	FBR	WASH 1400
Sr89	2.1(5)	7.8(3)	7.8(3)
Sr90	3.1(6)	1.2(4)	1.8(4)
Y91	2.4(5)	3.7(5)	2.0(5)
Ru103	6.2(4)	5.4(4)	5.4(4)
Ru106	2.2(6)	3.9(6)	3.9(6)
$Te129^m$	1.8(5)	1.5(5)	1.5(5)
$Te131^m$	1.7(4)	1.2(4)	1.1(4)
Te132	3.2(4)	6.4(3)	3.0(4)
I131	2.1(4)	2.3(3)	2.4(3)
I132	8.4(2)	9.5(2)	1.0(3)
I133	4.4(3)	3.4(3)	3.1(3)
I134	3.8(2)	5.4(2)	5.6(2)
I135	1.8(3)	1.7(3)	2.5(3)
Cs134	1.2(6)	4.0(4)	5.1(4)
Cs137	1.2(6)	3.0(4)	4.0(4)
Ba140	1.4(5)	4.4(3)	6.3(3)
Ce144	1.7(6)	2.9(6)	2.9(6)

Table 5.1(a) (continued)

Isotope	Thyroid			"Total Body"
	Sauron	FBR	WASH-1400	Sauron
Sr89	0	1.5(3)	9.2(2)	1.2(4)
Sr90	0	8.1(3)	1.0(3)	1.6(6)
Y91	0	2.3(1)	9.8(1)	9.2(3)
Ru103	0	8.1(2)	4.3(2)	7.0(2)
Ru106	0	4.1(3)	6.2(2)	9.2(3)
$Te129^m$	6.4(3)	9.4(2)	3.2(2)	3.5(3)
$Te131^m$	2.0(3)	1.2(5)	8.7(4)	1.1(3)
T132	2.6(3)	2.0(5)	9.7(4)	2.2(3)
I131	1.7(6)	1.0(6)	1.0(6)	2.8(3)
I132	5.5(4)	5.4(3)	6.6(3)	1.4(2)
I133	3.9(5)	1.6(5)	1.8(5)	5.6(2)
I134	2.6(4)	9.3(2)	1.1(3)	6.0(1)
I135	1.1(5)	3.0(4)	4.4(4)	3.1(2)
Cs134	0	3.9(4)	7.9(3)	5.7(4)
Cs137	0	2.7(4)	5.1(3)	3.5(4)
Ba140	0	1.3(3)	1.0(3)	7.0(3)
Ce144	0	1.3(4)	4.5(1)	6.6(4)

WASH-1400 values taken to 30 years, but both the others refer to 50 years.

Table 5.1(a) (continued)

Isotope	Total Bone		Marrow		Endosteal Surfaces (FBR only)
	Sauron	WASH-1400	FBR (red)	WASH1400 (Total)	
Sr89	1.9(5)	3.0(4)	3.2(4)	1.3(4)	3.2(4)
Sr90	2.6(7)	2.4(5)	2.8(6)	6.0(5)	2.8(6)
Y91	3.5(5)	1.9(4)	7.1(2)	9.3(3)	8.8(2)
Ru103	9.7(2)	8.8(2)	1.1(3)	1.1(3)	8.5(2)
Ru106	2.3(4)	5.9(3)	5.8(3)	6.2(3)	5.3(3)
$Te129^m$	1.8(4)	1.4(3)	2.6(3)	8.4(2)	2.6(3)
$Te131^m$	2.4(3)	2.5(2)	3.6(2)	3.1(2)	2.6(2)
Te132	3.2(3)	9.1(2)	1.7(3)	1.0(3)	1.8(3)
I131	3.2(3)	2.1(2)	1.3(2)	1.9(2)	1.2(2)
I132	1.4(2)	4.7(1)	1.6(1)	5.0(1)	1.3(1)
I133	1.1(3)	9.2(1)	3.0(1)	9.4(1)	2.5(1)
I134	7.1(1)	1.9(1)	6.8(0)	2.0(1)	5.4(0)
I135	2.8(2)	8.7(1)	2.8(1)	9.1(1)	2.3(1)
Cs134	3.7(4)	4.7(4)	4.0(4)	4.8(4)	3.7(4)
Cs137	6.0(4)	3.6(4)	2.8(4)	3.7(4)	2.7(4)
Ba140	9.4(4)	5.2(3)	4.6(4)	3.4(3)	1.9(4)
Ce144	1.2(6)	1.0(4)	1.8(3)	9.2(3)	1.6(3)

WASH-1400 values taken to 30 years, but both the others refer to 50 years.

Table 5.1(b) ICRP weighting factors (ICRP pub. 26)

Organ or Tissue	Weighting factor (Wt)
Gonads	0.25
Breast	0.15
Red Bone Marrow	0.12
Lung	0.12
Thyroid	0.03
Bone surfaces	0.03
Remainder*	0.30

*Where five other most irradiated organs, or tissues, (excluding the skin in most circumstances) are given a weight of 0.06 each, with irradiation of all other organs and tissues being neglected.

Committed dose equivalents are the time integrated dose equivalents received from any radioisotope absorbed at one time and delivered over a human life-time (50 years). If integrated for an infinite time this is referred to as a dose equivalent commitment . These two commitments are the same when the isotope's effective half-life is much less than 50 years. Problems arise for long lived isotopes, such as C-14(9). It was also recommended that "the Commission's dose limitations are intended to relate to the dose-equivalent commitment resulting from one year of a particular practice". The dose equivalent received in one year (possible from one incident, as could occur under accident conditions), over either a short period from short lived radioisotopes or a long period from less unstable isotopes, may be covered by that year's dose equivalent limits. The dose limitations have been set as limits on risks from doses likely to lead to stochastic effects. The limits are set so that whole body irradiation and non-uniform irradiation lead to the same limiting risk. This is contained in the condition below, for one year, where the organ dose equivalents (Ht) are weighted by factors (Wt) recommended in ICRP 26:

(5.3) $\Sigma_t Wt*Ht<H_{wb,1}$, where $H_{wb,1}$= annual whole body dose equivalent limit. The weighting values are displayed in table 5.1b.

The left-hand side of condition 5.3, say (5.4) $Z=\Sigma_t Wt*Ht$, can can be evaluated for single releases under a variety of conditions and compared to the appropriate limits for individual members of the public. For non-stochastic effects the total dose equivalent annual limit is 50 mSv, while the whole body (stochastic) annual limit for members of a critical group is 5 mSv. There are special conditions applicable to the eye lens and the skin regarding non-stochastic dose limits.

Variables, such as age and sex, are not considered to be significant in the setting of these limits, but need to be considered when evaluating dose equivalents and any derived limits. An example of this is given by Baverstock and Vennart (1977(55)) for derived emergency reference levels for ground contamination in the milk food chain in the U.K.

Section 5.1.3 Application of ICRP 26 to calculated doses for the WEERIE model

Only a limited range of organ committed dose equivalents from the SAURON model are used in WEERIE. Nine single organ doses are considered, which are: lungs; thyroid; bone; stomach; liver; kidneys; small intestine; upper large intestine and lower large intestine. The bone dose commitment does not discriminate between bone surfaces and red bone marrow. Also included, as mentioned in section 5.1.1 is the "total body" dose commitment for other organs and tissues, but the distribution of this quantity among the organs and tissues is not defined explicitly.

From this immediately available information condition 5.3 cannot be completely evaluated, but a major portion can be described. Here it is assumed that the bone dose commitment takes the total weighting of each section of the bone. The doses to the gonads and the breast are not given individually, but are included in the "total body" dose commitment. One assumption would be that both the breast and gonads each receive the "total body" inhalation dose commitment. The quantities of inhaled radionuclides depend greatly on the atmospheric dispersion for the release, where factors of two to ten could quite often occur between predicted and measured time integrated air concentrations. Also release pathways can not be accurately described. Hence the assumption on the inhalation dose commitments for the two organs should not be unduly pessimistic with regard to other factors in the calculation of doses.

For gas cooled carbon moderated thermal reactors the fission products to which the "total body" dose is most sensitive are listed in table 5.1c, where iodine-131 and tellurium-132 have also been included. The entries in this table display the products of the organ sensitivity factors (F rem/Ci(inhaled)) and the relevant weighting function (W) for the three major organs to receive significant doses as well as the "total body", using 0.4 for W ("total body")=W(breast+W(gonads) under these assumptions.

For the MAGNOX and AGR reactors the notional accidents considered will primarily release iodine, tellurium and caesium,

Table 5.1(c) Interpretation of "total body" dose in terms of ICRP 26 weighting terms in calculating weighted whole body doses from the available dose predictions in WEERIE.

Activity (kCi/AGR fuel channel)	Isotope	Product of (Fk*Wtk) for organ k				% of "total body" to this weighted dose (57% of weight)
		"total body" Wt=0.4	Thyroid Wt=0.03	Lungs Wt=0.12	Bone Wt=0.15	
100	Sr89	0.5(4)*	0.0	2.5(4)	2.9(4)	8.5
15	Sr90	0.4(6)	0.0	0.24(6)	3.0(6)	11
70	Ru106	1.2(3)	0.0	240(3)	3(3)	0.5
180	Te132	0.8(3)	0.1(3)	3.8(3)	0.5(3)	13
130	I131	1.2(3)	60(3)	2.4(3)	0.5(3)	1.9
22	Cs134	2.4(4)	0.0	14.4(4)	0.6(4)	14
19	Cs137	1.6(4)	0.0	14.4(4)	0.9(4)	9.4
160	Ce144	2.8(4)	0.0	21(4)	18(4)	6.7

* 0.5(4) = 5000

with significant quantities of ruthenium in some cases. The release fractions of strontium and the rare earths will generally be comparatively small, and iodine may be surpressed in cases where it reacts with MAGNOX vapour. With these limitations, it is unlikely that this estimate of the weighted whole body effective dose (Z in equation 5.4) would be in error by more than about 10%, where this error also depends on the organ sensitivities assumed.

The expected error in the value of "Z" will depend on the reactor type and release patterns. Elemental strontium is more volatile than its oxides while the reverse is true for ruthenium (44). For high burn-up fuel, as in FBR's and HTR's, build up of, for example, Cs134 may adversely affect this approximation. Fuels, such as bonded carbon coated oxide pellets in an HTR (Lewis), which could have relatively high metallic release fractions would also alter the degree of this approximation, particularly for releases in reducing atmospheres. Different fuel cladding and coolants, such as zircalloy and water in LWR's, have different release properties to reactors using steel and carbon dioxide for these two items respectively. Zircalloy reacts with oxygen relatively more than steel so could allow relatively higher releases of strontium but suppress releases of ruthenium and tellurium, by affecting the immediate atmosphere about the fuel. It should be noted tellurium is an oxygen group element so can react readily with zircalloy. General pellet-cladding interactions will affect details of any escape of activity.

These effects could alter this approximation of applying the weighting functions for the gonads and breast to the "total body" dose calculated within WEERIE. The accuracy is not significantly affected due to the organ sensitivities used at present. If new inhalation dose factors are introduced in the future, or exotic releases are considered, this approximation would have to be reviewed.

Section 5.2 Description of Notional accidents in an AGR

In this section each of the four notional AGR accidents will be described along with the calculated release of fission products to the atmosphere. The parameters of the escape process,

such as release fractions, rate of fuel involvement, plate-out rates, resuspension factors and overall leakage rates, are given.

Each case has a common fuel irradiation history, where the burn-up of 18000 MWd/Te is assumed to occur at a rating of 13 MW/Te, typical of an AGR. Time dependent flux, spectrum allowance factor and fission fractions (12) are incorporated in modelling the irradiation period, which is broken into nine 154 day steps. The fission product inventory is estimated, using this data, in the FISP section of the code WEERIE. This FISP routine (10) does not allow the formation of isotopes by neutron capture, only allowing for their decay by this nuclear process. A later program, FISP 4, Beynon 1973 (77) does allow for accretion by neutron capture, where a more detailed three group model of neutron flux, rather than a single group, is used. Both routines use a point model of a reactor.

The neglect of build up of isotopes by neutron capture events events in FISP only led to one radiologically significant isotope being grossly underestimated, see table 5.2. This isotope was Cs134 so the assumption was made that it would be released in the same ratio to Cs137 as it was produced in the reactor core. Not only do both have the same chemical properties but also these are long lived nuclides with respect to the time scale of any accidents and have no significant short lived precursors which could be affected by release conditions.

This is an appropriate time to mention briefly some of the design features of an AGR which should guarantee the safety of this system to such an extent that it has been constructed on sites much closer to large urban communities than earlier gas cooled reactors in the UK. One important feature is the ceramic fuel in steel cans which can withstand much higher operating and transient temperatures than uranium metal fuel with magnox cladding without releasing activity to the coolant. The coolant circuit itself is contained within a pre-stressed concrete pressure vessel along with the heat exhcangers. This greatly reduces the number and size of large penetrations and also the rates of depressurisation for a given, but improbable, failure. This pressure vessel is designed so that its failure during the operating life of the reactor is "incredible".

Table 5.2 Comparison of FISP4 (3 group flux model) to FISP (1 group flux model) for 1386 days irradiation in an AGR

Radiologically significant isotopes	Half life of isotopes[b]	Fission Product Inventory(Ci/Te)	
		FISP (no (n,γ) production	FISP-4 with (n,γ) production
Total Krypton	mixed	1.83(6)[a]	1.74(6)
Rb88	18 min.	2.59(5)	2.56(5)
Sr89	50 d.	3.35(5)	3.37(5)
Sr90	28 y.	5.07(4)	4.30(4)
Ru103/Rh103	39 d./57 min.	8.49(5)	9.67(5)
Ru106	369 d.	1.98(5)	2.18(5)
Te132	78 h.	5.15(5)	4.99(5)
Total Tellurium	mixed	2.73(6)	3.16(6)
Iodine-131	8 d.	3.54(5)	3.50(5)
Total Iodine	mixed	4.54(6)	4.86(6)
Total Xenon	mixed	3.77(6)	3.33(6)
Cs134	2.1 y.	1.80(1)	6.57(4)*
Cs137	30 y.	5.53(4)	5.62(4)
Ce144/Pr144	284 d./17 min.	4.60(5)	4.86(5)/4.88(5)

[a] 1.2(3)=1200 etc. [b] Tobias (1972)

*In FISP4 6.57(4) Ci/Te is produced by Cs133(n,γ)Cs134 against 1.65(1) Ci/Te produced by decay along the mass chain A=134.

Two main forms of penetrations still exist, namely the stand pipes over the fuel channels (for control rods and on-load refuelling) and the tunnels for the gas circulators. The former have been designed so that a failure is only a remote possibility, but if it did occur the following depressurisation transient would cause little, if any, economic damage to the plant and minimal radiological hazards off-site. The penetrations for the gas circulators are not expected to be breached, where double closures may be used. Even so the motor was mounted in the tunnel to reduce the chances of rotating plant damaging the closures and to provide a resistance to the flow, which would minimise the probability of coolant stagnating in the core, in the case of an "incredible" failure in this tunnel. Air has to be excluded from this tunnel to prevent a possible oil explosion at a faulty motor. Another possible means by which a depressurisation of the circuit could theoretically occur is if the by-pass system used to control the chemical composition of the coolant was to fail, causing depressurisation to atmospheric pressure in about an hour.

A great deal of effort has been expended to ensure that adequate cooling is provided to all fuel channels in the core in the event of faults in this reactor. The control system has been designed to cope with the interactions between the generation of power in the core, derived from normal operation or the radioactive decay heating after a reactor trip, the heat sink, in the form of the boilers and feed water supply, the generation of electrical power at the turbines and the supply of essential power if external sources fail. Great complexities arise when restarting forced flow after the reactor has been tripped and the gas circulators' speed has run down. It is essential to achieve a good level of cooling as the decay heat in the core is of order 100 MW immediately after the successful reactor trip. Even so the overall system is designed such that there is adequate time to prevent economic damage to the fuel and core structure, where the period malfunctions have to last before safety is impaired in these circumstances is always longer.

Some potential critical malfunction conditions have been investigated and the system has been determined to react satisfactorily. Flow in one channel has to be reduced by 40% of its intended operational level in a fuel channel, by blockage or graphite sleeve fracture, to cause fuel melting while the reactor is still operating, but the channel gas outlet temperature, or later the activity detectors, should trip the reactor to prevent fuel damage. It is theoretically possible for a channel to be blocked and the fuel to melt in an intact coolant circuit, where plate-out would occur, but activity would have to leak to the atmosphere through normal pathways at a very slow rate. This potential accident could only release, at most, 100 Ci of iodine-131, given pessimistic assumptions. Some depressurisation accidents have been considered, where a slow depressurisation may cause economic damage and safety damage if adequate cooling is not provided within about 10 minutes and 30 minutes respectively of the start of the accident.

In this work the notional AGR accidents which model pin failures could be described as having a definite but small probability of occurrence, but this would be much greater than any associated with the melt-out of fuel in a channel. The latter type could be described as "incredible". No specific significance should be attached to the use in this work of the failure of exactly 20 pins or the melt down of one fuel channel. These values were taken to show the relative sizes and types of releases which might occur for different accidents, but restricted to a scale which should not involve any catastrophic changes in the reactor structure which could lead to complexities outside the scope of the WEERIE models.

In all the accident sequences studied it is assumed that the reactor is shut down two minutes before any release from the fuel begins. No significant changes in the consequences are produced by using a different delay of up to about 10 minutes. The isotopes used in FISP generally have half lives greater than a few minutes, so this delay can be used to allow for the decay of shorter lived precursors already assumed in the data incorporated within the model. Some form of time difference may be expected between shut down of the reactor and

damage to the fuel which permits escape of radionuclides. The two minute delay used here for these modelled AGR accidents is purely notional. In some accident sequences this delay may be negligible or, even more improbably, reversed if the reactor is not tripped rapidly.

Once the amount of activity released in a notional accident has been calculated there are further limitations on estimation of any doses resulting from dispersion in the atmosphere. The Gaussian dispersion parameters used in WEERIE are strictly valid only for ground level releases, so elevated releases are not considered in the following incidents. The effects of buoyant and self heating plume rise are not modelled for these releases. In depressurisation events the escaping coolant could contain a large enough heat content to produce appreciable rises in some circumstances. The interaction of buoyancy forces and building wakes is a complicated problem. Self heating plumes could only occur for major accidents, and would also be dependent on the condition of the atmosphere.

Section 5.2.1 Description of notional depressurisation accident with simple cladding failure on twenty pins

This notional accident is intended to demonstrate some features of simple cladding failure which may occur on a major depressurisation in an AGR. Five time steps are considered within the release, so that the internal time dependent structure of the release can be examined.

The major depressurisation is assumed to occur with a half life of 9 minutes (Woollatt), which means the incident should tail off in about a half hour to one hour. The cladding of twenty pins is assumed to fail, with 80% of this fuel being involved at a linear rate within four minutes. The remaining 20% is assumed to be released at a rate decreasing exponentially, as allowed in the WEERIE circuit behaviour model, with a characteristic time of one minute. The total mass of fuel involved is given by (5.5) $M = M_1+M_2$ (Te) , where $M_1=r_{1*}t_p$ (5.6) , with t_p as the time in seconds when 80% of the fuel has been involved at a linear rate in the release to the coolant. Other terms are defined below:

(5.7) $M_2 = \int_{tp}^{tr} e^{-\alpha t} \cdot r_2 . dt = (e^{-\alpha tp} - e^{-\alpha tr}) . r_2/\alpha$ Te.

(5.8) $M_1/M_2 = 4/1 = (r_1/r_2)*(t_p*\alpha)/(e^{-\alpha tp} - e^{-\alpha tr})$. Assuming $\alpha = 4/t_p$ (5.9) so that the whole fuel involvement should occur effectively within $2t_p$, where t_r is such that

(5.7a) $M_2 = (e^{-\alpha tp})*r_2/\alpha$. From (5.8) and (5.9) this gives (5.10) $r_2 = r_1 . e^4$ Te/second. This form of release will be assumed for all the four cases, but with different values of t_p for a given mass M of fuel involved.

Only a small fraction of the fission product inventory in the fuel pins, but no actinides, is assumed to escape on clad failure. Element dependent release fractions correspond to a portion of the "free" isotopes existing in any spaces outside the oxide fuel ceramic, but contained by the cladding under normal operating conditions.

The "free" isotopes in a fuel pin will tend to consist preferentially of the longer lived isotopes. This is due to the diffusion rates of isotopes through the ceramic to the gap about the fuel. The fuel tends to fragment with increasing burn-up, under the effects of stresses, densification and general pellet-cladding interactions which can alter the diffusion paths isotopes have to travel to become "free". Also grain boundary movements within the crystalline structure of the fuel could affect the constitution of the "free" isotopes. A pessimistic assumption has been made that the release fractions used for each element would be independent of the half-lives of the radionuclides involved, as the temperature conditions within the damaged fuel would possibly have an important influence on releases during the accident.

Many studies of the release fractions of isotopes from uranium dioxide fuels have been made. From these studies it can be assumed that 6 Ci of I131 is "free" in an AGR pin, corresponding to 1.37% of the total I131 inventory of the pin, but only 2 Ci(0.46%) is released on a simple cladding failure (Woollatt 1978 (78)). This last value is similar to that

derived from experiments undertaken by the UKAEA (Hillary and Taylor, 1972 (79)). In these experiments it was also found that Csl37 releases followed that of Il31 quite closely for can punctures at about 1000°C. Other elements which are likely to display similar release behaviour to caesium and iodine are: germanium, arsenic, selenium, bromine, rubidium, cadmium, antimony, tellurium (as elements) and tritium (as some hydride rather than a gas). Inert gases are reported to have a release fraction of about 6% under these conditions. Although the alkaline earths, strontium and barium, are more volatile than the oxide forms, they still have low release fractions. Beattie (53) quotes releases of $3.1.10^{-3}$% and $1.1.10^{-3}$% for Sr and Ba respectively from UO_2 fuel again at about 1000° C, where this is in agreement with other sources of information (44, 79-82). Rare earths, including Yttrium, Zirconium, Niobium, Silver, Lanthanum, Cerium, Praseodymium, Neodymium, Promethium, Samarium, Europium, Gadolinium and Terbium, are assumed to be well retained by the fuel at about 1000° C with a release fraction of 10^{-4}%. If actinides were to be released they would probably behave in a similar fashion to the rare earths. Other elements, including Ruthenium, were assumed to escape in quantities intermediate to those of caesium and strontium:

$R(Ru)=(R(Sr)*R(Cs))^{-\frac{1}{2}}=4.10^{-2}$%. These release fractions are displayed in table 5.3.

A simplified model of fission product behaviour in the coolant circuit is assumed, where only iodine is plated out on interior surfaces. Further it is assumed that 90% of the iodine is in elemental form with a half life of 3 minutes in the coolant (78, Macdonald 1971 (83)), while the remaining 10% is methyl iodide which effectively does not plate out. The mean plate-out rate for iodine is $\lambda_I^p = 0.9*0.693/180 = 3.465.10^{-3} sec^{-1}$. Resuspension of Xenon from the plated out Iodine is assumed to occur in the coolant circuit. No filtration is allowed for the escaping coolant and coolant borne fission products which leak directly to the atmosphere with an effective half life of 9 minutes for this major depressurisation.

Table 5.3 Elemental release fractions for a notional simple pin failure in an AGR

Elements	Release Fraction
Xe,Kr	0.06
I,Cs(Te,Ge,As,Se,Br, Rb,Cd,Sb,H^3)	0.0046
(Ru,Mo,Tc,Rh,Pd, Ca,Zn,In,Sn)	0.0004
Sr	0.000031
Ba	0.000011
(Y,Zr,Nb,Ag,La,Ce, Pr,Nd,Pm,Sm,Eu,Gd,Tb)	0.000001

Table 5.4 Atoms released from the simple twenty pin failure on a major AGR depressurisation.

Isotope	Release Fraction (R)	Inventory in 20 pins (N^{o}·) T	Half Life	Maximum Potential Release	Calculated Releases	
					No. of atoms	Curies
$Kr85^m$	0.06	2.31(18)*	4.5 h	1.39(17)	1.23(17)	140
Kr85	0.06	2.80(21)	11 y	1.68(20)	1.53(20)	8.8
Sr90	0.000031	5.6(22)	28 y	1.7(18)	1.55(18)	0.034
Ru103	0.0004	2.5(21)	39 d	1.0(18)	9.05(17)	5.0
Ru106	0.0004	9.5(21)	369d	3.8(18)	3.42(18)	2
Te132	0.0046	2.2(20)	78 h	1.0(18)	9.03(17)	60
I131	0.0046	3.65(20)	8 d	1.68(18)	4.77(17)	12.8
I135	0.0046	2.44(19)	6.7 h	1.02(17)	3.09(16)	23
$Xe131^m$	0.06	5.4 (18)	12 d	3.24(17)	2.95(17)	5.3
$Xe133^m$	0.06	2.09(18)	52.5 h	1.25(17)	1.14(17)	11.4
Xe133	0.06	4.77(20)	5.3 d	2.86(19)	2.47(19)	1010
Cs134	0.0046	6.3(21)	2 y	2.83(19)	2.55(19)	7.3
Cs137	0.0046	7.7(22)	30 y	3.54(20)	3.18(20)	6.3

*(1.2(3)=1200)

Iodine released to the atmosphere is assumed to have a deposition velocity in air of 1.2 cm/sec. The chemical forms iodine may take include elemental iodine, methyl iodide and iodine associated with aerosol particles, where the proportion of elemental iodine will probably dominate the deposition rates close to the source. With the source depletion model used this deposition velocity for iodine might possibly have to be reduced once dry deposition has removed a large fraction of elemental iodine. This could occur within 30 km of the source under stable conditions and at much larger distances as the conditions become more unstable. There is an option in the modified depletion model where this effect can be approximated, provided the change required in the deposition velocity is not too large. However as the proportions of the different physical forms of iodine are uncertain this option will not be used here. In addition daughter isotopes produced mainly in the plume may have significantly different deposition properties to those isotopes of the same element which were released from the nuclear installation. When stable dispersion conditions are used results will only be given to about 30 km, as severe depletion of iodine will have occurred by this distance and results may no longer be adequately described by a constant high deposition velocity for material released at the source or by a simple Gaussian model. Except for non-depositing inert gases the rest of the release is assumed to be small aerosol particles, with a deposition velocity typically 0.3 cm/sec. Hence a three group deposition model can be used.

The releases from this modelled event were stored for five time steps: 0-240 secs; 240-480 secs; 480-720 secs; 720-960 secs and 960-1800 secs, by which time the majority of the release has occurred. Results from a detailed breakdown of the release pattern are given in a later section, while the gross releases are described here.

Table 5.4 gives the inventory of the twenty pins for some isotopes along with the calculated and 'maximum' potential releases. For ling lived isotopes the 'maximum potential release' can be defined effectively as: $Q_{ij}^{mp}=R_{ij}*I_{ij}(pin)$, the

product of the pin inventory (I) and the ij^{th} isotope's release fraction (R), ignoring precursors, plate-out and other effects. Hence this can be used to identify the effects of plate-out and contributions from short lived precursors. In the case of I131 only 30% of the 'maximum potential release' occurs due to plate-out. Isotopes which are not plated-out in this notional accident seem to have been reduced by the truncation of the modelled incident to only half an hour, but the 10% loss should not be significant in comparison to other uncertainties. There are no major effects of resuspension in the released quantities of xenon isotopes, such as $Xe131^m$, $Xe133^m$ and Xe133. This is due to the relatively short time scale of the accident compared to the half-lives of the iodine isotopes concerned.

The total release contains of the order of at least 1kCi of mixed fission products but only 12.8 Ci of Iodine-131.

Section 5.2.2 Release from a more prolonged clad failure on a major depressurisation in an AGR

This notional accident is intended to be a more pessimistic interpretation of the previous pin failure accident. The irradiation history, with the two minute cooling period mentioned earlier, is retained, as well as the total mass (M) of the 20 pins involved (see equation 5.5 etc.).

The release fractions used in this case are higher. All the "free" I131 in each pin (6Ci) is assumed to be released. Thus the iodine release fraction is increased by a factor of 3. In addition to this all other elements, except for the inert gases, are assumed to have a similar increase in the relevant release fractions. From the data available for releases of inert gases from uranium dioxide fuel an upper value of the fractional release of 10% would be more representative than an increase by a factor of three to 18% (Hillary and Taylor). This also allows the description of an accident which is less dominated by inert gases escaping to the atmosphere.

A second parameter altered was the time t_p in which 80% of the release from the fuel pins occurs. This was extended to 8 minutes, so that the time steps used to describe the internal structure of the release were modified to four and prolonged to a full hour. (i.e., 0-480,480-960,960-1800,1800-3600 secs).

The gross releases of selected isotopes are presented in table 5.5. There is no significant truncation of the release when the time steps are extended to one hour. Some effects of plate-out are evident in the releases of iodine isotopes. Again no major effects have been produced by resuspension in this short accident. This second release contains less than 3kCi of mixed fission products associated with 38.5Ci of I131, reflecting the relative change of release fractions of the inert gases and the other radioisotopes from those in the first accident.

Section 5.2.3 Notional release due to channel melt out with an intact coolant circuit

This case is intended to represent a sequence of events where all the fuel in an average channel melts while the coolant circuit is intact but leaking to the atmosphere at an average operational rate. This permits a study of the effects of filtration on the notional release. The initial inventory of the fuel has the same irradiation history as previously described, where the reactor is again assumed to be shut-down two minutes before the fuel begins to release fission products.

For the fuel to melt in one channel while the reactor has just been shut down it may be assumed there is poor coolant flow through that channel. This means that radioisotopes from the fuel will only slowly enter the coolant circuit. The present model represents this by assuming that 80% of the fission products is involved after 2 hours, which is a much longer time than in the two releases described earlier. A complete fuel channel consists of a single stringer of seven elements each with 36 pins, totalling 252 pins (78).

A coolant circuit normally operates with an effective, but small, (9) leakage rate to the atmosphere, assumed to be 3% per day in this case. Final clean-up of the circuit is presumed to begin 24 hours after the start of the incident. This marks the end of the release studied here, although inert gases may still escape during this last stage, probably with some time delay while passing through the appropriate filters. During the release it is assumed a by-pass system is started, one hour from the onset of the release, which absorbs methyl iodide at a

Table 5.5 Release from the more prolonged pin failure on a major AGR depressurisation

Isotope	Release Fraction	Potential Release No.	Calculated Release	
			No.	Curies
$Kr85^m$	0.10	2.31(17) *	2.26(17)	260
Kr85	0.10	2.80(20)	2.80(20)	15
Sr90	0.000093	5.3(18)	5.26(18)	0.11
Ru103	0.0012	3.0(18)	3.0(18)	17
Ru106	0.0012	1.1(19)	1.1(19)	6.6
Te132	0.0137	3.01(18)	3.02(18)	200
I131	0.0137	5.0(18)	1.42(18)	38.5
I135	0.0137	3.34(17)	9.17(16)	70
$Xe133^m$	0.10	2.09(17)	1.53(17)	15
Xe133	0.10	4.77(19)	4.77(19)	1970
Cs134	0.0137	8.5(18)	8.5(18)	24.1
Cs137	0.0137	1.06(20)	1.06(20)	20.9

* (1.2(3)=1200)

Table 5.6 Filtration factors used in the two sequences for the single channel melt-out in an intact coolant circuit.

Time Steps (hours)	Filtration factors	
	Sequence 1	Sequence 2
0-1	0	0
1-2	0.97	0.5
2-4	0.97	0.5
4-12	0.97	0.9
12-24	0.97	0.97

rate with a "plate-out" half life equivalent to 1.6 hours. This effect can be represented by an additional plate-out rate for iodine, so $\overline{\lambda_I^p}$=0.693(0.9/180 + 0.1/(1.6*3600)) sec^{-1} after the first hour. The majority of the channel inventory will be involved within the first three hours, so it is assumed that plate-out only leaves methyl iodide in the coolant circuit with a plate out rate of λ_I^p=0.693/(1.6*3600) sec^{-1}. This is represented later by a four group deposition model to cope with the later portion of the release containing only methyl iodide, where the deposition velocity for iodine is reduced to 1mm/sec. while that for the other halogen, bromine, is unchanged.

It is further assumed that measures are taken to reduce the atmospheric release of radionuclides after the initial hour. This is modelled by assuming that filtration factors (Fl) can be applied to the release from the reactor. These filtration factors have been varied during the release so as to investigate the gross sensitivity of this mechanism. No filtration factors are applied to the inert gases, tritium or iodine, where the last element is the only one with plate-out reductions. The variation of filtration factors assumed during the five time steps is shown in table 5.6. In addition the second time step was assessed with a filtration factor of 0.9. A major assumption in the simple filtration model is that all daughters of isotopes which are produced by radioactive decay of parent isotopes on the filters immediately resuspend and escape directly to the atmosphere. This will act as a delaying term in the release of a fraction of the later isotopes in decay chains, but without reduction by that daughter's filtration factor or leakage rate from the containment.

Release fractions of the fission products have been taken from several sets of recommendations in an attempt to provide a wide selection range for input data. It is known that uranium dioxide crystal matrix does not retain fission products well above about 1500° C to 1700° C, depending on irradiation and physical damage. Table 5.7 contains the release fractions used in this case of a single channel melt-out. The complete melting of the fuel is represented by the high, 99.9%, release fractions for the inert gases, tritium and the halogens. The results of experiments show a tendency for the releases of tellurium and

Table 5.7 Release fractions for a notional channel melt-out in an AGR

Elements	Release Fraction
Kr, Xe, I, Br, H^3	0.999
Te	0.99
Cs, Rb	0.966
Ru	0.791
Ge, As, Se, Cd	0.8
Ga, Mo, Tc, Sn, Sb, In	0.2
Ba	0.029
Sr, Ag, Pd, Rh, Y, Zr, Nb, Zn, La, Ce, Pr, Nd, Pm, Sm, Eu, Gd, Tb	0.006

the alkalis to be slightly lower ((53)(44)), as in table 5.7. In a carbon dioxide atmosphere a 79.1% release of ruthenium has been measured, (53) and has been extended to cover other elements of a similar volatility. This high release fraction for ruthenium suggests a non-reducing atmosphere which explains the low release fractions for barium (2.9%) and strontium (0.6%) reported from the same source. Non-volatile elements have been given the same release fraction as strontium. A group of elements of intermediate volatility are assumed to be released at a level of 20%. The comparatively high volatility of ruthenium oxides has been considered in the process of assigning release fractions to elements without widely reported experimental basis.

Any actinides escaping from the fuel would have a release fraction similar to that of the rare earths, as an upper limit in most cases. Radioisotopes of radon, a heavy gas, could be an exception to this, but only Rn222 has an appreciable half life, which is slightly less than four days. Evidence from test rigs suggests that the actinides rapidly plate-out on any relatively cool surfaces within the coolant circuit. As the coolant circuit is intact, it is assumed that negligible actinide activity escapes to the atmosphere. This may not be the case if a depressurisation occurred with fuel melting, but this is dealt with in more detail in the description of the fourth notional AGR accident.

Gross releases of selected isotopes from this notional accident, spanning twenty four hours, are given in table 5.8 for the two complete sequences of different filtration parameters. The release of inert gases, and long lived isotopes of iodine without significant precursors, are not affected by the filtration factors, due to the effective circuit behaviour modelling already described. The other isotopes show releases which are increased about three times in the case with low filtration efficiencies. The large release of inert gases results from two factors. The first is the high release fractions combined with a null effect by the filters. The second is that some inert gas isotopes have precursors which are more abundant in the irradiated fuel than these isotopes, such as with I135 and Xe135, where the immediate precursor is contained within the reactor. In the case of I135 92% decays to Xe135 within 24

Table 5.8 Activity released by the two sequences of filtration on the single channel (notional) melt-out with an intact coolant circuit

Isotopes	Total Channel Inventory(kCi)*	Released Activity (Ci)	
		Sequence 1	Sequence 2
$Kr85^m$	35	230	230
Kr85	2.0	57	57
Sr90	15	0.098	0.29
Ru103	170	150	450
Ru106	70	62	180
$Te129^m$	8.4	9.4	28
$Te131^m$	19	17	55
Te132	180	190	620
I132	190	3100	3100
I131	130	17	17
I135	240	23	23
Cs134	22	24	72
Cs137	19	21	63

*At time of initial shut-down

24 hours, so the major portion, over 70%, of Xe135 is due to production after shutdown of the reactor. This phenomenon is of more importance in the control of reactors due to the very high thermal neutron capture cross-section ("reactivity poisoning" effect) of Xe135.

This notional accident sequence releases only about 17 Ci of I131, but of order 20,000 Ci of inert gases and other fission products with half lives of at least several hours. Also released are quantities of long lived caesium isotopes (Cs134, Cs137), where the escape may involve more than about 100 Ci of each when poor filtration efficiencies are assumed. Ruthenium isotopes, such as Ru103, and Ru106, can be released in quantities of the order of or greater than 100 Ci, with a similar release of Te132 (the precursor of I132). This leads to a more complex dose pattern resulting from the dispersion in the atmosphere of this release compared to that of either of the previous multi-pin failure cases.

Section 5.2.4 Notional single channel AGR melt-out associated with a major depressurisation.

This major depressurisation case involves the same amount of fuel as the previous case described in section 5.2.3, where the same release fractions are used but combined with a much shorter release period. This assumes the atmosphere in the fuel channel is non-reducing, so depressing the releases of strontium relative to ruthenium. The likelihood of this type of accident is probably of such remoteness that any detailed changes in a few of the elemental release fractions would be of little significance compared to the large uncertainties surrounding any relevant accident sequences. Plate-out of iodine and subsequent resuspension of xenon are dealt with as in the two previous major depressurisation incidents. No filtration of the escape to the atmosphere in this melt out case is assumed.

An assumption has to be made about the time scale for the whole channel to melt. The source of heat (Hd) in the shutdown reactor would be due to radioactive decay processes, which is about 5% of the operating level. The single core could contain approximately 400 channels generating a thermal power of about 1500MW. The heat generation from the release should be below

1MW so self heating plume rise can be neglected (51,52). The mass of fuel (Mc) in a single channel of seven elements is almost 360 kg with a mean specific heat capacity (C_f) of about 350 J/(kg.°K) in the temperature range of concern. The appropriate time (dt) for the fuel to melt, with a mean rise in temperature (dT) of about 1800°K is:

(5.11) $dt(secs)=dT^{*}Mc^{*}C_f/Hd$ = 1200 s (to 2sf). In the model an extension of this period to only cover that in which 80% of the fuel melts was made as a token allowance for residual cooling due to low gas flows at reduced pressures and any radiative cooling at high temperatures. Five time steps were used for this release covering a full hour: 0-480 secs; 480-1200 secs; 1200-1800 secs; 1800-2700 secs and 2700-3600 secs.

The gross releases are displayed in table 5.9; obviously this is the most severe of the notional accidents studied. The release of about 30 kCi of I131 means this is a serious accident, especially with the accompanying releases of ruthenium, caesium and tellurium radioisotopes. The release of inert gases is of the order of a few hundred thousand curies.

In this notional accident actinides could be released, where a pessimistic release fraction is similar to that for the release of strontium (0.6%). A reasonable assumption would be that the great majority of the refractory actinidies rapidly plate-out within the complex coolant circuit of the AGR. The form of these actinides could be as small particles which could be bonded together by the less inert fission product compounds. This could even lead to any radon radioisotopes being trapped within the internally deposited material. The total single channel activities of some actinides are given in table 5.10, taken from the prediction of two heavy element computer models, HYLAS(77) and HYACINTH(Harte, 1976 (84)) using the fuel irradiation history assumed previously. Also displayed are the maximum permissible air concentrations (see (84)) of the radionuclides as insoluble forms. From this table it can be observed that the hazard from any radon gas is negligible. (c.f. coal fired power stations, (9)). A significant potential hazard arises from the fissile isotopes and the transuranium elements.

Table 5.9 Activity released from the notional AGR single channel melt-out on a major depressurisation

Isotope (half-life)	Channel Inventory (kCi) at time of shut-down	Gross release (kCi)
$Kr85^m$	34.6	29
Kr85	2.0	1.8
Sr90	15	0.081
Ru103	170	120
Ru106	70	55
$Te129^m$	8.4	8.2
$Te131^m$	19	18
Te132	180	170
I131	130	34
I135	240	62
Cs134	22	21
Cs137	19	18
Ba140(12.8 d)	220	6.1
Ce144(284 d.)	160	1.0

Table 5.10 Heavy element inventories in an AGR

Isotopes	Channel Inventory (Ci)		MPC of insoluble particles in air (Ci/m^3)
	HYLAS predictions	HYACINTH predictions	
Rn222	(not in model)	2.2(-11)	1.0(-8)
U238	1.0(-1)	1.0(-1)	5.0(-11)
U239	2.3(6)	2.2(6)	1.0(-9)
Np239	2.3(6)	2.2(6)	2.0(-7)
Pu238	1.6(2)	1.8(2)	1.0(-11)
Pu239	6.0(1)	5.8(1)	1.0(-11)
Am241	3.0(1)	3.0(1)	4.0(-11)
Cm244	5.0(1)	7.5(1)	3.0(-11)

Table 5.11 shows the values of rem/Ci (inhaled) for some actinidies (6). Curium-244 only builds up significantly in high, hard neutron flux, as in FBR's rather than AGR's. Only uranium, plutonium and neptunium have been reported as being released from molten fuel in test rigs: usually only traces escape the high temperature regions. Using the channel inventories from table 5.10 for Pu239 and applying pessimistically the release fraction of strontium, about 0.4 Ci of Pu239 could be released to the atmosphere. This has to be compared to the releases of 80Ci of Sr90 and about 20 kCi each of Cs134 and Cs137. For the same breathing rate and dispersion conditions the relative doses after 50 years (6) to the endosteal bone surfaces, red bone marrow and the lung are shown in table 5.12. Doses from Pu238 and Cm244 could be larger than those of Pu239, but only by a factor of about two. The tissue most sensitive to these actinides appears to be the endosteal bone surfaces, but no significant errors would be brought into the description of the inhalation dose commitments of this notional accident by neglecting potential actinides releases. External exposures would not be affected by neglecting these actinides due to the dominant release of Cs137 which sets these levels for many decades.

Any plutonium which did escape to the atmosphere may be expected to be in the form of a heavy aerosol which has a high gravitational settling velocity, as the material may have densities similar to that of uranium dioxide (10 gm/cm^3). This would severely limit the extent of its dispersion in the atmosphere, so restricting doses, although there would be hazards in any decontamination work. This would also apply to any "clean up" operations taken against deposits of fission products, but this is not dealt with when considering these releases in the next section.

Section 5.3 Doses and exposures from four notional AGR accidents

Atmospheric conditions can be parameterised by Pasquill dispersion categories. This allows mean time integrated air concentrations to be calculated. These lead to inhalation doses which may be related to appropriate actions. Comparisons can

Table 5.11 Organ dose sensitivities for heavy elements (Kelly et al)

Isotopes	Organ sensitivities (rems(at 50 years)/Ci(inhaled))			
	Lung	Red bone marrow	Endosteal (bone) surfaces	Thyroid
Pu238	5.9(7)	1.2(7)	1.6(8)	1.9(6)
Pu239	6.0(7)	1.4(7)	1.8(8)	2.2(6)
Cm244	3.6(6)	1.9(7)	2.4(8)	2.9(6)
Np239 (oxide form)	1.6(1)	3.8(0)	4.8(1)	5.9(-1)
Am241	3.4(6)	3.8(7)	4.8(8)	6.0(6)

Table 5.12 Comparison of "relative" doses due to heavy elements and to long lived fission products for a release from the fuel in a single channel melt-out.

Isotope	Release Fraction	Released Activity (Ci)	Relative Doses (Kelly et al.) (i.e. Dose sensitivity* Released activity (10^8))		
			Endosteal bone surface	Red bone marrow	Lung
Cs134	0.966	21000	7.6	8.4	8.4
Cs137	0.966	18000	4.9	5.0	5.4
Sr90	0.006	81	2.3	2.3	0.01
Pu239	(0.006)	0.4	0.7	0.06	0.24

be made to Emergency Reference Levels (ERLs), set by the MRC (34) for use in the U.K. and to the recommendations of ICRP 26. Table 5.13 gives the ERLs currently applicable in this country, where the doses also apply to dose commitments. These are intended to be limits where action may be taken if a significant reduction in total risk can be achieved but are not absolute dose limits. The ICRP 26 recommendations for exposure of members of critical groups of the public are stricter requirements, for annual doses, with limits at 0.5 rem (whole body) for risk limitations in stochastic dose ranges and 5 rem (any organ or tissue) for prevention of non-stochastic effects.

Use of the present deposition model allows estimates of ground contamination to be made. These levels can be compared to Derived ERLs (Baverstock and Vennart (55)), see table 5.14, for the pasture-cow-milk ingestion dose pathway. External gamma and beta exposures received over an extended period after the accident may also be compared to the relevant limits. The consequences of the two accidents involving twenty pins will be dealt with separately from those involving the melt out of a single channel. The three depressurisation releases have a three group dry deposition model applied to represent plume depletion with a mixed release of elemental and other forms of iodine. The deposition velocities are shown in table 5.15. The prolonged release, over a whole day, from a single channel melt out contained in an intact pressure circuit is dealt with in more detail, as briefly described earlier.

Section 5.3.1 Cloud doses from failure of twenty pins on a major depressurisation

Temporal characteristics of the release will be discussed initially, after which the dose dependence on downwind travel is considered. Comparisons will also be made between the numerical estimate of the cloud gamma exposure and that of the semi-infinite cloud approximation.

Atmospheric dispersion is assumed to be that of average Pasquill category D weather with a mean windspeed of 5 ms^{-1}. The horizontal Gaussian dispersion parameters for category C are used as the release is extended over a period larger than

Table 5.13 ERL's in the U.K. (MRC)

ORGAN	ERL Dose (rems)
Whole body	10 (or 15 Roentgens in dry air)
Gonads	10
Bone:	
Red marrow	10
Endosteal surfaces	30
Lung	30
Thyroid	30
Superficial tissue (e.g. beta irradiation)	60
Any other tissues or organs	30

Table 5.14 DERL's for ground contamination giving doses via the pasture-milk food chain (MRC, Baverstock and Vennart, 1976)

Isotope	DERL (microCi/m^2)		Critical Organ
	Adult	Infant (6 months)	
Sr89	6400	190	Bone marrow
Sr90	26	6.6	Bone marrow
Cs137	36	18	Whole body
I131	27	1.8	Thyroid

Table 5.15 Deposition velocities used in the grouped element dependent deposition model

Elements	Deposition velocity cm/sec
Kr,Xe	0.0
I,Br(average)	1.2
All others (aerosols)	0.3

about 10 minutes (15), (53). The dispersion parameters used give mean values of time integrated concentrations. No allowances have been made for any effects of building induced turbulence, although it is assumed the release occurs at ground level. An inversion layer is not explicitly modelled, but as the dispersion parameters rely on validation from experiments an averaged effect on the cloud dosage is implicitly assumed in these calculations. Detailed surface roughness effects have not been considered in the description of the dispersion estimates in this study.

From the accumulation of time integrated air concentrations at a given point downwind of the release the build up of potential inhalation dose commitments can be estimated. An average breathing rate of $2.32.10^{-4}$ $m^3.s^{-1}$ has been assumed to apply when using equation 5.1 to convert time integrated air concentrations to dose commitments.

Examples of the internal time structure of releases are given in figure 5.1 for ground level on axis lung and thyroid dose commitments, 1 km downwind of the source for both releases. In each case the effect of iodine plate-out on the thyroid dose commitment, with an effective half life of 3 minutes, can be seen. Within about fifteen minutes of the start of the release the thyroid dose commitment is levelling off sharply, while that for the lung is still increasing but at a decreasing rate due to the depressurisation tailing off with a half life of 9 minutes. There appears to be no major differences resulting from the different rates of fuel involvement used in these cases. After half an hour the ratios of both the thyroid and the lung dose commitments are about 2.96:1, reflecting the factor of three introduced between the release fractions for elements, other than inert gases, in these incidents. Similar effects can be seen in figure 5.2 for the on axis ground contamination by I131 and Cs137 one kilometre downwind of the source.

Numerically calculated cloud gamma (Roentgens in dry air at STP) and cloud beta (rads in air) exposures are given in figure 5.3 where these apply to an on axis ground level exposure point 1 km downwind. The cloud beta exposure is based on local air concentrations, reflecting the short range of beta particles in air. After half an hour the ratios of the

Fig. 5.1 Build up in time of on-axis inhalation dose commitments 1 km downwind of the notional AGR accidents 1 and 2 dispersing under prolonged neutral conditions.

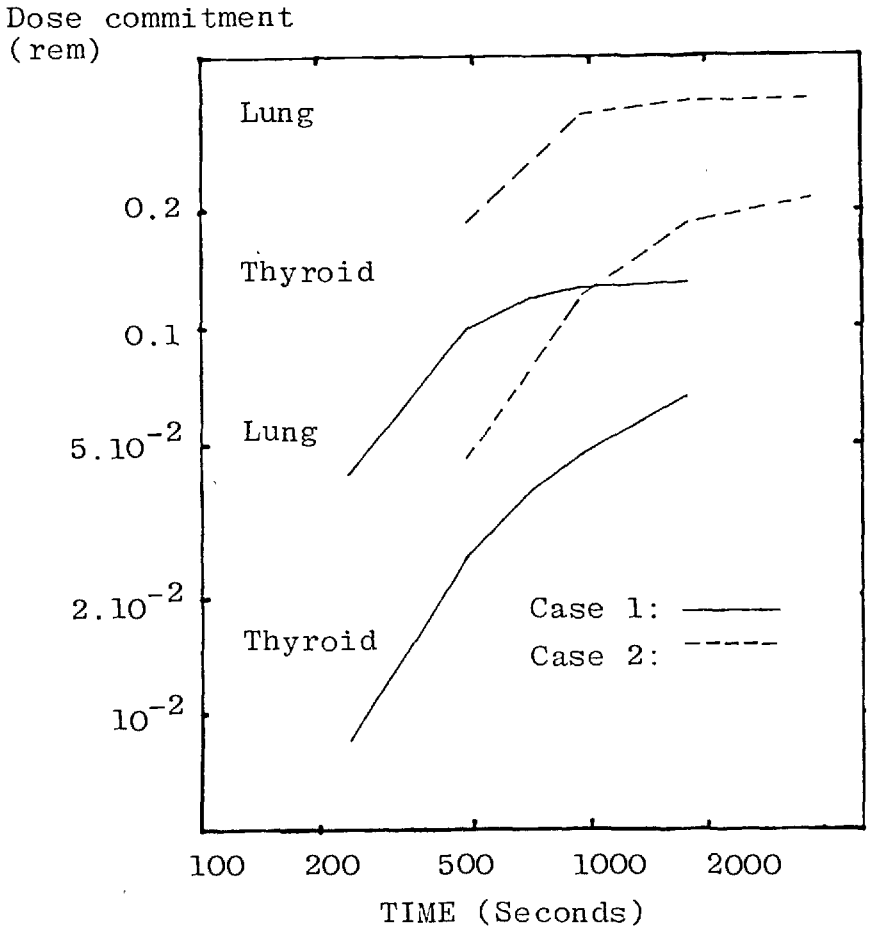

Figure 5.2 Building up in time of on-axis ground contamination 1 km downwind of the notional AGR accidents 1 and 2 dispersing under prolonged neutral conditions.

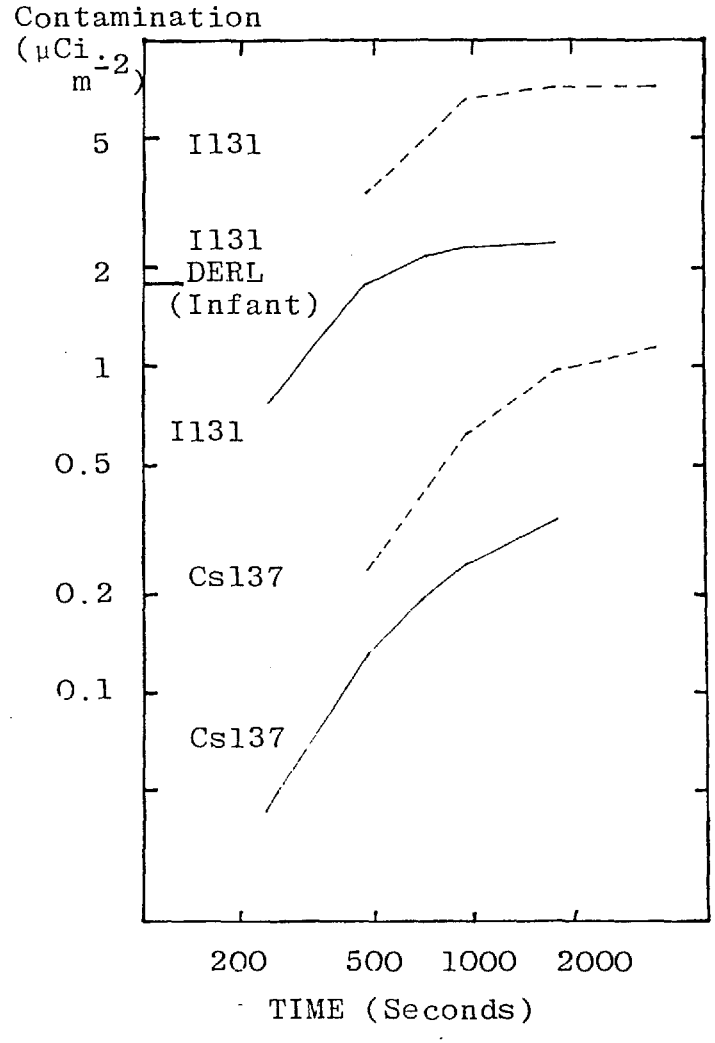

Figure 5.3 Build up in time of on-axis external cloud beta and gamma exposures in air 1 km downwind of the notional AGR accidents 1 and 2 dispersing under prolonged neutral conditions.

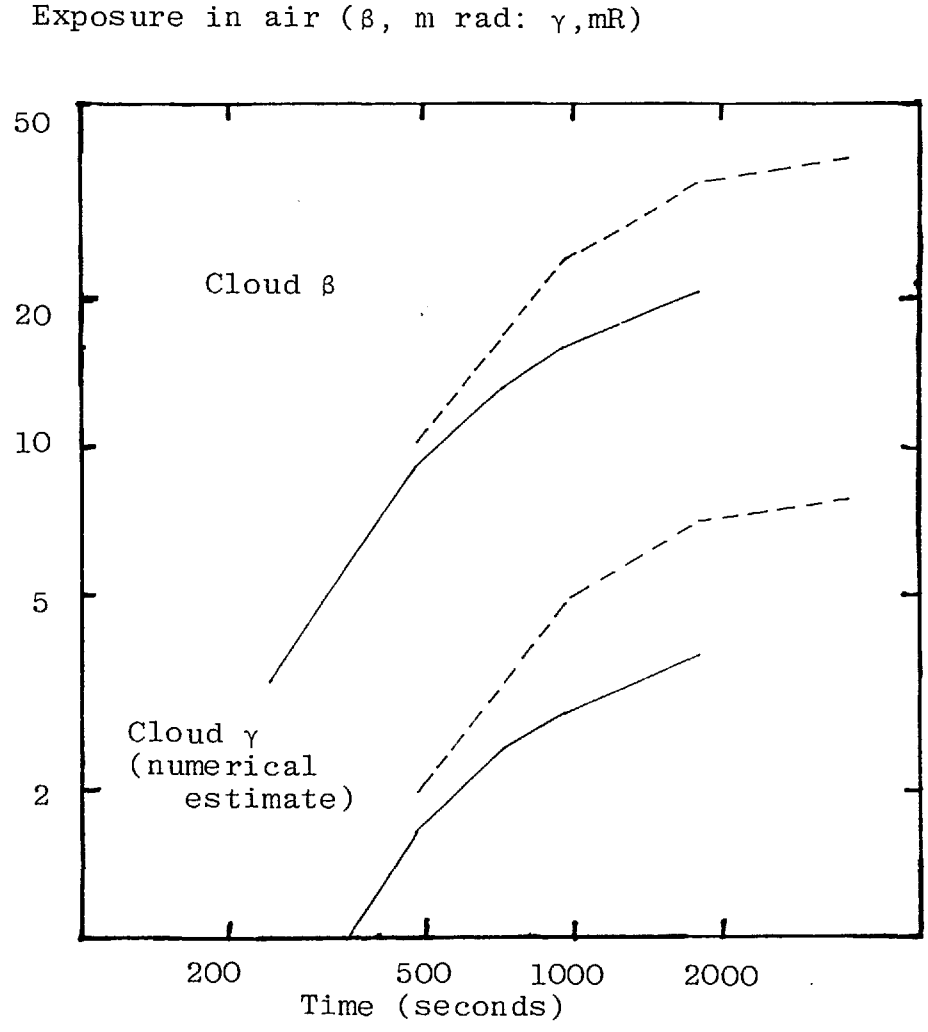

Figure 5.4 Downwind dependence of initial on-axis ground contamination due to the notional AGR accidents 1 and 2 dispersing under prolonged neutral conditions.

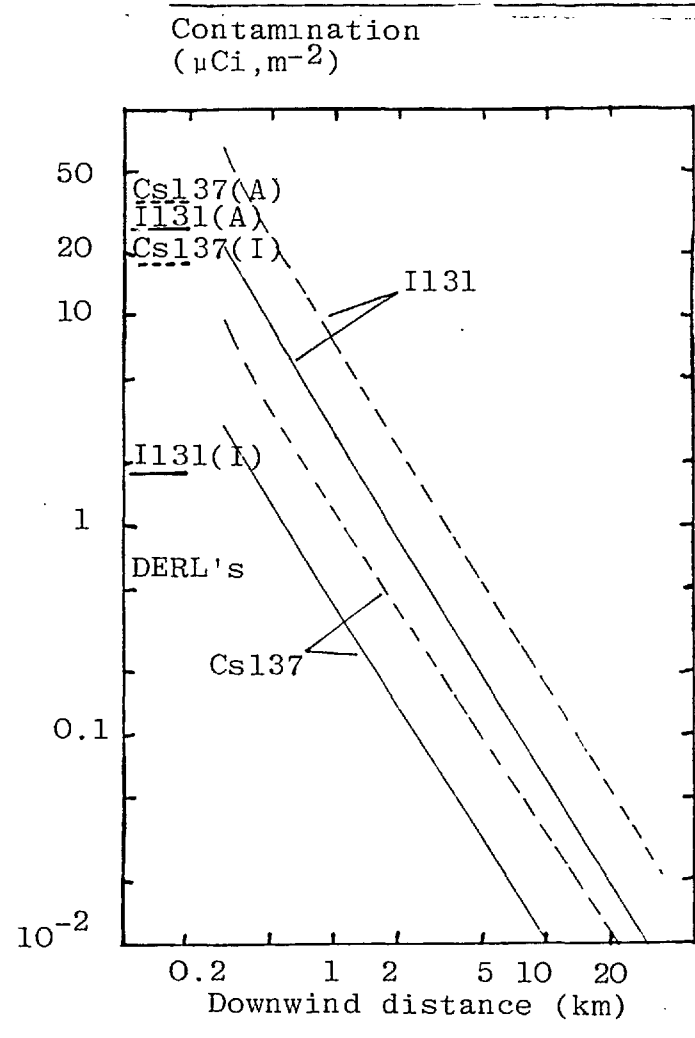

two releases for cloud gamma and cloud beta are 2.08:1 and 1.85:1 respectively. This shows that the inert gases contribute, as could be expected, more to these cloud exposures than to organ dose commitments where the relative increase in inert gas release fraction was only 1.67:1 rather than 3:1 for non-gaseous fission products. Also the cloud beta exposure is dependent slightly more on the inert gas component of the release than the cloud gamma exposure.

The downwind distance dependence of each of the on-axis inhalation dose commitments, cloud exposures and ground contaminations has been studied for these two releases. Predicted mean ground contaminations can most readily be compared to DERLs for these accidents. Figure 5.4 shows the on axis downwind distance dependence of I131 and Cs137 contamination compared to the adult and infant DERLs for the pasture-milk-food dose pathway. Here caesium ground contamination is unlikely to be a problem beyond the site boundary of a few hundred metres, for either release. Iodine-131 ground contamination, with respect to adults, would only be of slight significance in the larger of the releases within a downwind range of about ½ km under neutral dispersion conditions. The infant's DERL for I131 is more restrictive and contamination at levels above this value extend to downwind distances of about 1.3 km and 2.4 km for the simple and more prolonged twenty pin failure releases respectively. In the latter case the DERL is not exceeded at the 10% plume boundary beyond about 0.6 km downwind where the crosswind plume spread is about 0.265 km. This gives an estimate of the area of I131 contamination above the infant's DERL as approximately 0.32 km^2 (80 acres). The loss of production from this area of farm land is unlikely to be of significance in the supply of milk to the local or regional population.

The gross releases, described in tables 5.4 and 5.5, dispersing in the atmosphere under neutral category D weather are unlikely to produce unacceptably high levels of risk from inhalation dose commitments. The two largest single organ dose commitments are to the thyroid and lung, where these are generally about an order of magnitude greater than any other single organ inhalation dose commitment, including the "total body" internal irradiation dose.

These two organ doses, to the thyroid and the lung, are given in figure 5.5 for ground level on axis dose points at various downwind distances. No ERLs are exceeded, on average, by either release under these dispersion conditions beyond site boundary of about 200 metres. Even 300 metres downwind the mean on axis weighted inhalation dose commitments from the greater of the two releases produce an equivalent whole body dose of 0.471 rem, which is very close to the ICRP annual limit of 0.5 rem to members of the public: the "whole body" dose could just exceed this annual limit when the external cloud gamma exposure, of 0.026 R (numerical) to 0.24R (semi-infinite approximation), is considered, as these give extra whole body contributions of about 0.015 rem to 0.14 rem (33). The non-stochastic ICRP limit of 5 rem per year to any single organ probably will not be exceeded under neutral conditions beyond about 200 metres and then only for the thyroid dose commitment resulting from the larger release.

If the releases were to occur in stable Pasquill category F conditions (with the horizontal dispersion parameters for a short release) with a typically low windspeed of 2 metres/second, there is an increase of on axis cloud concentrations at short distances but predicted depletion from the narrower plume can reduce long range concentrations even with the low deposition velocities given in table 5.15; where $Q^*=0.38$ one kilometre downwind for $v_g=1.2$cm/sec in stable conditions. Beyond 10 km this may not accurately reflect the characteristics of say I131 if this was released in several different forms, unlike I132 produced mainly in the plume. . The smaller of the two releases is unlikely to lead to inhalation doses exceeding the relevant ERLs, while the greater release could produce organ doses close to these levels for the thyroid and lungs within about 300 metres downwind (see figure 5.6). Beyond 1 km the lung becomes the most irradiated single organ.

Uncertainties in the dose sensitivity of the lung to certain isotopes are not of major importance in these releases. In the later stages of the release, particularly in stable conditions when iodine is severely depleted far from the source, uncertainties of the dose delivered by Te132 to the thyroid may not be negligible.

Figure 5.5 Downwind dependence of initial on-axis inhalation dose commitments due to the notional AGR accidents 1 and 2 dispersing under prolonged neutral conditions.

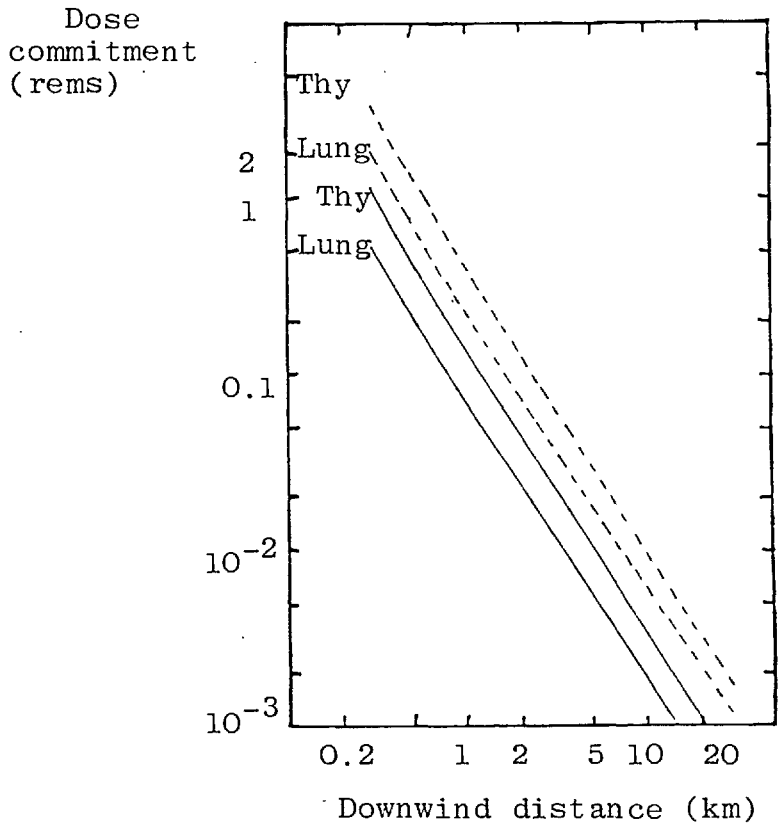

Figure 5.6 Downwind dependence of on-axis inhalation dose commitments due to a notional AGR accident 2 dispersing under stable short time scale conditions.

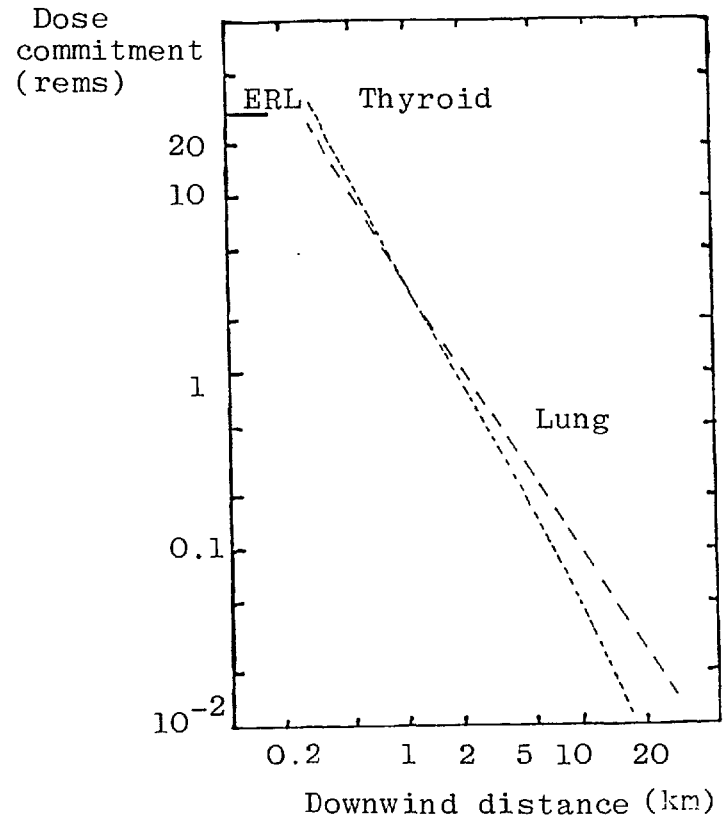

High levels of ground contamination could extend to about 6 km, see figure 5.7, but meandering of the plume in stable conditions could produce major local differences. Also, the contaminated area above DERL's, assuming a straight path under these non-dispersive conditions, is about 0.46 km^2 (115 acres) which is about a 50% increase over the equivalent area for neutral conditions. If the release occurred from a low stack a larger area might be contaminated but at lower levels. Also shown in figure 5.7 is the initial contamination due to I132, half life of 2.3 hours. This isotope is the comparatively short lived daughter of Tel32, half life of 78 hours, so under these conditions and deposition model most of the I132 beyond a few kilometres is produced in the plume. This is a demonstration of the relative increase of I132 contamination to that of both I131 and Csl37 due to the differences between the sources noted upon earlier (see Chapter 2).

For dispersion under stable conditions the whole body ICRP annual limit, for doses in the stochastic range of 0.5 rem would be exceeded at 1 km where the weighted whole body dose is 0.73 rem excluding 0.052 R to 0.43 R external cloud gamma exposure, for the larger pin failure release. Also the non-stochastic limit of 5 rem to any single organ would probably be exceeded under these stable conditions for both the thyroid and the lung to about 1 km in either of these notional ground level releases.

In figure 5.8 the downwind distance dependence of the cloud gamma and cloud beta exposures dispersing under category D weather conditions, as used for figures 5.4 and 5.5, are displayed. Even close to the reactor the ERLs are not approached. The cloud beta dose would be given primarily to any uncovered portions of the skin as well as the eyes, where clothing can provide effective shielding against beta radiation. The cloud gamma exposure can be estimated by a numerical calculation, using $2*9^3$ sampling points for an on axis exposure point and 9^3 for off axis exposure points, or a semi-infinite estimate based on the local gamma activity of the time integrated air concentrations. No allowance in either calculation has been made for the presence of the ground (see chapter 3). From figure 5.8,

Fig. 5.7 Downwind dependence of on-axis initial ground contamination due to a notional AGR accident 2 dispersing under stable short time scale conditions.

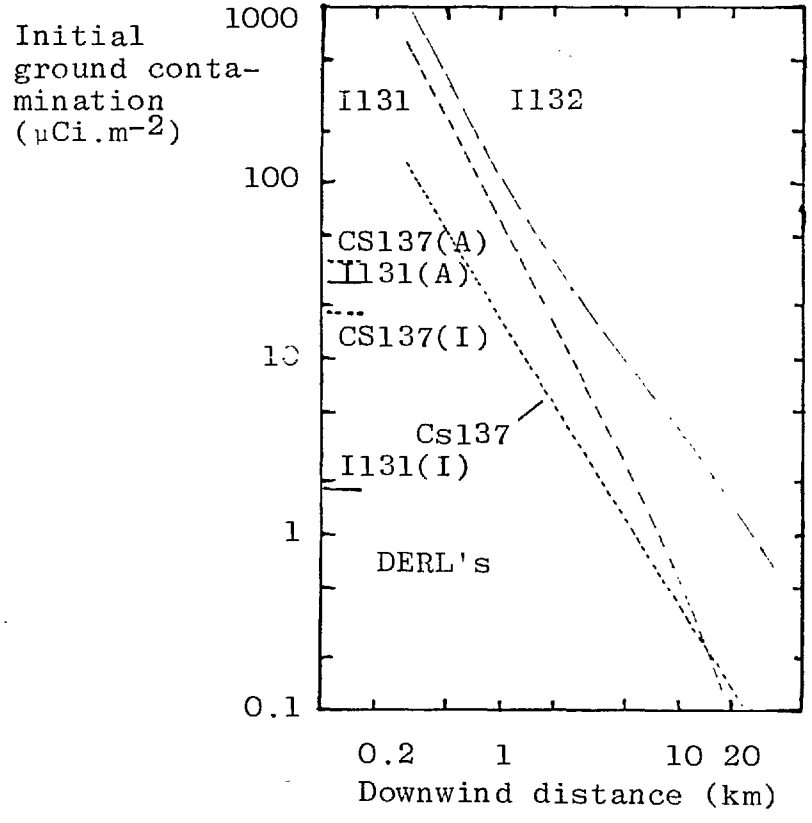

Fig. 5.8 Downwind dependence of initial on-axis external cloud exposures due to the notional AGR accidents 1 and 2 dispersing under prolonged neutral conditions.

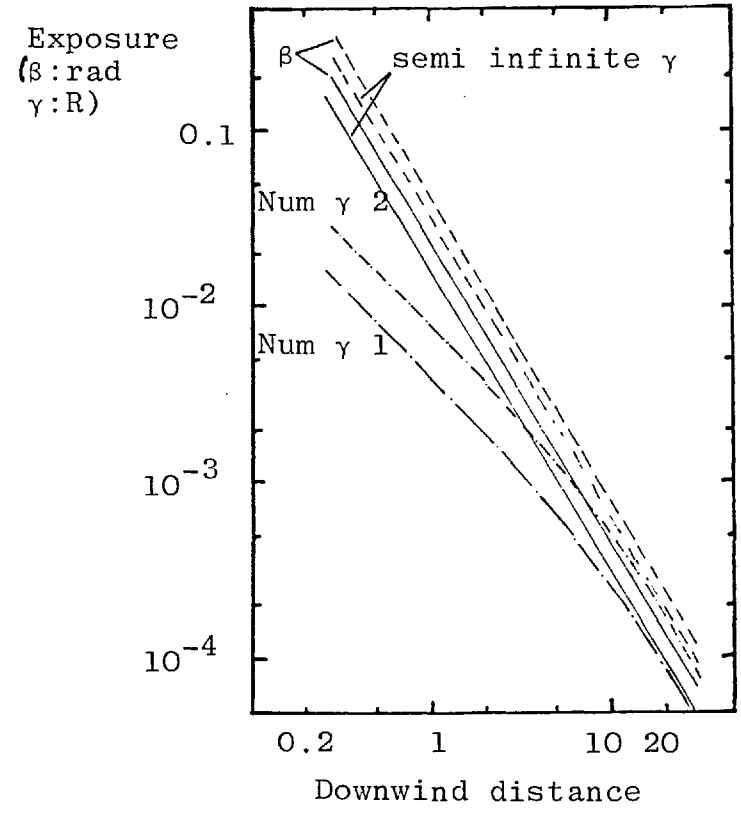

Figure 5.9 Downwind dependence of on-axis cloud gamma and beta exposures in air due to a notional AGR accident 2 dispersing under stable short time scale conditions.

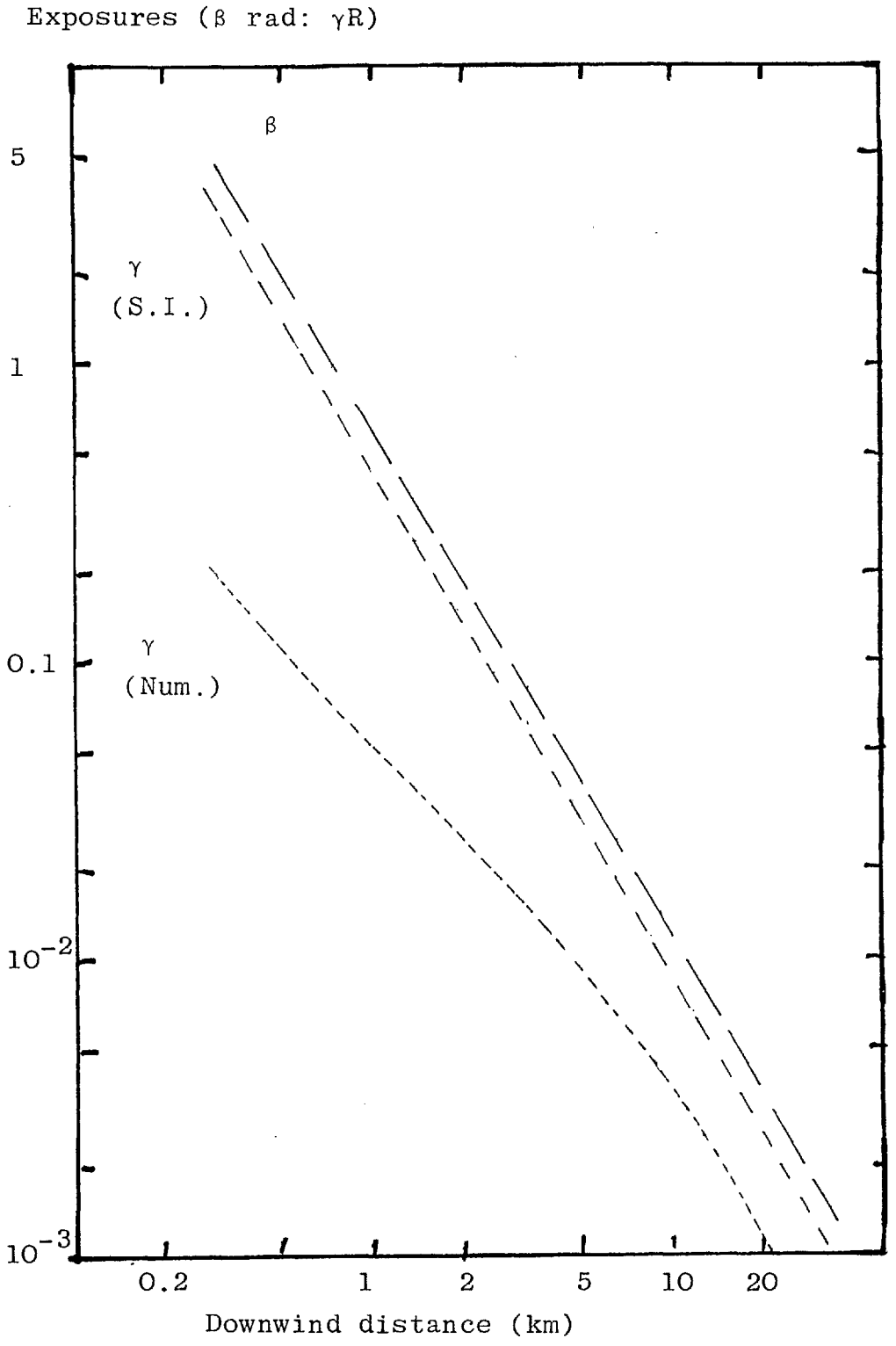

for both releases, the numerical cloud gamma estimate is always the lower, representing the leakage of photons from the finite plume. This difference, as expected, is larger at short distances where the plume is smaller, with dimensions similar or less than the mean free paths of gamma rays in air (typically 100m to 200m for energies of 0.5 MeV to 2MeV). For example, under these neutral conditions, at about 30 km downwind the plume is 9.5km wide and 0.3km high, while at 1 km downwind these dimensions are 440m and 70m respectively. For category F stable conditions these two dimensions are respectively, 2.9km and 0.13km at 30km downwind and only 140m and 30m, one kilometre from a ground level source. Figure 5.9 shows the expected greater difference between numerical and semi-infinite estimates of the cloud gamma in less dispersive conditions to those of figure 5.8.

To recap, only a severe release of volatiles from a failure of the cladding of twenty pins on a major depressurisation could lead to inhalation dose commitments greater than present ERLs, close to a site boundary several hundred metres downwind, and then only for a ground level release under stable conditions with poor dispersion. Iodine-131 contamination of pasture could be a problem under neutral dispersion conditions and become more extensive if stable conditions occurred at the time of the release. External cloud gamma and beta exposures are not significant when compared to these other factors for the dispersion conditions considered. External exposures from deposited materials will be considered in the next section.

Section 5.3.2 External Exposures due to ground contamination from clad failure incidents

In these clad failure depressurisation incidents the plume of airborne radionuclides takes a matter of about an hour to pass any given downwind exposure point. A deposit is left on the ground and other obstacles which may only be a small fraction of the plume material but is resident, and delivering exposures, in that locality for a time long compared to that of the passage of the plume. In this study exposures 1 m. above a smooth plane of this deposit have been calculated neglecting any shielding effects of ground roughness. The ageing of the deposit during the first year is considered, but allowances for weather-

ing or other redistributions of the material are not made. This restriction is imposed as it would be very difficult to follow all the pathways affecting doses in the environment, and would involve many problems beyond the scope of this study of the immediate impact of active releases to the atmosphere.

As the releases have been broken into time segments, or steps, this enables the gamma exposure rates from the ground deposites to be studied during the release period. The implications of this are demonstrated for the lesser clad failure release under neutral dispersion conditions. No exposure rate from ground activity is calculated during the initial step of the release. All the time integrated release from the first step is allowed to escape in this model at the end of this first step. Hence at the start of the second period the exposure rate from the modelled deposit is an overestimate (see figure 5.10), as no decay has been allowed while the time integrated release for the step is accumulated. By the end of the second period the exposure rate is an underestimate as the contribution from the second stage of the release is not included until the start of the next period. During the release this model can be used to set upper and lower bounds to the mean exposure rates from ground deposits. After the final release the estimate is an upper bound but will return to a 'true' mean value after a period sufficient to allow the transient effects of the stepped release to decay. The transients will extend for a time scale which depends on the steps used and the isotopes released, and should not be more prolonged than several times the release period, provided the steps are not too large.

Both the external beta and gamma exposure rates 1 km downwind for the two clad failure accidents are shown in figures 5.10 a and b respectively, to an ageing time of one year after dispersion in neutral conditions. The steps bound the exposure rates quite closely during the time in which the releases are assumed to occur. The maxima occur towards the end of the release giving exposure rates for the two cases (a) 1.1 mR/hr, (b) 3.2 mR/hr and ($_a$)7 mrad/hr, (b) 20 mrad/hr for ground gamma and beta exposures respectively. From inspection of the curves in these cases the transient effects of the stepped releases are expected to be minimal within three hours of the end of the release.

Figure 5.10a Effects of decay on external ground exposure rates for up to one year after a deposit is formed on-axis 1 km downwind of a notional AGR accident 1 dispersing under prolonged neutral conditions.

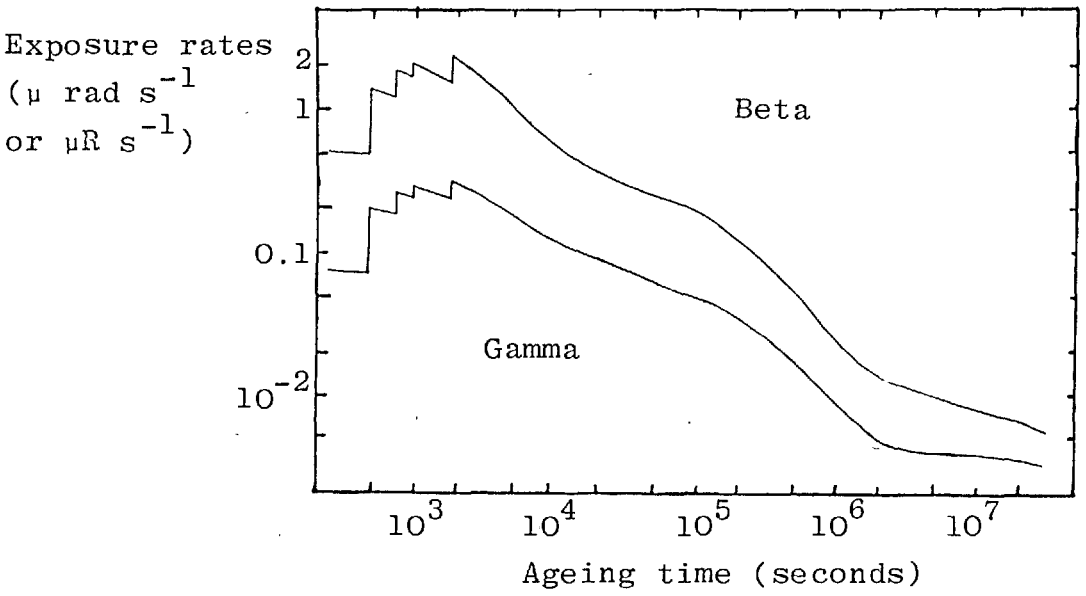

Figure 5.10b Effects of decay on external ground exposure rates for up to one year after a deposit is formed on-axis 1 km downwind of a notional AGR accident 2 dispersing under prolonged neutral conditions.

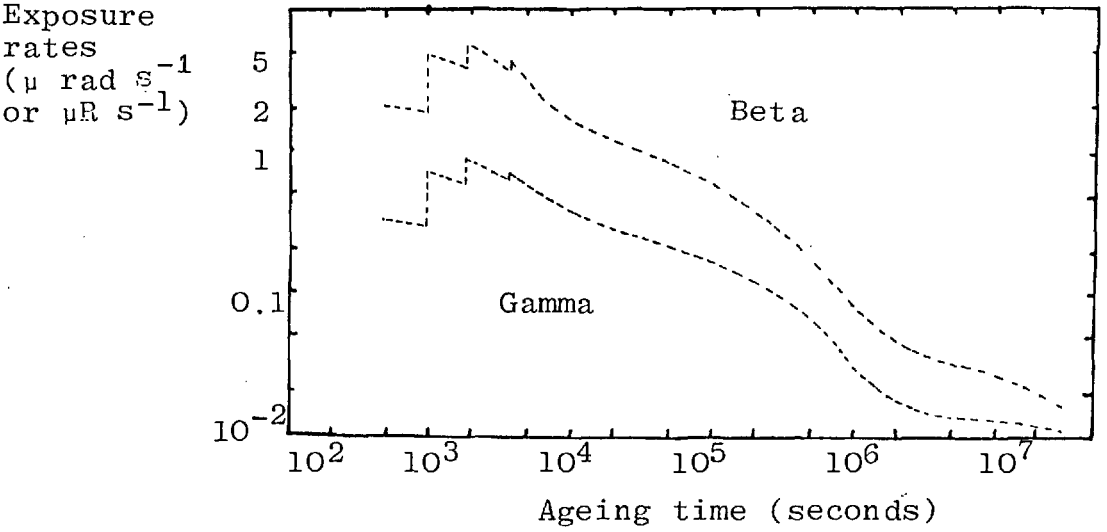

At short times the build up in time of these exposures from ground sources will be affected by the stepped releases. No activity is lost by this process, only its time of release and subsequent decay is altered. The total exposure from these sources, after a suitably long period, should accurately reflect the expected time dependence of this quantity. Figure 5.11 displays the time dependence of on axis external gamma and beta exposures for the lesser clad failure accident 1 km downwind with neutral dispersion conditions. This shows that exposures from deposited sources can exceed the relevant cloud exposures after about eight hours of the start of the release. After one year of decay the ground deposits have produced an exposure possibly over twenty times that of the cloud if no modifying factors are introduced. In this release the mean on axis external ground gamma exposure will probably not exceed about 0.15 R 1 km downwind under these neutral dispersion conditions. Also after cooling for about one year the beta exposure rate appears to be falling more rapidly than that due to gamma activity. This depends on the type of release considered (e.g. Clarke). The plateau in the gamma exposure rate reflects the quantities of long lived caesium isotopes released.

The downwind distance dependence of the mean on-axis ground exposure after one year ageing is shown in figure 5.12 for this lesser pin failure release under neutral conditions, along with the two cloud gamma estimates. From this it can be seen that the ground gamma exposure does not decrease as rapidly as the cloud gamma downwind. Several factors contribute to this effect. One is that many short lived isotopes can contribute significantly to the cloud exposure at short downwind distances, but give negligible contributions to the ground exposure after a year. Not only is this due to the short half lifes but also to comparatively poor deposition rates, such as for Kr88, $Xe133^{m}$ and $Te133^{m}$.

At short distances the size of the plume can limit the sources of cloud gamma exposures relatively more than those giving ground gamma exposures. The on axis cloud gamma has a large spatial range of source positions which can contribute significantly while the on axis ground exposure has a much more limited geometry, so is less affected by the plume dimensions.

Figure 5.11 Accumulation in time of on-axis cloud and ground external exposures 1 km downwind of a notional AGR accident 1 dispersing under prolonged neutral conditions.

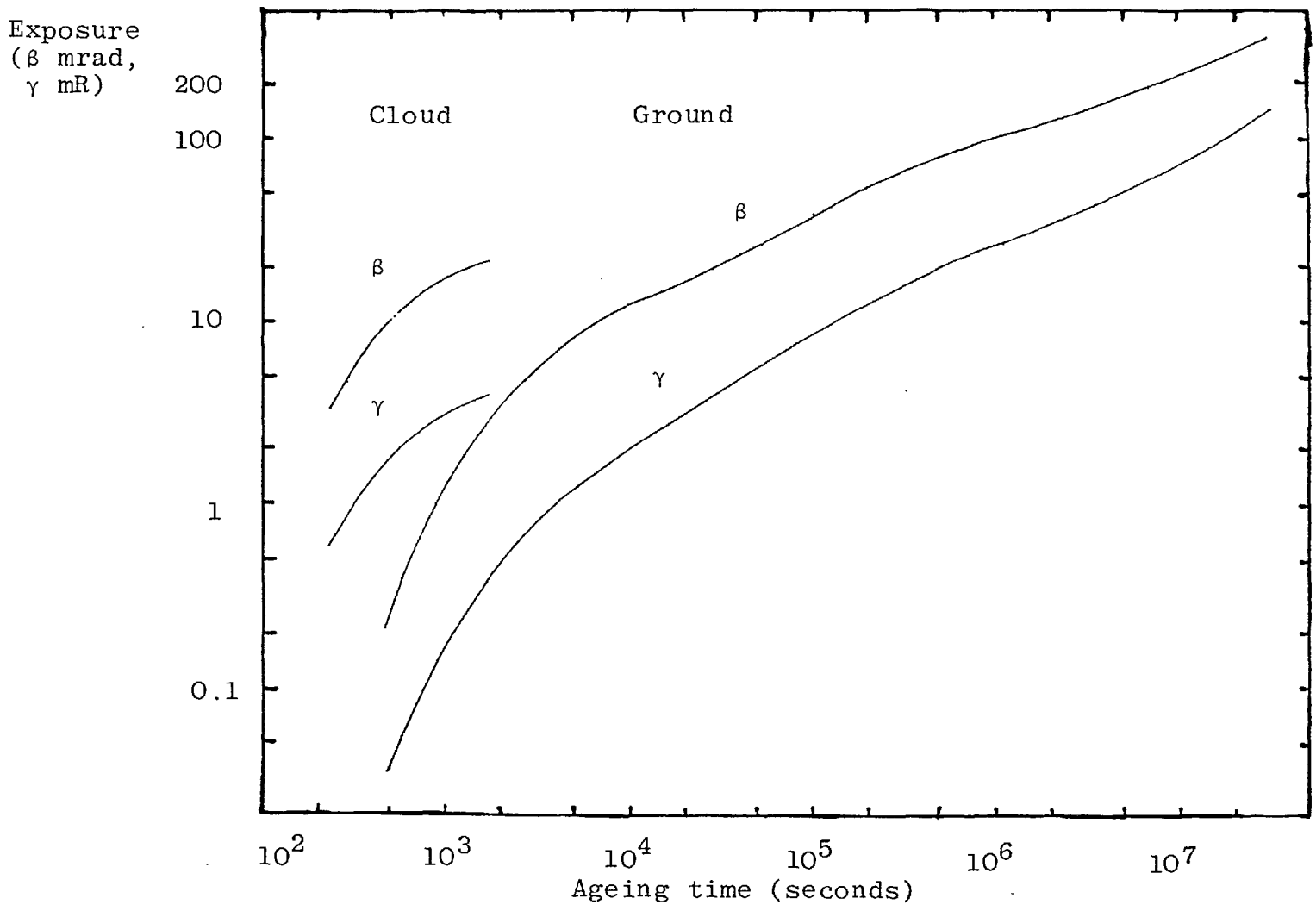

Figure 5.12 Downwind dependence of on-axis total cloud gamma and ground gamma (after 1 year) external exposures from a notional AGR accident 1 dispersing under prolonged neutral conditions.

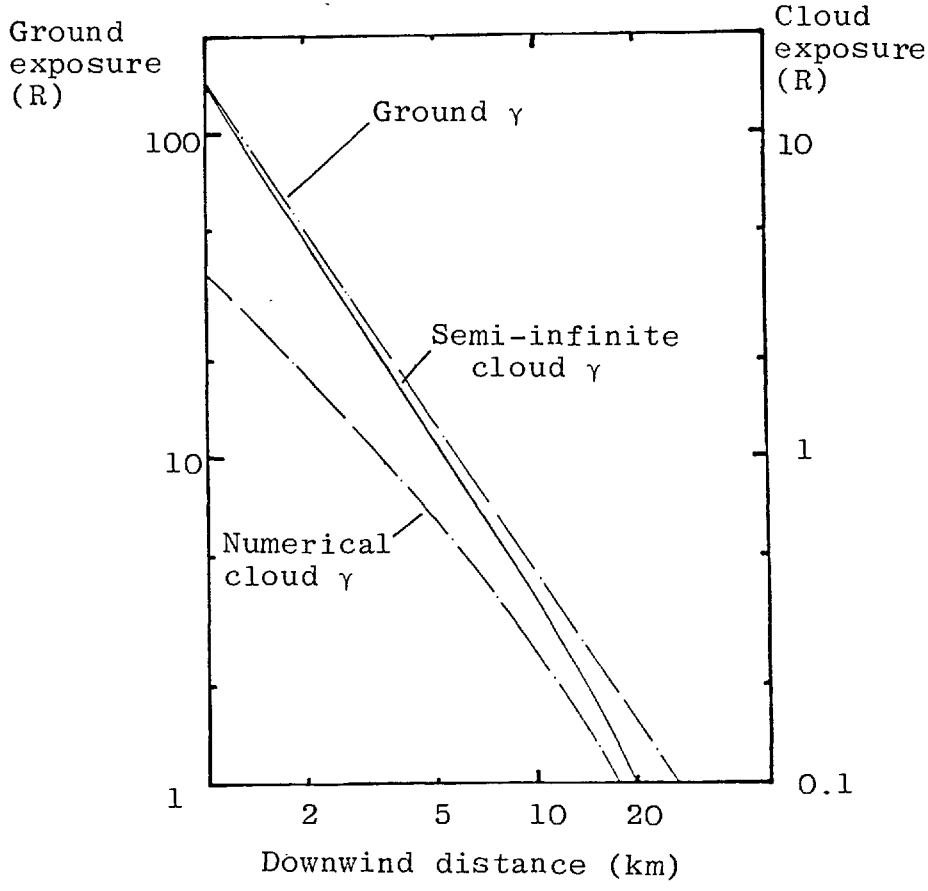

Figure 5.13 Downwind dependence of on-axis total cloud gamma and ground gamma (after 1 year) external exposures from a notional AGR accident 2 dispersing under prolonged neutral conditions.

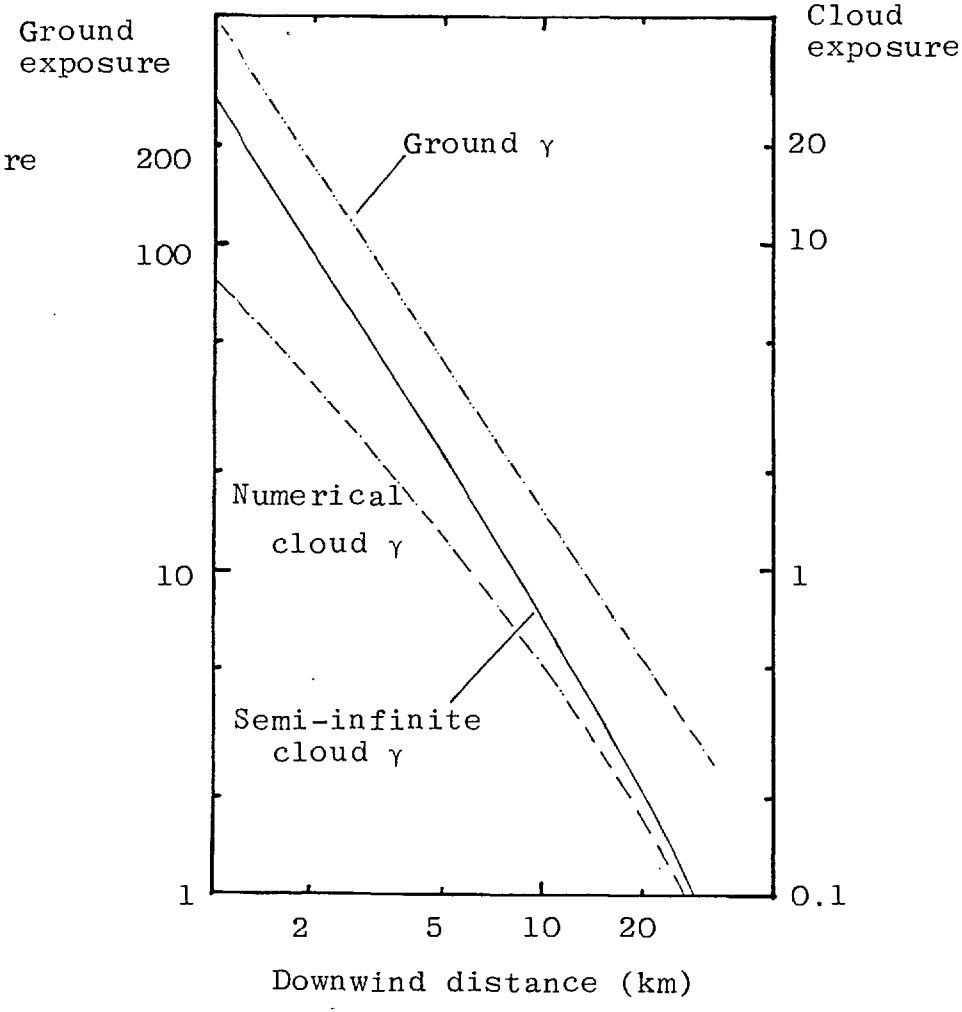

The ground gamma exposure rate within one year is dominated by contributions from caesium isotopes and other elements which were given a low deposition velocity. Compared to the deposition pattern of long lived iodine isotopes these other elements extend over a larger downwind range which is reflected in the ground gamma exposure. Similar trends are displayed by the greater pin failure case in figure 5.13.

Another method of presenting these results in more detail is used in figures 5.14(a) and (b). These display contours of the ratio of ground gamma to numerically calculated cloud gamma on-axis exposures for both pin failure releases, where diagram (b) refers to case 2. The contours of the deposit formed under neutral dispersion conditions are plotted on axes of downwind distance and ageing time. From both sets of curves it can be seen that ground deposition is relatively more important to external gamma exposures before about 10 km and after about 15 km downwind than within this range, at least during the first year for each release. This is due to restricted plume dispersion at short distances while at longer distances the cloud gamma exposure has already lost any contributions from short lived isotopes.

Cloud exposures rely mainly on contributions from inert gases (a) which in these accidents are much more abundant than depositing nuclides (b). The inert gases are not depleted by dry deposition but only by radioactive decay while travelling downwind ($g(x/(u^*t_c))$, where t_c is a characteristic decay time for the major contributors to cloud exposures. For depositing nuclides which contribute significantly to ground exposures a long decay half life is necessary so only depletion of the source term by dry deposition $Q^*(x)$ is important rather than radioactive decay in the plume. There are also different geometric terms for each type of exposure, depending on the relevant plume or deposit dimensions (N_p,N_d). Hence the ratio of ground to cloud gamma exposure rates x metres downwind after an ageing time of t is dependent on the factors: where $b'=\int_o^t b\lambda' dt'$

(5.12) $(N_d*Q^*(x)*b')/(N_p*g(x/(u*t_c))*a+N_p*Q^*(x)*b)$. When the quantity a is much greater than the amount of depositing mate-

Figure 5.14a Contours of the ratio of ground gamma to numerical estimate of cloud gamma exposures for decay time of deposits and downwind on-axis position for a notional AGR accident 1 dispersing under prolonged neutral conditions.

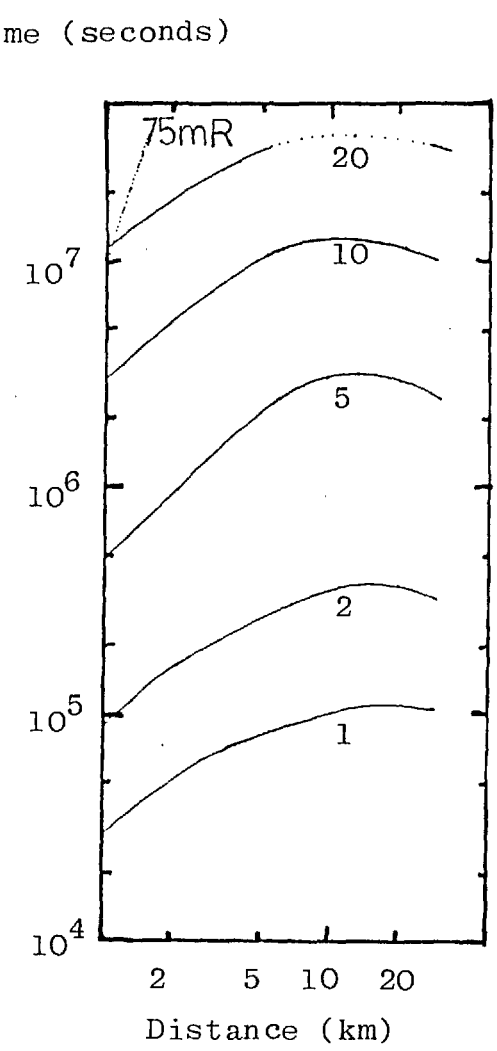

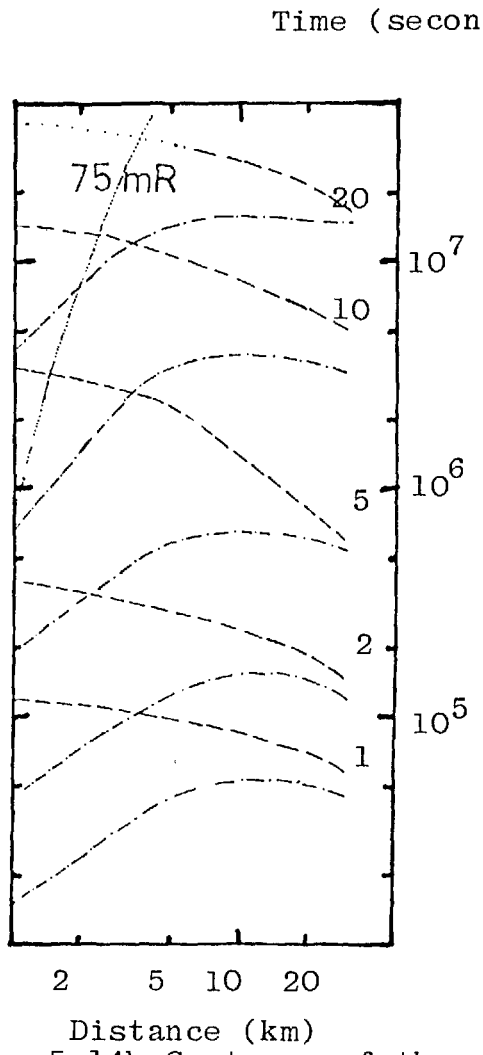

Figure 5.14b Contours of the ratio of ground beta to cloud beta exposures for decay time of deposit and downwind on-axis position for a notional AGR accident 2 dispersing under prolonged neutral conditions.

rial b the distance dependence will be determined by N_d/N_p and the competitive effect between Q^* and g, where the last two depend on windspeed and meteorological conditions.

For gamma exposures the effects of different geometries are shown in figure 5.14b where the cloud gamma is derived from both the numerical and semi-infinite estimates. The effect of dry deposition can be measured by the source depletion terms reaching 50% by 40km and over 100km for deposition velocities of 1.2cm/s and 0.3cm/s respectively under neutral conditions. The shorter distance corresponds to a travel time of about two hours, which has to be compared to the decay half lives of the major cloud gamma exposures: I132($T_{\frac{1}{2}}$=2.3hrs.); Kr87($T_{\frac{1}{2}}$=76mins.); $Te133^m$($T_{\frac{1}{2}}$=55mins.); Cs138($T_{\frac{1}{2}}$=33mins.) and Kr88($T_{\frac{1}{2}}$=176mins.). This suggests the cloud components decay more rapidly than the plume is depleted by deposition under neutral conditions with a characteristic time less than 1 hour, from the turning point in figure 5.14 , although the situation has further complexities than mentioned.

Consider the ratios of cloud and ground gamma for the two pin failure releases as being dependent on: b/(a+b) (Case 1); 3b/(5a/3+3b) (Case 2). As an inert gases are very much greater than b, non-gaseous elements, these two ratios are in proportions of 1:9/5 for the lesser and greater releases respectively. This explains the factor of approximately two between the contours in figures 5.14a and 5.14b, for corresponding times.

Also shown in figures 5.14a and b are isopleths of ground gamma exposure giving the ageing time and on axis downwind distance when this whole body external exposure exceeds 75 mR, about one tenth the ICRP whole body annual dose limit to members of the public. For the lesser release this does not occur at 1 kilometre downwind until about four months after the escape of activity. The release from Case 2 causes this exposure level to be reached after only about a week, at this distance. This difference in time scales is due to the dependence with which the exposure accumulates, as shown in figures 5.10 and 5.11.

Contours of the ratio of ground to cloud beta can be drawn, see figures 5.15a and b for the greater release under conditions D and F respectively, corresponding to those for gamma exposures in figure 5.14. Due to the short range of beta radia-

Figure 5.15a Contours of the ratio of ground beta to cloud beta exposures for decay time of deposit and downwind on-axis position for a notional AGR accident 2 dispersing under prolonged neutral conditions.

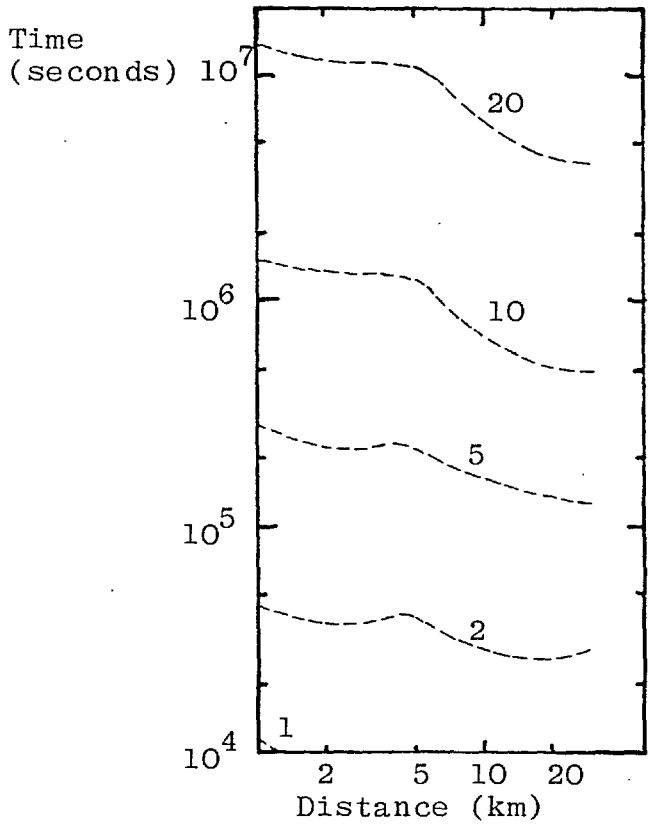

Figure 5.15b Contours of the ratio of ground beta to numerical estimate of cloud beta exposures for decay time of deposit and downwind on-axis position for a notional AGR accident 2 dispersing under stable, short time scale conditions.

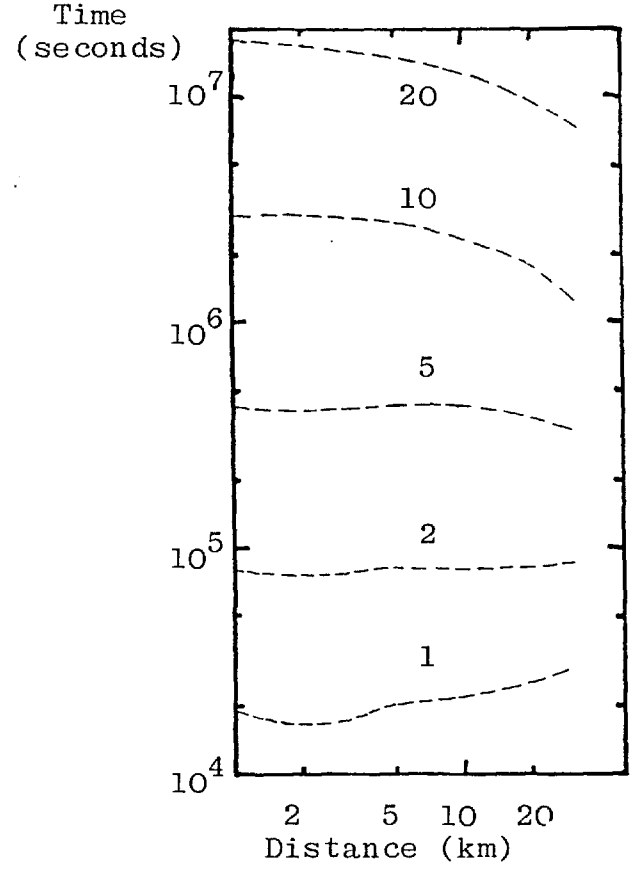

tion in air the exposure is only dependent on local levels of activity for both cloud and ground estimates. A consistent difference between these two exposures is due to the ground beta dose having been attenuated by one metre of air while that of the cloud is assumed to include "contact" doses. Attenuation of beta rays by air has most impact for energies below O.5MeV. Geometric factors are not relevant to distance dependences of beta ratios, only the competitive effects between decay and depletion remain. As could be expected these beta ratios show more resemblance to the gamma ratios with the semi-infinite cloud approximation, although there is a more complicated situation at short ageing times in category D conditions, see figure 5.15a, probably due to the behaviour of short lived isotopes and daughter products in the plume. The build up of ground beta exposure from long lived sources have to be of high energies, such as Ru106/Rh106, while low energy beta emitters (Te132, Kr88, Xe133, H^3, Cs134 and Cs137) contribute effectively only to the cloud dose. Under category F conditions the mean windspeed is 2 m/s so two hours travel corresponds to about 15 km. The source depletion terms reach 50% by about O.5 km and 15 km for v_g=1.2 and O.3 cm/s respectively in these stable conditions. This would have the effect of enhancing ground beta doses close to the source due to large amounts of iodine isotopes in the deposit, at quite short ageing times before the longer lived depositing nuclides dominate the ground beta exposure. A low windspeed tends to compress the length scale in stable dispersion conditions, as in figure 5.15b. Finally at ageing times of several months the long lived ground deposits impose the source depletion functional dependence on the ratio lines in figure 5.15b. Comparison of the curves in figures 5.15 a and 5.14 b shows that cloud gamma exposures relative to ground gamma exposures are more important than cloud beta to ground beta exposures at all times within a year of the release occurring and at most distances beyond 1 km of the source.

These results are strictly relevant to the particular deposition model used and its application to the isotopes considered in the two pin failure incidents. Characteristics of other releases will be considered later in the following sections.

Section 5.3.3 Cloud doses from notional AGR single channel melt-out accidents

These two notional accident scenarios both involve the same release fractions but develop along different paths before activity escapes to the atmosphere, as described earlier in this chapter. The consequences of these releases are also different in scale and type.

The contained single channel melt-out (Case 3) extends over a period of one day. This means that one meteorological condition is very unlikely to predict the consequences from the release realistically. A pessimistic assumption is made however that the wind direction does not change while activity escapes. Some allowance is made for a change of dispersion conditions by considering different categories applying to some portions of the release.

Before discussing Case 3 the major depressurisation single channel melt-out accident (Case 4) is described. The time scale of the depressurisation is assumed to be about one hour, as in the previous cases 1 and 2. The build up in time of dose commitments from Case 4 is shown in figure 5.16 for the thyroid, lung and bone on-axis doses under Pasquill-Smith modified category C conditions. Building entrainment and an inversion at a height of about 1 km have been incorporated. Smith's parametrization of dispersion has been followed, assuming a ground level release at midday in spring or autumn with partial cloud cover and an average roughness length of 30 cm along the whole path of the plume, for a 5m/s windspeed at 10 metres. The thyroid dose commitment again reflects the plate-out behaviour of iodine, while other elements do not have this allowance. The ERLs for both the lung and thyroid are exceeded within the first stages of the passage of the plume one kilometre downwind of the source. By the end of the release the gross bone dose commitment has exceeded 10rem, at this downwind distance where this may reflect possible early fatalities better than lung or thyroid organ doses. From figure 5.17 the external cloud gamma exposure can be predicted as not exceeding the relevant ERL, while the cloud beta dose is low compared to the ERL for irradiation of superficial tissues. Figure 5.18 displays the on-axis ground contamination of I131 and Cs137 greatly excee-

Figure 5.16 Build up in time of on-axis inhalation dose commitments 1 km downwind of a notional AGR accident 4 dispersing under slightly unstable conditions.

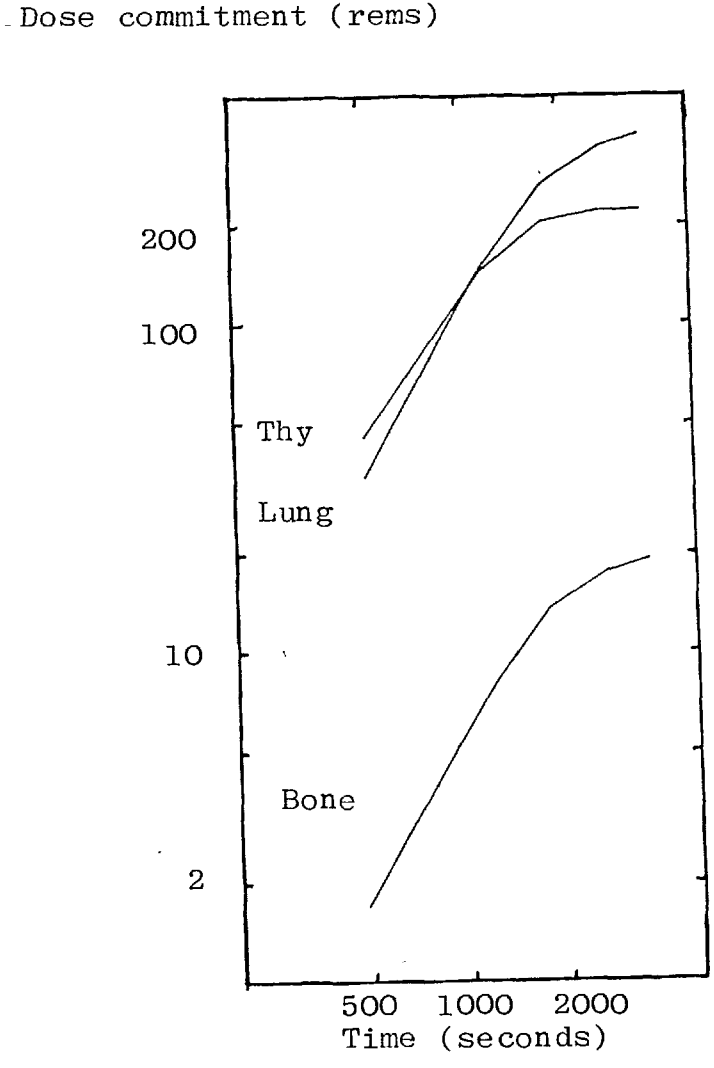

Figure 5.17 Build up in time of on-axis external cloud exposures, in air, 1 km downwind of a notional AGR accident 4 dispersing under slightly unstable conditions.

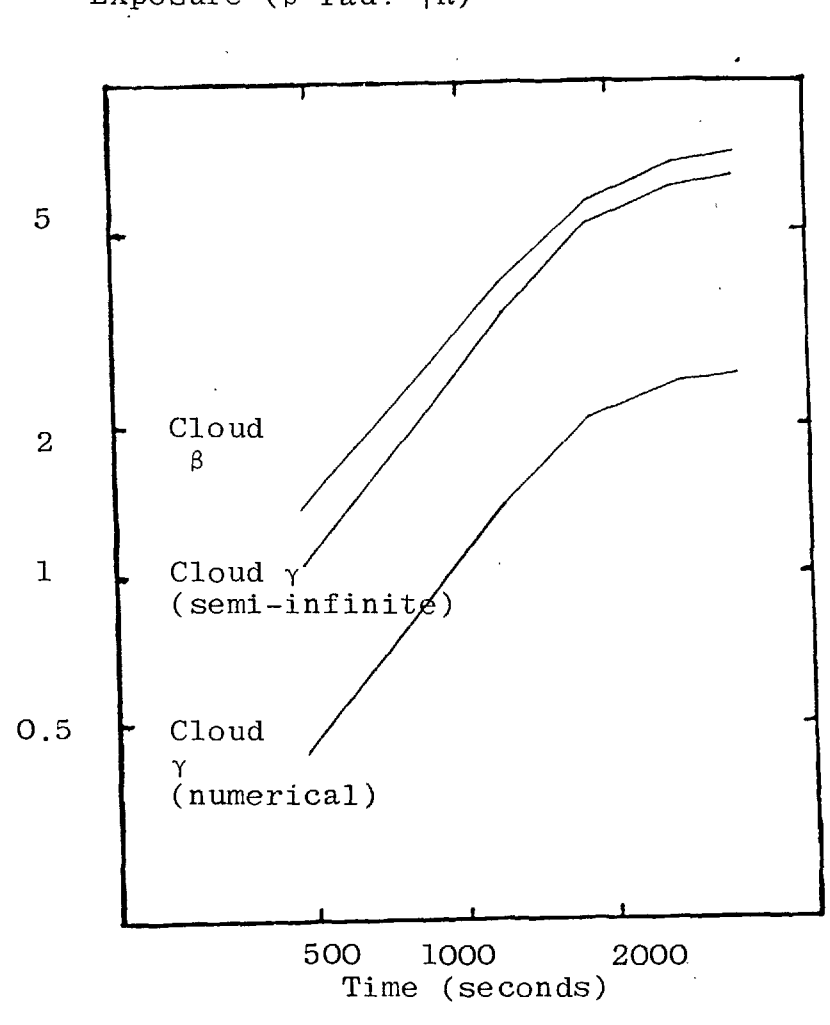

Figure 5.18 Build up in time of on-axis ground contamination 1 km downwind of a notional AGR accident 4 dispersing under slightly unstable conditions.

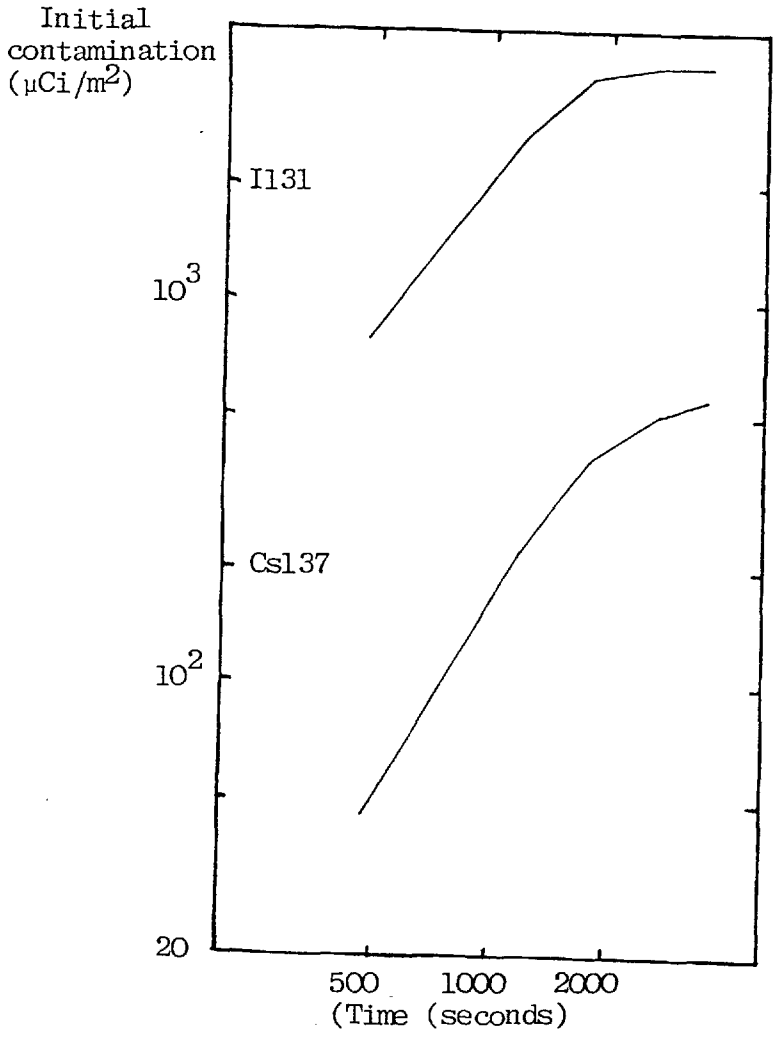

Figure 5.19 Downwind dependence of on-axis inhalation and weighted whole body dose commitments for the notional AGR accident 4 dispersing under slightly unstable conditions.

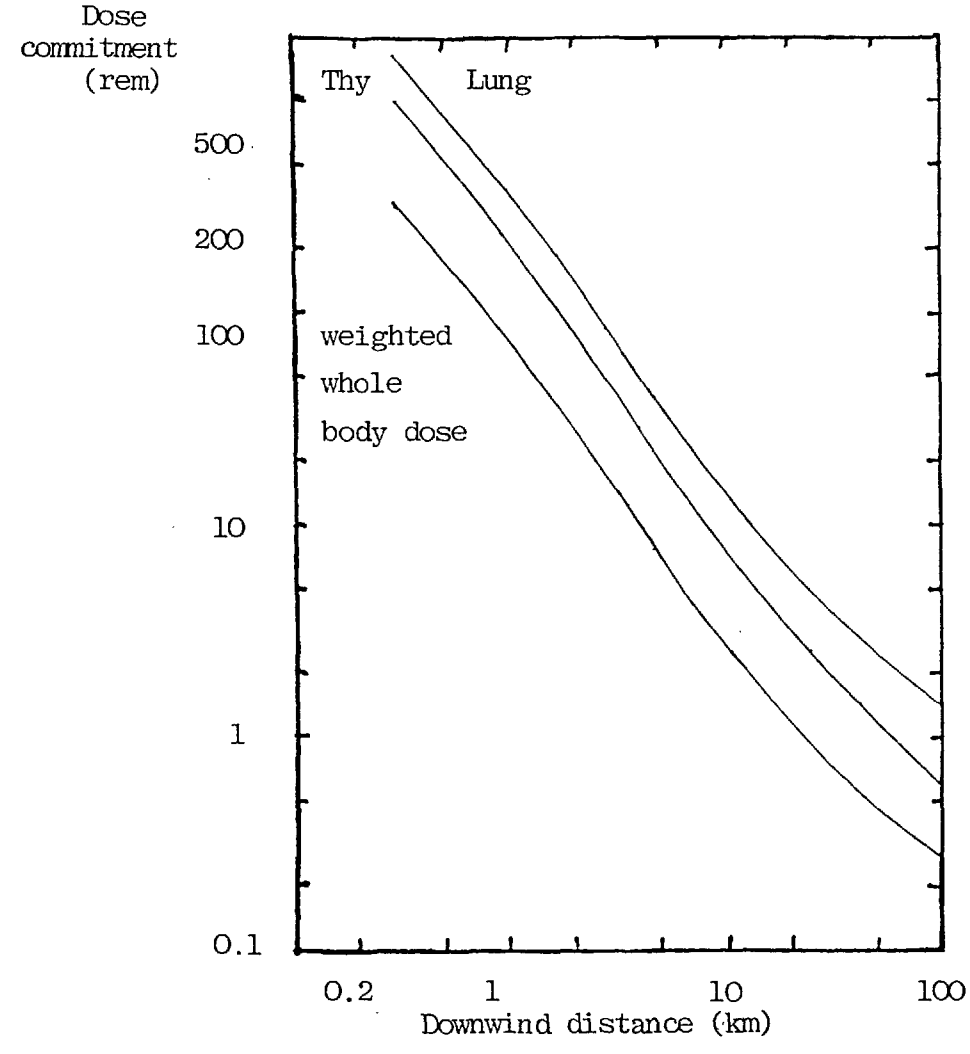

ding the relevant DERLs even after only a small part of the release has passed.

The downwind distance dependence of the on-axis thyroid and lung inhalation dose commitments to 100km is shown in figure 5.19. The threshold for early fatalities due to lung doses, received within one year, is about 2500 rads, so probably no early fatalities could be expected under these conditions beyond 300 metres. Whole body irradiation greater than 200 rads could produce early fatalities, due to bone marrow damage, but it is unlikely that any would occur for this release under slightly unstable conditions beyond several hundred metres. There is a slight difference in trends beyond about 30 kms due to the sensitivity of the thyroid dose commitment to the higher iodine deposition rate relative to other depositing elements. Uncertainties in organ sensitivities areless important in cases 3 and 4 as a greater range of isotopes are released and have an averaging effect over any discrepancies. Also shown on this figure is the weighted whole body dose commitment derived from the ICRP 26 factors and the single organ dose commitments. In this modelled incident the main contribution derives from the lung dose commitment. The ICRP stochastic whole body dose limit is exceeded within about 40 km of the source while the non-stochastic limit is exceeded within a shorter range extending to 5 km. The ERLs, derived by the MRC in the UK, are not exceeded beyond about 4 km and 6 km for the thyroid and lung respectively. The external cloud exposures under these slightly unstable conditions are given in figure 5.20. Neither the gamma or beta exposures are of great relative significance. Both estimates of the cloud gamma exposure are at least an order of magnitude less than the weighted whole body irradiation due to inhalation of radioisotopes. This reflects the large release fractions of elements other than gases and iodine in this notional accident.

Initial ground contamination out to 100 km by I132, I131 and Cs137 is shown in figure 5.21. Under these conditions deposition depletes the plume to 0.58 and 0.87 of the original source strength for travel to 110 km from the source, for deposition velocities of 12 mm/s and 3 mm/s respectively, so at

Figure 5.20 Downwind dependence of on-axis external cloud gamma and beta doses in air for the notional AGR accident 4 dispersing under slightly unstable conditions.

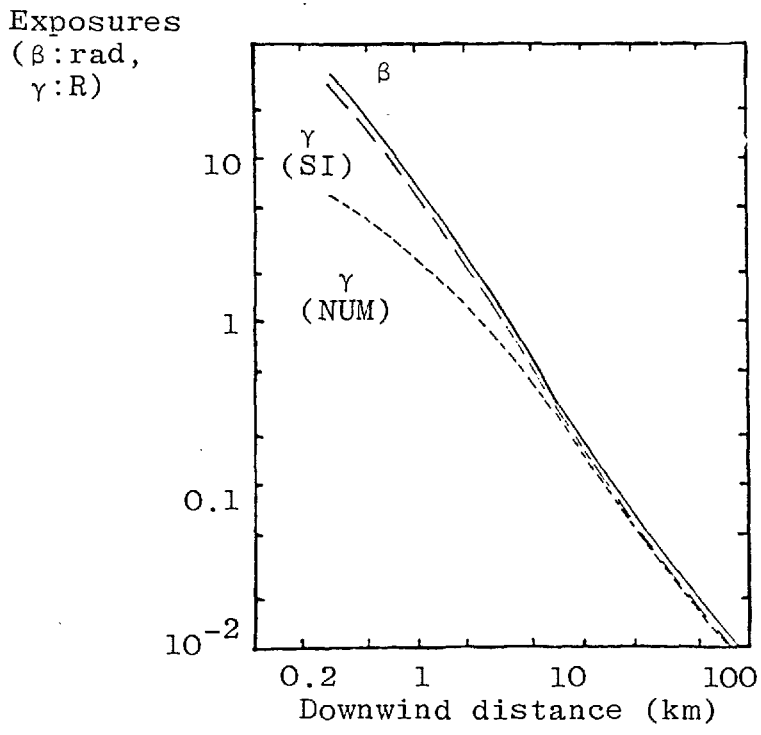

Figure 5.21 Downwind dependence of on-axis ground contamination for the notional AGR accident 4 dispersing under slightly unstable conditions.

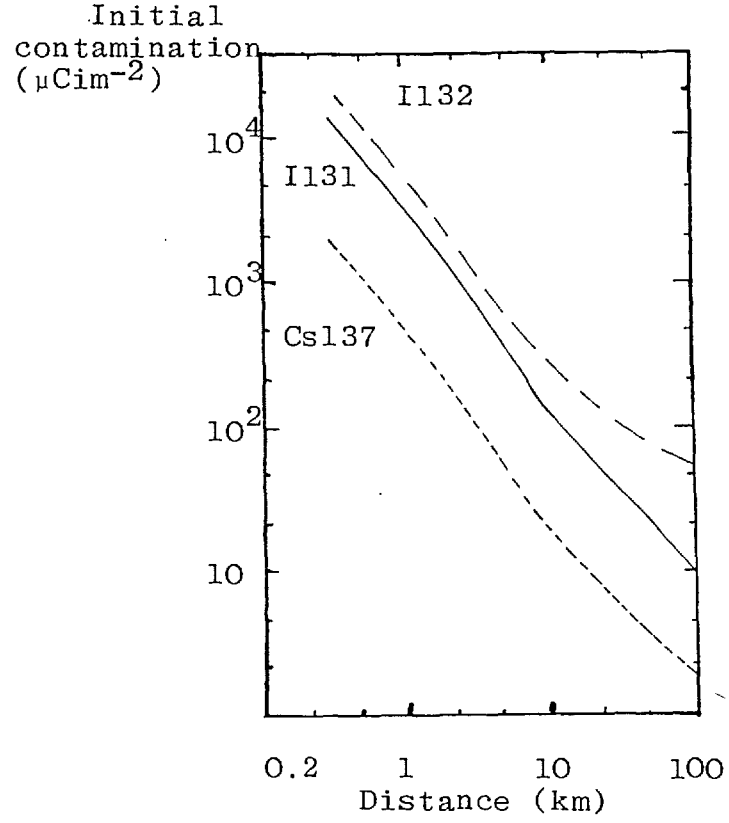

short distances depletion does not have a major effect and there should be no major problems about the iodine release consisting of several physical forms. Figure 5.21 shows high I131 contamination levels out to 100 km, where this is still above the DERL for an infant. The corresponding DERL for Cs137 is exceeded within about 11 km of the site. The build up of I132, produced from Te132 decays in the plume, can be seen by comparison of this contamination to that of I131 which mainly depends on the quantity released at the source. These factors suggest that external exposures will be significant from the deposited material, as will be discussed in the next section.

The consequences under slightly unstable conditions for this depressurisation melt-out accident are severe and become more so if stable category F weather is assumed for dispersion calculations. Figures 5.22a and b show some of the on-axis dose commitments and ground contamination, respectively, following this release occurring in stable conditions with the same grouped deposition model. The effect of the relatively high iodine deposition velocity is seen in both the thyroid dose commitment and the I131 ground contamination. Relative build up of iodine-132 by decays from Te132 in the plume has again been predicted. The lung and weighted whole body dose commitments follow similar curves to those of the weakly depositing elements, such as caesium and strontium. Early fatalities, and morbidity, may occur within 3 km due to the lung inhalation dose commitment, assuming most of the dose accrues within the first year. Damage to bone marrow, directly and by whole body irradiation, may be an important influence within several hundred metres of the release. Travel to 30 km under these stable conditions represents a period of over four hours but these conditions are unlikely to persist to 100 km.

Two interpretations of the notional contained single channel melt-out accident have been modelled using different filtration efficiencies; other variations could be envisaged due to changes in meteorology over the 24 hour release period. However for ease of comparison to the other notional accidents a single wind direction has been assumed for all meteorological conditions applied to the separate steps of the release.

Figure 5.22a Downwind dependence of on-axis inhalation and weighted whole body dose commitments for the notional AGR accident 4 dispersing under stable conditions.

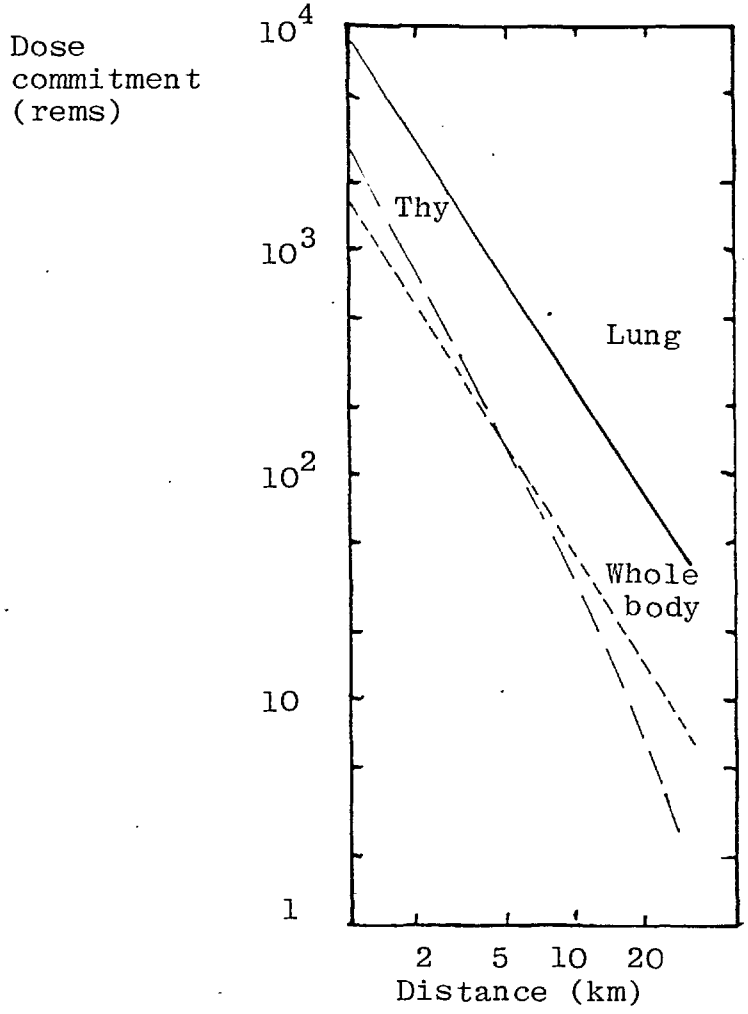

Figure 5.22b Downwind dependence of on-axis ground contamination for the notional AGR accident 4 dispersing under stable conditions.

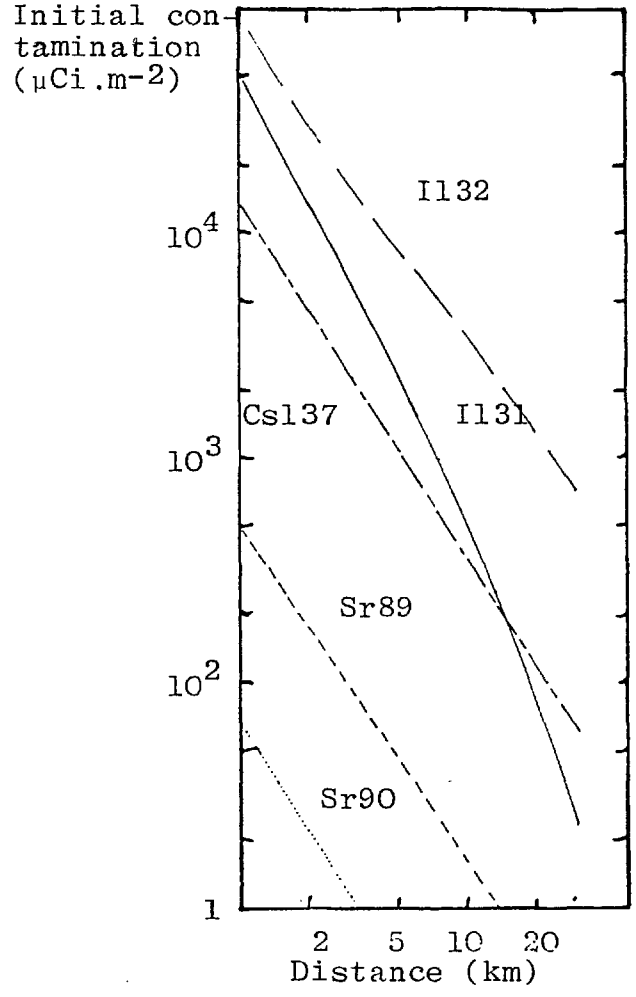

A pessimistic assumption about meteorology is to assume dispersion under category F conditions for the full 24 hours. The initial three short time steps are assumed to have lateral dispersion characterised by a short averaging time while the last two steps, covering 20 hours, is modelled by using parameters for a prolonged (category C (Beattie and Bryant 1970)) release. The resulting build up of potential on-axis inhalation dose commitments one kilometre downwind are presented in figure 5.23, with the effects of different filtration sequences 3.1 and 3.2. The effect of reducing the elemental filtration efficiencies from 0.97 to 0.50 is marked in the case of the lung and bone dose commitments. The iodine dominated thyroid dose commitment is only slightly dependent on the filtration factors in this descriptive accident. This corresponds to the assumption that only plate-out, and not filtration, influences iodine releases from the reactor. Filtration of tellurium, and any subsequent resuspension from the filters, only causes small percentage changes in the thyroid dose commitment at short times, but at late periods I132 is an important resuspension product. Also shown for the lung and bone doses is the effect of using 90% efficient filters during the second hour of the release. The ratios of the dose commitments to the lung for the three filtration factors due to the second hour of the release is, as could be expected, in the ratio
16.6:3.34:1=1-F(0.5):1-F(0.9):1-F(0.97).

Figure 5.24 shows that the on-axis cloud beta and cloud gamma exposures one kilometre downwind of the source are less dependent on the filtration fractions, due to the large contribution from inert gases. Complicated differential effects result from the model assuming that decays within the filters immediately release the daughter products to the atmosphere together with the resuspension from plated out iodine. These detailed differences have not been investigated further as the model of the filter systems is crude and no reasonable sequence appears capable of producing critical external cloud exposures for these particular releases. An example of allowing different meteorology for each of the time steps of case 3 is presented in figure 5.25 for inhalation dose commitments building up during the release for an on-axis exposure point 1 km downwind

Figure 5.23 Build up in time of on-axis inhalation dose commitments 1 km downwind of the notional filtered AGR accidents 3(1 and 2) dispersing under stable conditions.

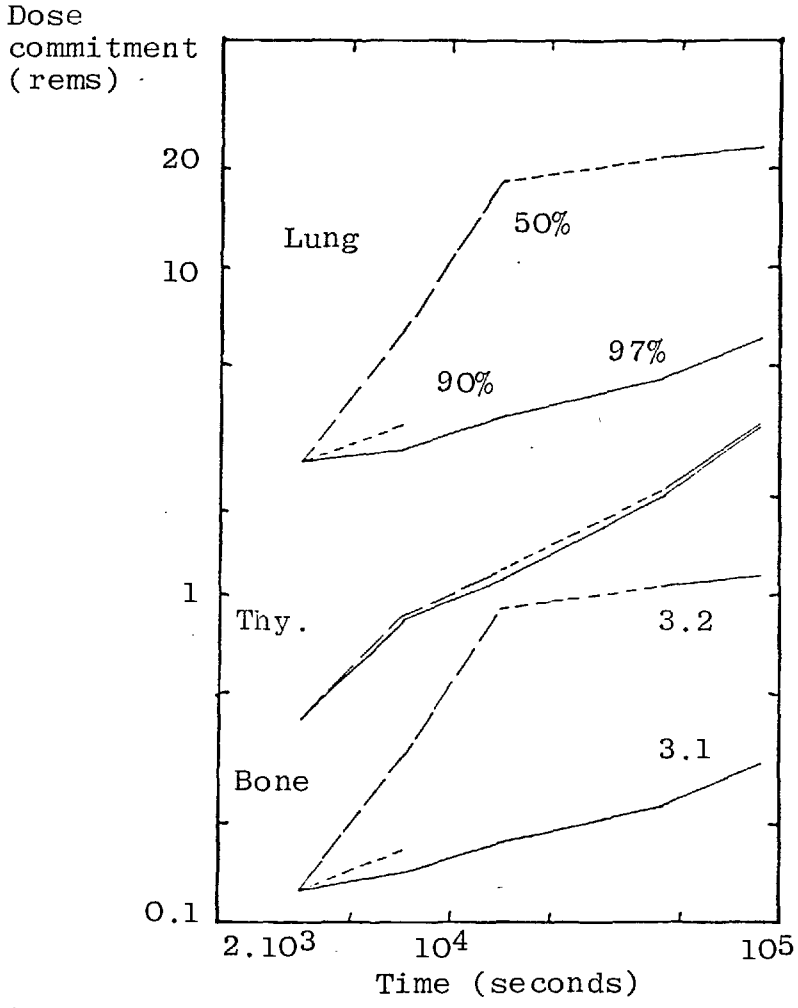

Figure 5.24 Build up in time of on-axis external cloud exposures 1 km downwind of the notional filtered AGR accidents 3(1 and 2) dispersing under stable conditions.

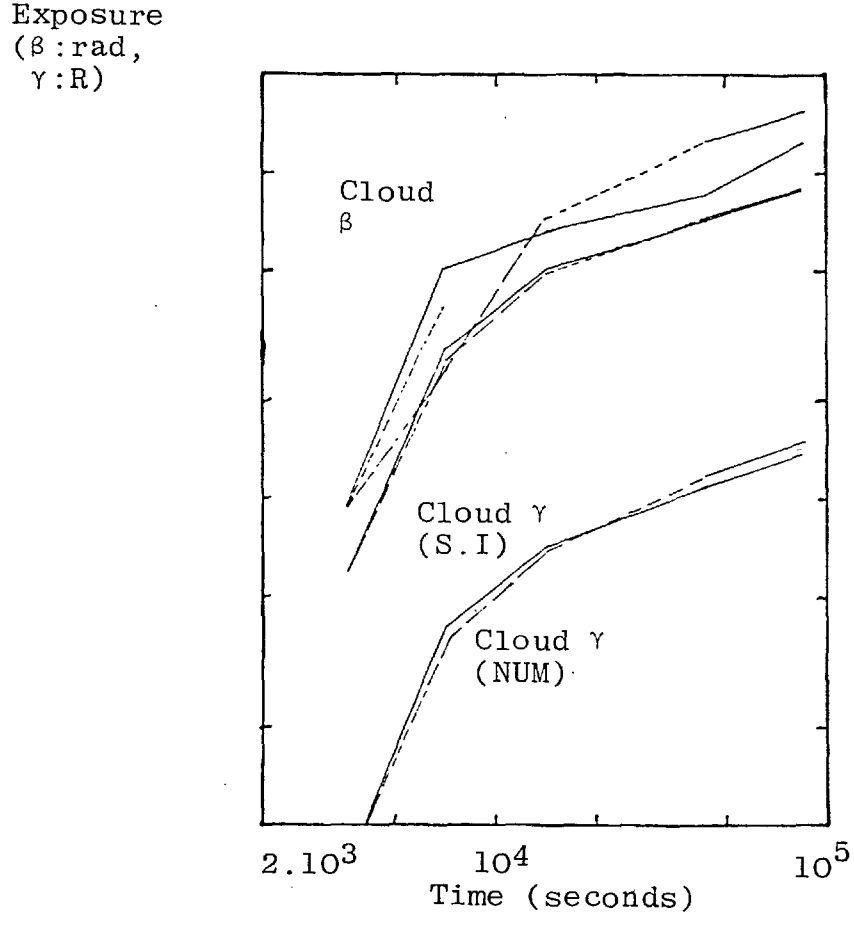

Figure 5.25 Effects of different dispersion conditions on the build up in time of on-axis inhalation doses from the notional AGR accident 3.1 . (F(u=2m/s,short) —— ——, F(u=2m/s,prolonged)————, D(u=5m/s,prolonged) -----)

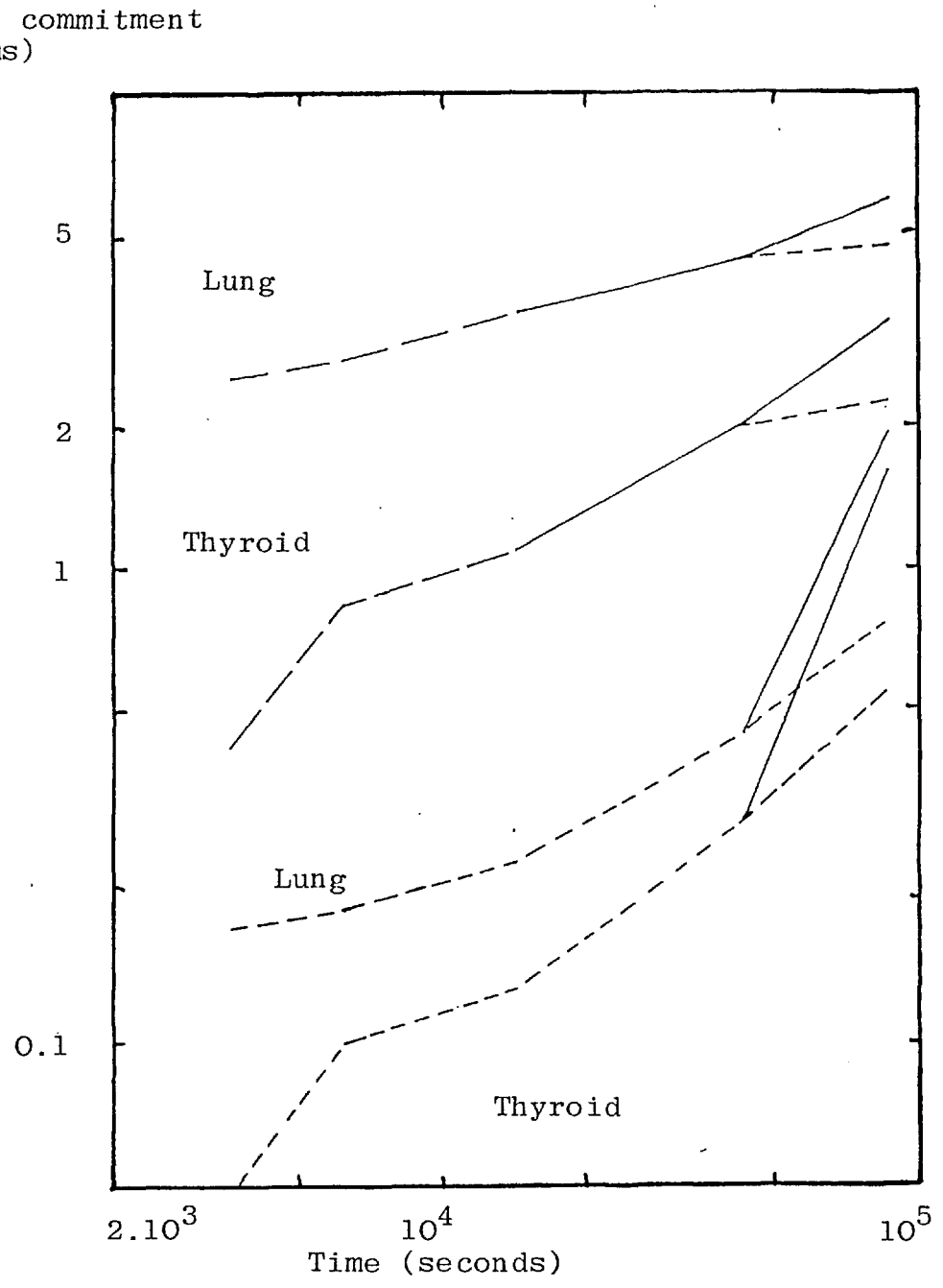

of the ground level source. These are for filtration sequence 1 with the first four steps released in one category, F or D, but the last prolonged step, from 12 to 24 hours, is given for both conditions as detailed in the figure. From this graph it can be seen that persistent stable weather during the first half of the release produces the severest conditions, irrespective of the dispersion category for the last half. However if the first half of the accident is assumed to disperse under neutral, Pasquill category D, conditions the total dose commitment from the whole accident can still be dominated by stable weather in the second half of the release as could occur during the night. The assumption of neutral dispersive conditions in the early stages of the accident decreases the lung dose proportionately more than that of the thyroid, due to a larger portion of the lung dose accruing in the first twelve hours. This is due to the modelling of the iodine plate-out, which means the iodine release after a half-day is primarily due to resuspension and assumed immediate escape of iodine isotopes from tellurium isotopes decaying on the filters, especially for I132.

Downwind distance dependences for on-axis inhalation dose commitments and ground contamination under neutral (category D) prolonged conditions are shown in figures 5.26a and b respectively for filtration sequence 1. These suggest that ERLs for inhalation dose commitments will most probably not be exceeded beyond a few hundred metres from the source, while the ICRP non-stochastic annual limit for single organs would be exceeded only over a slightly longer range, probably not beyond 0.6 km. The thyroid dose commitment curve approximately follows that of the lung dose commitment, due to there being little plume depletion within 30 km under these neutral dispersion conditions. Two thirds of the thyroid dose commitment is received in the last two steps, 20 hours, of the release when I132 is resuspended from the filters and delivers about 85% and 95% of the thyroid dose close to the source from the last two steps respectively. There will also be a large component from Tel32 decays in the cloud at fairly long distances from the reactor. Figure 5.26 b displays the initial I132 ground contamination from only the last twelve hours of the release, but the source I132 is deposited at only 0.1 cm/sec, as is all iodine due to the assumption that I131 is released at this

Figure 5.26a Downwind dependence of on-axis inhalation dose commitments from the notional AGR accident 3.1 dispersing under prolonged neutral conditions.

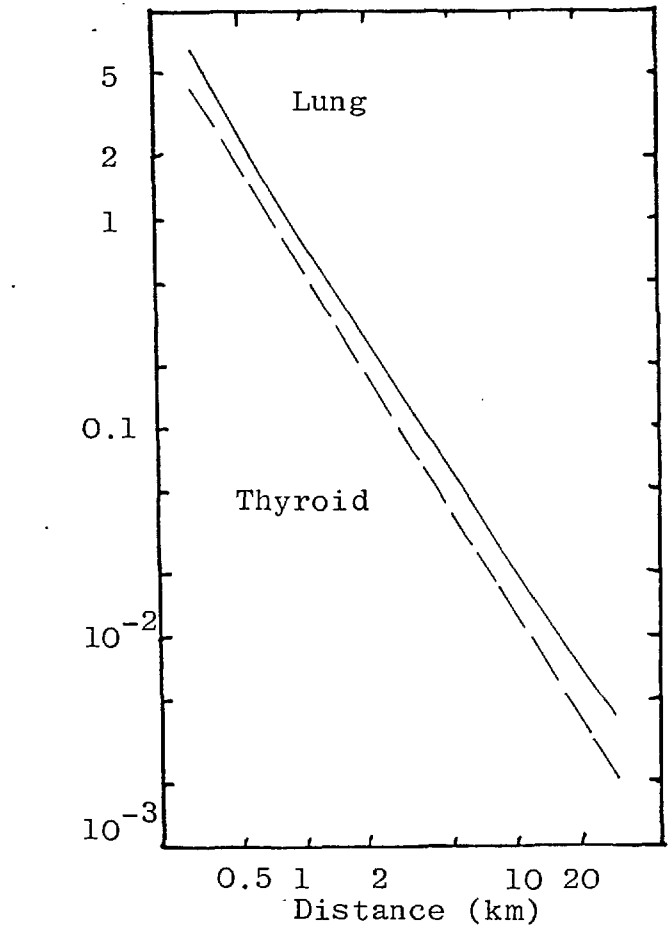

Figure 5.26b Downwind dependence of on-axis initial ground contamination from the notional AGR accident 3.1 dispersing under prolonged neutral conditions.

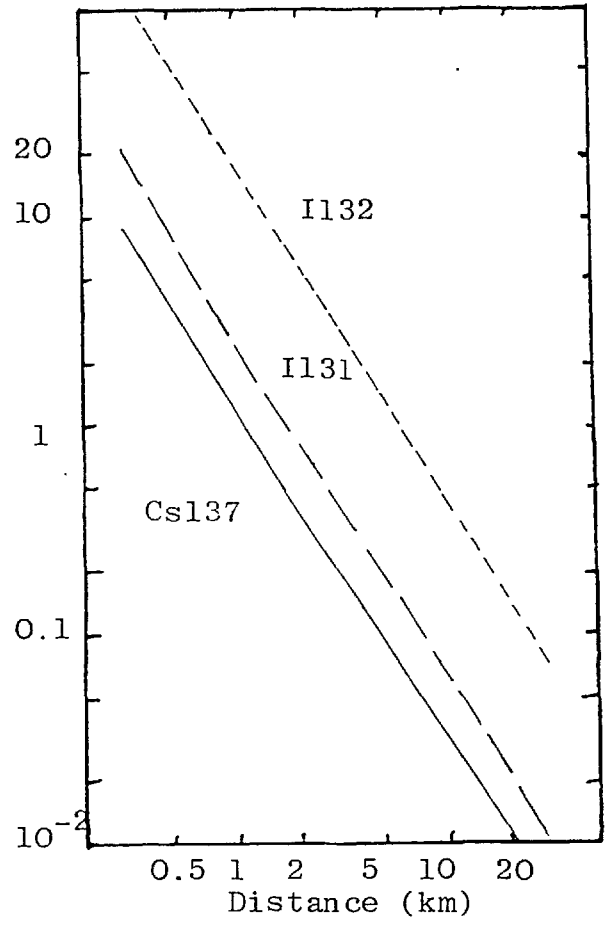

stage only as methyl iodide. The half life of I132 is 2.28 hours, corresponding to a travel distance of about 40 km in the plume when deposition is negligible. Longer lived iodine isotopes would contribute proportionately more at long distances. The ICRP stochastic whole body annual limit is not exceeded beyond 1 km where the pessimistically predicted mean weighted value is 0.13 rem, with at most 0.03 R cloud gamma exposure.

Total ground contamination is not of any significance beyond 1 km, when compared to DERLs for the grass-milk-food dose pathways for I131 and Cs137 under neutral conditions. The assumption of a low deposition velocity after four hours of the start of the release, corresponding to methyl iodide only, does not affect the I131 ground contamination by more than a factor of two in these conditions. Major differences could be produced by this assumption with the large I132 release, noted above, during the last twelve hours (see figure 5.26b). The form of this I132 resuspending from Te132 decays on the filters is uncertain, but might be in a form which would have a mean deposition velocity larger than that of methyl iodide. Hence different isotopes of one element may need to be described by different depletion rates during the latter stages of a prolonged release, and this may have to be extended to cover different chemical forms of single isotopes.

Under stable conditions, using prolonged lateral dispersion during the last two release steps, the resulting inhalation dose commitments for both filtration sequences are displayed in figure 5.27. In both cases lung doses are most critical, exceeding ERL's within 1 km, while mean thyroid doses only exceed these levels within about 300 metres of the site for both sequences. The worst filtration sequence results in a mean lung dose commitment above the ICRP annual non-stochastic limit out to about 3 km, where the mean on-axis weighted whole body dose is approximately 0.62 rem. This has to be compared to the corresponding distance of 1 km for the more efficient filtration scheme. This distance also applies to the limit of high thyroid doses for both sequences. Iodine is not directly acted on by the filters, only by plate-out, but the consequences are dominated by the releases from the filters during the last two steps

Figure 5.27 Downwind dependence of on-axis inhalation dose commitments for both notional AGR accidents 3(1 and 2) dispersing under stable conditions.

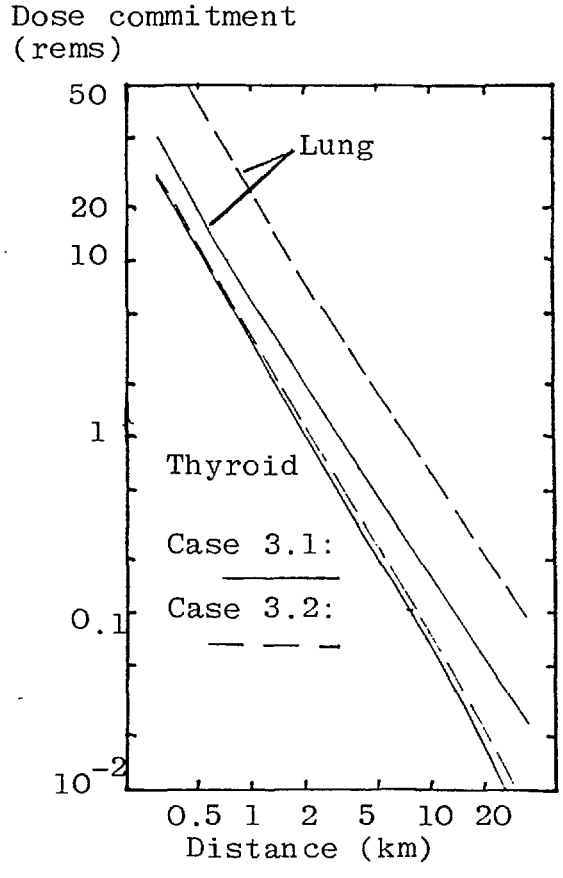

Figure 5.28 Downwind dependence of on-axis ground contamination for both notional AGR accidents 3(1 and 2) dispersing under stable conditions.

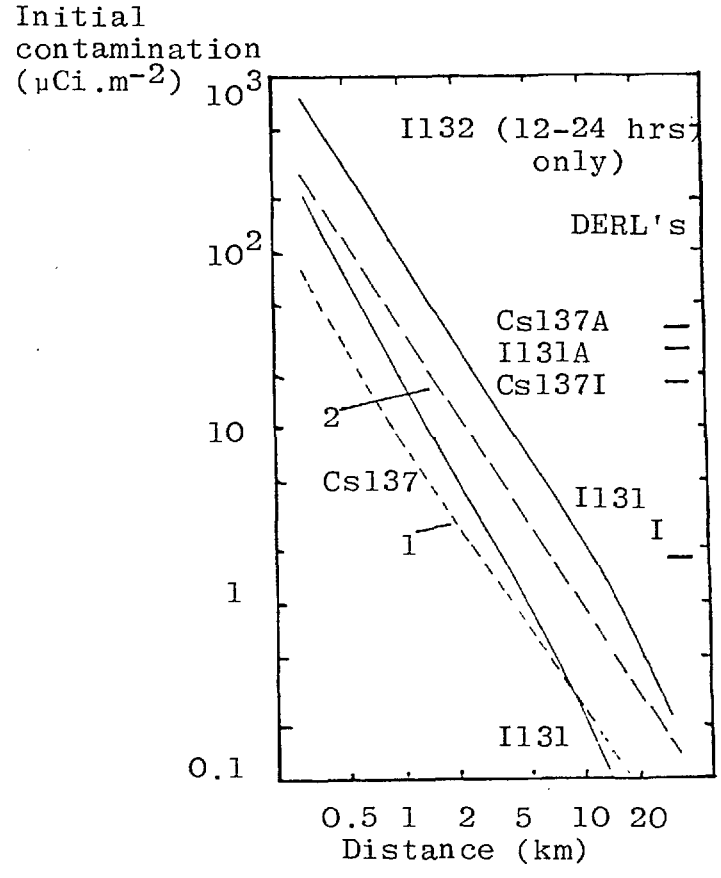

which are similar in both filtration schemes, but a low iodine deposition velocity is assumed in these periods.

Dose commitments from the two different filtration sequences can be compared relative to the thyroid dose commitment, as in table 5.16. The lower filtration efficiency sequence allows the lung and most other dose commitments to increase by about a factor of 5 relative to the thyroid dose (sequence 2). In this sequence the doses to both the compartments of the large intestine become comparable to the thyroid dose commitment. Both the stomach and small intestine dose commitments only change by a factor of about two for these cases, due to the dominance of doses from iodine isotopes, particularly I132 in the last twenty hours of the release. No account of different chemical forms affecting organ sensitivities has been considered for the later stages of the release, but this may be significant in prolonged releases.

The thyroid inhalation dose commitment in cases 3.1 and 3.2 only show a slight fall relative to lung doses by 30 km, unlike the total I131 to Cs137 ground contaminations in figure 5.28. This is due to a combination of production of I132 by decays from Te132 and the low deposition velocity assumed for iodine during the last two steps of the release from the intact coolant circuit. The decay of Te132 in the plume only becomes important when I132 originally released from the reactor has decayed while travelling downwind. The I131 ground contamination is dominated by the early releases, due to the effects of plate-out and the large iodine deposition velocity used, 1.2 cm/s compared to 0.1 cm/s in later stages, as figures 5.26b and 5.28 reflect. The importance of I132, released by this model directly from the filters, along with its production by "in cloud" decay of Te132, in the last stage of the accident is highlighted by these two figures.

This is an example of a restriction on the use of an element dependent deposition model in a situation where isotope dependent depletion could be of significance. Also the physical forms of each isotope has to be considered in the most stable dispersion conditions when predicting levels beyond 10 km. These points will be considered further in the discussion of external

Table 5.16 Single organ dose commitments, relative to that of the thyroid for single channel melt-out with an intact coolant circuit.

Single Organ (I:insoluble, S:soluble)	Inhalation organ dose commitments, normalised to that for the thyroid for the filtered releases	
	Sequence 1	Sequence 2
I Lungs	1.4	6.8
S Thyroid	1.0	1.0
S Bone	0.068	0.34
I LLI	0.22	1.1
I ULI	0.11	0.53
I Stomach	0.045	0.083
I SI	0.049	0.096
S Kidneys	0.087	0.39
S Liver	0.032	0.15
S "Total body"	0.017	0.073

exposures from the deposits formed by these notional releases in the next section.

Section 5.3.4 External exposures due to ground deposits from the notional single channel melt-out releases

In all the results of this chapter an element dependent deposition model is used which assumes that inert gases are not deposited. This means that uncertainties in the releases of xenon isotopes, due to assumptions about the filtration, plate-out and resuspension parameters for iodine, the immediate precursor of xenon isotopes, do not affect the ground contamination. This also applies to xenon decay daughters, which are not significant sources of caesium isotopes. The current model of resuspension to the atmosphere after decays on filters can produce large releases in the last stages of an incident, particularly for I132. However this crude assumption will not greatly affect the long term exposures from the deposit, as I132 has a short half life of 2.28 hrs. In general the long lived radioisotopes do not have any significant precursors which could yield significant activity resuspending from the filters.

When dealing with external exposures for the contained channel melt-out with a prolonged release period, it is pessimistically assumed that the ground deposits from each step have a common axis. The on-axis external ground gamma exposure rate 1 km downwind is shown in figure 5.29 (curve 1,1), for filtration sequence 1, released under neutral, category D dispersion conditions. This exposure rate remains approximately constant, at 0.5 mR/hr, during the day long release period, and probably for most of the second day after the start of the incident. Note that there is only an order of magnitude decrease in the exposure rate in the first year of this large scale accident, unlike the earlier pin failure cases where this quantity decreased by two orders of magnitude. Also shown are the contributions from each step of the release. This emphasises the importance of the assumed lack of filtration in the first hour, as well as the duration of the filtered (97%) release from the last two time steps. Figure 5.29 also gives the total and step contributions of the on-axis external ground gamma exposure 1 km downwind for filtration sequence 2 released under stable category F dispersion conditions (curve 2,1) with lateral dispersion, as

Figure 5.29 Effects of different dispersion conditions on the decay dependence of the total on-axis external ground gamma exposure rate from the notional AGR accident 3.1.

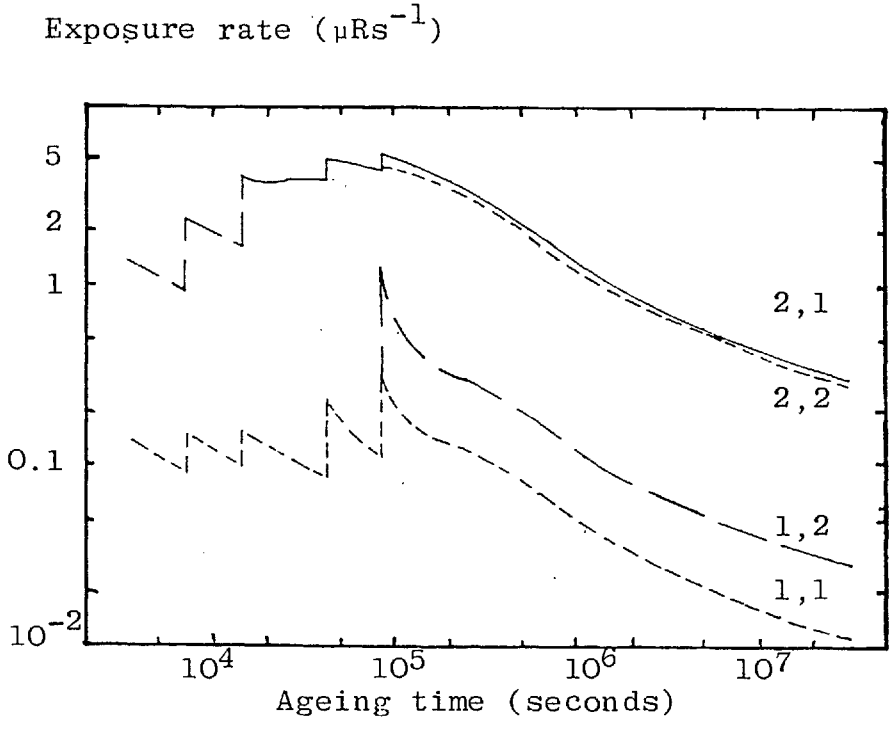

Figure 5.30 Build up in time of on-axis cloud and ground gamma exposure 1 km downwind of a notional AGR accident 3.1 dispersing under prolonged neutral conditions.

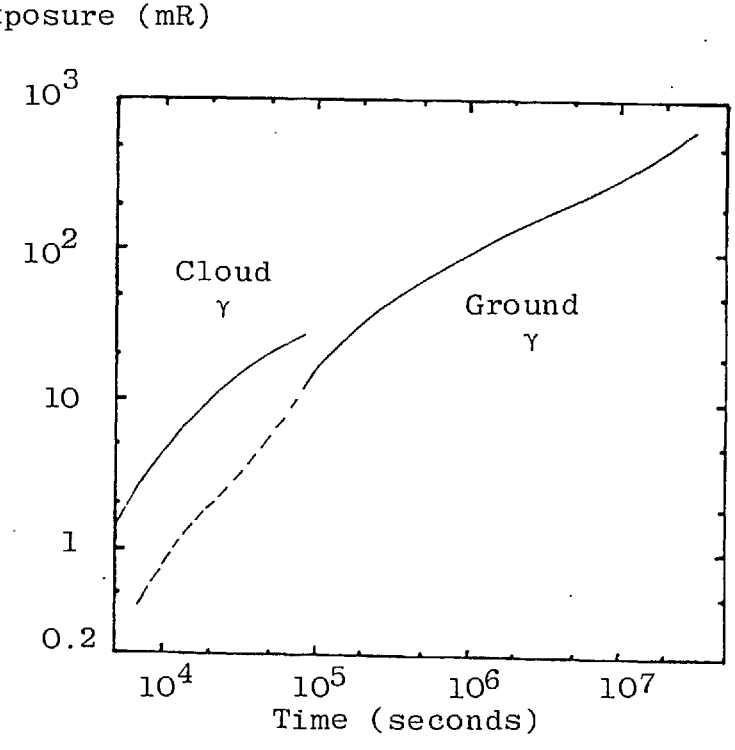

described earlier for figure 5.25 in the relevant section. In this case the steps from the second to fourth hours dominate due to the poor (50%) filtration factors and the short time-scale lateral dispersion parameters. The peak exposure rate in this case is about 14 mR/hr for most of the release period. There is a factor of about 35 between the two cases at short times, falling to about 20 at long times, where different dispersion assumptions account for up to about half this ratio. The remainder arises from increases in releases of both short and long lived isotopes. The application of prolonged lateral dispersion parameters for the last two steps reduce the consequences by a factor of three compared to those predicted with characteristically short release parameters. The sharp decrease in these rates for the last two steps, with a time scale of hours, is due largely to the I132 component resuspended to the atmosphere by Te132 decays on the filters. The above discussion demonstrates that one type of prolonged release has the potential to yield a large range of consequent ground gamma exposures.

The effects of changes in meteorological dispersion conditions for the last half of the release are also shown in figure 5.29. For sequence 1 the occurrence of stable conditions, possibly in the night, during the first hour or a large period of the remainder of the release could produce a significant increase in the long term exposure rate. An example (curve 1,2) has the last step dispersing under prolonged stable conditions and produces a threefold increase in the ground gamma exposure rate after ageing of the deposit by one year. When the first half of the filtration sequence 2 release disperses under stable conditions the last half cannot significantly affect the long term exposure rates. This is due to the comparatively small contribution to the total release of long lived caesium isotopes by the last steps, as shown by curves (2, 1) and (2,2) of figures 5.29 where the latter curve results from neutral meteorological conditions in the final stage of the accident.

The isotopes dominating these ground gamma exposure rates close to the source are given in the computer calculations, and tabulated in tables 5.17 and 5.18 for sequences 1 and 2 respectively.

Table 5.17 Time dependence of significant contributors to the external ground gamma exposure from sequence 1 filtered release at short downwind distances with neutral dispersion conditions

Time after start of release	Dominant isotopes in given energy groups*				
	1 0-0.39MeV	2 0.39-0.68MeV	3 0.68-0.8.8MeV	4 0.88-1.28MeV	5 1.28+MeV
First 4 hr.	Te/I132	Ru103,I133	I132,Ru105(I134)	I132,I135(I134)	I135,I132
Up to 1 d.	Te132,$Tc99^m$(I131)	Ru103,I132	I132(Cs134)	I132,$Te131^m$	I132(La140)
2nd day	"	"	I132,Cs134	"	"
3rd day	"	"	"	I132,La140($Te131^m$)	I132(La140)
day 12	Te132,$Tc99^m$,I131	Ru103,Cs134	I132,Cs134	La140, I132	"
Day 35	(Ce141,Te129,I131)	"	Cs134,$Ba137^{n_i}$	Cs134,Rh106	La140,Cs134
day 70	(Te129,Ce141)	"	"	"	Cs134(La140)
day 170	(Ce144,Ru103)	Cs134,Rh106	"	Cs134	Cs134
1 year	(Ce144,Sb125)	"	$Ba137^m$,Cs134	"	"

*i: (isotope n) this isotope does not contribute significantly to the total ground gamma exposure rate.

ii; " the main isotopes have not changed since the previous time.

At early stages in both filtered releases iodine and tellurium isotopes are of most concern. The most persistent of these two elements giving significant contributions to the ground gamma exposure is Te132($t_{\frac{1}{2}}$=78hrs.), with its short lived daughter I132($t_{\frac{1}{2}}$=2.2hrs.) which gives a high yield of gamma radiation on decay. The contributions from I131 ($t_{\frac{1}{2}}$=8d) are swamped by the quantities of low energy gamma emitters released in later steps of the release. Ruthenium isotopes persist for longer periods, particularly Ru103($t_{\frac{1}{2}}$=40d) and Ru106($t_{\frac{1}{2}}$=369d), where the latter has a short lived gamma emitting daughter Rh106. The caesium isotopes Cs134($t_{\frac{1}{2}}$=2.28y) and Cs137($t_{\frac{1}{2}}$=30y), by its gamma emitting daughter $Ba137^{m}$($t_{\frac{1}{2}}$=2½min.), contribute greatly to the external gamma exposure after about a month, finally producing over 80% of the total exposure rate after one year of decay. By this stage the mean group 3 energy of 0.76MeV used in the calculation overestimates the main single photon occurring in this group, which is that at 0.66MeV from $Ba137^{m}$.

Small, high energy contributions at intermediate times result from La140 ($t_{\frac{1}{2}}$=40 hrs.) which is the daughter of Ba140 ($t_{\frac{1}{2}}$=12.8d). Low energy photons due to $Tc99^{m}$ ($t_{\frac{1}{2}}$=6 hrs.), the short lived daughter of Mo99($t_{\frac{1}{2}}$=66 hrs.), gives a contribution which is superceeded by Ce141($t_{\frac{1}{2}}$=32.5d), Te129(short lived daughter of $Te129^{m}$, $t_{\frac{1}{2}}$=33.5d), Ce144($t_{\frac{1}{2}}$=284d) and Sb125($t_{\frac{1}{2}}$=2.5y). In both case 3.1 and 3.2 it is only a few of several hundred isotopes which produce major contributions to the ground gamma exposure rates. The ageing behaviour of the total exposure rate is similar in form for both cases. Note that the exposure rate at one year has not levelled off as much as was found in the pin failure cases. This is due to the relatively larger component of intermediate and long lived isotopes escaping during these filtered releases.

The build up in time to one year of on-axis external gamma exposure 1 metre above the deposit of mixed fission products from the first filtration sequence release is shown in figure 5.30 together with the numerical estimate of the cloud gamma exposure. The exposure from the ground again exceeds the external cloud gamma exposure 1 km downwind about a day after the end of the release for dispersion under neutral stability

Table 5.18 Time dependence of significant contributors to the external ground gamma exposure from sequence 2 filtered release at short downwind distances with stable dispersion conditions.

Time after start of release	Dominant Isotope				
	1 0.-0.39MeV	2 0.39-0.68MeV	3 0.68-0.88MeV	4 0.88-1.28MeV	5 1.28+MeV
First 4 hr.	Te132, I131 $Tc99^m$	Ru103, I133	I132, I134 Ru105	I134, $Te133^m$, I132	I135, Rb88, Cs138 $Te133^m$
Up to 1 d.	Te132, $Tc99^m$	Ru103, I132	I132, Ru105, Cs134	I132, $Te131^m$	I132, La140
2nd day	"	"	I132, Cs134	"	"
3rd day	"	Ru103	"	I132, $Te131^m$	"
day 12	"	Ru103, Cs134	"	I132, Cs134	La140, I132
day 35	(Ce141, Te129)	"	Cs134, $Ba137^m$	Cs134, Rh106	Cs134, La140, Rh106
day 70	(Te129, Ce141)	"	"	"	Cs134, La140, Rh106, Pr144
day 170	(Ce144, Ru103) Cs134, Rh106	"	"	"	Cs134, Rh106, (Pr144, La140)
1 year	(Ce144, Sb125)	"	$Ba137^m$, Cs134	"	Cs134, Rh106

*i; (isotope n) this isotope does not contribute significantly to the total ground gamma exposure rate.

ii; " the main isotopes have not changed since the previous time.

conditions. The downwind distance and ageing time dependences of the on-axis ground exposure are shown in figure 5.31, with contours of equal exposure. The detailed dependences within a day of the release will be affected by the process of using stepped releases. Ground roughness effects could be accommodated by reducing the contour values by an appropriate factor, usually quoted as about 0.5 but this is dependent on local conditions. These exposures are greater, or comparable, to a typical background irradiation level out to several kilometres.

External beta exposure rates, for the deposit from the sequence 1 release, are shown in figure 5.32 for neutral dispersion conditions throughout and also the case where the first four hours disperse under stable conditions, with the individual step contributions also shown. As before, for the ground gamma exposure rate, any portion of the sequence 1 release which disperses under stable conditions dominates the whole ground beta exposure rate as the deposit ages, see curve two. The beta exposure rate of the deposit formed from the third and fourth hours under stable conditions approximately equals the total beta exposure rate for the whole release when dispersed under neutral category D conditions, see curve 1. Figure 5.33 (a and b) shows the age and downwind distance dependences of the ground beta exposure in air on the axis of the plume for dispersal occurring in Pasquill category D and F weather respectively. The ageing time starts one day after the release ends, so as to avoid any problems created by using stepped fractions of the release. Under continuous stable category F conditions for the sequence 2 release the on-axis ground gamma and beta exposure history up to one year are shown in figures 5.34a and b, respectively. The contours in figure 5.34b are about 5 times those in figure 5.33b, due to the greater release of depositing activity. The form of the ground gamma contours in figure 5.34a show the effects of plume depletion at long distances, under stable conditions, when compared to those of figure 5.31. This can also be seen when the beta exposures shown in figures 5.33a and 5.34b are compared.

Case 4 produces much greater levels of ground contamination, as noted in the previous section. This is displayed in figure

Figure 5.31 Contours of on-axis external ground gamma exposure in air (milli-Roentgens) for a notional AGR accident 3.1 released under prolonged neutral conditions.

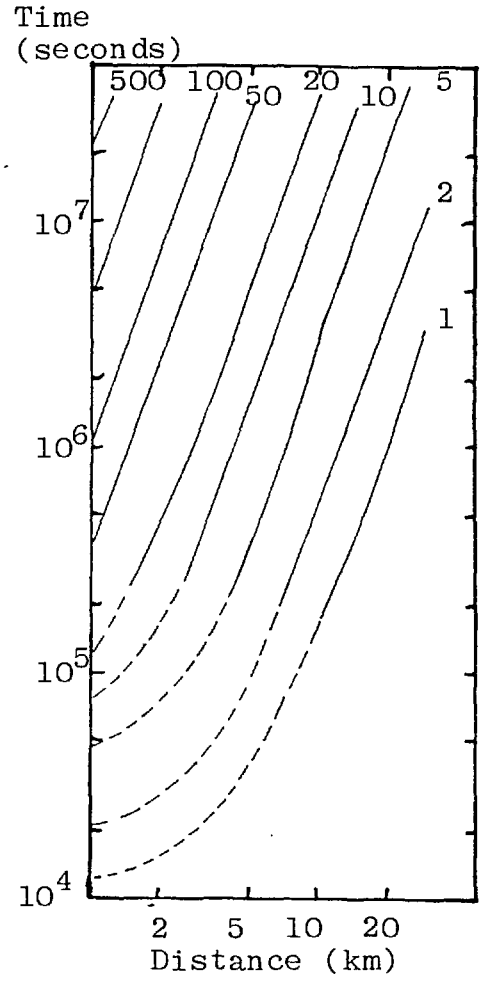

Figure 5.32 Effects of different dispersion conditions on the decay dependence of the on-axis external ground beta dose rate from the notional AGR accident 3.1.

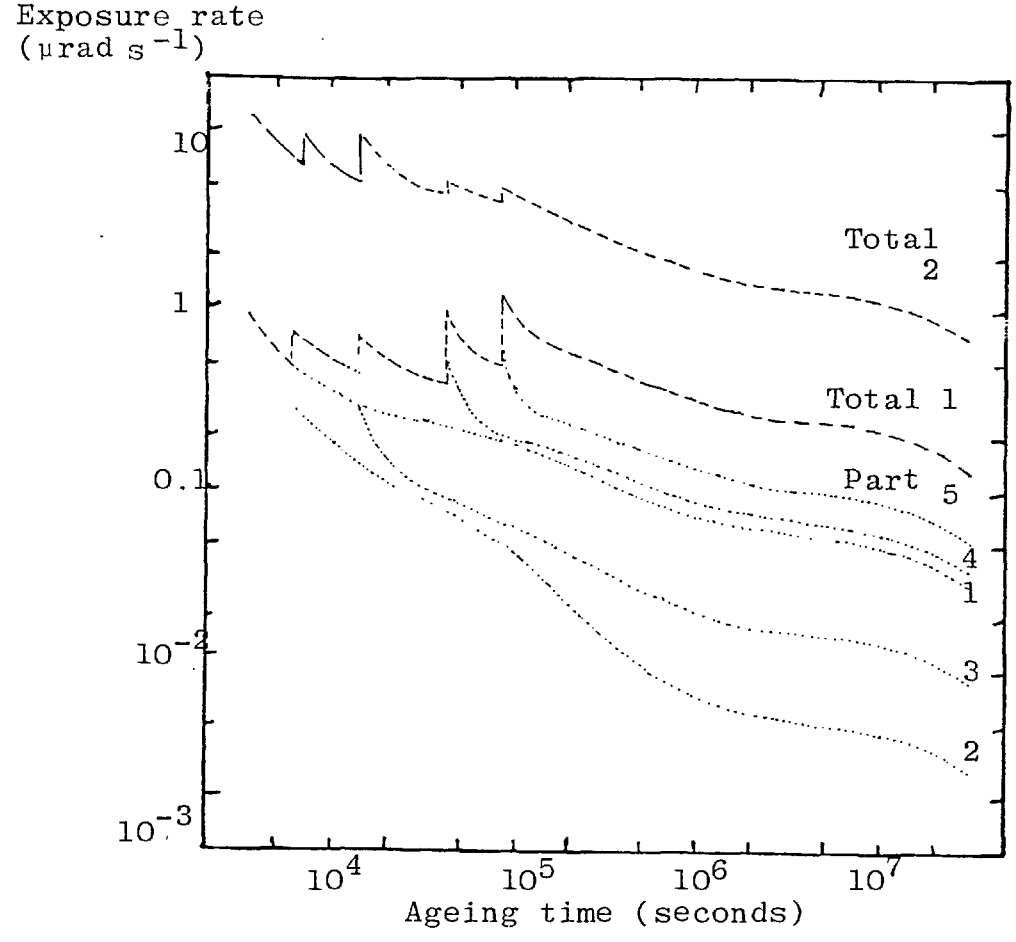

Fig. 5.33a Contours of on-axis external ground beta dose in air (millirads), for a notional AGR accident 3.1 released under prolonged neutral conditions.

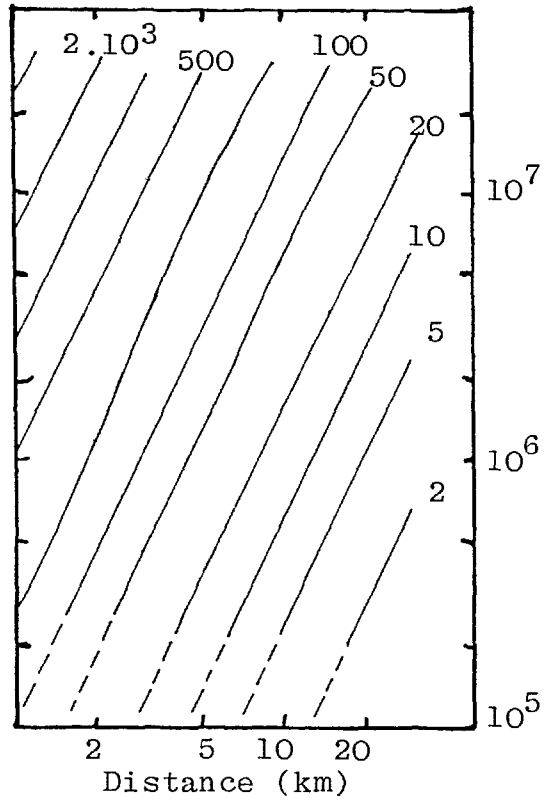

Figure 5.33b Contours of on-axis external ground beta dose in air (millirads) for a notional AGR accident 3.1 released under stable conditions.

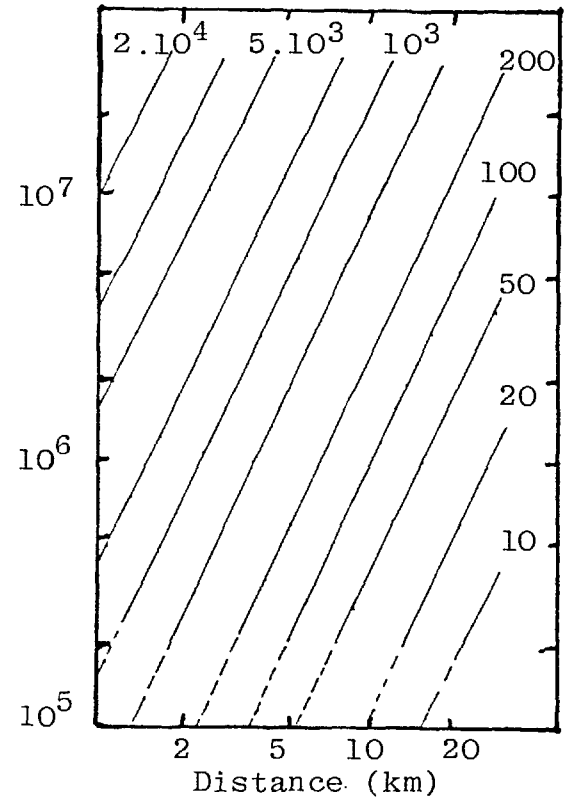

Figure 5.34a Contours of on-axis external ground gamma exposure in air (milli-Roentgens) for a notional AGR accident 3.2 released under stable conditions.

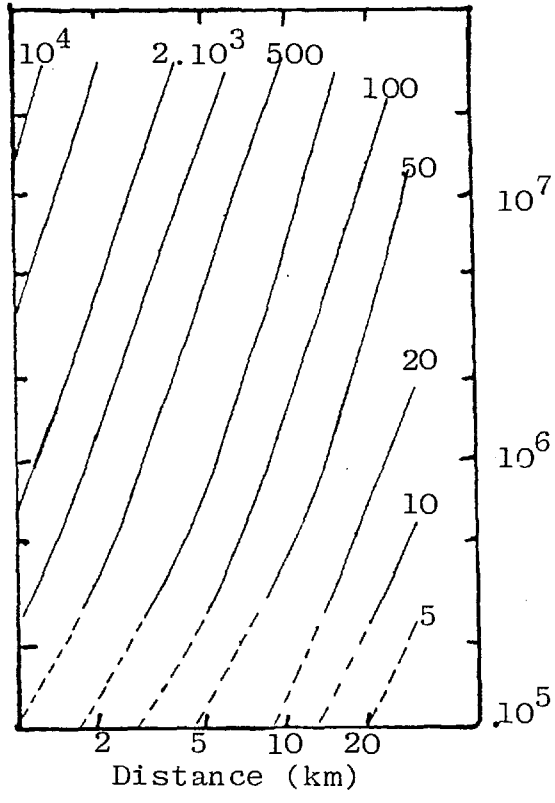

Figure 5.34b Contours of on-axis external ground beta dose in air (millirads) for a notional AGR accident 3.2 released under stable conditions.

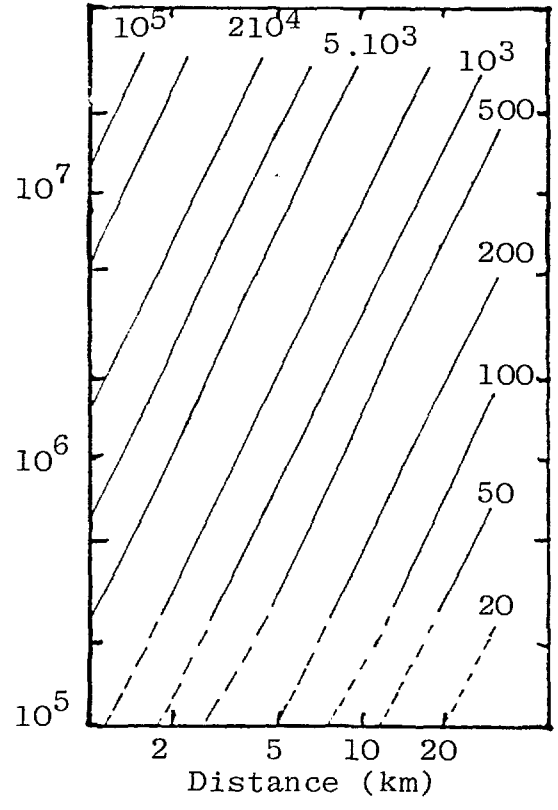

5.35 by the on-axis ground gamma exposure rate 1 km downwind of the source, after dispersion under Pasquill-Smith C conditions. For several hours during and after the release the ground exposure rate exceeds 0.7R/hr, and is still over 18mR/hr after one year ageing, neglecting any modifying effects. The gamma exposure from the ground deposit exceeds the cloud gamma exposure after two hours from the end of the release, which is much sooner than for the pin failure depressurisation releases or the contained channel melt-out accident. Gross gamma exposures building up in time are shown in figure 5.36, where the ground exposure exceeds the numerical cloud gamma estimate 1 km downwind by more than a factor of 100 after ageing of the deposit by one year. Both the last two graphs refer to deposition under slightly unstable conditions, which do not produce large depletion factors, and the ground gamma exposures reflect the large release fractions assumed. The total exposure of about 300 R during the first year, 1 km downwind, is unacceptably high and evacuation followed by decontamination would be required.

The full ageing and distance dependence of the ground gamma exposure is shown in figure 5.37a for the depressurisation release occurring under slightly unstable conditions. Even 30 km downwind the exposure can exceed 1 R (about 0.7 rem, (33)) within about one month and so also exceeds the ICRP stochastic annual limit on whole body dose to members of the public. The non-stochastic ICRP annual limit, in this case for irradiation of the whole body, is not exceeded in the first year beyond about 10 km of this ground level source. Any contamination by Cs137 becoming fixed in the soil could produce a hazard over an extended period, where figure 5.21 can be used to estimate the affected area. Neglecting weathering and ground roughness a Cs137 contamination level of about 6 microCi/m^2 could produce an exposure of over 0.5 R in air each year, only falling off with a half life similar to 30 years. The area could extend to 30 km along the axis of the deposit and about 5 km along the 10% plume boundaries, representing a large area of about 8.7 km^2 (2100 acres).

The ratios of ground to cloud exposures are plotted against ageing time and travel distance in figure 5.37b. This shows, as for the smaller notional depressurisation releases (cases 1 and 2), the effects of a narrow plume at short distances and

Figure 5.35 Decay of on-axis external ground gamma exposure rate 1 km downwind from a notional AGR accident 4 released under slightly unstable conditions.

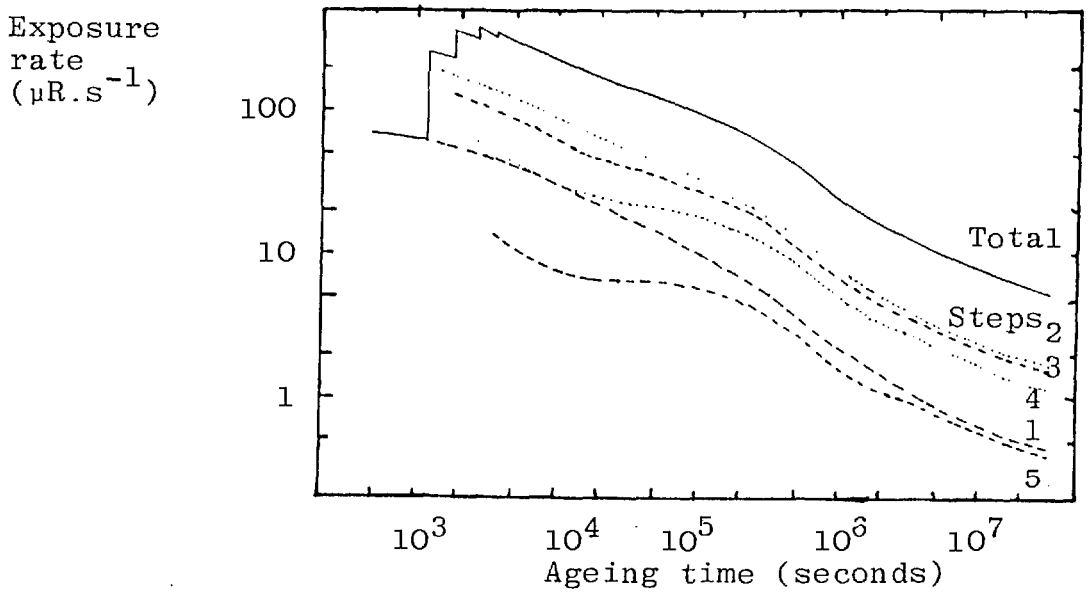

Figure 5.36 Build up in time of on-axis external ground and cloud gamma exposure 1 km downwind of a notional AGR accident 4 dispersing under slightly unstable conditions.

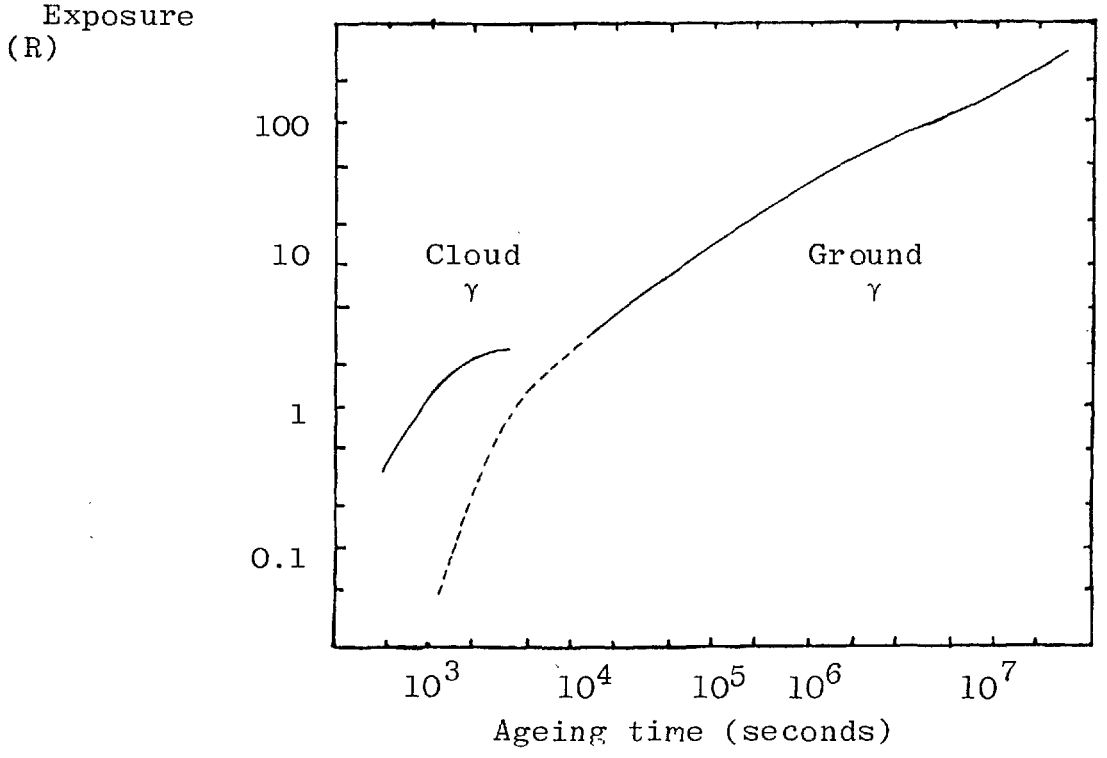

Figure 5.37b Ratio of on-axis ground to cloud gamma exposures in air after a notional AGR accident 4 is released under slightly unstable conditions.

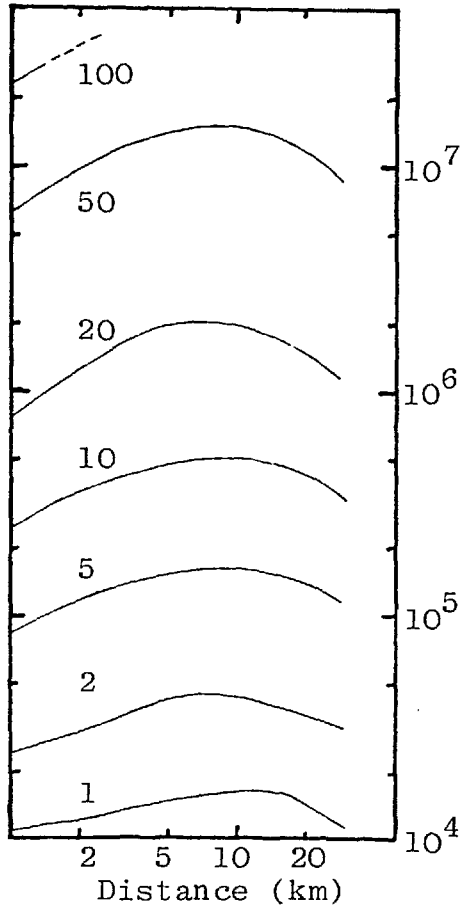

Figure 5.37a Contours of on-axis external ground gamma exposure in air for the notional AGR accident 4 released in slightly unstable conditions. (in Roentgens).

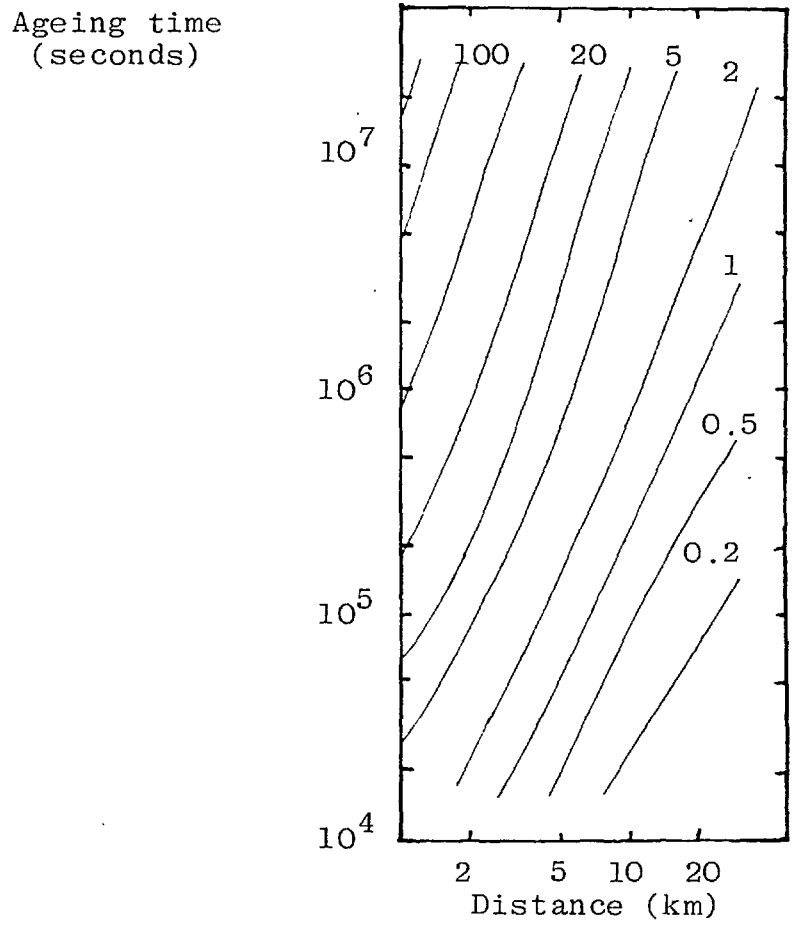

the decay of short lived isotopes in the plume by greater distances. The size of the release is represented by contours appearing at shorter distances and more occurring within one year.

The effects of ground gamma exposures from this single channel depressurisation accident are severe even under slightly unstable conditions. A brief example of potential consequences for this release dispersing in stable conditions follows, where only the exposure on axis 1 km downwind is described.

Figure 5.38 shows the on-axis external gamma exposure rate from the deposit formed under stable, low windspeed conditions 1 km downwind of the source. For about three hours, during and immediately after the release, this exposure rate exceeds 12 R/hr and falls after one year to 0.42R/hr, assuming no ameliorating factors. Obviously this would make a large area uninhabitable and could make early fatalities a major consequence in this interpretation of the release. The high on-axis gamma exposure rate from the deposited material 1 km downwind is shown in figure 5.39 along with the ageing dependence. This ground exposure exceeds that due to the cloud almost immediately after the passage of the plume, but downwind diffusion time has been neglected in these dispersion calculations. Also the effects of the stepped release would affect the time dependence of this exposure at short times. After ageing by one year the deposit has delivered a gamma exposure almost 400 times that of the cloud at this short downwind distance.

Isotopes which deliver major contributions to the ground gamma exposure during the ageing process of the deposit from this single channel melt-out depressurisation incident are shown in table 5.19. Iodine isotopes, given a comparatively high deposition velocity in the grouped depletion model, initially dominate the exposure rates. Later the caesium isotopes Cs134 and $Cs137/Ba137^{m}$ produce most of the exposure after several months. Ruthenium isotopes, Ru103 at short times and Ru106/Rh106 at longer times, give significant contributions to this external gamma exposure during the first year of decay.

Figure 5.38 Decay of on-axis external ground gamma exposure rate 1 km downwind from a notional AGR accident 4 released under stable conditions.

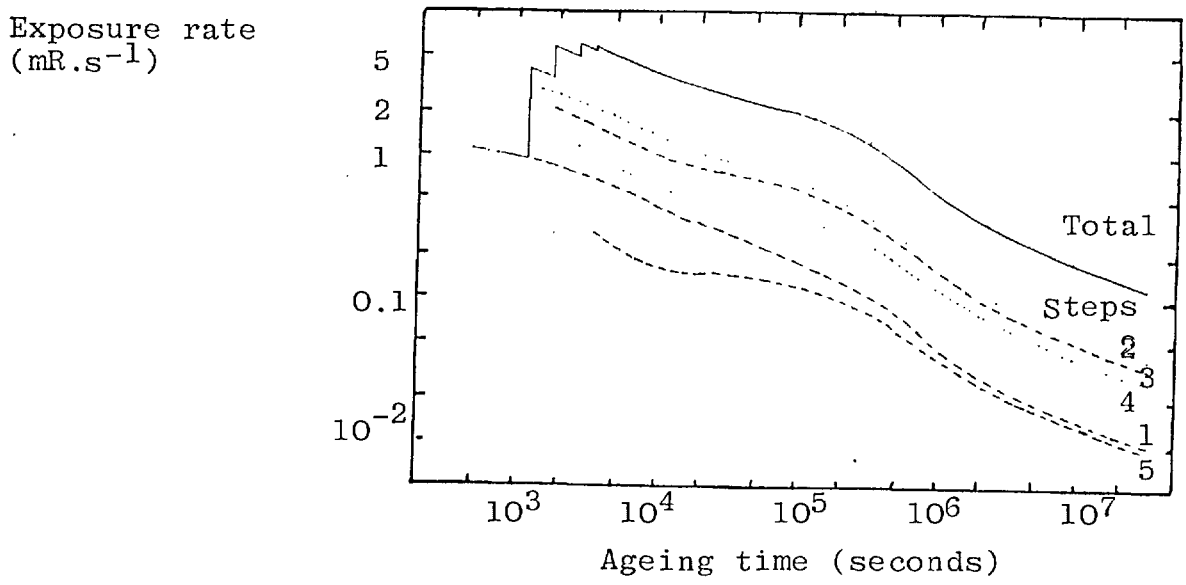

Figure 5.39 Build up in time of on-axis external ground and cloud gamma exposure 1 km downwind of a notional AGR accident 4 dispersing under stable conditions.

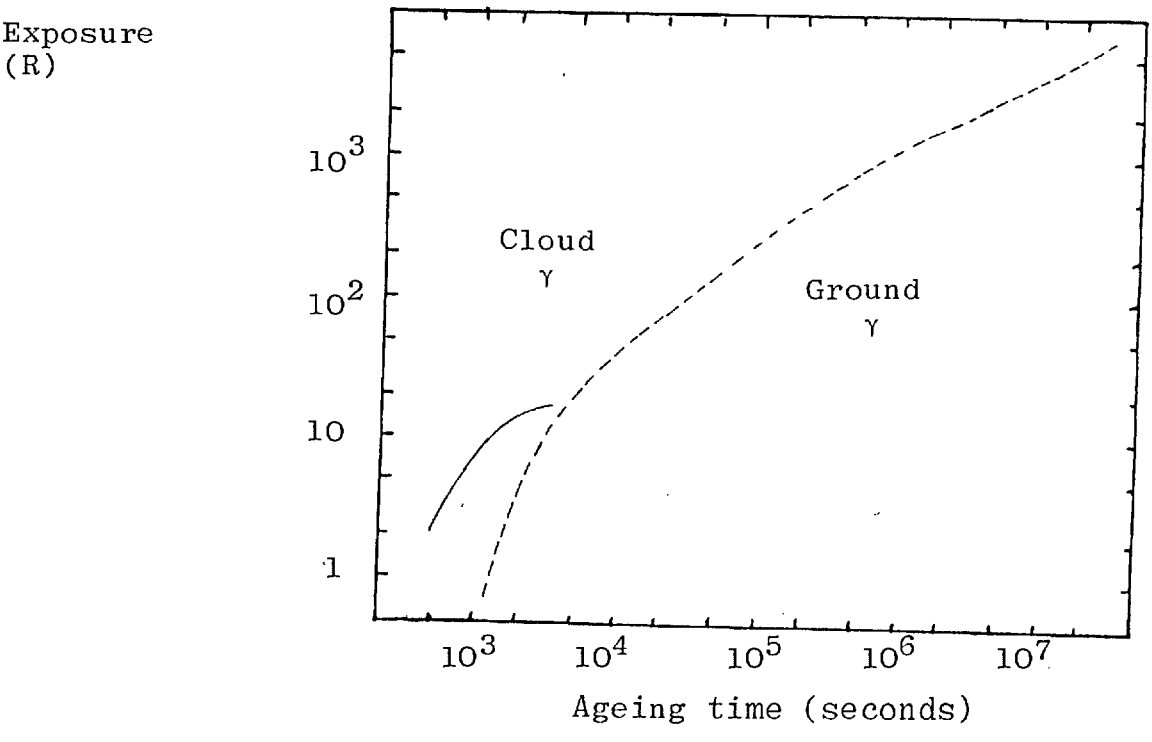

Table 5.19 Time dependence of significant contributors to the external ground gamma exposure from the single channel melt-out depressurisation release at short downwind distances with slightly unstable dispersion conditions.

Time after start of release	Dominant Isotopes				
	1 0-0.39MeV	2 0.39-0.68MeV	3 0.68-0.88MeV	4 0.88-1.28MeV	5 1.28+MeV
First 4 hr.	Te132, I131, $Tc99^m$	I133, Ru103	I132, I134	I134, $Te133^m$ I135	I135, I132, Cs138
Up to 1 d.	Te132, I131,	I133, Ru103	I132, Cs134	I132, I135	I132, I135, $Te131^m$
2nd day	"	Ru103, I132	"	I132, I135 $Te131^m$	I132, La140 $Te131^m$
3rd day	"	"	"	"	"
day 12	I131, Te132	Ru103	"	I132, Cs134	La140, I132
day 35	I131 (Ce141)	Ru103, Cs134	Cs134, $Ba137^m$	Cs134, Rh106	Cs134, La140 (Pr144)
day 70	I131(Te129, Ce141)	"	"	"	"
day 170	(Ce144, Ru103)	Cs134, Rh106	"	"	Cs134, Rh106 (Pr144)
1 year	(Ce144, Sb125)	"	$Ba137^m$, Cs134	"	Cs134, Rh106

Figure 5.40 Decay of on-axis external beta dose rate 1 km downwind from a notional AGR accident 4 released under slightly unstable conditions.

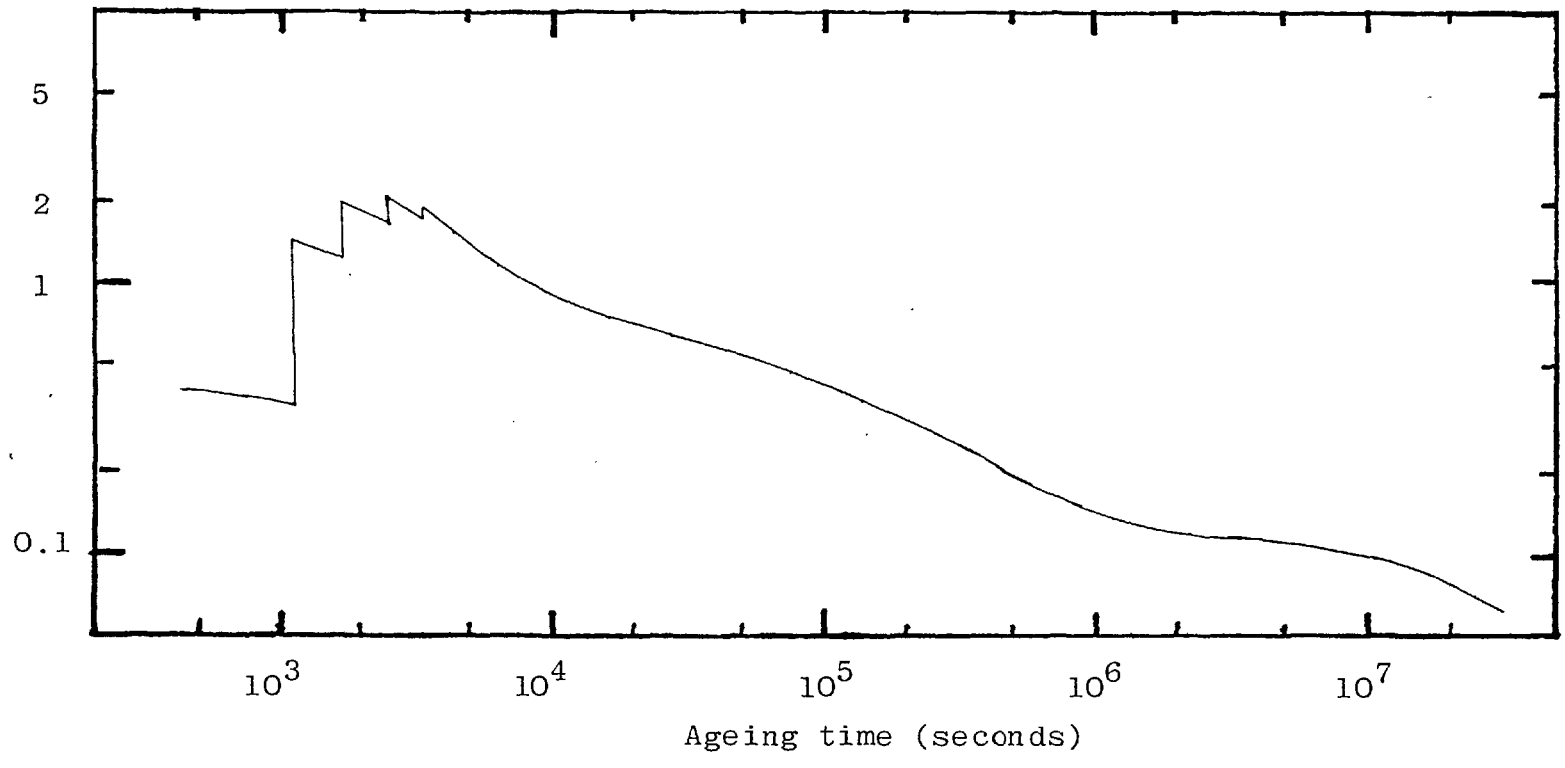

The portion of the release from 480 seconds to 1800 seconds dominates this depressurisation release, both for inhalation and external cloud and ground doses. This is again shown by the step components of the release in figure 5.40, giving the time dependence of the on-axis beta exposure rate from material 1 km downwind under slightly unstable conditions. This peaks at about 6 rad/hr during the release, but decreases more rapidly immediately after the end of the release than the ground gamma exposure rate. Towards the end of the first year the beta exposure rate reaches a slight plateau not found for the gamma exposure rate in figures 5.35 or 5.38. The isotope Rh106, the short lived daughter of Ru106($t_{\frac{1}{2}}$=369d), has a mean beta decay energy of 1.4 MeV, while other long lived isotopes and associated radionuclides do not produce such high beta decay energies.

No further consequences will be discussed, as an adequate description of these releases has been given in the preceding sections. Collective dose commitments to groups of population will be discussed in the next chapter, while the remaining section of this chapter briefly displays some attempts to produce "diagnostic" predictions.

Section 5.4 Use of WEERIE to provide "diagnostic" quantities for the four AGR cases

If an accident were to occur it would be of obvious benefit to have methods available which would permit identification of the release on the basis of a few quite rapid field measurements. The CEGB have estimated time integrated air concentrations and associated gross decay counts which can be related to ERL's of organ dose (36). Other indicators which may be of use, besides the gross beta and gamma count rate, are:

i. Gross cloud gamma/beta ratios of exposure (rates),
ii. Ground gamma exposure rates at short times,
iii. Energy spectra of gamma (external) exposure.

The next three subsections will briefly describe some applications of the methods developed to predict gross decay counts and the other parameters.

Section 5.4.1 Gross decay counts from airborne radionuclides

There are many problems associated with physically sampling a plume of mixed radioactive nuclides in the atmosphere. These

difficulties would be enhanced if a comparatively simple quantity such as a decay rate count were to be used in predicting a complicated parameter such as inhalation doses likely to be received by a member of the public.

The sampling procedure itself can cause problems, as not only the properties of turbulent diffusion in the atmosphere have to be considered but also the limitations of the available counting system. At present the emergency plans involve taking an air sample by drawing air through a filter. The decay rate of material on the filter is assessed and related, through previously calculated factors, to potential organ doses. Such filters would only provide a delay period of a few score seconds to inert gases, which can contribute greatly to cloud beta, and to a certain extent to cloud gamma, exposures. This delay is quite short compared to typical half lives of the inert gas isotopes involved, so such measurements would not directly allow the release of inert gases to be quantified.

The sampling time has to be sufficient to provide adequate averaging over typical eddies met in the atmosphere. Other requirements are that a sufficient active aerosol sample is obtained to give good counting statistics, but too much activity can cause a decrease in counting efficiency due to the dead time of the detector. Once the sample has been gathered there are still factors affecting the counting rate which are particular to the counting geometry and detector type. No direct detailed information is available to allow,in this study,for all these factors, so the rest of this section will deal only in terms of time integrated air concentration (disintegration per m^3).

Current CEGB beta/gamma action levels (BGAL), primarily for fission products, are quoted (36) in units of disintegrations per minute per cubic metre, where if this level is maintained for a period of four hours an ERL will be exceeded. Hence the time integrated air concentration levels producing the relevant ERL from these mixed beta/gamma disintegrations can be derived assuming this constant level by applying a factor of 240 minutes, so $D(dis.\bar{m}^3.ERL^{-1})=BGAL(ERL^{-1}(\text{in 4 hr}).\ dis.m^{-3})*240$ mins.

Table 5.20 gives these time integrated air disintegration values for four accident sequences, with the appropriate critical organ.

Table 5.20 Time integrated disintegration count to give doses equal to organ ERL's for radiologically, and related, significant isotopes (Macdonald et al (CEGB))

Type of release	Critical Organ	ERL(rem)	Total beta/gamma level to give 1 ERL ($dis./m^3$)*
Minor depressurisation with pin failure	Thyroid	30	1.8(10)
Major depressurisation with pin failure	LUNG	30	5.5(9)/1.8(10)†
Major depressurisation with pin failure, but zero plate-out	Lung	30	3.1(9)/6.5(9)†
Single stringer fuel melt-out	Thyroid	30	4.3(10)

*1.2(3) = 1200 etc.

† 10% reduction in the release of ruthenium

The details of these accidents were not given explicitly (36) while the disintegrations considered only apply to "mixtures of isotopes of a single element plus associated precursors and daughter products". Direct comparisons between the results in table 5.20 and those from this study cannot be made, but could give qualitative agreement. Most of the AGR cases quoted by the CEGB apply plate-out factors to all isotopes, whereas this study only applies this effect to iodine isotopes so relatively enhancing the importance of other elements.

Here the time integrated activities (dis/m^3) are taken for each non-gaseous fission product within the radiologically significant decay chains of the elements: strontium, ruthenium, iodine and caesium. All decays due to inert gases within these chains are neglected as are decays of elements in other chains. This assumption will artificially enhance the effectiveness of the "measured" total decays which are assumed to contribute to organ doses, especially for the releases containing proportionately large releases of inert gases, such as the contained single channel melt-out incident.

The time integrated disintegrations per ERL to the critical organ derived from these calculations, for each of the four notional AGR releases, are given in table 5.21, where variations due to different travel times and associated plume depletion are also shown. This table shows how the type of sequence affects this diagnostic quantity, although not all incidents considered have a severity in which the relevant ERLs for inhalation doses to organs are exceeded beyond 1 km downwind of the source. The lung action level varies from $2.1.10^{10}$ to $1.3.10^{11}$, rather than from $3.1.10^{9}$ to $1.8.10^{10}$ in the CEGB calculations. The difference between the two sets will depend on the descriptions of particular accidents as well as assumptions about which radionuclides contribute to the total "measured" count, so may not be contradictory. A factor of 5 can be produced between the different accident sequences, where the effect of different windspeeds can also affect the result for the lung value. Lower windspeeds allow more of the shorter lived, generally less radiologically significant, isotopes to decay, so relatively enhancing the doses from the plume for a given disintegration rate.

Table 5.21

Beta/gamma action levels derived from the four notional AGR accidents.

Accident	Organ	On-axis time integrated concentrations (dis./m^3)*		
		1km(D,U=5m/s)	1km(F,U=2m/s)	3km(F,U=2m/s)
1	Thyroid	8.4(10)†	-	-
2	Thyroid	7.7(10)	1.2(11)	1.7(11)
	Lung		1.3(11)	1.3(11)
3.1:				
hrs:0-1	Lung	3.4(10)	2.8(10)	2.8(10)
	Thyroid	1.2(11)	1.6(11)	2.4(11)
1-4	Lung	3.6(10)	2.5(10)	2.4(10)
	Thyroid	3.2(10)	3.3(10)	4.7(10)
0-4	Lung	3.5(10)	2.7(10)	2.7(10)
	Thyroid	6.3(10)	8.4(10)	1.2(11)
3.2:				
hrs:0-1	Lung	-	2.8(10)	2.8(10)
	Thyroid	-	1.6(11)	2.4(11)
1-4	Lung	-	2.1(10)	2.2(10)
	Thyroid	-	4.4(11)	5.2(11)
0-4	Lung	-	2.2(10)	2.3(10)
	Thyroid	-	3.4(11)	4.3(11)
4	Lung	4.2(10)▽	3.6(10)	-
	Thyroid	7.2(10)▽	1.2(11)	-

* for radiologically significant, and related, isotopes

† 1.2(3) = 1200 etc.

▽ slightly unstable, category C (Pasquill-Smith), dispersion conditions for column 1 entries for the major depressurisation single channel melt-out.

The thyroid action level is found to have a broader range of values, than for the lungs, under the circumstances studied here, while the CEGB published results show a narrower range. This could be due to the effects of the three group deposition model reducing thyroid doses relatively more than lung doses under stable conditions, so that the constitution of the airborne activity varies with travel by an additional factor to radioactive decay. In the pin failure type of releases the lung can become the critical organ under stable conditions where iodine isotopes are depleted preferentially from the plume where this depends on the physical form of the released iodine. Filtration affects the total number of disintegrations, arising from the contained single channel melt-out case, when inert gases are ignored but are a large portion of the releases; the model only subjected iodine to plate-out, and the thyroid dose did not vary greatly between the different sequences. In consequence the thyroid disintegration action level in the second to fourth hours of each filtration sequence show an order of magnitude difference, being lower when higher efficiency filters are applied to the escaping activity.

This brief discussion highlights some of the problems which have to be dealt with when trying to predict gross disintegration levels related to single organ inhalation ERLs. These difficulties have to be regarded in the perspective of actually obtaining field measurements. The position of the sample relative to the axis of the plume may be poorly known: in fact if manually operated samples are used it may be considered that too high a level of risk is attached to any attempts to make measurements close to the axis of some types of release. If a ten minute sample is used and only a limited time scale is available after the sampler has been correctly placed and started, the turbulent diffusion in the atmosphere may still produce random fluctuations in the measurement which could be misleading. The probability of this occurring would depend on a combination of the sampling time, the meteorological conditions and the travel time in the plume from the source to the detector. Elevated releases may delay this initial assessment if the plume can only be sampled within, say, about ten metres of the ground. Automatic monitors at the site boundary may be circumvented by the release in this

case and possibly also if there was a narrow jet-like high momentum release. Measurements close to the site may be unduly pessimistic due to the presence of relatively high levels of short lived nuclides and inert gas isotopes which do not contribute significantly to inhalation doses further downwind. Releases with high sensible heat content may produce plume rise effects which also cause problems in sampling the plume and predicting potential downwind consequences.

A simple gross measurement of airborne activity may be useful in assessing the general magnitude of a release, but has many limitations which have to be recognised in the particular circumstances surrounding the escape of activity. Other assessment methods have to be used in parallel.

Section 5.4.2 Application of gamma exposure rate measurements

Exposure rates, due to gamma rays from the plume and the deposit, are supposed to be measured under accident situations (36). Detailed isotopic identification takes several hours of analysis, so cannot be used immediately in the assessment of any release. Some details of calculated gross and simple energy grouped exposure spectra are discussed below.

The information in WEERIE only permits gamma exposure calculations by means of energy deposition build up factors. Hence any photon flux predicted at a given exposure point is in terms of the source energy photons, so does not relate directly to the flux of photons which would be measured, as the scattered component would be degraded in energy. The cloud gamma flux predicted in WEERIE may be a reasonable approximation if the unscattered component of exposure is dominant. This would occur principally for points close to the axis of the plume at distances such that contributions from distant parts of the plume are negligible (i.e. few high energy emitters). This produces complications which are difficult to deal with accurately. An assumption will be made that measurements of gamma rays are such that exposure and its first time derivatives are the measured variables, or those pertaining to energy deposition. The following discussion attempts to identify fairly simple gross characteristics of external gamma exposures during the passage

of the plume within the limitations described above. A further uncertainty in these calculations, relying on the stepped nature of the modelled release, is that longitudinal dispersion of the plume is neglected, so that no effects of merging of the stepped cloud results can be studied. These effects would be dependent on the windspeed and the dispersion conditions during the release as well as the time scale of the accident.

Initially results from the three notional depressurisation incidents will be outlined, see table 5.22. The releases become progressively worse for the cases a to c: a, Simple 20 pin failure; b, More severe 20 pin failure; c, Single channel melt-out (earlier referred to as cases 1, 2 and 4 respectively). The last has entries for slightly unstable conditions and stable conditions 1 km downwind on the plume axis while the others refer to neutral dispersion conditions. The grouped energy spectrum of the cloud gamma exposures do not show any major differences between the depressurisation releases. A slight difference between the pin failure and channel melt out cases is that the latter has proportionately more gamma exposure derived from isotopes emitting photons in the range 0.64 MeV to 1.28 MeV.

As the releases have been broken into steps average exposure rates due to the cloud gamma exposures can be calculated and compared to those from deposited material. The initial ground gamma exposure rates for each step were used but may err by, at least, a factor of two towards pessimism, especially at late stages in the major depressurisations. The ratios of mean cloud to initial ground gamma exposure rates for each step has been calculated. This shows that the more serious releases have relatively higher ground gamma exposure rates, particularly in the early stages of the depressurisation. These differences become less distinct towards the end of the releases, probably due to plate-out reducing the iodine content of the later stages of the releases which gives a major portion of the initial ground gamma exposure rates.

In the field it would be difficult to distinguish the exposure rate from material deposited early in the release to that

Table 5.22

Details of external gamma exposures during the notional depressurisation accidents.

Quantity	Notional Accident			
	Case A	Case B	Case C	
Dispersion category	D O 5 P	D O 5 P	C O 5 S	F O 2 S
Downwind distance	1 km	1 km	1 km	1 km
Numerical cloud gamma exposure by group energy, E_2=0.64MeV (% contributions)	28.0±0.5*	24.5±0.1	23-31*	23-31
E_4=1.28MeV	50-44	52-44	65.4±0.4	63.9±0.5
E_5=1.88MeV	68-63	66.0±1.4	85-81	81.3±1.2
E_6=2.35MeV	84-78	84-76	92-89	91-88
Ratio† of mean cloud to initial ground gamma exposure rates				
(a) for individual steps				
(start) 0-8 mins.	32-36	12	9	4
(mid) 8-30 mins.	43-14	14-11	8±1	3.5±0.3
(end) 30-60 mins.	-	5	9	3.5
(b) for accumulating initial ground gamma rates				
(start) 0-8 mins.	32-36	12	9	5
(mid) 8-30 mins.	12-3	7-3	5-1	2-0.5
(end) 30-60 mins.	-	0.4	0.4	0.16
Ground gamma exposure rates for individual steps (% contributions by energy group)				
E_2=0.64 MeV	15.5-11.6	16-14	19-25	20-26
E_4=1.28 MeV	67-46	69-50	72.3±0.5	72.3±0.3
E_5=1.88 MeV	90-75	91-76	94-88	92-89
E_6=2.35 MeV	95-84	97-84	97-94	96-94

*Where no monotonic trend exists during the release period a mean is quoted. Where a monotonic trend does exist the upper and lower limits are quoted in the correct time sequence to show increasing or decreasing trends.

†Uncertainties, possibly of factors of at least 2 could arise from effects of stepped releases on the ground gamma exposure rate, as during the release only upper and lower bounds can be estimated reasonably.

from later contamination. Hence the ratios of cloud gamma to accumulating ground gamma exposure rates are also given in table 5.22. The simple pin failure case is still fairly distinct from the other cases, due to the relatively low proportion of depositing nuclides in the release. In case c the different dispersion conditions produce a factor of about two in this ratio.

Finally from table 5.22 the grouped source energy contributions to the ground gamma exposure rate are detailed. The only slight difference is that the pin failure releases have exposure rates at energies below 1.88 MeV which decrease more rapidly during the depressurisation than for the channel melt-out case. This is due to the proportionately high energy contributions from inert gases and daughters, particularly Kr88/Rb88. Not only does this reflect the smaller amount of fuel involved in the pin failure cases but also the short time in which the activity escapes into the coolant. Case c has large contributions from many isotopes at these energies below 1.88 MeV and, due to the longer fuel involvement period, the proportion of low energy exposure, less than 0.64 MeV, increases during the release, but the proportion above 1.28 MeV is approximately constant.

From the above discussion it can be concluded that the type of release for a depressurisation incident may not be readily deduced with certainty from external gamma measurements. Gross gamma levels combined with disintegration counts of the passing cloud may be of more immediate use. A serious problem with these modelled depressurisations is the short time scale for the release, about an hour, during which it may be difficult to obtain a reasonably wide ranging set of measurements on the constituents of the plume.

This last point, of the speed of assessment, is also of concern for any releases from an intact coolant circuit, but the resultant plume can be located and studied in more detail close to the site at later times, so reducing time spent in transmitting necessary information to the emergency controller. The gamma details for the filtration sequences, 1 and 2, are given in table 5.23 for neutral and stable conditions, respectively, for an on-axis sampling point 1 km downwind. One

Table 5.23

Details of gamma exposures for the filtered releases from the channel melt-out in an intact coolant circuit.

Quantity	Notional Accident					
	Sequence 1			Sequence 2		
Dispersion conditions	D 0 5 P			F 0 2 S		
Time of step release	0-1 hr.	1-2 hr.	2-4 hr.	0-1 hr.	1-2 hr.	2-4hr
Filtration	0.0	0.97	0.97	0.0	0.5	0.5
Grouped energy contributions to the cloud gamma exposure, numerical estimate (% by energy group)						
E_2=0.64 MeV	37.8	95.4	72.6	44.9	77.0	83.8
E_4=1.28 MeV	70.3	96.9	78.6	72.4	86.9	90.5
E_5=1.88 MeV	84.8	97.7	81.8	84.9	91.1	92.9
E_6=2.35 MeV	91.6	98.5	87.2	91.1	94.1	95.2
(group 7 only)	7.7	1.5	9.4	7.8	5.4	4.5
Ratios* of mean cloud to initial ground gamma exposure rates						
(a) individual steps	1.5	22	3.7	0.97	2.6	1.9
(b) accumulating	1.5	6.5	0.83	0.97	1.3	0.85
% contributions to the ground gamma exposure rate, for individual steps by the group energy:						
E_2=0.64 MeV	22.1	17.8	17.7	23.5	27.3	36.3
E_4=1.28 MeV	72.0	75.9	77.7	72.6	75.6	81.1
E_5=1.88 MeV	90.7	96.9	94.1	90.4	91.3	91.7
E_6=2.35 MeV	95.5	98.0	95.5	95.1	94.3	93.4
(group 7 only)	4.0	2.0	4.3	4.4	5.4	6.3

*See text and table 5.22 for comments on the uncertainties in this ratio.

immediate effect on the cloud gamma exposure spectrum due to the application of the filters is a large relative enhancement of the low energy component, below 0.64 MeV. This is due to the inert gases which escape without being reduced by filtration effects. These gas isotopes, particularly Xe133, $Xe133^{m}$ Xe135 and $Xe131^{m}$, produce mainly low energy photons.

Only 40% of the fuel is involved by 1 hour and 80% after two, so this second hour is still affected significantly by any surviving short lived isotopes just escaping from the fuel. During the third and fourth hours fewer short lived isotopes are present in the release, while iodine releases are suppressed by plate-out but resuspension from the filters begins to have a noticeable effect. The efficiency of the filters can produce different types of gamma exposure spectra. High efficiency filters effectively retain most of the non-gaseous material, excluding iodine in this model. After all the fuel has been involved in the sequence 1 release, during the third and fourth hours, there is a fall in the proportion of low (less than 0.64 MeV at source) photons delivering exposures, while about 10% of the exposure is delivered from Kr88($t_{\frac{1}{2}}$=172 min) and its short lived daughter Rb88($t_{\frac{1}{2}}$=18 min) in the comparatively high energy range (2.35 to 2.7) MeV. In the sequence 3.1, with low efficiency filtration, there is less difference between the second and next two hours than in the other sequence 3.2.

Lower windspeed under stable conditions, assumed here, effectively reduces downwind contributions from short lived isotopes, but has little effect on the first hours' unfiltered release. About 5% of the cloud gamma exposure after the first hour of the second filtered release is produced by Kr88/Rb88 at source energies around 2.5 MeV.

The ratios of cloud gamma mean exposure rates to the individual step and accumulating initial ground gamma exposure rates are also given in table 5.23. By the end of the first hour there is little difference in these exposure rates, although it must be remembered that the nature of the stepped releases enhances the initial ground gamma exposure rate which is assumed to start at the end of the given step release period. Stable

dispersion conditions during the first hour enhance the importance of ground gamma contamination relative to that resulting from the cloud. For the higher efficiency filtered release under neutral conditions the mean cloud gamma exposure rates are more important, when compared to the initial exposure rates from the deposit, than with the lower efficiency filters in stable conditions. Details of these ratios are complicated but tend, except for the second hour of sequence 1, to be lower than those met in the early and middle stages of the major depressurisation accidents. This reflects the importance of large release fractions for non-gaseous isotopes on a single channel melt-out even when the escaping activity is treated by filters.

Ground gamma exposure spectra do not show any marked features for either of the filtered channel melt-out releases. During sequence 2 the Rb88 2.5 MeV exposure component, with smaller contributions from Cs138($t_{\frac{1}{2}}$=33 min), is slightly larger than in the high efficiency filtered release. The other qualitative difference is in the contributions in the sequence 2 release from the low energy gamma emitters, source photons below 0.64 MeV, which deliver up to twice as much of the total exposure rate than in sequence 1.

Details of the external gamma exposure spectra could provide some qualitative properties of releases which could be used to infer some of the contents of a plume. These results need much more scrutiny to establish quantitative relationships for the different releases and also more sensitivity tests to the numerous parameters describing each accident. Problems may arise in distinguishing between photons emitted from the cloud and those from the ground deposit, especially the scattered components. The short duration of some depressurisation events may pose practical difficulties in taking rapid measurements of any radioactive release to the atmosphere.

Section 5.4.3. Ratios of beta to gamma exposures and exposure rates

One method which could be employed to locate a plume in the atmosphere is the measurements of beta to gamma exposure ratios in the atmosphere.

A major difference between the properties of beta and gamma radiation is the attenuation in the atmosphere by scattering and absorption, where the charged beta radiation has a much shorter range than photons. Hence away from the plume only the penetrating photons will deliver finite exposures. Due to the geometry of the plume and that of the deposit the direct photons from the cloud will be more important to external exposures. Only close to the plume will beta exposures be measurable and dependent on the local cloud concentrations, as is the semi-infinite cloud gamma approximation. This is shown in figure 5.41a for a notional single channel MAGNOX depressurisation accident (60), 100 m downwind under Pasquill-Smith category C conditions with building entrainment. Due to the elemental release fractions from the fuel these results will be qualitatively correct for most types of unplanned rapid fission product releases. The semi-infinite cloud gamma approximation follows the local cloud concentrations as would the cloud beta exposures. Also shown is the crosswind dependence when the iodine release is reduced from 10% to 1%, causing a 40% overall reduction in the cloud gamma exposure. Similar curves can be drawn for the gamma exposure rate 1 metre above the ground contamination, but due to the more limited geometry the ground gamma exposure rate follows the local concentration more closely than that from the cloud within the 10% plume boundaries, see figure 5.41 b. This ground gamma exposure decreases more rapidly with crosswind distance than does that of the cloud gamma numerical estimate.

The ratios of gross cloud beta to the numerical estimate of the cloud gamma may be of some use when identifying releases. In both the pin failure cases there is a steady decrease in this ratio as the depressurisation continues. This ratio varies during the release period, as shown in table 5.24. This shows the relative effects of proportionally less inert gases in the larger, Case 2, release. For dispersion under stable conditions this is larger for case 2.

For these two pin failure releases the ratios of ground beta to ground gamma initial exposure rates for the individual steps progressively increase as shown in table 5.24. These

Figure 5.41b. Crosswind dependence of predicted initial numerical and local ground gamma exposure rates in air, 100 metres downwind, for a notional MAGNOX single channel melt-out under slightly unstable conditions with modelled building entrainment (iodine release 10%).

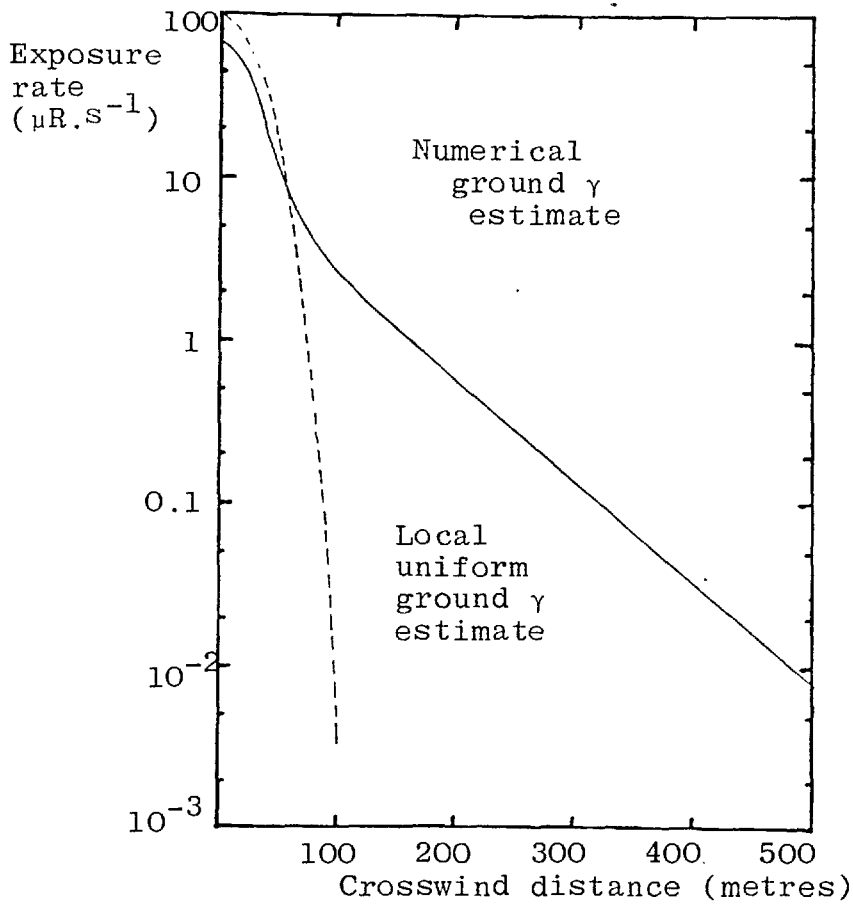

Figure 5.41a. Crosswind dependence of predicted numerical and local cloud gamma exposures, 100 metres downwind of a notional MAGNOX single channel melt-out released under slightly unstable conditions, with modelled building entrainment, showing the effects of reducing iodine escape from 10% to 1%.

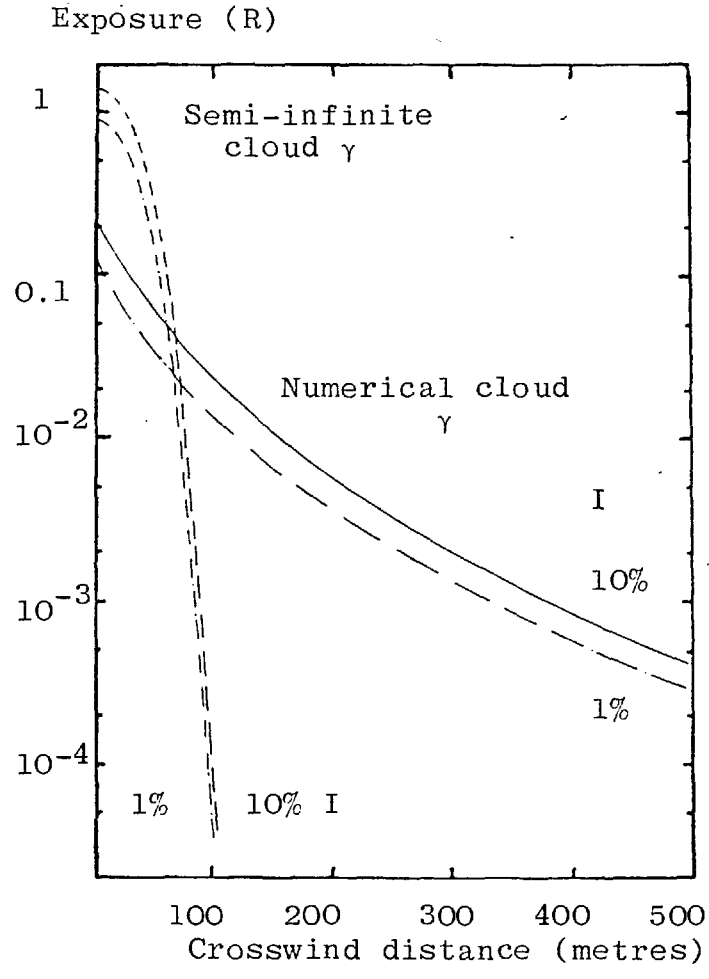

last two sets of ratios are very close as they are practically independent of the gas release fractions when the grouped element dependent deposition model is used. This shows a larger variation than for the cloud beta/gamma ratios which may reflect the plate-out of the iodine isotopes with high gamma production efficiencies. This trend is followed for the case 4 release and the ratio of initial on-axis ground beta and gamma exposure rates 1 km downwind varies over a similar range. For this more severe depressurisation incident the ratio of cloud beta to cloud gamma exposures lies very close to 2.7 throughout the release and does not vary monotonically during this period. This last ratio is lower than the previous values, reflecting the release of many more isotopes which have low ratios of (beta decay energy)/(gamma decay energy) compared to those of the pin failure cases. Also the attenuation of low energy beta particles by one metre of air has to be allowed for when comparing beta/gamma ratios from ground deposits.

A more complicated situation arises for the individual steps of the single channel release of fission products from an intact pressure circuit, sequences 3.1 and 3.2. Each first step shows the effect of different meteorology on the unfiltered slow release. The effects of filtration are of a similar magnitude to the meteorological influences.

Again differentiating between cloud and ground exposures may cause problems when conducting emergency beta/gamma measurements about a nuclear power installation after or during a release to the atmosphere. After further detailed study, with particular attention being paid to the definition of a wide range of accidents, these gross beta/gamma ratios may eventually be of direct use in rapidly identifying the type of release in an emergency when combined with other measurements.

Section 5.5 Summary and Conclusions

A range of notional AGR releases has been described. These have demonstrated successfully the methods discussed in chapters 2 and 3 for improving depletion and external exposure calculations. Some potential diagnostic parameters have been identified.

The dose patterns resulting from these notional releases will be applied in the next chapter to the study of collective quantities and site assessment.

Table 5.24 Beta to gamma ratios 1 km downwind of source

Release	Met conditions	Cloud β/γ		Ground β/γ	
		Initial value	Final value	Initial value	Final value
1	D	5.7	5.1	6.6	9.4
2	D	5.1	4.7	6.5	9.2
2	F	11.5	10.8	-	-
4	F	2.7	2.7	6.3	7.9
4	F	2.7	2.7	7.7	8.8
3.1	D	-	-	6.8	5.1
3.2	F	-	-	8.2	8.2

C H A P T E R S I X

Collective dose commitments and site assessment

Section 6.1 Introduction

There are many problems associated with the calculation and interpretation of collective dose commitments to a population group, particularly when a broad spectrum of the public surrounding any site is involved. The application of population census data to these calculations is demonstrated, where some limitations have been discussed in general terms in Chapter 4. Any collective doses from artificial sources of radiation in the environment have to be compared with those resulting from the normal background irradiation. The relative detriments of practices can be made by comparison of particular collective dose commitments (UNSCEAR, 1977).

In this chapter some practical examples of collective doses resulting from the series of notional AGR releases are analysed. These results are calculated by routines within one program, EXTRA, which deals with several aspects of collective dose evaluation. This is followed by a comparison of sites for the most serious notional AGR accident: that of a single channel melt-out associated with a major depressurisation, using slightly unstable dispersion conditions with an approximation of the effects of building entrainment.

The discussion then proceeds to the application of weighting functions on real population distributions for assessing the suitability of any given site as a location for a nuclear power station, as regards risks to the public. Different types of site and sector weighting functions applied to different ranges will be considered. The sensitivity of the results to the different factors will be analysed, where the angular width of the sector is an additional parameter for the latter weighting function. These results should provide useful information to guide the development of any assessment schemes for sites on a probabilistic basis. In an attempt to formalise the characteristics of the radial distribution of weighted population totals about a site a "quality" factor is defined and discussed as a site dependent quantity for comparative purposes.

It has been noted (Charlesworth and Gronow, 1967 (87)) that, "account can be taken of the relative prevalence of different wind directions and the frequency of different weather categories in those directions where these may have significance". This is a site dependent factor which has to be considered in any study concerned with the probability of any given level of risk. The effects on site and sector risk values are shown for an assumed windrose of one dispersion category. Future developments of weighting factors may take the effects of emergency measures into account, so finally an example of a hypothetical evacuation is modelled, using the computer program EXTRA.

Section 6.2 The potential effects on population groups of the notional AGR releases

The populations about a selection of nuclear power installations are used to display potential, but improbable, collective consequences resulting from the notional AGR releases described in the previous chapter. These collective doses are calculated within the program EXTRA, which is described briefly below:

The program EXTRA consists of modified and extended site assessment routines originally intended to follow the methods of the NII (41). The additional features of the new program include:

i. Census data editing facility, to relocate and add population about the site.

ii. The next sector to be assessed can be chosen by
   a) automatic step by a preselected angle in a clockwise direction;
   or b) a switch to any sector

iii. The downwind dose relationship can be altered by
   a) A uniform factor, without destroying original values
   or b) Read in a new set of values.

iv. Windrose weighting facility for each 10° sector, starting from 0° N.

v. Calculation of site and "worst" sector "quality" factors.

The first point allows not only the local population distribution to be represented more accurately (if this information is

available and is compatible with the census data base), but also allows the collective doses designed after evacuations to be modelled when used in conjunction with point three above. The second new option allows the detailed consequences for any or all sectors about a site to be studied more efficiently. The last two features will be dealt with in later sections. A 'free format' routine has also been incorporated to simplify the input data, particularly for the population editing facility.

The following subsections will deal with the results within 30° sectors out to 30 km for all the AGR accidents at one site, and collective whole body dose commitments within $22\frac{1}{2}^{\circ}$ sectors out to 100 km for nine sites.

Section 6.2.1 Comparison of collective doses for notional AGR releases at one site

Dispersion in the atmosphere can at best be predicted to within about a factor of three, which means that the shape of the plume in a gaussian model may not be a good approximation for a single release. Surface irregularities can produce large local influences on atmospheric dispersion. To reflect this uncertainty, and also the uncertainties in using residential population census data, the lateral spread of the plume is represented by a uniform box when calculating collective doses.

The uniform lateral box concentrations for the ground level releases studied are set to the average value within the 10% limits of the plume, where this can be calculated to be 56.5% of the peak on-axis plume concentration at a given downwind distance. This factor can be directly applied to inhalation dose commitments, but when long term ground contamination effects are considered this neglects the penetrating nature of the gamma rays producing exposures beyond the plume limits. For ease of calculating and interpreting collective dose commitments a sector subtending a fixed angle (α) from the source at all downwind distances is preferred. This enables the population groups to be rapidly identified, but will also mask the effects of the duration of the release on lateral dispersion. The typical lateral width of a plume means that the angle (β) subtended by the 10% limits of the plume tends to decrease at long distances. To allow for this

effect the mean box dose level has to be modified so that the value applied to population distributions is given by,

(6.1) $D_{box,\alpha\ sector}=0.565*D_{plume\ peak}*\beta/\alpha$, where α is chosen to be 30° in this first set of examples. This formulation means that this final dose level depends primarily on the vertical dispersion of different meteorological conditions on a release.

The collective doses to the population within 30km of site 1 are calculated, where the population data are in the form of gross numbers for individual enumeration districts where the population centroid is located to within a 100 metre square in the national grid coordinate system. If this centroid lies within the 30° sector of interest the population it represents is weighted by the dose associated with its distance from the site. The dose at a given downwind distance, which, as explained above, has a uniform crosswind distribution within the 30° sector, is calculated by interpolation between a set of previously determined values. These contributions from each enumeration district are accumulated with distance from the site and printed, with the accumulated population within each sector, at distances of 2,3,5,8,12,16 and 30 km.

When the detailed distribution of population about site 1 is considered one enumeration district is found to cover most of the area close to the semi-urban site, see figure 6.1. Due to the very irregular shape of this enumeration district its population centroid (A) is almost 3 km from the site, at the edge of the urban area. Within this particular area there is a small village of approximately 200 people only about 1.5 km from the centre of the site. The editing facility has been used to relocate these villagers from the ED population centroid to the position of the village.

The worst 30° sector, with the largest collective dose by 30 km, was chosen to compare the consequences of the four notional AGR releases. Each release was swept around the site population distribution in steps of 6°. It was found that the same sector, centred on 324° from 0° N, was the worst by 30 km for all releases. This is due to the downwind distance dependence of the inhalation doses resulting from these releases not being greatly dissimilar when averaged over a 30° sector, but this also depends on the particular population distribution.

Figure 6.1 Example of a very irregularly shaped Enumeration District including site one.

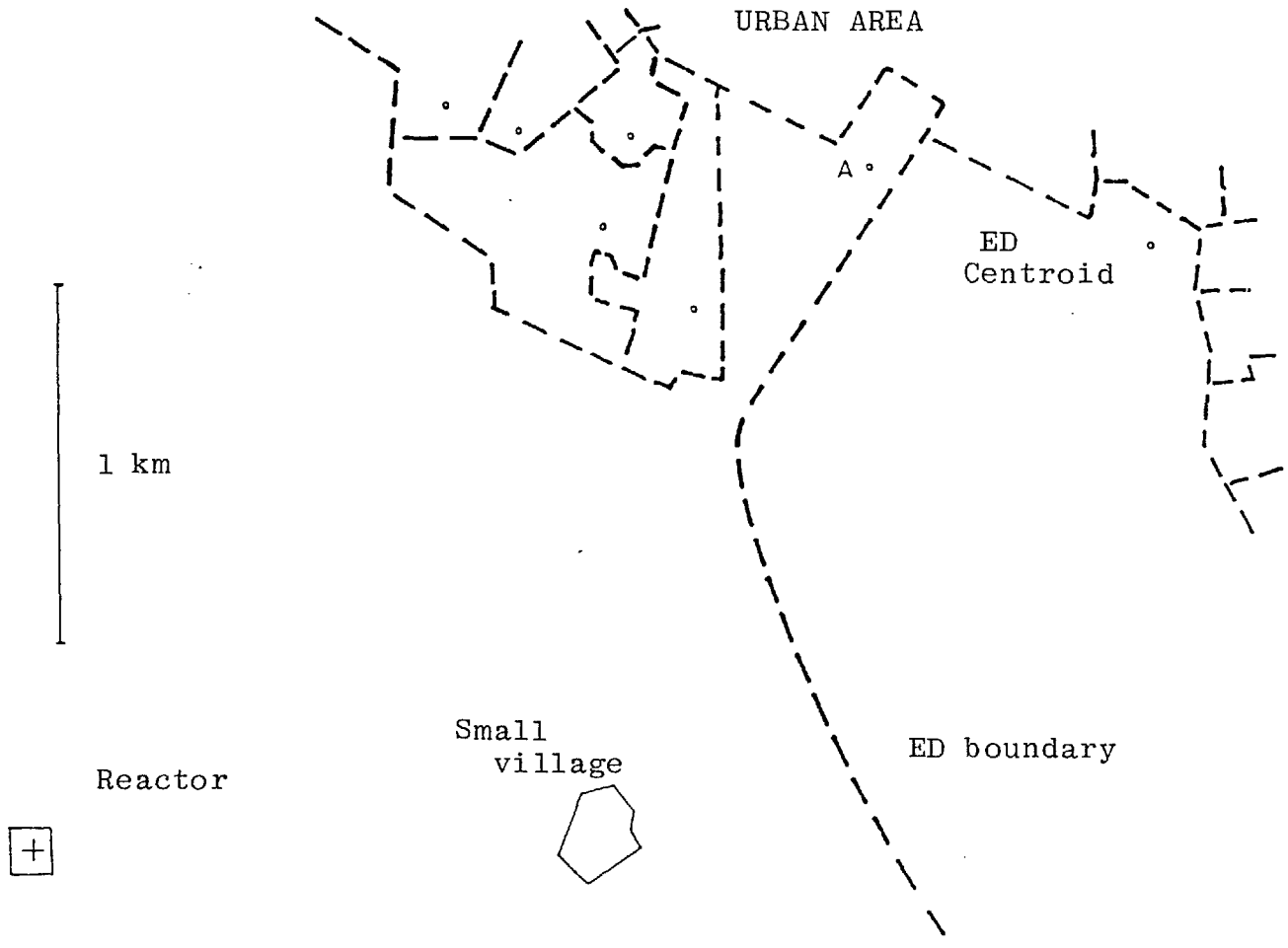

The full angular distribution of the collective weighted whole body doses within each 30° sector from the notional single channel melt-out major depressurisation accident dispersing under slightly unstable conditions is plotted in figure 6.2. The worst sector receives most of the total collective dose within 8 km of the site. The correction for the small village in fact removes people from the worst 30° sector even though this results in more people closer to the site. There is a broad sector from 180° to 250°, clockwise from north, where the collective dose in a 30° sector is comparable to the consequences of the worst sector at 30 km, but is delivered mainly between 8 and 16 km. If the probability of the wind blowing in a given direction was taken into account the sector with the greatest risk by 30 km may be different from that derived by this simple assessment.

The collective doses delivered to the population in the "worst" sector at this site are given in table 6.1 for a selection of doses and exposures resulting from the range of AGR releases. The collective dose is shown as it accumulates downwind along the sector, where none occurs within 2 km of the site for this "worst" sector. The accumulating sector population total within each of the downwind distance boundaries is given in this table. About three quarters of the total collective dose within the 30° sector out to 30 km from any release is delivered within the first 8 km which only contains about one quarter of the total sector population.

These collective dose commitments can be interpreted in terms of the numbers of fatal cancers which could develop in the exposed population within, say, 20 years for leukaemia and a longer period for most other forms of cancer. When groups of people are exposed to low radiation doses, in the stochastic range, the number of fatal cancers which could be expected per 10^6 man-rad (low LET irradiation) are about 100, with about twenty cases of lung cancer and five fatal thyroid malignancies (38). These values interpreted for an individual are comparable to the ICRP-26 stochastic specific risk factors of 10^{-4}rem^{-1}, 2.10^{-5}rem^{-1} and 5.10^{-6}rem^{-1} for the whole body, lung and thyroid respectively. Non-stochastic effects may occur close to the source only for persons exposed to the release from the single channel melt-out associated with a major depressurisation. Any non-stochastic

Figure 6.2 Angular dependence about site one, centred on a 30^{0} sector extending 30 km from the site, of the potential collective weighted whole body dose commitment from the cloud of a notional AGR accident 4 dispersing under slightly unstable conditions, with the intermediate distance dependence shown.

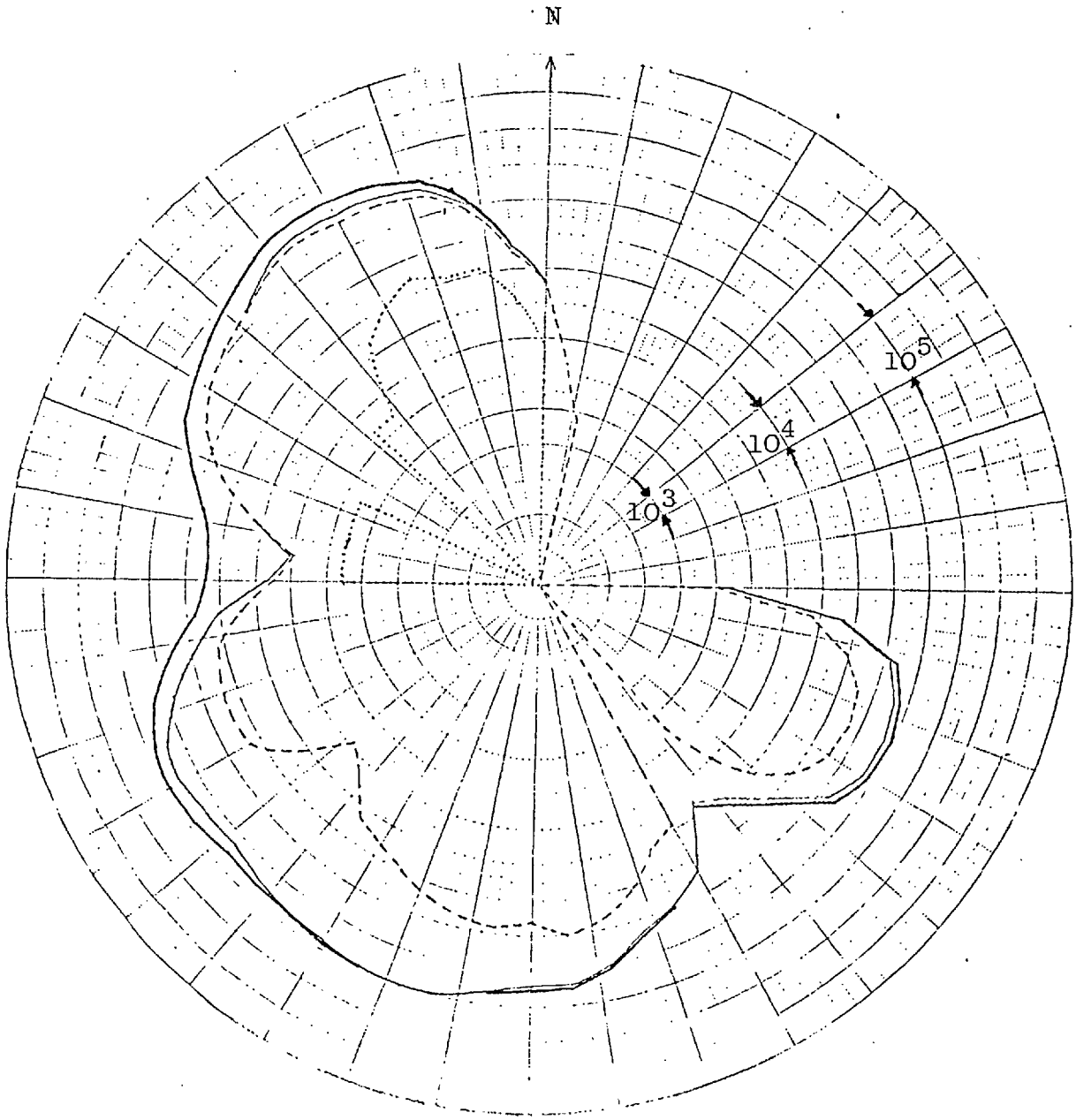

3 km . . . ; 8 km - - - - ;
16 km ——— ; 30 km ———— .

Table 6.1 Collective doses in the worst 30° sector at site 1

Source release	Dose	Units	Met. con.	Collective dose by the given distance					
				3 km	5 km	8 km	12 km	16 km	30km
4	Weighted whole body	man-rem	C'5S'	1.24(4)	4.30(4)	9.45(4)	1.02(5)	1.04(5)	1.35(5)
4	lungs	man-rem	"	6.46(4)	2.28(5)	5.03(5)	5.40(5)	5.58(5)	7.11(5)
3.1	lungs	man-rem	D5P	1.70(2)	5.98(2)	1.31(3)	1.40(3)	1.44(3)	1.74(3)
2	lungs	man-rem	F2S	2.3(2)	7.91(2)	1.72(3)	1.83(3)	1.89(3)	2.31(3)
2	thyroid	man-rem	D5P	8.34(1)	2.85(2)	6.14(2)	6.55(2)	6.72(2)	8.08(2)
1	"	man-rem	D5P	2.87(1)	1.0 (2)	2.18(2)	2.32(2)	2.38(2)	2.79(2)
External ground gamma in first year.	Whole body	man-roentgen							
4	"	"	D5P	5.42(4)	1.94(5)	4.33(5)	4.64(5)	4.78(5)	5.93(5)
2	"	"	"	1.13(2)	4.03(2)	8.94(2)	9.54(2)	9.81(2)	1.19(3)
1	"	"	"	3.33(1)	1.18(2)	2.62(2)	2.79(2)	2.87(2)	3.48(2)
Accumulating sector population				2341	16288	56141	65599	73939	207260

detriment, such as lung morbidity, is not considered in this study due to all the uncertainties involved.

Potential risk (G_F^I) can be defined as the probability of death for an individual from a given sequence of events (eg(35)). The potential risk of developing a fatal cancer within a lifetime from a given dose commitment (D) arising from a given year's practice, where the probability of receiving this dose level is P(D), can be given as $G_F^I = D.f_I.P(D)$, where f_I is the mean frequency of developing a fatal cancer per unit dose commitment (or the specific risk factor). An individual's mean potential risk rate can be defined as $\dot{G}_F^I = G_F^I/T \text{ yr}^{-1}$, where T(years) is an appropriate period such as the latent period for the development of a cancer or leukaemia. Once the dose commitment has been delivered then P(D)=1 . A collective dose commitment (Q) to a population group (C) can be associated with a given level of potential risk $G_F^C = Q.f_C.P(Q)$, where f_C is the number of fatal cancers developing per unit collective dose, and P(Q) is unity once an event giving a collective dose Q occurs. This risk now relates to a detriment to the health of the population group C. This value G_F^C can be interpreted as the potential number of fatalities in the population group C , so that a mean casualty rate for this can be defined as $\dot{G}_F^C = G_F^C/T \text{ yr}^{-1}$. If the population group C contains N people then the mean potential individual risk rate is $\dot{G}_F^{I'} = \dot{G}_F^C/N \text{ yr}^{-1}$, and a similar definition can be used for an individual's mean lifetime risk if in the exposed group C. There are many problems in estimating the values, and the meaning in relation to other human activities, of the terms used in the above definitions (38, ICRP 26, ICRP 27, (35)). The relative detriment for certain practices can be given by ratios of an organ's collective dose commitment for a given population group which has a specific response to this stimulation.

For the worst release, under slightly unstable conditions, about 14 latent fatalities may occur within 30 km of the site in this sector as estimated from the weighted whole body dose commitment. The collective lung dose commitment to the exposed population is the dominant contribution to this estimate, so a predominance of fatal lung cancers might be expected from this release as the frequency of fatalities from the same LET external

and internal doses is expected to be similar. Other inhalation dose commitments from the three lesser releases suggest the occurrence of less than one latent fatality, where mostly neutral dispersion conditions are used. Under stable conditions the prolonged filtered single channel melt-out release sequences may produce single figure latent fatalities, in the unlikely event of the whole release occurring in this one "worst" sector or the other highly populated sectors about this site. There is about a factor of 20 to 30 reduction in the collective inhalation doses between dispersion in neutral and stable conditions for a given release.

In the two pin failure cases, for dispersion under neutral conditions, the external gamma exposure after one year from the deposit could produce a similar number of fatalities as those resulting from inhalation doses delivered in stable atmospheric conditions, assuming the specific risk factors quoted earlier to apply. This suggests that several hundred fatalities may result over an extended period of many decades due to external irradiation from contamination in the most serious AGR release considered in chapter 5 if no ameliorating action was taken. The ground gamma exposure in the first year from this severest AGR depressurisation accident, under slightly unstable weather conditions, may result in long term casualties of order fifty, where any decontamination has been ignored. The plume under these Pasquill-Smith category C conditions is found to be narrower at large distances than the prolonged plume under neutral conditions, so is diluted relatively more when uniformly spread over a 30° sector. This effect, combined with the spatial population distribution about site 1 and the nature of the unfiltered melt-out release, results in the latent fatalities from the first year of ground gamma exposure in the severest case only being a factor of four above those due to inhalation doses, where this differential is much less than that found for the pin failure cases after dispersion in neutral conditions.

These potential, but improbable, collective doses to members of the public can be compared to the annual collective doses to workers, and personnel of external contractors, at a nuclear power station. The collective occupational dose is delivered

during such procedures as normal operation, inspection, maintenance, refuelling and any special operations, and is mainly in the form of external irradiation. Table 6.2 gives some annual collective doses for a variety of reactors where both the age and power of the reactor are important factors. The experience of most reactors is that the annual station collective dose is about several hundred man-rems, except where special operations are performed. These values are comparable to the whole body exposures after one year from the deposits resulting from the pin failure releases, but the mean individual exposure should be much less for members of the public. The severest depressurisation accident would result in a much larger collective dose, probably with the mean individual dose for the worst population group being comparable to the annual value for the workforce.

All stages of the nuclear fuel cycle result in doses being received by workers and members of the general public. Fabrication and reprocessing spent fuel are of greater detriment than transport of radioactive materials (Macdonald (97)). Storage of waste products, not only after treating spent fuel but also from mining and processing of uranium ores, can be potential sources of hazards. Generally it is required that doses to the public are at least an order of magnitude less than those received due to an occupation, where this should be reflected in the safety measures to prevent excessive releases of radioactivity to the environment.

The probabilities of these types of AGR accidents occurring in particular dispersion conditions are not known and can only be estimated by detailed analysis of the characteristics of the reactor and the site. An approximate upper limit can be obtained if the reactor is assumed to conform to an interpretation of a Farmer curve (35). This sets a target of a maximum allowable probability for the occurrence of any accident which should be met by the design and operation of a given reactor type. The target probability (F_p) is inversely proportional to the curies of I131 released (Ci_{I131})

(6.2) $F_p = 1/Ci_{I131}$ yr^{-1}, but has a maximum probability for any small releases, less than 100 Ci, of about $10^{-2} yr^{-1}$. These

Table 6.2 Typical annual collective dose commitments to nuclear workers (BNES, 1978 (98))

Description of annual staff collective dose	Number exposed	Collective dose (man-rem)	
		Mean	particular years
Typical PWR's (Germany)			
Demonstration	-	860	600-1300
First Generation	-	440	300-550
Second Generation	-	320	175-450
Particular reactors			
KWW(670 MW(e)) (1976) (commissioned 1972)	-	-	310
(1977)	-	-	320
KRB I (250 MW(e))(1976)(commissioned 1966)	670	-	550
Millstone-2 (USA)(2600 MW(t)) First full fuel cycle, includes 1400 man-rems from once in a lifetime operations	-	-	1800
Gas cooled Graphite moderated reactors (UK)			
Dungeness-A (commissioned 1966)	-	150	128-323
1976 history (5% of station dose from contracted workers)	560	-	154

values are intended only as an order of magnitude guide and real reactors are expected to have characteristics which are better than the Farmer curve. This should be the case for the AGR with its many design characteristics which would limit accidental releases.

From this Farmer curve and descriptions of the four notional AGR accidents in chapter five upper limits to the probability of occurrence are about $10^{-2}yr^{-1}$, for pin failures and filtered channel melt-out sequences, and $3.10^{-5}yr^{-1}$ for the channel melt-out associated with a major depressurisation. A complete analysis of the three smallest releases would probably separate the estimates of the frequency of occurrence of the relevant accidents.

A crude frequency to latent casualty plot can be obtained based on the preceding discussion for the "worst" sector at site 1 out to 30 km. Results are plotted in figure 6.3 where only the expected upper limit to the mean number of latent fatalities has been calculated with no indication of the variance about the mean. Differences of more than an order of magnitude could exist between the two sets of collective doses and any expected latent fatalities for the filtered release sequences. The probability of a given level of performance by filters, and more generally the effects of plate-out, would be a major factor in determining the consequences of this type of release from an intact coolant circuit.

Section 6.2.2 Survey of collective doses resulting from a notional major AGR depressurisation and single channel melt-out at sites in the UK.

Of the notional AGR releases the major depressurisation with a single channel melt-out is used here to assess potential collective sector doses about some sites for nuclear power stations in the UK. It should be emphasized that this accident has been selected principally for its mixed fission product characteristics and that its remote probability should be born in mind. This release is used as a vehicle to describe the effects of population distributed about sites with particular reference to the concept of a worst sector for collective

values are intended only as an order of magnitude guide and real reactors are expected to have characteristics which are better than the Farmer curve.

From this Farmer curve and the descriptions of the four notional AGR accidents in chapter five the upper limits to the probability of occurrence are about $10^{-2}yr^{-1}$, for the pin failures and the filtered channel melt-out sequences, and $3.10^{-5}yr^{-1}$ for the channel melt-out associated with a major depressurisation. A complete analysis of the three smallest releases would probably separate the estimates of the frequency of occurrence of the relevant accidents.

A crude frequency to latent casualty plot can be obtained with the information derived in the preceding discussion for the "worst" sector at site 1 out to 30 km. The results are plotted in figure 6.3 where only the expected upper limit to the probability of an accident is shown. Only an estimate of the mean number of latent fatalities has been calculated with no indication of the variance about the mean. Differences of more than an order of magnitude could exist between the two sets of collective doses and any expected latent fatalities for the filtered release sequences. The probability of a given level of performance by the filters, and more generally the effects of plate-out, would be a major factor in determining the consequences of this type of release from an intact coolant circuit.

A major engineering and calculational effort would be required to further quantify these and other consequences for all the AGR's in the UK.

Section 6.2.2 Survey of collective doses resulting from a notional major AGR depressurisation and single channel melt-out at sites in the UK.

Of the notional AGR releases the major depressurisation with a single channel melt-out is used here to assess potential collective sector doses about some sites for nuclear power stations in the UK. This release is used as a vehicle to describe the effects of population distributed about sites with particular reference to the concept of a worst sector for collective

Figure 6.3 Simplified example of probability-latent fatality distribution for site one for the range of notional AGR accidents considered in chapter five.

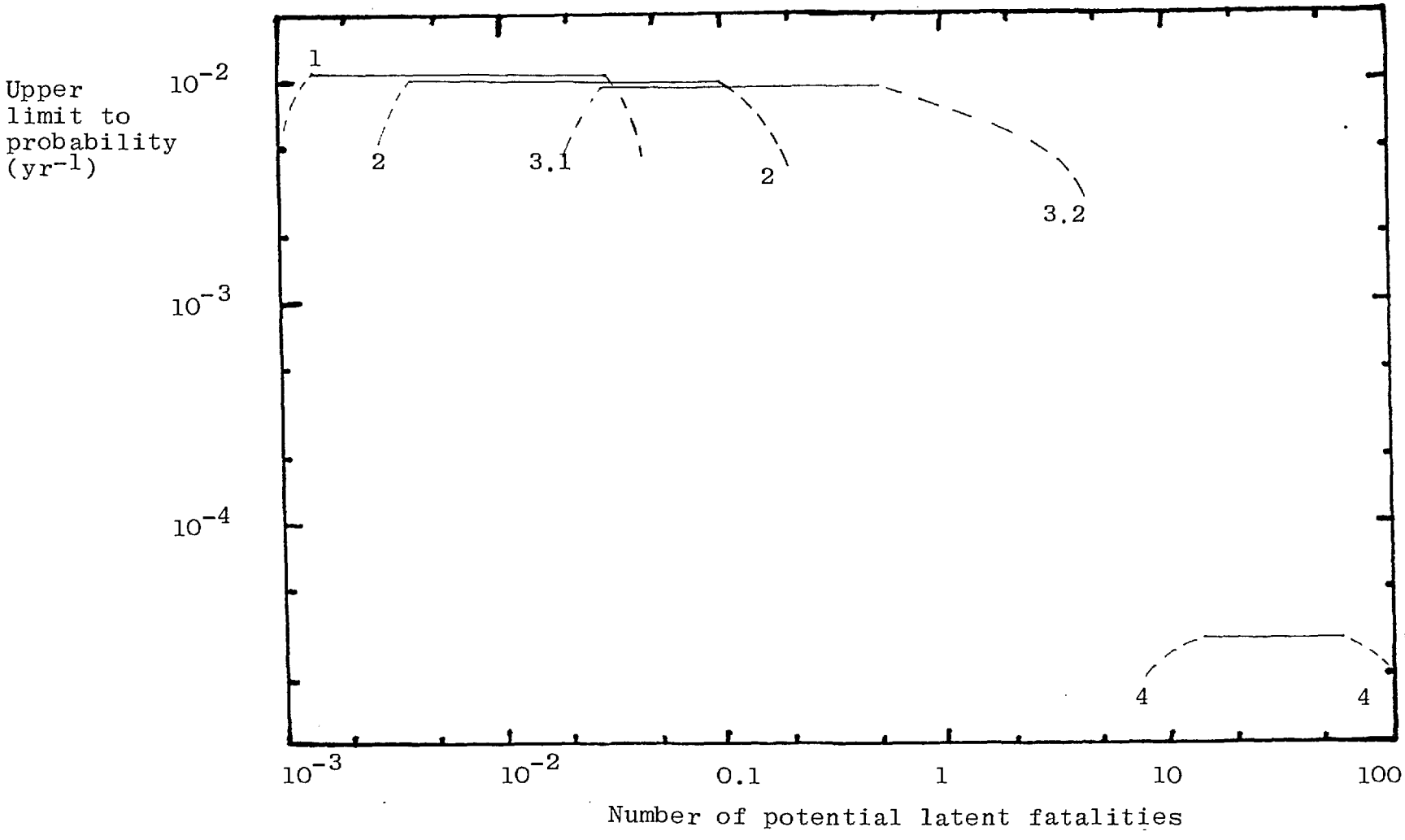

doses at a given site. The weighted whole body dose is applied in the calculations for the case where dispersion occurs under slightly unstable conditions in the atmosphere. This notional short time-scale release has not been limited by the WEERIE modelling procedure unlike the prolonged filtered releases and contains a broad range of fission products compared to the other notional releases.

Initially the sites are surveyed for 30° sectors out to 30 km using the enumeration district 1971 100% census data. Secondly the collective doses within a 22½° sector out to 100 km, representing a travel time of 5.6 hours under the assumed meteorological conditions, are considered using the ward and civil parish data from the 1971 census. In both cases the lateral spread of the plume is represented by a uniform dose level over the whole sector at any given distance, as described in the previous section. Many influences could affect the trajectory and the concentration profile of the plume while it travels 100 km, so these results can only be used as a general indication for individual sites.

Section 6.2.2.1 Collective 30° sector doses out to 30 km for eight sites

These collective weighted whole body dose commitments for 30° sectors are plotted in figures 6.2 and 6.4 to 6.10 for sites 1 to 8 respectively. Site dependent meteorology has not been accounted for in these results. The sector was stepped round by 6° which produces a reasonably continuous plot for a site. The editing facility was only used on site 1 as details of all sites were not readily available. This would only affect the results for sparsely populated rural areas within a few kilometres of a site, but villages of several hundred people, and larger communities, should be represented quite accurately.

To summarize for site 1 a "worst" 30° sector, especially close to the site, could be different if site dependent meteorology was used. Site 2, see figure 6.4, is in another semi-urban position but has a much more clearly defined worst sector at all distances out to 30 km. The "worst" sector for this second site has a collective dose which is slightly greater, by a few percent, than site 1 although the general level about site 1 is higher.

Figure 6.4 Angular dependence about site two, centred on a 300 sector extending 30 km from the site, of the potential collective weighted whole body dose commitment from the cloud of a notional AGR accident 4 dispersing under slightly unstable conditions, with the intermediate distance dependence shown.

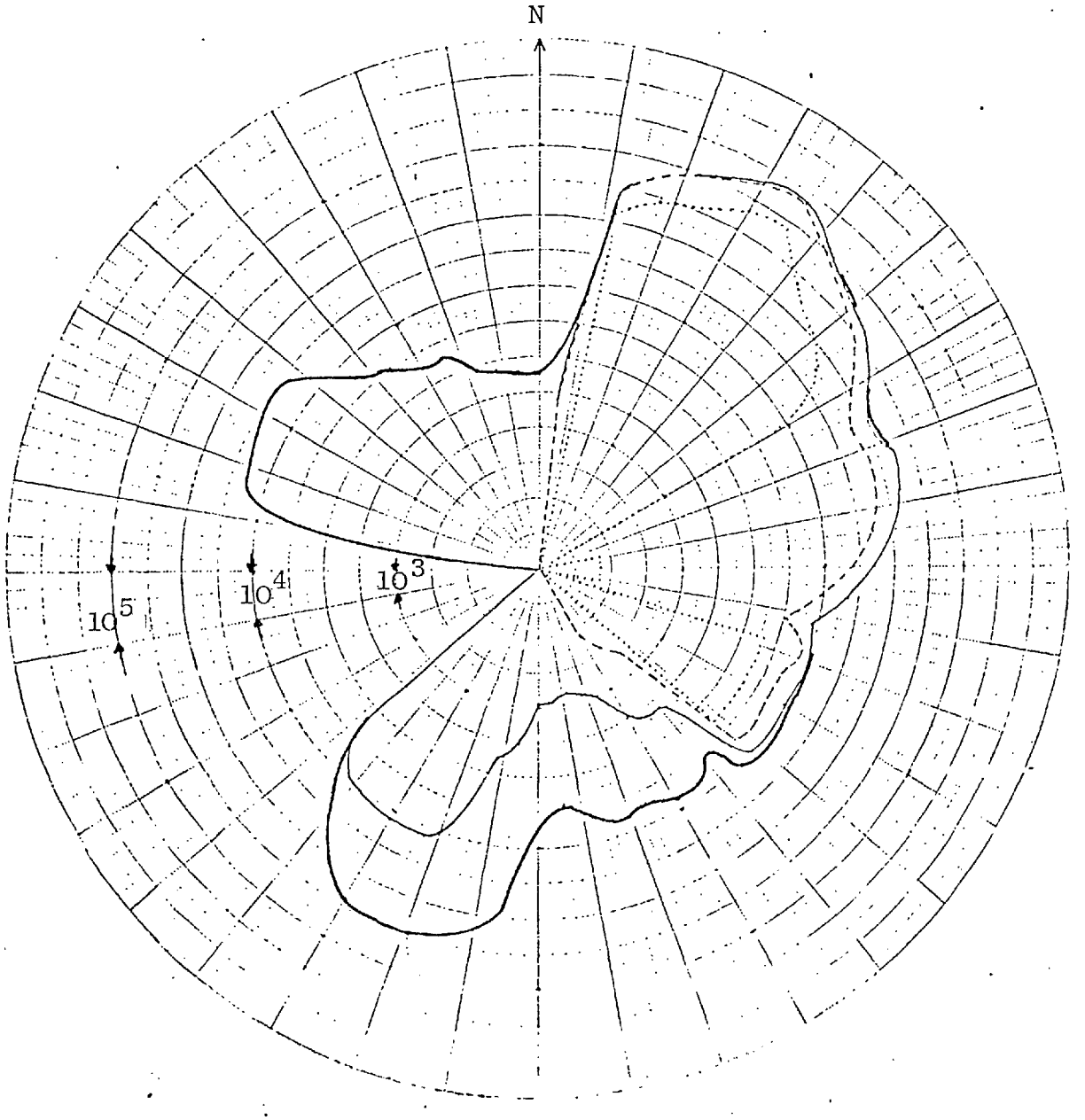

Sites 3 and 4, in figures 6.5 and 6.6 respectively, could be described as rural but are further removed from the open sea than the previous two sites. For site 3 the worst sector by 30 km is determined by the population distribution beyond 16 km which contributes over 80% of the collective sector dose. By coincidence this sector is roughly aligned with the worst sectors at shorter distances from the site. Although the collective dose in this worst sector of the third site is very close to those of the earlier two sites by 30 km it has proportionately smaller contributions from short distances. There is a general background about site 3 with only one other range of sectors which is comparable to the worst sector within 8 km of the site. Site 4 has a similar angular pattern but the worst sector at 30 km does not coincide with the worst sector at shorter distances. As sites 3 and 4 are quite closely related geographically, the longer range characteristics have similarities. There are two comparable sectors of concern within 16 km of the fourth site where one has a significant contribution within 3 km of the site.

Site 5, a rural coastal site, has a worst sector by 30 km which is dominated by the population beyond 16 km, but there is another unrelated sector of almost equal collective dose which has much greater short range contributions. Neither of these sectors contain the population within 3 km of the site. For site 6, about 60 km removed from site 4, the collective 30° sector dose to 30 km has several peaks, of about 2.10^{4} man-rems, for this dose pattern. This situation means that the method of choosing the worst sector could quite easily alter the worst sector radically, especially if site dependent meteorology was applied. The "worst" sector at 30 km also coincides with the worst sector to 16 km, but the worst sector within both 8 km and 3 km of the site is in another direction. One of the major peaks in the 30° sector collective dose at 30 km does not have any contributions from within 16 km of the site, and most of that population actually lies in the range 22 km to 30 km.

The final two sites, 7 and 8, to be considered in this section are coastal with mainly sparsely populated countryside within 30 km of each site. For site 7 there is one community just within 3 km of the site which clearly determines the worst

Figure 6.5 Angular dependence about site three, centred on a 30° sector extending 30 km from the site, of the potential collective weighted whole body dose commitment from the cloud of a notional AGR accident 4 dispersing under slightly unstable conditions, with the intermediate distance dependence shown.

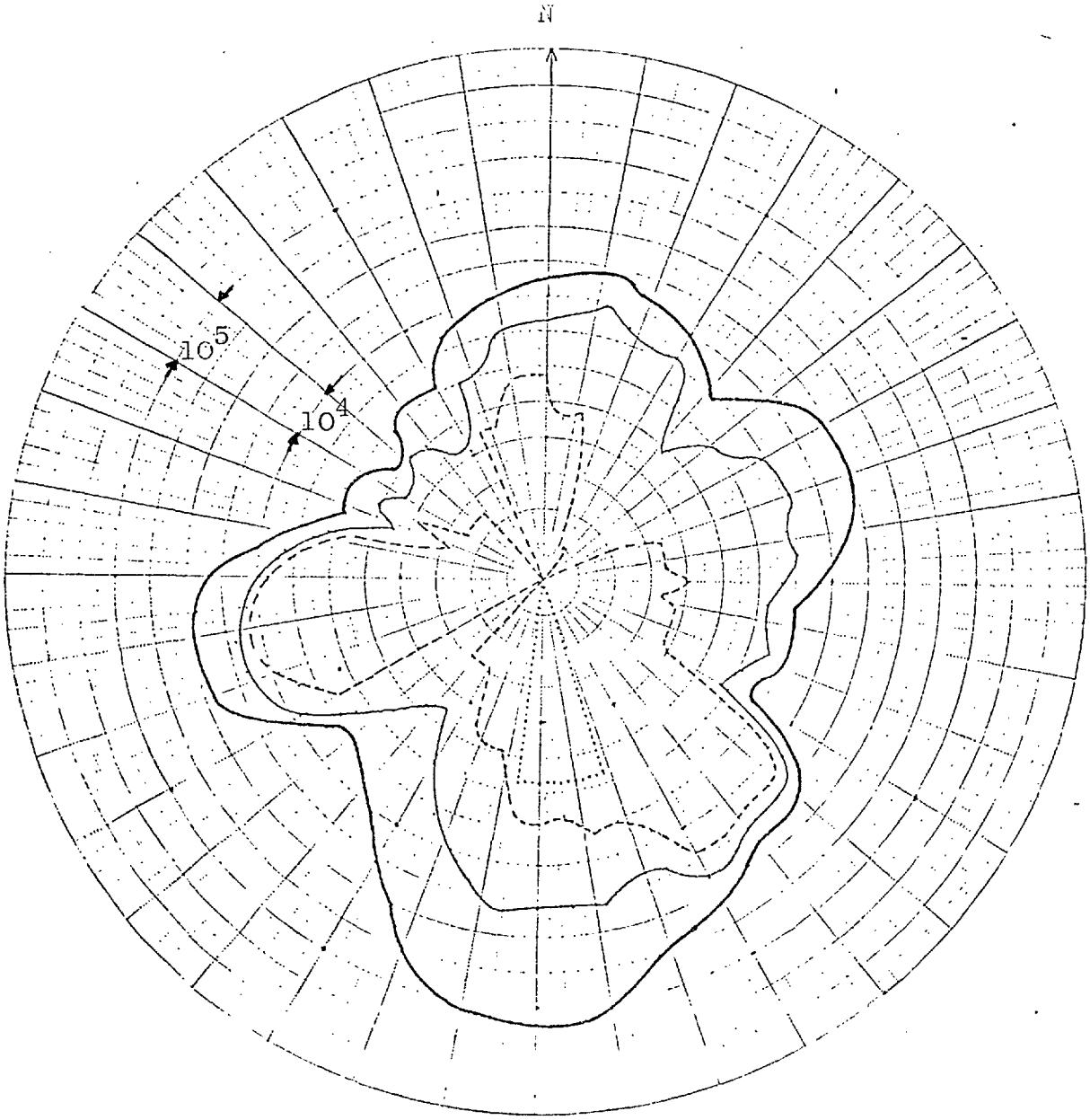

Figure 6.6 Angular dependence about site four, centred on a 30° sector extending 30 km from the site, of the potential collective weighted whole body dose commitment from the cloud of a notional AGR accident 4 dispersing under slightly unstable conditions, with the intermediate distance dependence shown.

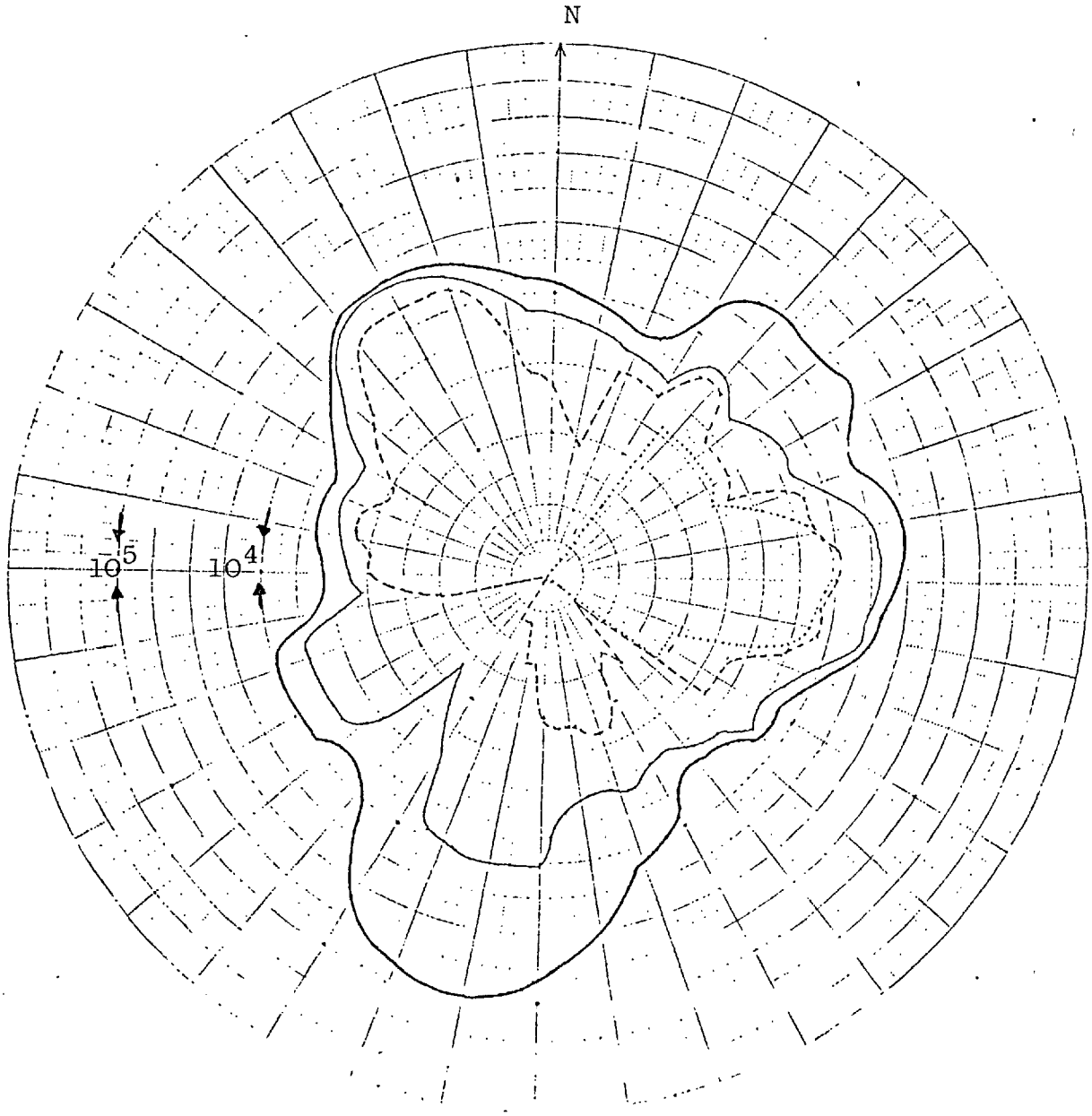

Figure 6.7 Angular dependence about site five, centred on a 30° sector extending 30 km from the site, of the potential collective weighted whole body dose commitment from the cloud of a notional AGR accident 4 dispersing under slightly unstable conditions, with the intermediate distance dependence shown.

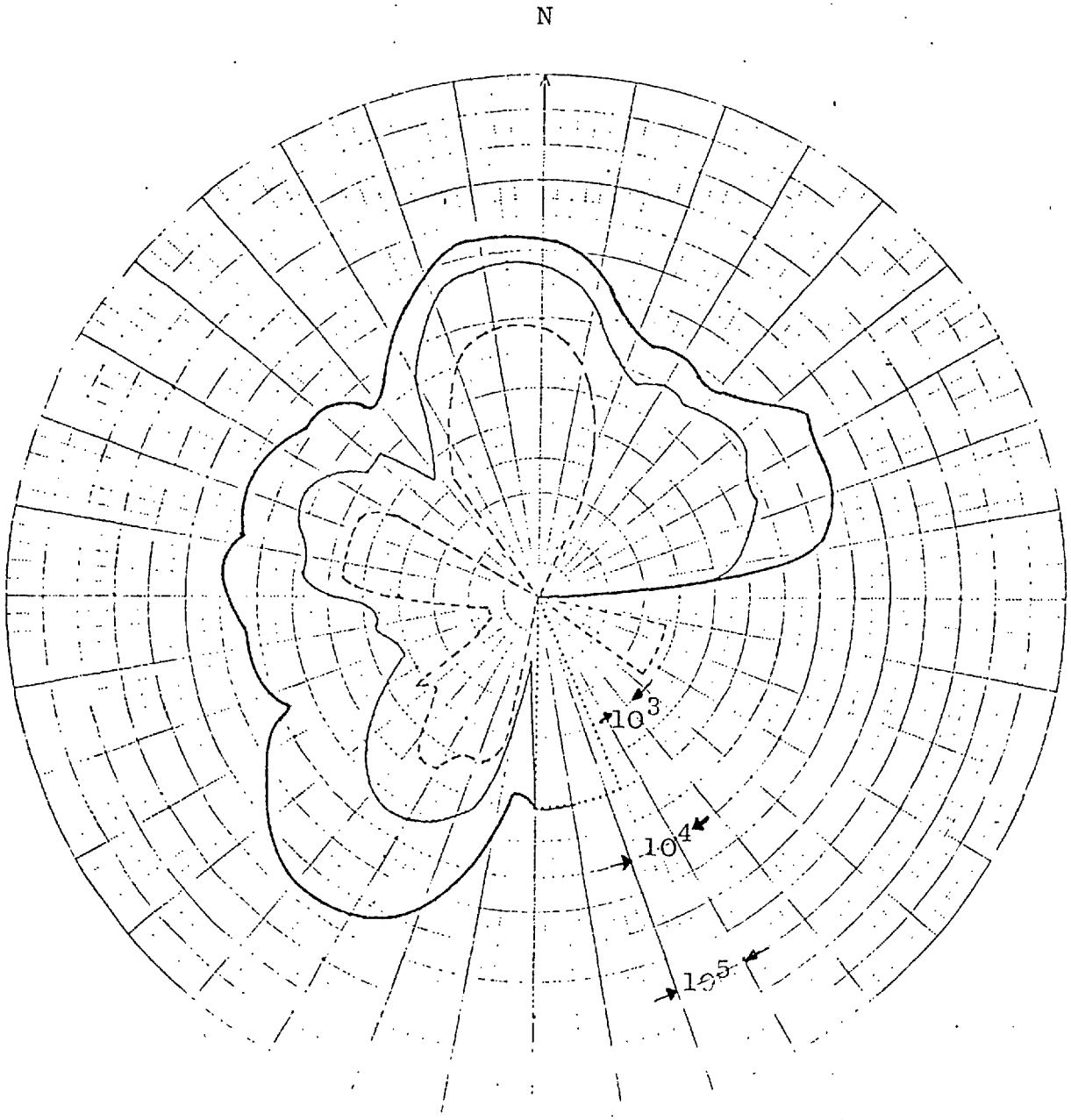

Figure 6.8 Angular dependence about site six, centred on a 30° sector extending 30 km from the site, of the potential collective weighted whole body dose commitment from the cloud of a notional AGR accident 4 dispersing under slightly unstable conditions, with the intermediate distance dependence shown.

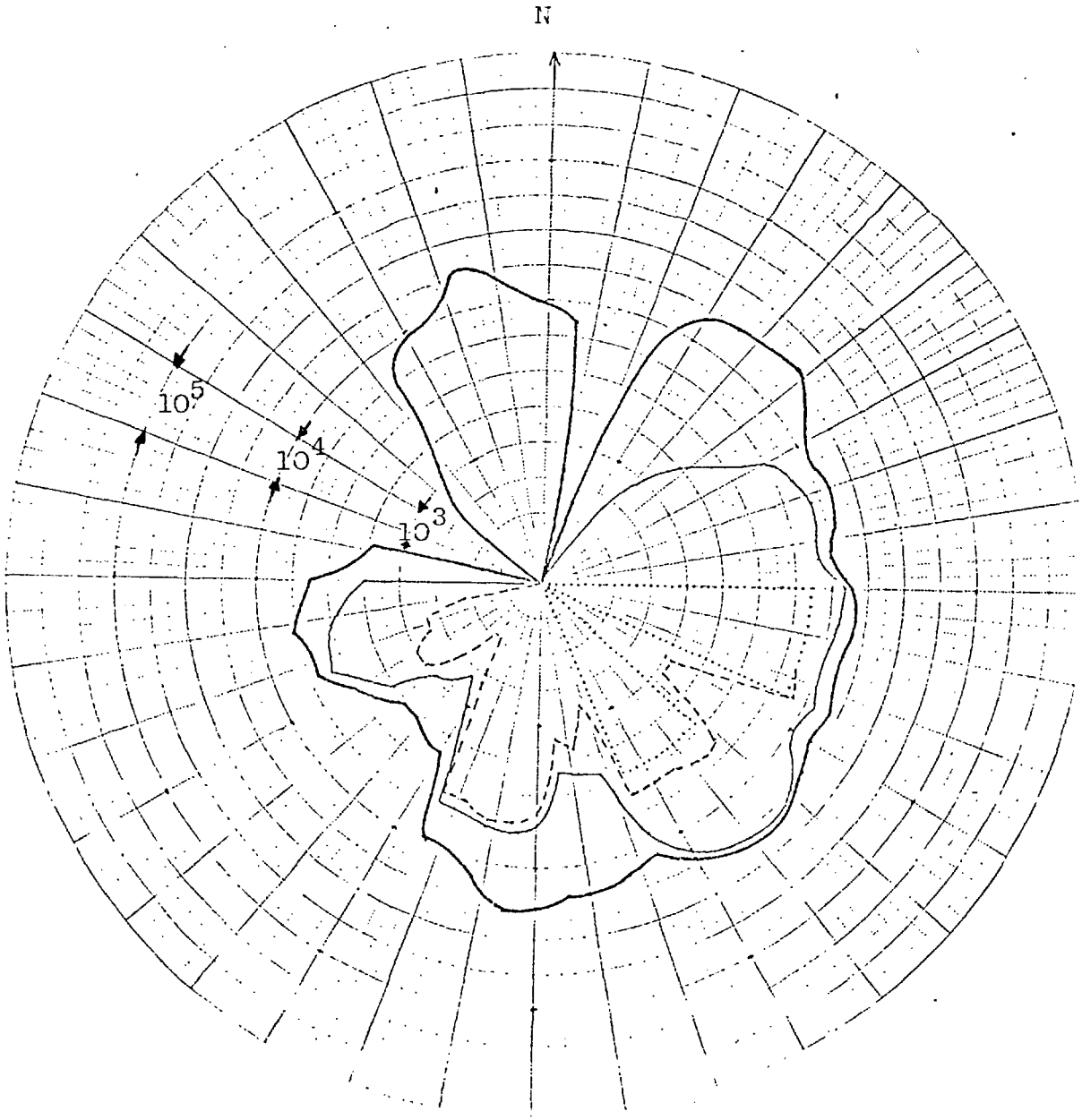

30° sector at all distances out to 30 km. Within 8 km of the eighth site there are few people so the worst sector is determined by the more distant centres of population. In this case site dependent meteorology may be an important factor in redefining a "worst" sector.

The expected number of latent fatal cancers from this notional release in the worst 30° sectors by 3, 8, 16 and 30 km for each site are displayed in table 6.3 where the orientation of the central line of the sector is also given, in degrees clockwise from 0° north. The total number of fatalities per 10^6man-rad, due to external exposure by low LET radiation of a standard population, is about 100 (38). It should be noted that the doses used in this section for the study of collective dose are weighted (ICRP-26) whole body values, derived by weighting appropriate single organ doses, so the result should be roughly equivalent to that from a uniform whole body irradiation, but possibly with a different frequency for each type of fatal cancer developing in the population. In the particular case of this dose pattern the lung dose commitment is the determining factor. These fatalities would probably occur over a period of several decades and have to be considered in the perspective of the size of exposed population group.

The "worst" potential casualty rates for the total population groups within the 30° sectors, at distances defined in table 6.3, about each site are given in table 6.4. The cases which involve population totals of only a few hundred close to the site, especially at sites 6,8,5 and 3, may not reflect the actual residential distribution due to the structure of the local enumeration districts. Also these small groups may not be representative of a "normal" population, so they could have a substantially different response to the collective doses than the assumed standard population. These casualty rates relate to a period of about 30 years so a factor of about $3.10^{-2}yr^{-1}$ could be applied to the figures in table 6.4 to give a pessimistic estimate of the individual annual risk of death in the exposed population group due to this release occurring. Close to a site this could reach 3.10^{-y} r^{-1}, but is typically nearer 3.10^{-5} yr^{-1}, and decreases to about $2.10^{-6}yr^{-1}$ for the worst sector population within 30 km of the site. The overall risk is many orders of magnitude less than these last results, as the probability of the accident occurring,

Figure 6.9 Angular dependence about site seven, centred on a 30° sector extending 30 km from the site, of the potential collective weighted whole body dose commitment from the cloud of a notional AGR accident 4 dispersing under slightly unstable conditions, with the intermediate distance dependence shown.

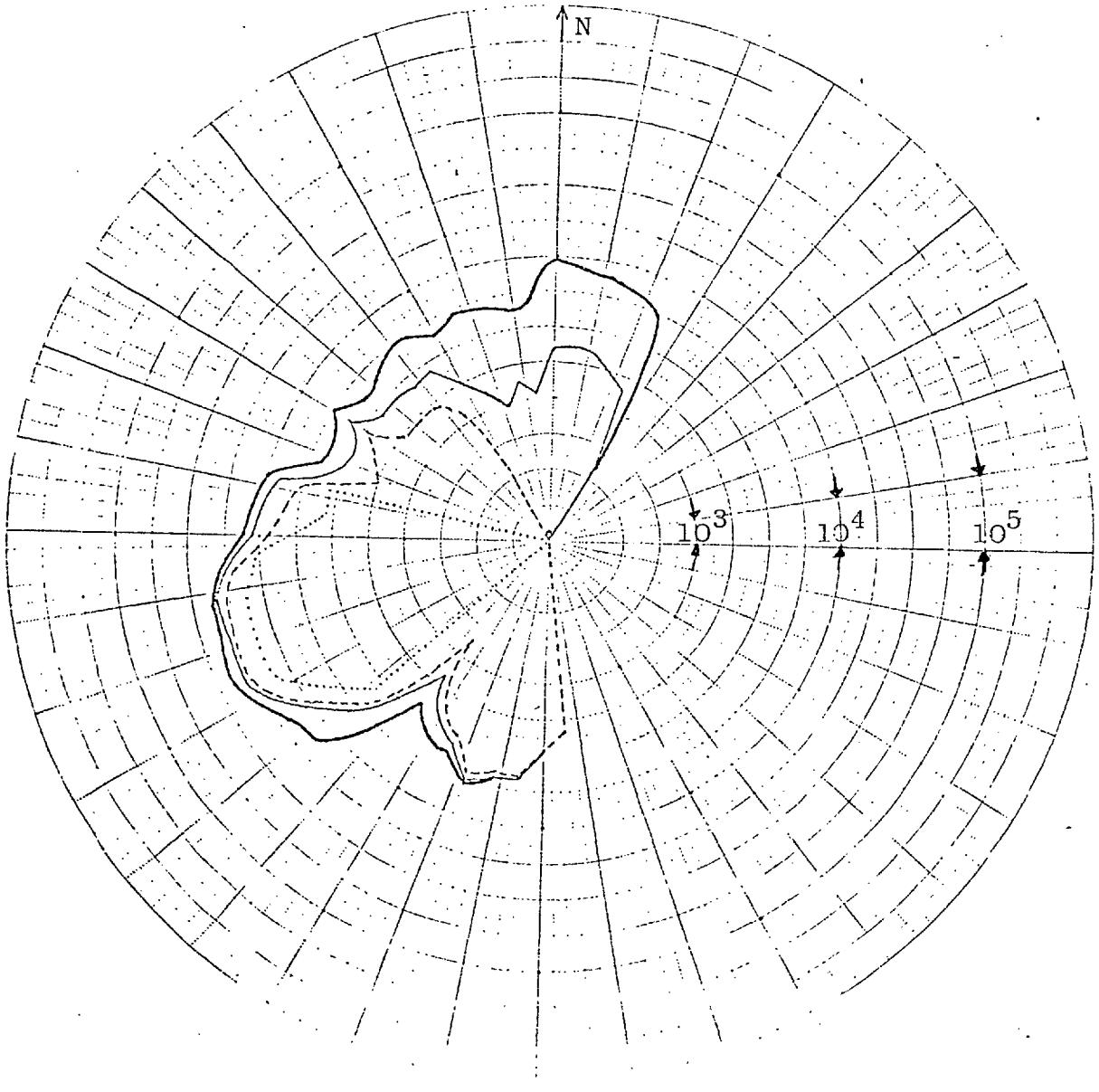

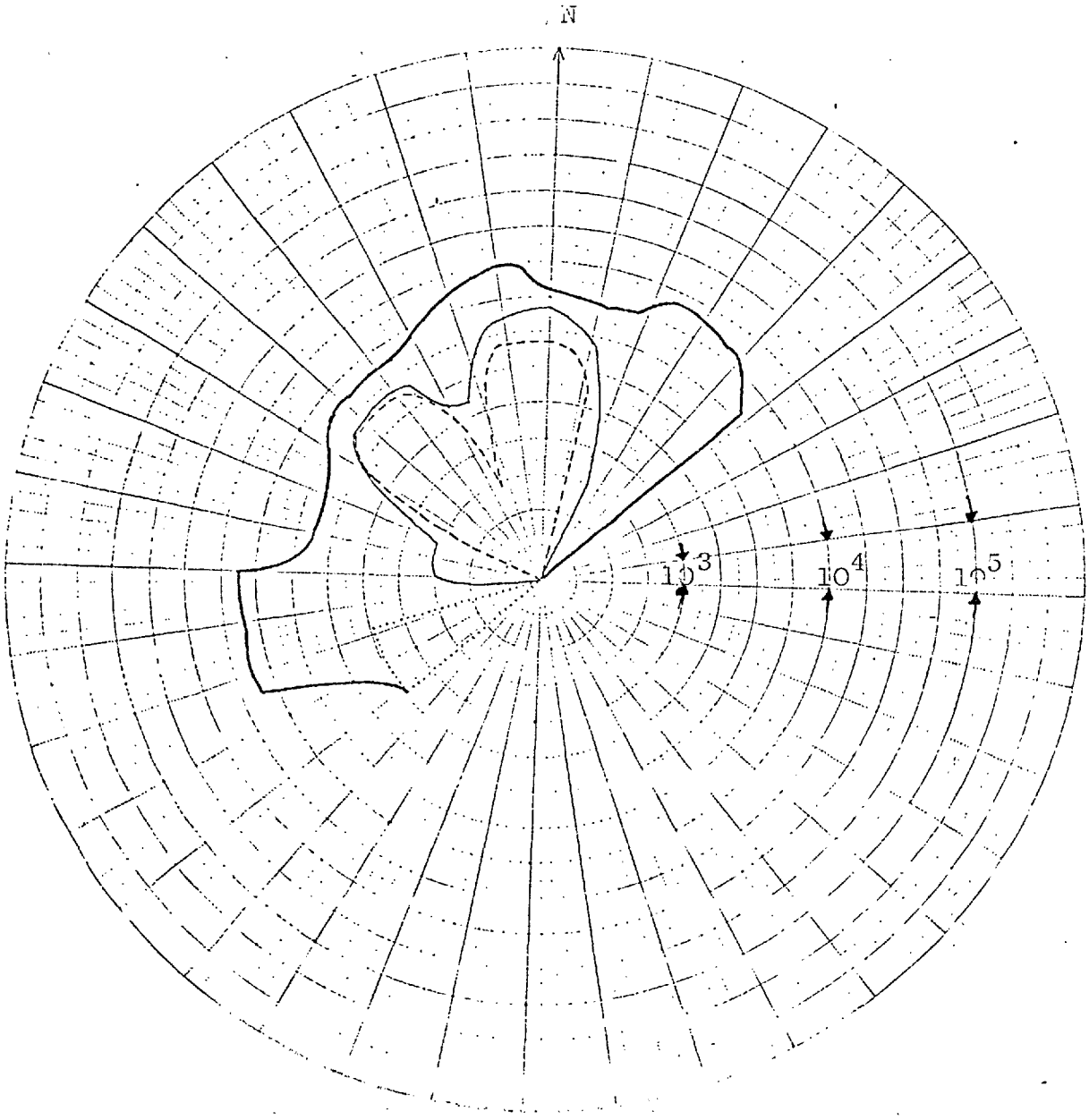

Figure 6.10 Angular dependence about site eight, centred on a 30° sector extending 30 km from the site, of the potential collective weighted whole body dose commitment from the cloud of a notional AGR accident 4 dispersing under slightly unstable conditions, with the intermediate distance dependence shown.

Table 6.3 Distribution of possible latent fatalities in the worst 30° sector out to 30 km for eight sites due to the channel, notional, melt-out on a major depressurisation, under slightly unstable dispersion conditions.

Site	Distance ranges (*where a number is bracketed the number of fatalities is below 1)											
	0-3 km			0-8 km			0-16 km			0-30 km		
	Axis	No. of fatal cancers	Total Pop.	Axis	No. of fatal cancers	Total Pop.	Axis	No. of fatal cancers	TOTAL Pop.	Axis	No. of fatal cancers	Total Pop.
1	336	2	4426	324	10	56141	324	10	73939	324	13	207260
2	36	9	6668	36	14	39884	36	15	52982	36	15	55137
3	174	(0.3)*	338	144	2	12089	150	2	33402	180	13	502501
4	90	1	1618	330	1	7042	330	2	19709	192	10	457693
5	168	(0.3)*	249	354	1	3845	354	3	47445	216	5	229125
6	102	(0.7)*	94	102	(0.7)*	94	138	2	36362	138	2	46832
7	246	1	2709	246	2	2913	246	2	7369	246	2	28959
8	240	(0.2)*	148	O(N)	(0.5)*	3560	O(N)	1	9939	354	2	57851

Table 6.4 Individual expectation of a fatal cancer, once the notional release occurs, at various sites for the worst 30° sectors to given distances.

Site.	Individual expectation of developing a fatal cancer (†bracketed entries are where probably less than one fatality develops in the exposed group)			
	by 3 km	by 8 km	by 16 km	by 30 km
1	4.5(-4)*	1.8(-4)	1.4(-4)	6.3(-5)
2	1.3(-3)	3.5(-4)	2.8(-4)	2.7(-4)
3	(8.9(-4))†	1.7(-4)	6.0(-5)	2.6(-5)
4	6.2(-4)	1.4(-4)	1.0(-4)	2.2(-5)
5	(1.2(-3))†	1.0(-3)	6.3(-5)	2.2(-5)
6	(7.3(-3))†	(7.3(-3))†	5.5(-5)	4.3(-5)
7	3.7(-4)	4.1(-4)	2.7(-4)	6.9(-5)
8	(1.4(-3))†	(1.4(-4))†	1.09(-4)	3.5(-5)

*4.5(-4)=0.00045

estimated to be of order $3.10^{-5}yr^{-1}$, has to be incorporated. The final risk values compare very favourably to the total and accidental death rates in the UK population which are both of order $10^{-3}yr^{-1}$ (ICRP-27, 35).

Another useful comparison which can be made is that between the accidental collective doses and those due to natural background radiation. Environmental background radiation, combined with an almost equal contribution from medical and other practices in the USA, result in a whole body dose of order 200 mrem/yr and about 100 mrem/yr in parts of the UK. The latter value gives collective doses to the "worst" sector (30°) populations out to 30 km of 3.10^3 to 5.10^4 man-rems, depending on the gross populations given in table 6.3. This range overlaps with the typical range of worst collective sector weighted whole body doses resulting from the passage of the cloud, under category C conditions, due to the highly improbable AGR single channel melt-out and major depressurisation accident. The collective exposure which might be, pessimistically, delivered in the first year by the ground contamination resulting from this release tends to be about one order of magnitude greater than the collective dose attributed to the natural background irradiation.

The next section is intended to give estimates of the consequences and risks to populations in sectors about nuclear power installations out to larger distances than in this section. Particular attention will be paid to information which may be of use in site assessment.

Section 6.2.2.2 Collective $22\frac{1}{2}^{\circ}$ sector doses out to 100 km for nine sites in the UK

The detail contained in the enumeration district (ED) census data is not essential when estimating collective doses to 100 km. Ward and Civil Parish (W/CP), each of which combine the total population of a group of ED's, should give an adequate representation of the collective dose (see discussion in chapter 4).

Rural areas have the poorest resolution when W/CP data are used, where this will be worse than that for single rural ED's. In Scotland the situation for rural parts is worse than that for England and Wales due to the lower population density and the compensating increase in the areas covered by each ED. Any

rural population within 8 km of a site will only be poorly represented in this assessment of collective doses out to 100 km in this section. This should not affect total collective doses which tend to be dominated by dense population areas which are well resolved by the W/CP data.

Only the $22\frac{1}{2}^{\circ}$ sector with the largest collective dose by 100 km is considered for each site. The weighting function is, again, the weighted whole body dose from the notional single channel AGR melt-out on a major depressurisation, released under Pasquill-Smith category C conditions, and has been appropriately modified for use in a $22\frac{1}{2}^{\circ}$ sector as is shown in figure 6.11. Two methods of assessing the collective dose are used: discrete and interpolated. Discrete weighting is where the whole sector population within radial delimeters r_{i-1} and r_i is multiplied by the weighting function at $r_i'=(r_{i-1}+r_i)/2$. Interpolated sector collective doses weight the individual W/CP's by the factor appropriate to that population's distance from the site. The collective $22\frac{1}{2}^{\circ}$ sector doses are defined by those doses occurring in fourty-five consecutive $\frac{1}{2}^{\circ}$ sectors. This means that the "worst" sector is chosen to the nearest $\frac{1}{2}^{\circ}$ by the discrete weighting system.

Table 6.5 gives the radial distribution of collective doses in the "worst" $22\frac{1}{2}^{\circ}$ sector out to 100 km, where the final total is compared to that estimated by using an interpolated weighting function. These two values of the total sector collective dose are found to agree to within about 8%. This means that the simpler discrete weighting system is of adequate accuracy provided the population is spatially well dispersed within each weighting zone. The angle, clockwise from 0° north, at which the worst $22\frac{1}{2}^{\circ}$ sector starts is also given.

Several of these "worst" sectors are the same as are found in the previous section, for 30° sectors out to 30 km. This occurs for sites 1,3,4 and 7, where the contributions by 30 km, as a fraction of the total risk by 100 km, are 0.54, 0.89, 0.79 and 0.56 respectively. Site 7 contains a small town of about 3000 people just within 3 km of the site. This dominates the worst sector for both ED and W/CP data when used, to 30 km and 100 km, in estimating this type of collective dose. In fact the

Figure 6.11 Weighting function for a $22\frac{1}{2}^{o}$ sector out to a distance of 100km, derived from individual weighted whole body dose commitment from the cloud after a release from a notional AGR accident 4 dispersing under slightly unstable conditions.

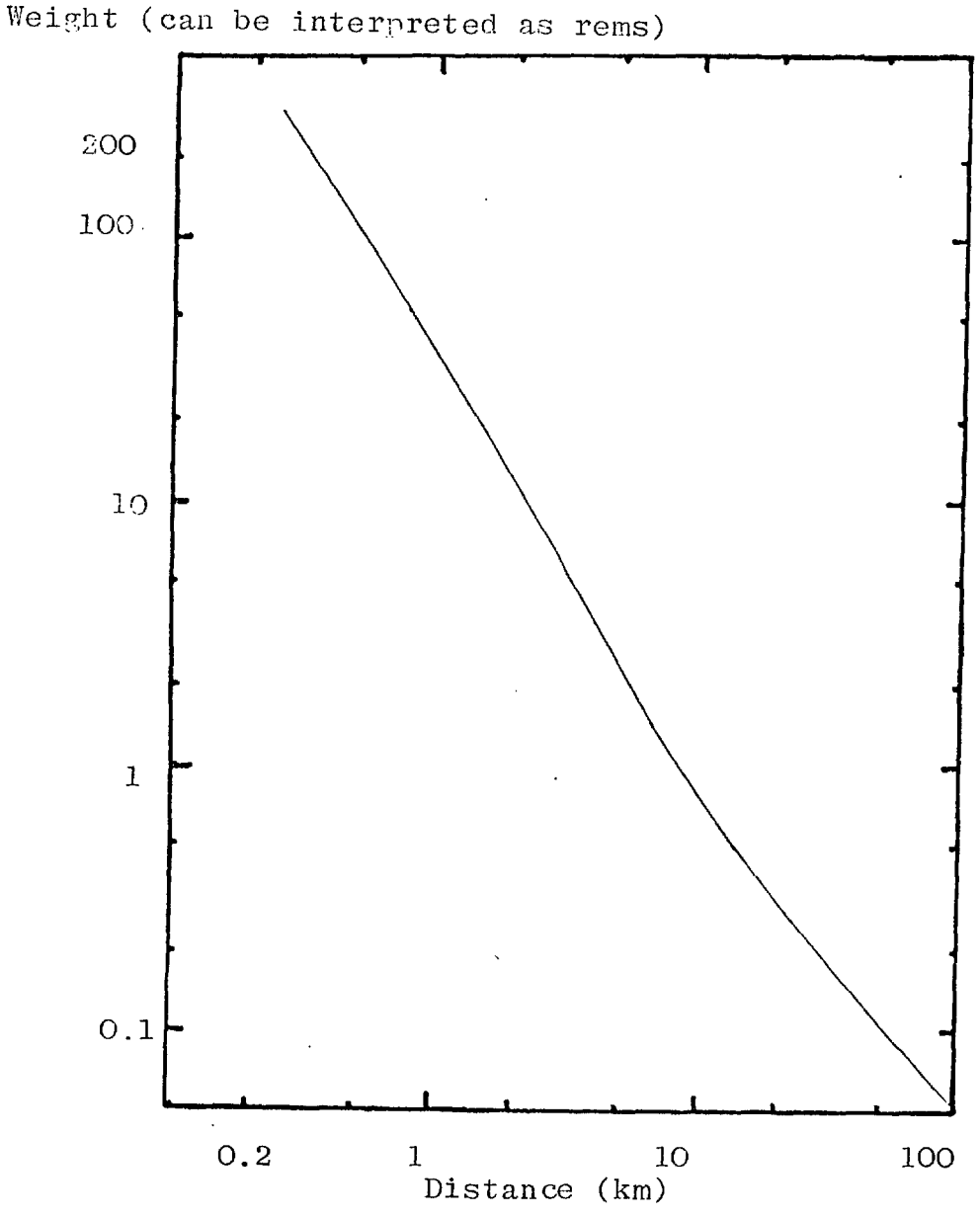

Table 6.5 Potential collective doses to the worst $22\frac{1}{2}^{\circ}$ sector at each of nine sites from the notional AGR single channel melt-out and major depressurisation.

Site	Starting Angle (to $\frac{1}{2}^{\circ}$)	Collective dose (man-rems) in the given sector by the distances: (Discrete weighting: bracketted values at 100km are from interpolated weight)							
		0-5 km	0-8 km	0-12 km	0-16 km	0-30 km	0-50 km	0-75 km	0-100 km
1	$317\frac{1}{2}$	7.96(4)	1.45(5)	1.56(5)	1.59(5)	1.90(5)	3.24(5)	3.48(5)	3.49(5) (3.43(5))
2	136	-	-	-	9.53(2)	7.42(3)	5.12(4)	1.48(5)	2.30(5) (2.35(5))
3	$165\frac{1}{2}$	4.37(3)	7.74(3)	1.13(4)	2.51(4)	1.33(5)	1.41(5)	1.44(5)	1.49(5) (1.59(5))
4	$177\frac{1}{2}$	3.62(2)	5.91(2)	1.08(4)	1.08(4)	1.13(5)	1.34(5)	1.39(5)	1.45(5) (1.43(5))
5	$236\frac{1}{2}$	-	-	-	6.77(2)	3.06(3)	3.36(4)	2.75(5)	5.41(5) (5.40(5))
6	39	-	-	8.52(2)	1.31(3)	1.68(4)	7.32(4)	9.42(4)	1.08(5) (1.05(5))
7	234	3.94(4)	4.03(4)	4.09(4)	4.15(4)	4.64(4)	6.83(4)	7.37(4)	8.33(4) (7.62(4))
8	301	-	6.60(3)	6.60(3)	6.88(3)	9.08(3)	2.04(4)	4.42(4)	2.61(5) (2.54(5))
9	$60\frac{1}{2}$	-	-	-	4.34(3)	2.15(4)	1.83(5)	2.12(5)	2.30(5) (2.26(5))

situation appears to be worse in the case of an assessment using W/CP data as this community draws in the population of the surrounding rural ED's to artificially increase the total sector population at this point. Even so site 7 has the lowest "worst" collective dose in a $22\frac{1}{2}^{\circ}$ sector out to 100 km when this pessimistic effect at a short distance is included.

At the other extreme the collective dose out to 100 km for some sites is dominated by the contributions beyond 75 km. Both sites 5 and 8 fall into this category with fractions of 0.50 and 0.83 in the last zone respectively. These worst sectors are in different directions to any sectors of concern out to 30 km identified in figures 6.7 and 6.10. The reason for this characteristic is that a metropolitan area lies just within 100 km of these two sites. A similar situation arises for both sites 2 and 9, which are closer to other areas of very high population density. At these two sites the particular conurbations are located about 50 km from the sites, where the last 50 km of the worst sector contributes 78% of the total risk in this direction at site 2 and in the case of site 9 the zone from 30 km to 50 km contributes 69% of the appropriate total sector risk. Finally site 6 also has a large contribution in the zone from 30 km to 50 km, about 50% of the total to 100 km, but this is derived more from a collection of separate towns and cities rather than one major population centre. The evolution of these population centres may have to be considered when choosing sites in the UK for long term developments in the nuclear power industry.

When considering these results it should be noted that the area of each sector beyond 50 km is 75% of the total sector area. The fact that the population at short distances from the site can still dominate the total collective dose reflects the non-uniform spatial distributions about sites in the UK and the form of the dose weighting function for sectors. Another factor which has to be considered is that major urban areas can have such large populations that they dominate a collective dose assessment even though individuals from smaller communities close to the site may be weighted by a dose term which is over two orders of magnitude greater than that at the other extreme of distance from the site.

Using the same value of expected latent fatalities per 10^6man-rads of LET external radiation, as in the previous section, an estimate of the number of casualities can be made from the values given in table 6.5. These are displayed in table 6.6 along with the distances by which most of these fatalities might occur. Also given in this table are the total sector populations out to this distance together with the mean probability of a fatality per member of this most exposed population group derived from these results, once this notional accident has been assumed to occur.

Those sites where the majority of the potential latent fatalities would occur beyond at least 50 km downwind in the worst sector have the lowest risk of individual members of the exposed population group to develop fatal cancers due to this release. In these cases the expected probability of individuals developing fatal diseases, once the accident has occurred and dispersed in the worst sector of the given site, ranges from 3 to 9 in 10^6, with a mean of 5 in 10^6. For those sites where the majority of latent fatalities occur within 30 km this rate for individuals has increased to the range 12 to 19 in 10^6, with a mean of 15 in 10^6. The exception is site 7 where the critical community is very close to the reactor. For this worst sector the individual potential probability of developing a fatal cancer could be as high as 700 in 10^6, for that portion of the worst sector population which could have half the total casualty incidence. This is similar to those values derived in the previous section for populations close to site. The low background of population in the rural areas about site 7 means that the next major collective dose contribution does not occur until the 30 to 50 km zone. At this larger distance the individual fatality probability, once the release has occurred in this worst sector, has decreased to 33 in 10^6 which is much closer to the values of other sites.

The annual collective doses to the population groups given in table 6.6 due to natural background radiation range from about 2.10^4 to 7.10^5 man-rem for these nine sites. This range includes all the collective worst sector doses shown in table 6.5. Hence the consequences, in terms of fatal cancers, from inhalation doses resulting from the passing cloud of radionuclides

Table 6.6 Major contributions to the potential fatal cancers in the worst $22\frac{1}{2}^{\circ}$ sectors within 100 km for the notional weighted whole body dose function.

Site	Distance(r_M) by which most cancers occur (kilometres)	No. of fatal cancers a, by r_M.b ., by 100km		Exposed population by r_M, in millions	Individual expectation of developing a fatal cancer ($*10^{-6}$)
		a	b		
1	30	19	35	1.0	19
2	75	15	24	5.0	3
3	30	13	16	0.9	14
4	30	11	15	0.9	12
5	75	28	54	6.4	4
6	50	7	11	2.2	3
7	i;5	4	8	0.006	700
	ii;50	6	8	0.18	33
8	100	26	26	7.1	4
9	50	18	23	2.0	9

under these conditions could be difficult to distinguish from those of the natural background radiation. The risks from external gamma exposure from deposited material may be more significant than those from inhalation doses, as discussed earlier, but ameliorating action can be taken against the effects of ground contamination.

Many factors have been omitted from this brief study, where releases from a stack, changes of meteorological conditions during travel downwind (not necessarily centred on a straight line from the release point) and topographical effects could greatly influence the results. The variation in the final results produced by a full assessment of the major effects would provide a greater understanding of the characteristics of collective doses to population groups about nuclear power reactors, and other installations. There are more difficulties in attempting to assess collective doses resulting from contamination (see chapters 1, 3 and 4).

Section 6.3 Site Assessment

This section will compare the results of site and sector weighting functions derived by the NII to those from applying different weighting functions derived from the previous section. Due to the different releases and organ doses assumed in the two methods only relative site properties can be studied. The NII functions result from dose commitments to the thyroid of an average member of the public for a nominal release of iodine-131 which disperses under stable atmospheric conditions and is characterised by prolonged lateral dispersion parameters. These weighting functions are in terms of mrem/Ci(I131).

The weighting functions of the NII were originally used out to 20 miles but can be interpreted for new metric distances out to 30 km (18.6 miles). The age distribution of the UK population is taken into account (see review (32)) in the thyroid sensitivity to I131. The sector weighting function is derived by the method explained earlier in section 6.2.1, so the effects of changing the angular width of a sector can be investigated.

Using the Pasquill gaussian plume parameters for stable category F conditions a curve of $1/(2\pi \cdot \sigma_y \sigma_z)$ can be drawn which

should be similar in form to the NII site weighting function when using the recommended values of σ_y for lateral dispersion (see figure 6.12). The nominal I131 release is assumed to be at ground level and deposition is negligible. This curve can be used to extend the thyroid weighting functions to 100 km, as has been done in figures 6.13 and 6.14, for the site and a $22\frac{1}{2}^{\circ}$ sector respectively. Stable conditions normally do not last long enough for material to travel this distance at a typically low wind speed of 2 m/sec, so this extension is pessimistic as the later sections of the curves would usually show the effects of more dispersive conditions. There are differences between the references (2) and (32) as to the values of the weighting functions within 1 mile of the site so an intermediate line has been taken and the subsequent consequences for site assessment discussed later. The site weighting function is just the peak on-axis dose multiplied by 0.565 to give the mean dose level within the 10% plume boundaries at ground level. This function is applied to the surrounding population equally in all directions to obtain a total site weighted population value, which has a dependence on distance from the site. Limiting site and sector curves have been derived (2) which individual site characteristics must not exceed during the expected commercial lifetime of that site and reactor.

The weighted whole body dose from the notional single channel AGR melt-out on a major depressurisation can provide a sector weighting function, see figure 6.11. An appropriate site weighting function, figure 6.15, can also be derived for this release of mixed fission products under slightly unstable conditions and assuming a three group element dependent deposition model.

There are several reasons for choosing the severest notional AGR release to derive site and sector weighting functions, for a comparison to results obtained by the methods of the NII. This notional AGR release contains a wide range of isotopes of all physical and radiological properties rather than just volatiles, as in the lesser releases modelled in chapter five. Also this mixture of many isotopes is at the other extreme to the nominal release of a single isotope with a particular affinity to only one organ, as done by the NII choosing iodine-131. The organ doses which are used as the basis of the weigh-

Figure 6.12 Dilution factor, extrapolated to 100 km, for non-depositing nuclides dispersing under stable, low windspeed conditions.

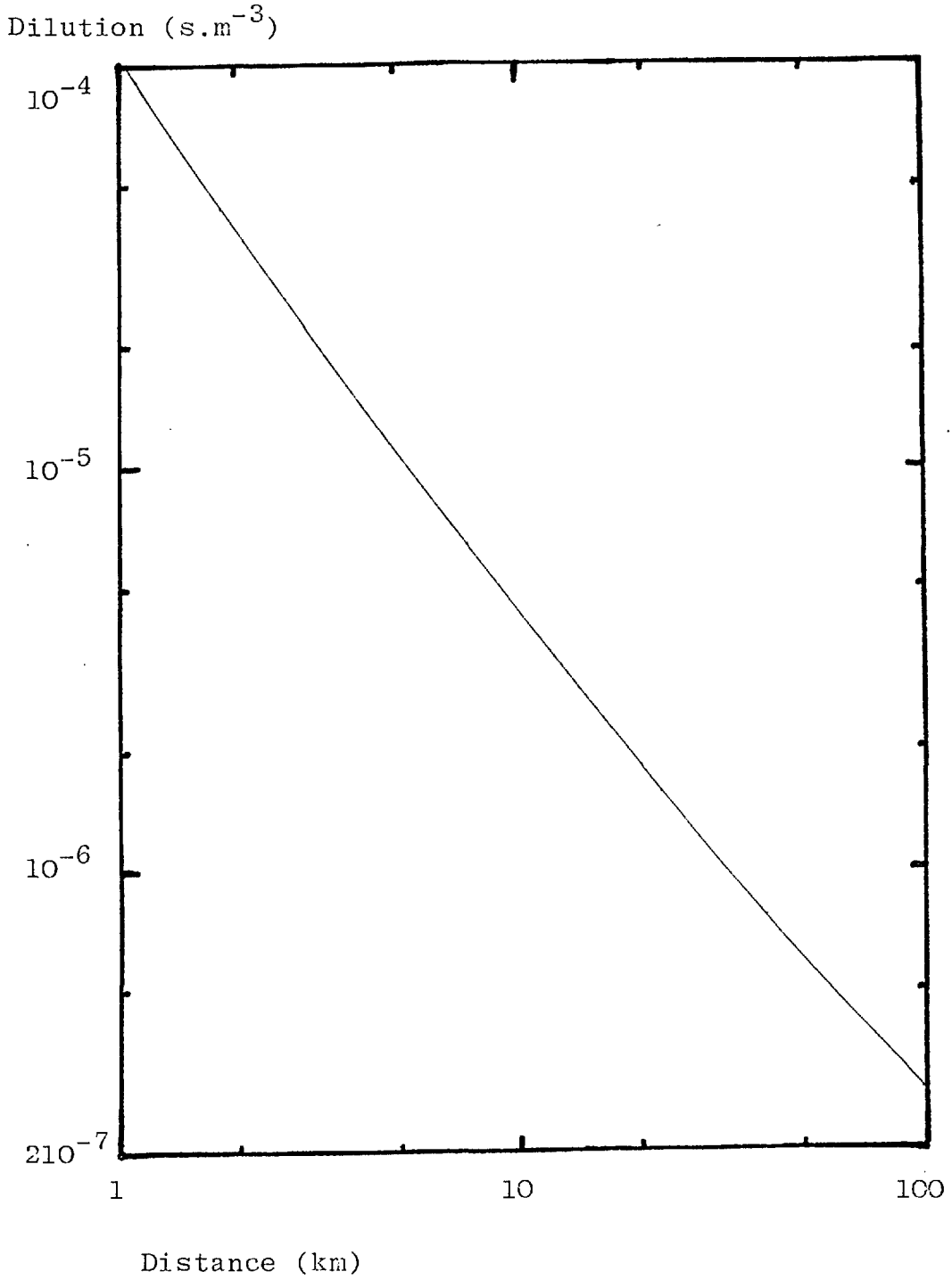

Figure 6.13 NII site weighting function, extrapolated to 100 km, derived from nominal inhalation dose commitments to the thyroid from non-depositing I-131 dispersing under stable conditions.

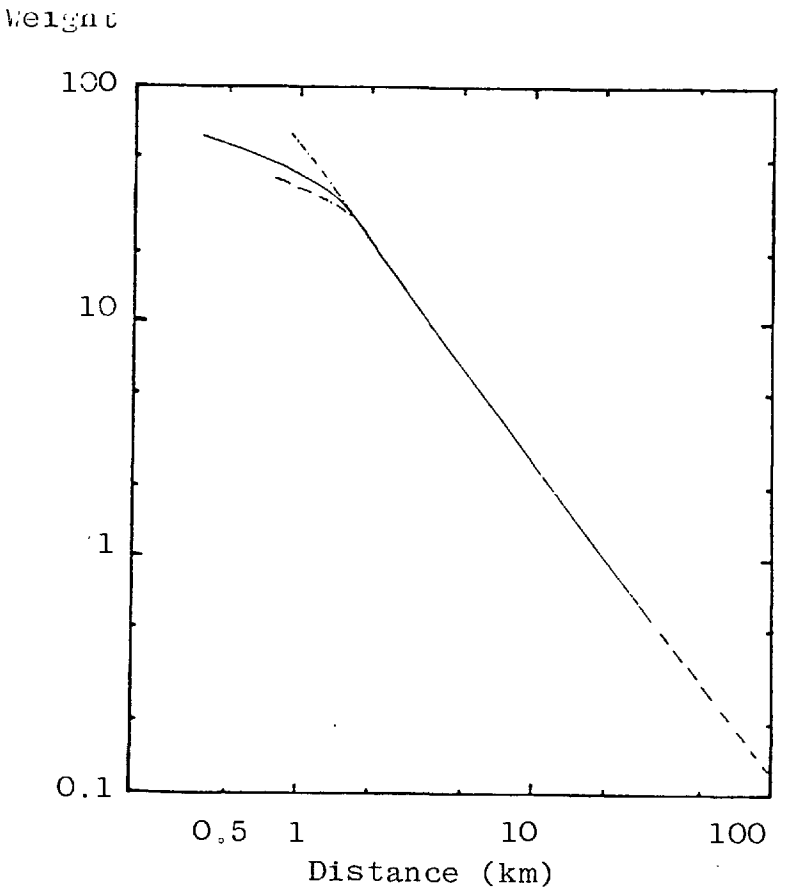

Figure 6.14 NII 22½° sector weighting function, extrapolated to 100 km, derived from nominal inhalation dose commitments to the thyroid from non-depositing I-131 dispersing under stable conditions.

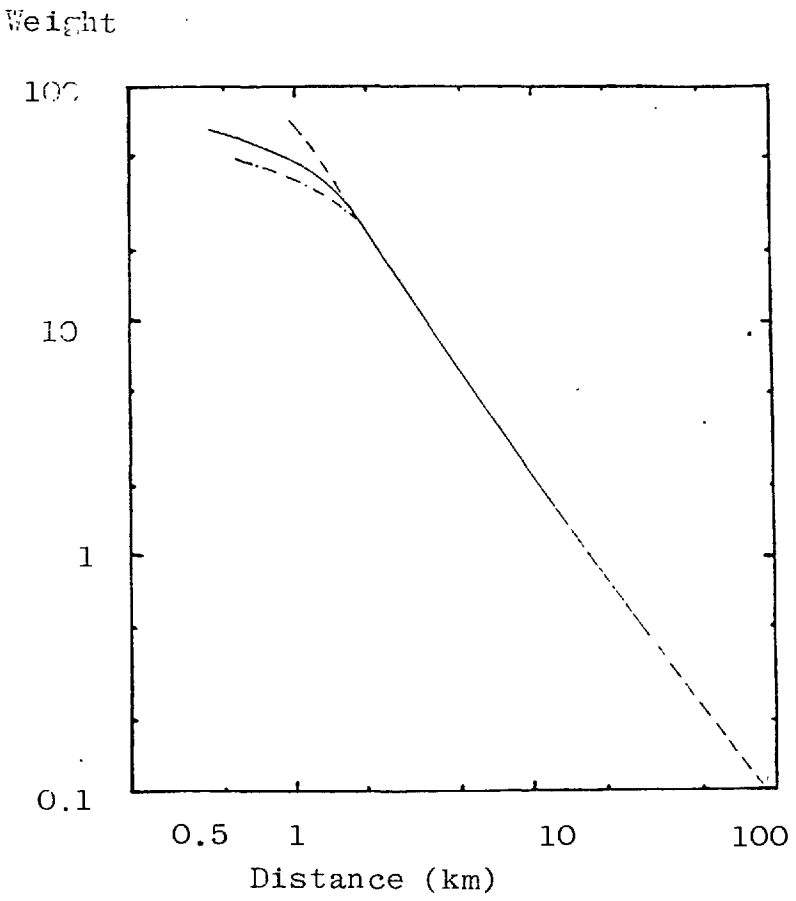

ting functions derived from this notional AGR accident is the whole body, rather than the thyroid for the nominal iodine-131 release. A given dose in either organ is considered to be radiologically less significant to the thyroid for the general health of a typical population (ICRP 26).

Added realism is given to these AGR based functions as the release is depleted by element dependent dry deposition, rather than the non-depositing behaviour assumed for iodine-131 in the NII weighting functions. High windspeed weather conditions, with an inversion, have been chosen so as to give a more typical method of modelling the transport of material in the atmosphere to 100 km from the ground level source than stable low windspeed conditions.

Due to the interpretations of the weighting functions at short distances, less than 1 mile (1.6 km) from the site, the NII based functions used here show a marked reduction closer to the site when compared to the forms of the axial dispersion curve, figure 6.12, and the whole body weighting functions in figures 6.11 and 6.15. Even without this interpretation the AGR derived functions may result in pessimistic site conditions. There is an exclusion area, extending to 1 km from an AGR with a prestressed concrete pressure vessel for residential population implicit in the limiting siting criteria (Gronow and Gausden, 1973). The discussion of these weighting functions by Shaw and Palabrica also questions the averaging process within the 10% plume limits as well as the sensitivity of the thyroid to mixed releases of radioisotopes of iodine and associated nuclides.

The results of applying these weighting functions to the residential population distributions about the real sites (1 to 9) will be discussed in the following sections. Comparisons will be made between the use of W/CP and ED census data as well as discrete and interpolation methods of applying the weighting functions within 30 km. The effects of different angular widths of sectors will be discussed along with extensions of the weighting functions to 100 km.

Figure 6.15 Weighting function for the whole site out to a distance of 100 km, derived from individual weighted whole body dose commitment from the cloud after a release from a notional AGR accident 4 dispersing under slightly unstable conditions.

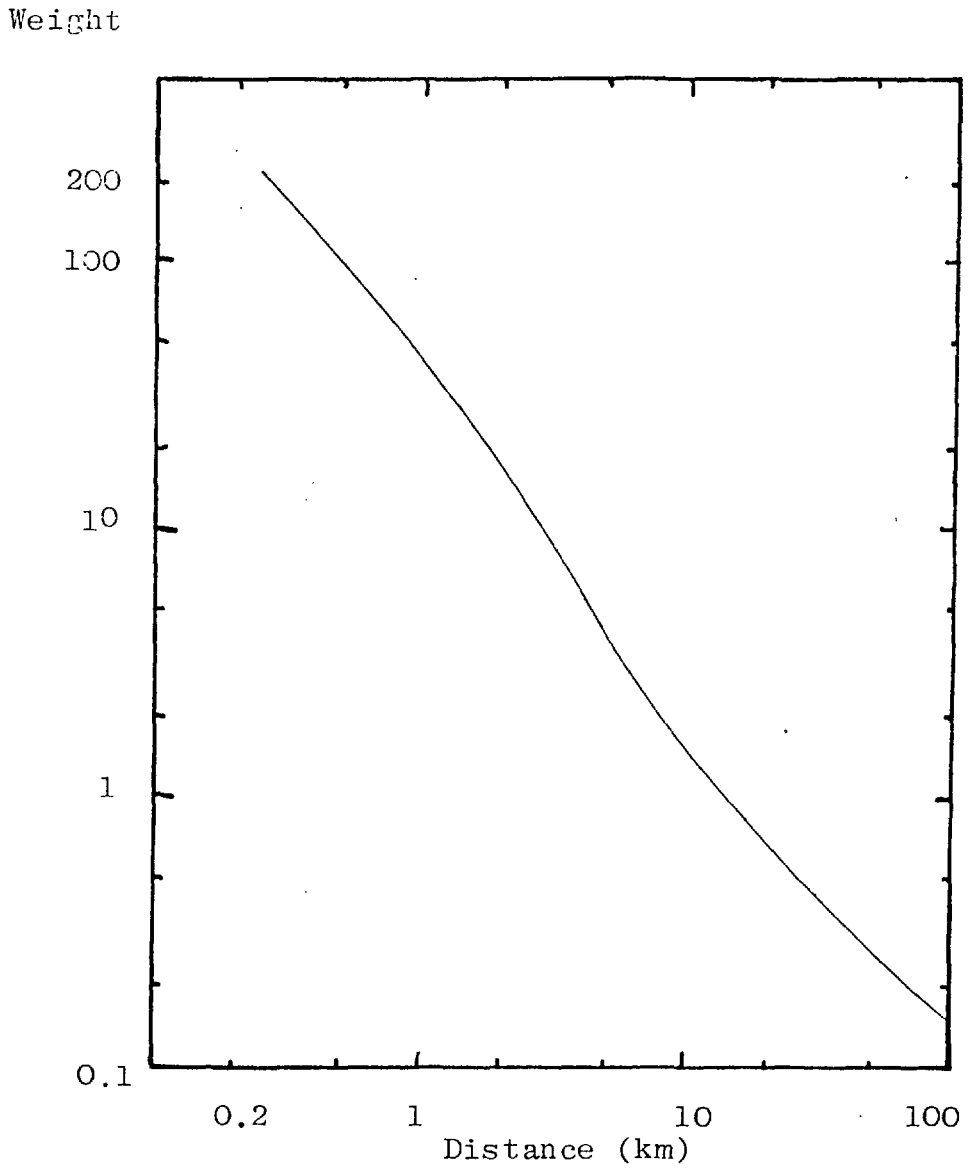

Section 6.3.1 Comparison of site and sector weighted populations in the locality of eight sites.

The use of NII weighting functions out to 30 km for $22\frac{1}{2}^{\circ}$ sectors will be discussed initially followed by those results for 30° sectors out to 20 miles. The effects of using W/CP or ED population census data and the associated accuracy for the location of "worst" sectors will be discussed. Differences in the site and sector weighted population totals for combinations of population data and discrete or interpolated weighting functions are considered. Discrete and interpolated weighting can be formulated as below:

Discrete weight for population K ($P(r_k)$),
where $r_{i-1}<r_k<r_i$ is $W(r_k)=W((r_i+r_{i-1})/2)=W(r_i')$

Interpolated weight for population K ($P(r_k)$),
where $r_{i-1}<r_k<r_i$ is $W(r_k)$ estimated by an interpolation scheme between the set of values of $W(r_i')$ in logarithmic coordinates.

The site weighting function, from figure 6.13, has been applied to the populations within 30 km of each of the sites 1 to 8. Table 6.7 gives the results for the two population sets, W/CP and ED, with the discrete and interpolated weighting systems.

Site 1 is clearly the poorest of the eight sites out to 30 km. Sites 2 and 3 have similar site weighted population totals by 30 km but some of this is produced at short distances about site 2, which could be a less desirable characteristic. Site 4 may have a smaller total site risk than sites 1 to 3 but it has a greater contribution at short distances than site 3, but this could be due to the details of the local ED structure rather than a true residential population. The site weighted population totals decrease to the values for sites 7 and 8, but, as noted earlier, site 7 has relatively large contributions at short distances. For these eight sites there is only an order of magnitude difference between the extreme sites by 30 km, where this relative difference increases as smaller radial distances are considered. A wider selection of sites, to include the remoter locations in the UK, can extend the lower limit of this range by a further order of magnitude. The upper limit of these sites is very close to the site limiting criterion so no

Table 6.7 Site weighted population totals with distance from site

		Distance (km)							
		0.5-1	2	3	5	8	12	16	30
1	*WCP/I			9.56(4)	2.64(5)	9.53(5)	1.60(8)	1.84(6)	2.18(6)
	ED/D			7.21(4)	3.19(5)	1.03(6)	1.68(6)	1.86(6)	2.21(6)
	E/I			6.80(4)	2.93(5)	9.68(5)	1.66(6)	1.85(6)	2.20(6)
2	W/I		1.66(5)	1.78(5)	3.16(5)	5.90(5)	6.65(5)	7.33(5)	1.05(6)
	E/D	2.68(4)	1.46(5)	1.95(5)	3.25(5)	5.81(5)	6.59(5)	7.28(5)	1.04(6)
	E/I	2.73(4)	1.35(5)	1.86(5)	3.17(5)	5.58(5)	6.48(5)	7.17(5)	1.03(6)
3	W/I			1.18(4)	1.27(4)	1.15(5)	2.16(5)	3.64(5)	1.10(6)
	E/D			5.51(3)	1.04(4)	1.52(5)	2.15(5)	3.71(5)	1.06(6)
	E/D			7.35(3)	1.24(4)	1.52(5)	2.17(5)	3.67(5)	1.10(6)
4	W/I			3.94(4)	9.99(4)	1.32(5)	2.54(5)	3.40(5)	9.35(5)
	E/D		5.89(3)	3.91(4)	1.04(5)	1.44(5)	2.45(5)	3.43(5)	9.78(5)
	E/I		4.62(3)	3.55(4)	9.79(4)	1.36(5)	2.43(5)	3.41(5)	9.44(5)
5	W/I		1.80(4)	1.80(4)	5.77(4)	7.03(4)	1.04(5)	2.40(5)	6.45(5)
	E/D		7.97(3)	7.97(3)	5.56(4)	7.02(4)	1.09(5)	2.40(5)	6.62(5)
	E/I		7.76(3)	7.76(3)	5.25(4)	6.75(4)	1.04(5)	2.31(5)	6.45(5)
6	W/I		3.66(4)	3.66(4)	3.74(4)	5.83(4)	1.08(5)	1.90(5)	4.60(5)
	E/D	4.89(3)	1.43(4)	1.43(4)	2.44(4)	4.11(4)	1.06(5)	1.77(5)	4.41(5)
	E/I	5.20(3)	1.26(3)	1.26(4)	2.57(4)	4.23(4)	1.03(5)	1.77(5)	4.42(5)
7	W/I			6.56(4)	7.65(4)	9.63(4)	1.13(5)	1.34(5)	2.06(5)
	E/D		1.07(4)	5.49(4)	8.74(4)	1.06(5)	1.21(5)	1.42(5)	2.22(5)
	E/I		9.09(3)	4.90(4)	8.60(4)	1.05(5)	1.21(5)	1.42(5)	2.14(5)
8	W/I					3.75(4)	4.35(4)	5.22(4)	2.22(5)
	E/D		4.74(3)	4.74(3)	9.84(3)	3.83(4)	4.77(4)	5.61(4)	2.42(5)
	E/I		4.13(3)	4.13(3)	9.61(3)	3.93(4)	4.96(4)	5.84(4)	2.27(5)

* W W/CP population data
E ED " "
D/I discrete / interpolated weight

other with a higher site risk factor could be considered for the AGR's with a prestressed concrete pressure vessel.

By 30 km the differences between the three combinations of methods is less than 10%, and in many cases only about 1% (see chapter 4). In rural areas the differences in the resolution of the W/CP and ED population data is most apparent, especially at short distances for the most isolated site 8. With the structure of the intervals over 70% of the relevant area about each site is contained in the annulus from 16 km to 30 km, where W/CP data is of adequate resolution. This last zone can dominate the characteristics of some sites so producing apparent agreement between the different methods of calculation for the whole site. In fact there is good agreement, at most 10% deviation, for all sites to within 8 km (5 miles), and even closer for the semi-urban sites 1 and 2. This common agreement is dependent on the population distributions about some very different types of site, so is an important factor when assessing the mode of weighted population calculation.

A more severe test is a comparison of the "worst" $22\frac{1}{2}^{\circ}$ sectors about these eight sites. A sector has proportionately more perimeter for a given area than the concentric circles evaluated in the last paragraph, so greater fluctuations can be expected in the population centroids which are contained by particular sector and zone boundaries. Also the sensitivity of the direction of the "worst" sector to the type of population statistics can be investigated.

Discrete weighting functions were used, as is done by the NII, to choose the "worst" $22\frac{1}{2}^{\circ}$ sector, where the radial distance dependence of the resulting sector weighted populations are given in table 6.8 for each site. For comparison the total sector weighted population using interpolation methods for the chosen worst sector are also given for each population set (W/CP or ED). The initial angle clockwise from 0° north by which the worst $22\frac{1}{2}^{\circ}$ sectors can be identified are entered in table 6.8, where these were calculated to the nearest $\frac{1}{2}^{\circ}$. The difference between the worst $22\frac{1}{2}^{\circ}$ sectors chosen using discrete weighting for W/CP and ED population sets was about 3° at most. This is good agreement as one W/CP centroid may contain the population for more than a dozen ED's, so can represent an area with dimensions several times those of the small census units.

Table 6.8 Comparison of W/CP and ED worst sector weighted populations.

r km	1		2		3		4	
	WCP	ED	WCP	ED	WCP	ED	WCP	ED
	317½	314½	24	22½	165½	168½	177½	179
Discrete								
1				2.99(4)				
2			1.75(5)	1.24(5)				
3	1.21(5)	3.86(4)	1.75(5)	1.73(5)	8.94(3)	5.58(3)		
5	1.70(5)	1.38(5)	2.85(5)	2.82(5)	8.94(3)	7.27(3)	8.65(2)	8.65(2)
8	3.54(5)	2.70(5)	3.68(5)	3.35(5)	1.84(4)	1.48(4)	1.51(3)	1.49(3)
12	3.85(5)	2.87(5)	3.77(5)	3.41(5)	2.86(4)	2.18(4)	3.07(4)	2.93(4)
16	3.94(5)	2.98(5)	3.86(5)	3.50(5)	6.84(4)	5.48(4)	3.07(4)	3.44(4)
30	4.73(5)	3.83(5)	3.91(5)	3.51(5)	3.48(5)	3.38(5)	2.96(5)	3.04(5)
Interpolated								
30	4.70(5)	3.90(5)	4.20(5)	3.52(5)	3.76(5)	3.70(5)	2.71(5)	2.77(5)

r km	5		6		7		8	
	WCP	ED	WCP	EP	WCP	ED	WCP	ED
	207½	206½	126½	127	234	237½	340½	337½
Discrete								
2			4.96(4)	1.00(4)				
3			4.96(4)	1.00(4)	8.05(4)	4.47(4)		
5		2.81(3)	5.04(4)	1.08(4)	8.05(4)	5.17(4)		4.93(3)
8		4.78(3)	6.20(4)	1.53(4)	8.32(4)	5.46(4)	1.48(4)	1.77(4)
12	8.69(3)	1.30(4)	6.66(4)	3.17(4)	8.48(4)	5.66(4)	1.97(4)	2.15(4)
16	1.63(4)	1.94(4)	1.11(5)	6.83(4)	8.65(4)	5.82(4)	2.04(4)	2.22(4)
30	1.51(5)	1.50(5)	1.17(5)	7.42(4)	9.92(4)	6.57(4)	5.24(4)	5.56(4)
Interpolated				7.27(4)	8.31(4)	6.35(4)	4.33(4)	5.00(4)
30	1.25(5)	1.26(5)	1.07(5)					

The worst sector weighted population totals about these eight sites range, again, within one order of magnitude. The ED populations with interpolated weighting functions can be regarded as the most probable values and are usually within 10% of the discretely weighted ED data by the final distance of 30 km. Greater differences, of up to about 20%, can exist between the two weighting methods applied to W/CP population distributions in the worst sector. There is a slight trend for the interpolated results to be pessimistic for the larger total sector values and optimistic for the less critical worst sectors when compared to the discretely weighted values, but this is probably not significant as only eight sites are sampled.

Weighted W/CP population sets for the more populated worst sectors are within about 25% of the estimates using ED data. This uncertainty in sector risk can extent to about 40% for the more sparsely populated sites, particularly site 7. As expected larger differences occur between the results using both population data sets at short distances from a site. Where the critical group contributing to the worst sector weighted population total is close to the site, this effect can dominate the final difference at 30 km, such as sites 6 and 7 (table 6.8). There are several situations in which these differences can arise. In some cases, such as sites 5 and 8, the ED population can lie much closer to the site than the appropriate W/CP, so can contribute more to the total sector weighted population. W/CP's close to a site can draw people into the worst sector from ED's which are actually outside the worst sector. This effect at short distances can still be important out to 30 km, as in the rural sites 6 and 7 and the semi-urban sites 1 and 2, although there are other complexities within 12 km of the sites 1 and 2. Differences produced at short ranges are normally relatively unimportant where the population in the last zone, beyond 16 km, dominates, as for sites 3, 4 and 5.

The worst $22\frac{1}{2}^{\circ}$ sectors using the NII discrete weighting function overlap significantly with the worst 30° sectors in figures 6.2 and 6.4 to 6.10 derived by interpolation of a weighted whole body dose from a mixed fission product release.

These narrow NII derived worst sectors to 30km can also be compared to those sectors for these sites derived by using the same basic weighting function but for 30° sectors out to 20 miles (32 km). The gross weighted population (ED data) in each worst sector can be compared as the weighting functions take into account the angular width of the sector (see section 6.2.1), as is done in table 6.9 along with the centre lines of the worst sectors.

Given a uniform population distribution about a site there should be no difference between the weighted population totals associated with 22½° and 30° sectors when the sector weighting function is defined as in section 6.2.1. For non-uniform population distributions the narrower worst sectors will tend to be more sensitive to the most densely populated areas close to each site. The total worst 22½° sector value can be expected to be greater than that for the 30° worst sectors, as only the most populated portions of the 30° sectors will contribute to the narrow sector. The greater range, to 20 miles, for these 30° sectors may add a small contribution to counteract the effects of the narrower sectors. If a large population centre lies between 30 km and 32 km there may be a major change in the total worst sector weighted population and, possibly, in the direction of this sector.

The results in table 6.9 show that the narrower sectors generally have a larger total risk than those for the 30° sectors, as was suggested in the previous paragraph. Even so most sites have very similar directions for the worst sectors, where the centre lines only deviate by a few degrees. There are two exceptions in sites 6 and 8.

Site 6 has the most extreme difference where totally separate sectors have been chosen by these two methods. The worst 30° sector out to 20 miles (32 km) only has contributions from population groups beyond 16 km, where this is a series of towns and cities. These long range groups just dominate the short range contributions in other sectors. The use of discrete weighting in producing this risk value and choosing the worst sector may not be the best representation, as the corresponding interpolated sector total is over 20% lower, but at $7.65.10^4$ is still larger than the 22½° sector risk to 30 km (discrete weighting). When the site 6 characteristic from figure 6.8 is

TABLE 6.9

Comparison of sites' worst sector risk factors when considered to 30 km and 20 miles for $22\frac{1}{2}^{\circ}$ and 30° sectors respectively (AGR weighting function)

Site	$22\frac{1}{2}^{\circ}$ sector to 30 km axis of worst sector	Sector risk (discrete ED data)	30° sector to 20 miles axis of worst sector	Sector risk (discrete ED data)
1	326	3.82(5)	328	3.55(5)
2	34	3.51(5)	36	3.10(5)
3	180	3.38(5)	177	2.91(5)
4	190	3.04(5)	192	2.62(5)
5	218	1.50(5)	217	1.28(5)
6	138	7.42(4)	347	9.73(4)
7	249	6.57(4)	247	5.81(4)
8	349	5.56(4)	355	4.18(4)

studied there are several almost equally important 30° sectors when an interpolated whole body weighting function is used to 30 km, so the "worst" sector at this site is particularly sensitive to the calculational methods.

The other exception occurs for the relatively isolated site 8, where the sparsely populated rural areas have large ED's which do not give as good resolution, on average, as in other sites. The difference of the weighting function at the extreme edges of the ED's to the value at the population centroid may be a significant effect at short distances even in the interpolation method of risk estimate. These effects could mean that differential effects due to the size of the worst sector could be more important for this site than for more populated sites.

The results of this section show that discrete weighting functions out to about 30 km may be adequate for whole site assessment purposes but have to be considered carefully when applied to assessing "worst" sector. The population about a site may mean that a worst sector is critically dependent on the selection process, as for site 6. Detailed close-in (less than 5 km) distributions should be used for the most accurate results. Also the radial distribution of weighted population along the worst sector, or generally for the whole site, may be important in assessing potential early fatalities from a major accident.

Section 6.3.2 Site and Sector assessment extended to 100 km from a site

In this section a comparison will be made between the extended thyroid weighting function and the whole body weighted dose commitment derived for the severest notional AGR accident. Ward and Civil Parish population census data are used for these results out to 100 km and should be of adequate resolution due to the dominance of the more distant populations about the majority of sites.

Both discrete and interpolated results for site weighted population totals are given in table 6.10. Due to the application and definition of the site weighting function this can be used as a method of relative comparison of the spatial population distributions about sites. As noted earlier beyond 8 km

Table 6.10 NII site weighted population values

Site	Distance (km)							
	5	8	12	16	30	50	75	100
1 D	3.06(5)	1.05(6)	1.64(6)	1.85(6)	2.20(6)	2.75(6)	2.89(6)	3.04(6)
I	2.64(5)	9.53(5)	1.60(6)	1.84(6)	2.18(6)	2.72(6)	2.87(6)	3.01(6)
2 D	2.97(5)	5.89(5)	6.56(5)	7.24(5)	1.04(6)	1.37(6)	2.18(6)	2.69(6)
I	3.16(5)	5.90(5)	6.65(5)	7.32(5)	1.05(6)	1.39(6)	2.14(6)	2.67(6)
3 D	9.73(3)	1.56(5)	2.17(5)	3.69(5)	1.05(6)	1.64(6)	1.93(6)	2.21(6)
I	1.27(4)	1.55(5)	2.16(5)	3.64(5)	1.09(6)	1.69(6)	1.99(6)	2.26(6)
4 D	1.06(5)	1.37(5)	2.58(5)	3.46(5)	9.69(5)	1.46(6)	1.82(6)	2.21(6)
I	9.99(4)	1.32(5)	2.54(5)	3.40(5)	9.35(5)	1.45(6)	1.84(6)	2.20(6)
5 D	6.20(4)	7.43(4)	1.10(5)	2.52(5)	6.66(5)	1.12(6)	2.15(6)	2.93(6)
I	5.77(4)	7.03(4)	1.04(5)	2.40(5)	6.65(5)	1.10(6)	2.07(6)	2.89(6)
6 D	4.75(4)	7.02(4)	1.23(5)	2.01(5)	4.71(5)	1.02(6)	1.40(6)	1.56(6)
I	3.74(4)	5.83(4)	1.08(5)	1.90(5)	4.60(5)	9.94(5)	1.39(6)	1.55(6)
7 D	8.97(4)	1.10(5)	1.26(5)	1.47(5)	2.26(5)	4.03(5)	5.40(5)	6.44(5)
I	7.65(4)	9.63(5)	1.13(5)	1.34(5)	2.05(5)	3.92(5)	5.40(5)	6.36(5)
8 D	0	3.65(4)	4.25(4)	5.07(4)	2.37(5)	4.12(5)	6.95(5)	1.33(6)
I	0	3.75(4)	4.35(4)	5.22(4)	2.22(5)	3.90(5)	6.76(5)	1.28(6)
9 D	4.95(4)	4.97(4)	1.57(5)	2.19(5)	4.88(5)	1.12(6)	1.26(6)	1.32(6)
I	4.89(4)	4.91(4)	1.56(5)	2.21(5)	4.64(5)	1.09(6)	1.24(6)	1.30(6)

Note: D - Discrete (centre of zone) weighting
I - Interpolated weighting factor applied to each W/CP

the interpolated and discrete estimates of weighted population for any site are in good agreement. Several sites, 2 to 5 inclusive and site 8, have larger contributions from the 75 km to 100 km annulus than has site 1. Only a factor of five spans the range of all these site weighted population totals, reflecting the fairly high population densities found over a large portion of Britain, particularly in England. It is also more difficult to distinguish between these relative levels associated with each site than is the case for results out to 30 km (see table 6.7).

The discretely weighted site populations, derived from the weighted (ICRP-26) whole body dose due to the worst AGR accident released under slightly unstable conditions, are given, accumulating out to 100 km, for each of these nine sites in table 6.11. It should be stressed that these values cannot be directly compared to those based on thyroid dose commitments, only the relative results within each set can be usefully compared. The discrete whole body site weighting function in the last two zones are in the ratio 1:0.78, while the respective extended thyroid function has a ratio of 1:0.55. This reflects the imposition of a 1 km high inversion on the dispersion under category C conditions, while the nominal iodine release is assumed not to reach any explicit inversion, under category F conditions, so continues to mix vertically but at a reduced rate far from the source. The effect of this different distance dependence is to make both sites 2 and 5 worse than site 1, due to distant metropolitan areas receiving relatively greater weighting with this second site assessment function. Also site 8 now exceeds sites 6 and 9 in overall risk due to a similar effect. A factor of five still covers the range of all site risk totals out to 100 km, only the relative values of the sites have been altered by using a different site weighting function.

When the two appropriate $22\frac{1}{2}^{\circ}$ sector weighting functions are applied, discretely, to the population distributions about each site the worst sector direction predicted by both functions is found to be the same to within the $\frac{1}{2}^{\circ}$ resolution available. As discussed in section 6.2 these worst sectors by 100 km are not always related to the worst sectors by 30 km for a given

Table 6.11 Site weighted population values based on the notional whole body dose function for nine sites.

Site	Collective site weighted population totals by the distances (discrete method)							
	5 km	8 km	12 km	16 km	30 km	50 km	75 km	100 km
1	2.06(5)	6.32(5)	9.88(5)	1.12(6)	1.36(6)	1.81(6)	1.95(6)	2.16(6)
2	2.12(5)	3.80(5)	4.20(5)	4.63(5)	6.80(5)	9.51(5)	1.75(6)	2.46(6)
3	6.97(3)	9.13(4)	1.28(5)	2.21(5)	6.87(5)	1.17(6)	1.46(6)	1.85(6)
4	7.16(4)	8.92(4)	1.62(5)	2.16(5)	6.41(5)	1.05(6)	1.40(6)	1.94(6)
5	4.22(4)	4.92(4)	7.07(4)	1.58(5)	4.41(5)	8.13(5)	1.84(6)	2.93(6)
6	3.64(4)	4.94(4)	8.15(4)	1.29(5)	3.14(5)	7.66(5)	1.14(6)	1.37(6)
7	6.41(4)	7.58(4)	8.51(4)	9.81(4)	1.52(5)	2.98(5)	4.34(5)	5.79(5)
8	-	2.10(4)	2.46(4)	2.96(4)	1.57(5)	3.01(5)	5.81(5)	1.47(6)
9	3.18(4)	3.19(4)	9.67(4)	1.35(5)	3.18(5)	8.35(5)	9.80(5)	1.06(6)

site. The weighted whole body results have already been given in absolute values (see table 6.5), which can be interpreted directly as an appropriate collective dose to a population group. Here each set of worst sector risks is normalised to the appropriate worst sector total by 100 km for site one, where these ratios are displayed in table 6.12.

Those sites, 1, 3 and 7, where both worst sectors to 100 km include some people within three kilometres of the site centre have relatively larger contributions at short ranges with the weighted whole body sector function. As has been noted earlier the interpretation of the thyroid based function, within the first kilometre, may account for a portion of this effect. At the other extreme of distance the thyroid dose based sector weighting function is found to weight the most distant population by a smaller extent than the AGR release based function, where a similar effect was found for the site weighting functions in the final zone. Only one site (5) has a "worst" sector of relatively higher weighted population than that of site 1 by 100 km. The relative differences between sites 1 and 5 are 16% and 55% for the nominal iodine and AGR based release functions respectively. These different excess values are due to the distance dependences of the functions beyond 30 km. In the case of site 7 about half the nominal collective dose to the population in the worst sector accrues within 3 km of the site, where the thyroid based function is relatively more optimistic than that based on the weighted whole body dose. The relative reduction caused by this effect is retained out to distances beyond 50 km, where the thyroid based function again shows relative optimism.

The thyroid based sector weighting function produces a factor of about 5 which will cover the range of extreme worst sector weighted population values for both weighting functions out to 100 km. This similarity was also found between the site values. A further similarity for these weighted population totals out to 100 km is that the same factor covers both the site and sector ranges of results, reflecting the interaction of the W/CP based population data for each site and the different weighting functions. The inherent assumptions of a straight

Table 6.12

Normalised worst sector risks to 100 km (discretely weighted) for NII and notional AGR based sector functions.

Site	Normalised worst sector (to site 1 at 100km) by a given distance							
	5 km	8 km	12 km	16 km	30 km	50 km	75 km	100 km
1T*	0.209	0.435	0.473	0.484	0.581	0.942	0.998	1.0
W*	0.228	0.415	0.447	0.456	0.544	0.928	0.997	1.0
2T	-	-	-	0.003	0.024	0.141	0.367	0.526
W	-	-	-	0.003	0.021	0.147	0.424	0.659
3T	0.011	0.023	0.035	0.084	0.428	0.450	0.451	0.466
W	0.013	0.022	0.032	0.072	0.381	0.404	0.413	0.427
4T	0.001	0.002	0.038	0.038	0.364	0.418	0.431	0.442
W	0.001	0.002	0.031	0.031	0.324	0.384	0.398	0.415
5T	-	-	-	0.002	0.010	0.092	0.658	1.16
W	-	-	-	0.002	0.009	0.096	0.788	1.55
6T	-	-	0.003	0.005	0.054	0.205	0.254	0.280
W	-	-	0.002	0.004	0.048	0.210	0.270	0.309
7T	0.099	0.102	0.104	0.106	0.122	0.181	0.194	0.211
W	0.112	0.115	0.117	0.119	0.133	0.196	0.211	0.239
8T	-	0.023	0.023	0.024	0.031	0.061	0.117	0.523
W	-	0.019	0.019	0.020	0.026	0.058	0.127	0.748
9T	-	-	-	0.015	0.070	0.504	0.574	0.607
W	-	-	-	0.012	0.062	0.524	0.607	0.659

*T=Thyroid based NII function, W=Whole body dose based AGR function.

trajectory for the release is used to derive these functions may not be valid in all conditions out to 100 km, particularly for stable dispersion in the atmosphere.

This and previous sections have shown that the relative quality of sites and the associated worst sectors depends on the detailed calculational methods applied. Some quite extreme differences have been produced when considering the definition of a "worst" sector solely by a total nominal collective dose to the population within a certain distance of a site. The next section will give a method which attempts to further quantify the effects of the radial distribution of a population group about a site.

Section 6.4 Site and sector assessment to produce a "quality" factor

Limiting site and sector curves have been published which are intended to apply to the siting of AGR's with concrete pressure vessels. These criteria appear to require an exclusion area extending to about 1 km from the site. The methods of applying the weighting functions and producing the site dependent characteristic "risk" curves are also given, where the derivation includes many factors from earlier work (Charlesworth and Gronow 1967 (87)). These limiting criteria (R_l) are defined within zones as below,

(6.4) $R_l^k(r_i) = \sum_{j=1}^{i} {}^{i}p_{l_j}^{k} * W_j^k$, where k is either for the whole site (si) or the most densely populated sector (se), r_i is the outer radius of zone i where a uniform weighting function W_i^k is applied to any population P_i^k within the zone boundaries from r_{i-1} to r_i and P_l^k is the limiting population for a given area at any site. This extends to the N^{th} zone where r_N=20 miles (or a metric equivalent), and r_0 is the centre of the site. The weighting functions, as explained earlier, are based on inhalation dose commitments to the thyroid and their use has been demonstrated in an earlier section.

The sector cumulative characteristic curve is intended to indicate the "risk" to the most populated sector at any site while the cumulative site characteristic curve displays a "risk" to the whole site. As noted earlier the relative prevalence of different wind directions and the frequency of different

weather categories in those directions could be taken into account, if of significance. In most cases a uniform windrose will be applied in each site assessment, as in previous sections, and only two notional examples of non-uniform windroses given. The weighting functions have been derived for only one weather category, so the full variations in the extent of dispersion at any one site are not considered here, although some indications of possible consequences have been given in earlier sections of this chapter.

For existing sites these limiting curves should not be exceeded at any distance from the site within the outer boundary r_N. This condition is given below for both the whole site and most populated sector,

(6.5) $R^k_{\text{site } s}(r_i) < R^k_1(r_i)$ for all $r_i < r_N$. The weighted population defined in terms of these weighting functions, at each site can be estimated by this procedure out to r_n. Although the weighting functions preferentially weight nearby population groups, due to the form of atmospheric dispersion, their proximith to the site may further enhance risks as there would be less time for any emergency procedures than for more removed communities.

Measuring the nearness of particular site and sector weighted population totals to the limiting values can be used to assess the relative merits of the particular detailed population distribution within a distance or r_N. A relative "risk" factor (f^k) can be defined as below, normalised to the limiting NII weighted population values,

(6.6) $$f^k(r_N) = \frac{\int_{r_0}^{r_N} R^k_{\text{site } s}(r)\, dr}{\int_{r_0}^{r_N} R^k_1(r)\, dr}$$. With the present definition of R^k_1 being in terms of uniform (discrete) weighting for each zone (based on boundaries defined in miles (Charlesworth and Gronow 1973)), the integration in equation 6.6 has to be replaced by a numerical procedure. It is assumed that the weighting factors for a particular site increase linearly from r_{i-1} to r_i, which smoothes out some of the site characteristics, where 6.6 now becomes:

$$(6.7)\quad f^k(r_N)=\frac{\sum_{i=1}^{N}(R^k_{\text{site s}}(r_i)+R^k_{\text{site s}}(r_{i-1}))*(r_i-r_{i-1})/2}{\sum_{i=1}^{N}(R^k_1(r_i)+R^k_1(r_i))*(r_i-r_{i-1})/2}\,.$$

The calculation can be rewritten in terms of a summation about each of the weighting values,

$$(6.8)\quad \sum_{i=1}^{N}(R^k_m(r_i)+R^k_m(r_{i-1}))*(r_i-r_{i-1})/2=\sum_{i=1\ m}^{N} R^k(r_i)*(r_{i+1}-r_{i-1})/2,$$

where $r_0=0$ and for $i>N$, $r_i=r_N$. This means the larger intervals in the zonal scheme weight the relevant more distant factors proportionately more, so this new "risk" factor may reflect latent cancer induction effects better than any early fatalities or morbidity effects at a site after an accident. An additional condition to that of 6.5 can be defined from these new relative "risk" factor for any site as: (6.9) $f^k_{\text{site s}}(r_i)<1$.

This site or worst sector "risk" factor, f^k, has been evaluated using the weighting values for 30° sectors (2) out to 20 miles for sites 1 to 8 using ED population census data. The results are given in table 6.13, where these factors have been derived by discrete weighting of the relevant population. The total site population does not always reflect the site "risk" factors, due to the spatial distribution of population especially in rural sites.

These sites at present have either Magnox or Advanced Gas cooled Reactors operating on them and in some cases two reactors. All these sites could accommodate an AGR under the siting criteria applied in these calculations. If reactor parks were to be designed, with several reactors at one site, careful consideration would have to be given to the independence of the rectors under fault conditions. Operational, continuous releases may impose a limit on the number of reactors at one park, rather than this site assessment scheme. Assuming the reactors to operate independently the number of reactors (N^R) in any one park could be increased until the site and (or) sector weighted population tests reached the limiting values, where the population groups at risk are factored up by this number of reactors N^R.

Table 6.13 Relative risk factors for site and sector to 20 miles at eight sites.

Site	Axis of worst 30° sector	Total site population by r_N=20 miles (in $*10^6$)	$R^{si}(r_N)$ Limit=3.82 (6)	$f^{si}(r_N)$	$R^{se}(r_N)$ Limit= 1.27 (6)	$f^{se}(r_N)$
1	328	1.07	2.16(6)	0.640	3.55(5)	0.321
2	36	0.62	1.08(6)	0.310	3.10(5)	0.369
3	177	1.14	1.16(6)	0.218	2.91(5)	0.142
4	192	0.99	9.85(5)	0.182	2.62(5)	0.101
5	217	0.73	7.32(5)	0.137	1.28(5)	0.055
6	347	0.53	5.23(5)	0.094	9.70(4)	0.033
7	247	0.17	2.37(5)	0.061	5.81(4)	0.058
8	355	0.25	2.31(5)	0.038	4.18(4)	0.025

In general the relative"risk" factor, f, for the worst sector tends to be less than the overall site relative "risk" factor, except for site 2. This is due to the detailed differences in the weighting functions where the site weights are just dependent on the peak axial concentrations and, unlike the sector weights, are not modified by any factors dealing with the lateral spread of material in the atmosphere, which tend to further reduce the weights at large distances.

The accuracy of these values can be estimated by an inspection of the "risk" values calculated by using continuous (interpolated) weighting functions, as described earlier. Table 6.14 gives the ratios of the discrete to interpolated site and 30° sector weighted population values at r_N(=20 miles) for these sites 1 to 8. The site weighted population factors are quite accurately assessed by 20 miles while there is more variance for the sector weighted population factors, where the extreme value at site 6 is due to a large population beyond 14 miles, as described earlier. At shorter distances the agreement between the estimates is expected to worsen. Due to the definition of this relative "risk" factor, f^k, the accumulating weighted population at large distances from the site is given more importance, where most of the population about a site tends to be in these outer zones, so this factor, f^k, is not very dependent on close in details of a site.

A quality factor for a site or sector may be expected to increase with decreasing levels of risk. The "risk" factor (f) can be converted to a form of quality factor as in the two equations below:

(6.10a) $Q_a^k = 1/f^k$, $Q_a^k > 1$;

(6.10b) $Q_b^k = -\ln(f^k)$, $Q_b^k > 0$. These values are displayed for all eight sites in table 6.15, where a difference of 0.693 in Q_b^k represents a factor of two in the relevant quality of a site or sector. A factor of about 15 covers the site qualities, Q_a, and a similar range occurs for the worst sector quality factors. This range of values is greater than that found in the total site and sector weighted populations, see table 6.13. The quality factors Q_a are more readily interpreted than the logarithmic based factors Q_b.

Table 6.14 Differences in the total site and sector weighted population by 20 miles due to discrete or interpolated weighting methods.

Site	$(R_D^{si}(r_N)/R_I^{si}(r_N))$	$(R_D^{se}(r_N)/R_I^{se}(r_N))$
1	0.96	0.97
2	1.03	1.04
3	0.98	0.89
4	1.01	1.04
5	1.07	1.13
6	1.04	1.27
7	1.04	0.97
8	1.03	1.01

Table 6.15 Quality factors for site and worst sector derived from the limiting site and sector risks

Site	$Q_a>1$		$Q_b>0$	
	site	worst sector	site	worst sector
1	1.56	3.11	0.447	1.14
2	3.22	2.71	1.17	0.998
3	4.60	7.03	1.53	1.95
4	5.51	9.84	1.71	2.29
5	7.33	18.3	1.99	2.90
6	10.6	30.5	2.36	3.42
7	16.4	17.1	2.80	2.84
8	26.0	39.4	3.26	3.67

The final topic in this section deals with a simple example of the effect of accounting for the frequency of different wind directions, under one weather condition. A notional windrose was assumed, see figure 6.16, which gave weights, W_j^R, to 10° intervals, j=1 to 36. The windrose is applied as a multiplicative factor within equation 6.4 so that the simple weighting function is replaced by $W_{ij}^{*k}=W_i^k \cdot W_j^R$. This is normalised by the condition below:

(6.11) $\Sigma_{j=1}^{36} (W_j^R-1)=0$, where j refers to angles from $(j-1).10^\circ$ to $(j.10-1)^\circ$. A uniform windrose has all W^R equal to unity.

The effects of this extra wind direction weighting function for the category F release of iodine assessment scheme are only given for the two sites 2 and 5. The whole site weighted population, $R^{si}(r_N)$ can be expected not to be greatly influenced by the application of the windrose. The population distribution at most sites would extend over a sufficient portion of the windrose so that an averaging process occurrs between the communities with weights $W_j^R < 1$ and $W_j^R > 1$. This expectation is borne out by these two sites for the nominal windrose (see table 6.16). If data for the frequency of category F dispersion conditions at all UK sites were applied some sites' characteristics may be altered by greater margins than in this example, where most change could occur within sites 7 and 8 as only about half the full windrose contains populated areas for these two rural, coastal sites.

When the worst sector, with the greatest total weighted population $R^{se}(r_N)$, is to be chosen after the application of the windrose factors, more significant changes could be expected than in the whole site as the population in a 30° sector would not have the averaging properties of the whole site as referred to above. The worst sector results with the windrose modifications are shown in table 6.16 for sites 2 and 5. For site 2 the direction of the worst 30° sector does not change. Not only is this worst sector more than twice the next worst sector, see figure 6.4, so that the range of the assumed windrose weights 0.7 to 1.4 can not overcome this difference, it also lies in a direction which the assumed windrose favours more than an average uniform windrose. This additional weighting reduces

Figure 6.16 Notional non-uniform windrose, divided into 10° sectors.

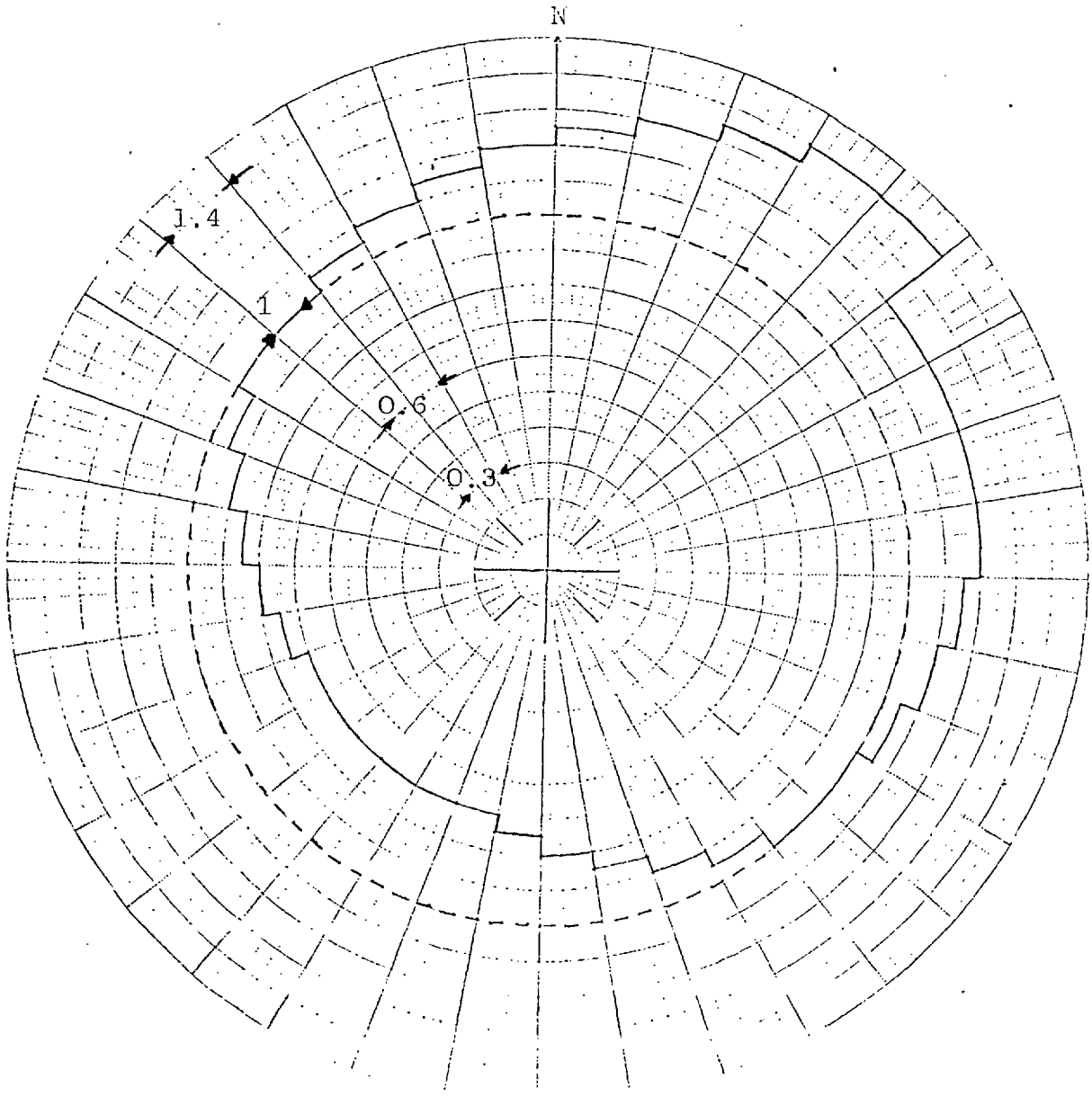

TABLE 6.16

Comparison of uniform and simple non-uniform windroses applied to AGR sector and site wieghting functions (30° sectors out to 20 miles)

Quantity	Site 2		Site 5	
	Uniform	Non-uniform	Uniform	Non-uniform
Site risk				
(inter., ED)	1.05(6)	1.17(6)	6.88(5)	6.66(5)
Qa (site)	3.37	2.78	8.01	7.92
Sector risk (angle)	36°	36°	217°	357°
(discrete, ED)	3.10(5)	4.28(5)	1.28(5)	1.33(5)
(inter., ED)	3.00(5)	4.13(5)	1.13(5)	1.27(5)
Qa (sector)	2.71	1.97	18.3	9.22

the "quality" factor of this worst sector by about 33% while the total sector weighted population has been increased by about 40%.

Site 5 exhibits a different effect of the windrose, which is a complete change of worst sector direction from 217° from north to 357° from north. There is only a small increase, less than 10%, in the total sector weighted population between these two cases, but the quality factor has been reduced by about 50%. From an inspection of figure 6.7 these two sectors have almost equal potential collective doses with a uniform windrose, with a difference of about 10% in favour of that centred on 217° from N, but that sector about 357° from N has much larger contributions from population groups closer to the site. These two sectors at site 5 are weighted by W^R of 0.7 about 217° and 1.15 to 1.25 about 357°. Note that using a non-uniform windrose also slightly affects the relative differences between the discrete and continuous total sector weighted populations, where any effect would in general be very site dependent.

This discussion has displayed that site factors may be quite readily calculated, if only relative comparisons are to be made on a single weather category, but exhibit slight dependences on the range of site weighting functions used here. The concept of a single "worst" highly populated sector for each site is much more dependent on the definition of sector boundaries and the details of the sector weighting function applied. A comparison of site characteristics to the limiting criteria has resulted in the definition of site and sector radially dependent relative "risk" and "quality" factors. Emergency measures, such as evacuation, may allow these weighting functions to be modified close to the site, and a simple example is given in the final section of this chapter.

Section 6.5 Modelling and assessing an evacuation

As noted in an earlier section of this chapter the modified site assessment computer program now allows evacuations to be modelled. In the following discussion a simple evacuation scheme for the small village marked in figure 6.1 at site 1 is detailed.

The lung inhalation dose commitment from the notional filtered AGR release after a single channel meltout in an intact coolant circuit is the basis of the time dependent dose commitment factors used. The release from sequence 1 is factored up so that the on-axis dose, 1 km downwind from the site, after 24 hours dispersing in average prolonged neutral conditions equals the ERL for the lungs. The dose commitment from the release with lower efficiency filters, sequence 2, has the same factor applied, so gives correspondingly larger dose commitments. These doses are uniformly spread over a 30° sector centred on the small village (A), which is 1.6 km distant from site 1, where the relative locations are given in more detail in figure 6.17. This uniform spread is intended to average over any fluctuations in the distribution of plume material during the period of evacuation.

Two time structures (a and b) of the evacuation are examined, starting, respectively, one hour and two hours after the release commences. After each evacuation starts the evacuees split into two groups which are assumed to move 700 metres every 10 minutes to the locations, B and C, in figure 6.17, but one small group, of 5, remains in the village throughout the release. One evacuated group, of 95, leaves the 30° sector immediately in this simplified model, while the other group, of 100, exits after 10 minutes. Ten people are assumed to enter the area to aid in the origanisation of the evacuation.

Using the knowledge of the release building up in time and the associated lung inhalation dose commitment 1 km downwind (see chapter 5) the fractions of the total dose commitment delivered during each of these small time periods of the evacuation can be estimated. The fraction, which depends on the starting time of the evacuation and the efficiencies of the filters acting on the release, combined with the multiplying factor assumed earlier, can be applied to the total lung dose by an option in the computer program which calculates potential collective dose commitments.

A breakdown of the collective doses received by each of the groups defined above during this evacuation, along with mean individual dose commitments, is given in table 6.17. When

Figure 6.17 Diagram showing relative locations of the reactor at site one and evacuees before and during a notional cross-wind evacuation.

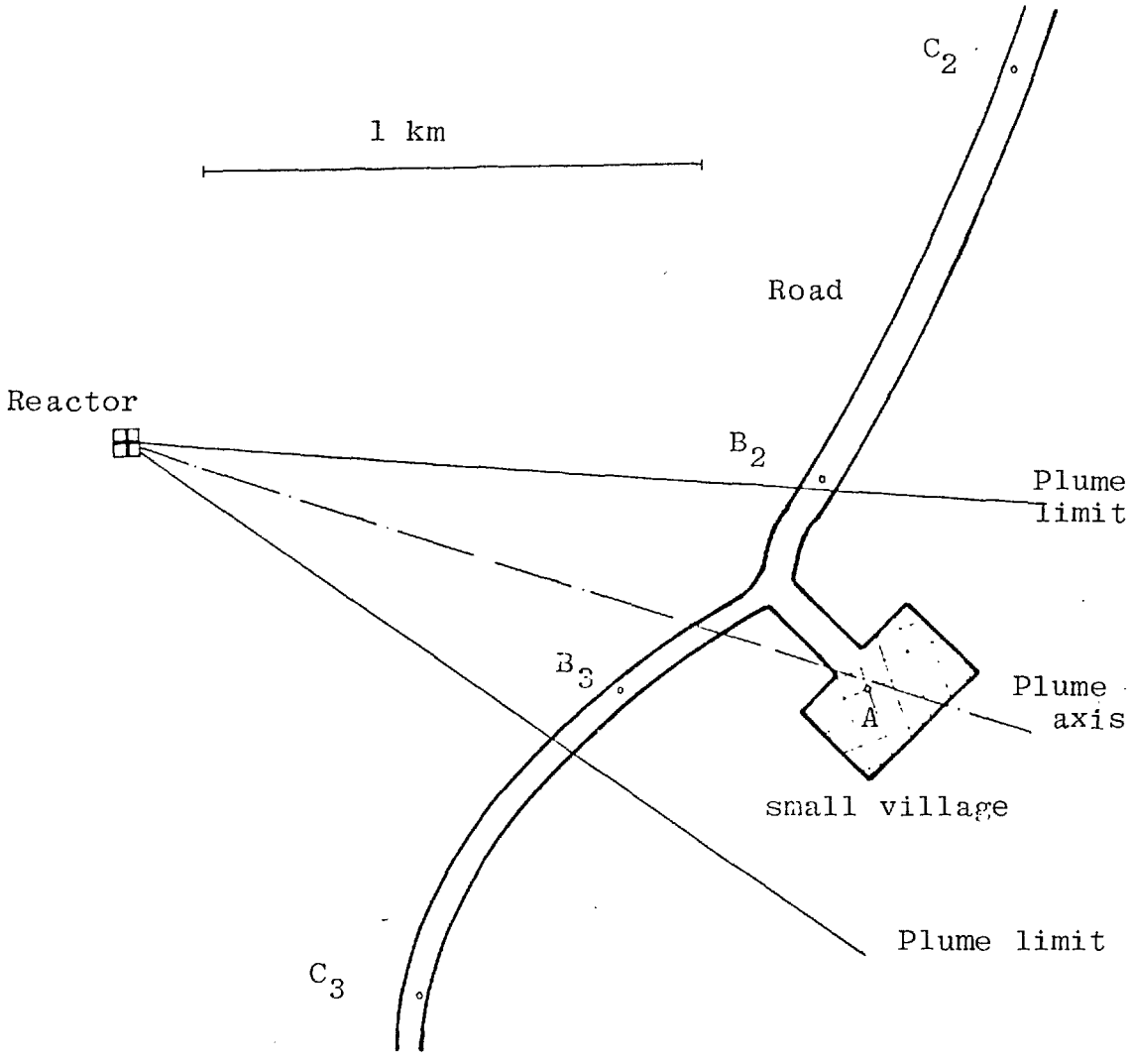

Table 6.17 Breakdown of collective and mean individual doses to groups within the notional evacuation scheme

	Evacuation Schemes								
	No evacuation	Evacuation after 1 hr.				Evacuation after 2 hrs.			
	Total villagers	Non-evacuees	Evacuees	Evacuators	total	Non-evacuees	Evacuees	Evacuators	total
Number of people from 3.1	200	5	195	10	210	5	195	10	210
mean individual(rem)	21	21	5.0	0.1	5.1	21	5.1	0.2	5.6
collective dose (man-rems)	4200	105	970	1	1080	105	1070	2	1180
from 3.2									
mean individual(rem)	80	80	11	2.1	12	80	24	3.0	25
collective dose	16000	400	2100	21	2500	400	4800	30	5200

any of these modelled evacuations are carried out under these particular conditions there is always an overall reduction in the total collective dose to the members of the whole exposed group. This occurs even when the number of exposed individuals is increased by the evacuators and the evacuation path initially involves approaching the reactor and being exposed to greater dose rates for a short time.

The evacuation provides a dose reduction factor, to the residential population, of about 4 for highly filtered releases and between 6 and 3 for lower efficiency filters acting on the release. In these examples the dose to the evacuees is primarily due to that received before evacuation commences as a crosswind rather than a downwind evacuation path is assumed. When the high efficiency filters are applied to the sequence 1 release after an hour the rate of delivering a lung dose commitment is markedly reduced and little is gained by evacuating after only one hour rather than two hours. With the low efficiency filters there is a stronger case for evacuation after one hour, rather than two, as the collective dose commitment more than doubles during this second hour. Shielding effects on external exposures, and the air flow through, houses and vehicles have to be considered when making a decision on evacuation and on other likely doses which could accrue and have been neglected in this simple treatment. It has been noted, in chapter 5, that in these filtered releases the cloud gamma exposure after the ini-tial hour is not of great significance relative to the whole release and the inhalation dose commitments. In both filtered release sequences the collective dose commitment to the evacuators is relatively small compared to that of the evacuees, but is much larger in absolute terms for the release acted on by the low efficiency filters. The individual dose commitment expected to be received by these evacuators may be relevant to the type of personnel chosen, or allowed to volunteer, as well as any protective devices they might carry.

The methods outlined here for modelling evacuation of population close to a site could be done in much greater detail, provided all the relevant data were available, including local dispersion conditions as well as effects of topographical features. Larger scale evacuations might be modelled in a similar fashion but the detailed time steps could rapidly become cumbersome. A possible solution to this problem could be to

modify all population centroid coordinates, and retain this modification for later calculational steps, so that these groups were progressively distanced from the site. Consideration of any detailed plans for a mass evacuation may provide alternative methods of calculating relevant collective doses.

The strategy of a mass evacuation would be more complicated, lasting for long periods, and probably involve higher non-radioactive risks than a small scale evacuation from the immediate vicinity of a site. Also modelling plume dispersal during the extended period required for mass evacuation would demand sensitivity tests to changes of dispersion conditions. At some sites, and potential sites, large scale evacuation may encompass hospitals which could greatly increase risks due to the transport of patients and interruption of medical services. The need for emergency plans to include the possibility of mass evacuation has been highlighted by the recent (March/April 1979) accident involving the core of the PWR at Three Mile Island (Penn., USA), although comparable accidents may be much more remote events in gas cooled reactors. In this case many residents left the area of their own volition, which may be a general effect which has to be considered for some types of large scale industrial accidents. Long term evacuation poses greater political and financial problems.

Section 6.6 Summary of Results

The previous section has shown that evacuation can be used to reduce the risk of population groups close to a site in the event of a release of radioactive fission products. This effect will be site dependent so should not be incorporated in any general site or sector weighting functions or related limiting criteria. Other sections of this chapter have shown that all sites cannot be simply assessed by any one set of fixed assumptions but each has to be considered in detail. A more comprehensive site assessment scheme would involve many of the points mentioned previously. The definition of a "worst" sector has to be considered in the light of any responsibilities or restrictions involved with that population group. The sensitivity of the results of any scheme to variations in the inherent assumptions would be a vital factor in defining confidence in the choice and long term surveilance of the site of a nuclear installation.

CHAPTER SEVEN

CONCLUSIONS AND SUGGESTIONS FOR FUTURE WORK

Section 7.1 Conclusions from this work

Improvements have been made to the dispersion and depletion routines in the WEERIE code as well as additions to the methods estimating external exposures. The ability to evaluate collective doses has been increased to provide information applicable to siting criteria and possible emergency procedures.

The conclusions from this work can be summarised as below:

i. The incorporation of a practical element dependent deposition model, for dry and wet depletion, is a significant improvement on the previous simple model allowing more detailed results to be readily obtained, with the major benefit occurring in predictions of ground contamination levels, as successfully demonstrated with a range of notional MAGNOX and AGR releases.

ii. Diagnostic properties derived from the improved predictions of inhalation dose commitments, external exposures, time integrated air concentrations, disintegration counts and ground contamination for the range of notional AGR releases suggested that external gamma spectra could be the most sensitive indicator of the type of release.

iii. The prolonged (1 day) notional AGR release, assuming operational leakage, emphasised the crude modelling of resuspension from filters and the problems of dealing with the transport of a radiologically significant element which exists in several different forms in a reactor.

iv. External gamma exposures from deposited activity at a given downwind distance can exceed the corresponding external cloud gamma exposures after about a day, when dispersion occurs in typical neutral conditions and depletion is only by dry deposition for the notional AGR releases, or a shorter period for the most extreme case considered. In these cases, except for a restricted range of conditions, external ground exposures only deliver doses which are more significant than inhalation doses over a prolonged period.

i. Redefinition of the routines which model the build up of activity in the reactor core to include heavy elements and activation products.

ii. Generalise and improve the model of transport of activity through a reactor to the atmosphere and so be able to cope with a wide range of reactor types and containment systems.

iii. Incorporate models to estimate potential doses from heavy elements released to the atmosphere.

iv. Include methods for deriving more realistic gamma spectra from airborne and deposited activity.

v. Parameterise the dispersion coefficients to allow a continuous range of conditions rather than discrete categories (e.g. in a form to use site dependent data.)

vi. Comparison of Gaussian dispersion models to more detailed models for special cases (e.g. fumigation, land-sea interface, plume rise etc.)

vii. Provide estimates for food chain doses from ground contamination (but this may lead to the development of a separate environmental code which could also allow for general weathering and other redistribution effects on amounts of activity which were initially predicted by WEERIE).

Future aims to improve methods for calculating collective doses and related site quantities include:

i. Derivation of weighting functions for various mixed fission product releases characteristic of categories of accidents in different reactor types e.g. LWR's.

ii. Allowance for site and time dependent dispersion and extension of the meteorological descriptions at the far downwind ranges of assessment areas.

iii. Further improvements to the resolution of population census data at short distances from the site, such as using 100 metre grid data.

v. Ground contamination for these notional AGR releases is above DERL's, for potential food chain doses, at larger downwind ranges than that for which inhalation dose commitments exceed ERL's.

vi. Weighted whole body collective dose commitments, using the recommendations of ICRP 26, can be used to estimate potential casualties at a site resulting from a notional mixed fission product release. This can be used to provide a means of comparing site qualities, by deriving appropriate site and sector weighting functions which are directly related to potential fatalities. In comparison the nominal iodine siting factors cannot be directly related to the source of the majority of potential casualties, or the critically exposed organ in all the cases discussed in this work.

vii. The selection of a worst sector has been shown to be sensitive to both the radius of the sector and its angular width, where if the latter is reduced this tends to produce the selection of higher density population groups. Also there may be several sectors of almost equal concern by a given distance, say 30 km, from a site and these may bear no relation to the population distribution in the immediate vicinity of the site.

viii. Centroid population census data (ED and W/CP) can be edited to allow for detailed site characteristics very close to a reactor and for evaluating local evacuation schemes. Regular 1 km and 100m grid data can represent a residential population to an equivalent degree of accuracy.

Section 7.2 Suggestions for future work

Two categories for possible future work can be identified as relating to the WEERIE code and methods for assessing collective quantities, such that a review of even extremely improbable releases from a reactor at any site could be undertaken.

Some major items for future work on the WEERIE code include the following topics:

iv. Effects of age, gender and diet on collective doses and consequences.

v. Detailed evaluation of collective doses to transitory population groups.

vi. For prolonged releases detailed cases could be considered, associated with real meteorology data, to evaluate collective doses.

vii. Methods for associating the probability of incurring at least a given collective dose with risks to health, or other appropriate quantities.

REFERENCES

(1) Flowers (Chairman) VIth Report, Royal Commission on Environmental Pollution "Nuclear Power and the Environment" (H.M.S.O., Cmnd 6618), 1976.

(2) W.S. Gronow and R. Gausden, IAEA proc. symp. Principles and standards of reactor safety. (1973).

(3) ICRP Publication 26 (Pergamon Press, 1977).

(4) R.H. Clarke, Hlth. Phys., 25, 267-280 (1973).

(5) F.O. Hoffman, C.W. Miller, D.L. Schaeffer and C.T. Garten Jnr., Nucl. Saf., 18, 343-354 (1977).

(6) G.N. Kelly, J.A. Jones and B.W. Hunt, NRPB-R53(1977).

(7) USEPA (Office of Radiation Programs, Washington, DC), Reactor Safety Study (WASH-1400): A review of the final report. (US Dept. Commerce, NTIS, PB-259442, 1976).

(8) ICRP Publication 29 (Pergamon Press, 1979).

(9) UNSCEAR, Sources and Effects of Ionizing Radiations. (U.N. 1977).

(10) R.H. Clarke, Hlth Phys, 23, 565-572, (1972).

(11) S. Nair, CEGB RD/B/N4138 (1977).

(12) J. Fitzpatrick, MSc. Dissertation, Imperial College, London (1974).

(13) R.H. Clarke, Ph.D. Thesis, Polytechnic of Central London (1973).

(14) W.F. Hilsmeier and F.A. Gifford, ORO 545 (1962) (also see (13))

(15) F. Pasquill, Met. Mag. 90, 33-49 (1961).

(16) L.S. Fryer and G.D. Kaiser, UKAEA, SRD R134 (1978).

(17) G.D. Kaiser, UKAEA, SRD R36 (1976).

(18) J.A. Martin Jnr., C.B. Nelson and P.A. Cuny. "A computer code for calculating doses, population doses and ground depositions due to atmospheric emissions of radionuclides". USEPA (Off. Rad. Progs., 1974).

(19) F.W. Stallman and F.B.K. Kam, USAEC (ORNL) ORNL-TM-4082 (1973).

(20) F.B. Smith, Internal Met. Off. Note, TDN 40(MET.O.14, 1973) and quoted in (24).

(21) H.M. ApSimon and A.J.H. Goddard, Proc. 4th Int. Cong. IRPA, Paris, 2, 603-606 (1977).

(22) P.R. Maul, Atmosph. Environ., 11, 1191-1195 (1977).

(23) R.A. Scriven and B.E.A. Fisher, Atmosph. Environ. 9, I 49,II 59 (1975).

(24) F. Pasquill, "Atmospheric Diffusion" (pub. Ellis Horwood, 1974).

(25) The Hon. Mr. Justice Parker: The Windscale Enquiry, Report by (HMSO, LONDON, 1978).

(26) J. Tadmor, Hlth Phys, 24, 37-42. (1973)

(27) L. Machta, G.J. Ferber and J.L. Heffter, Proc. Symp. Physical Behaviour of Radioactive contaminants in the atmosphere, IAEA-SM-181/7, 411-426(1974).

(28) B. Bolin, Int. J. Air Pollut., 2, 127-131 (1959).

(29) ICRP Publication 2 (Pergamon Press, 1959).

(30) Task Group on Lung Dynamics (ICRP), Hlth Phys., 12, 173-207 (1966).

(31) R.H. Clarke and R.E. Utting, CEGB Report RD/B/N1762 (1970)

(32) J. Shaw and R.J. Palabrica, Annals of Nucl. Sci. and Engineering, 1, 241-254 (1974)

(33) A.J.H. Goddard, G. Gouvras and S.J. Strachan, The American Nuclear Society Transactions, 31, 444 (1979) (jointly pub. by AMS and ENS)

(34) M.R.C., "Criteria for Controlling radiation doses to the public after accidental escape of radioactive material" (HMSO, 1975)

(35) G.R. Bell, Reactor Safety Analysis, 12, 49-72 (1977)

(36) H.F. Macdonald, P.J. Ballard, I.M.G. Thompson, E.P. Goldfinch and H.C. Orchard, J. Br. Nucl. Energy Soc., 16, 177-186 (1977).

(37) ICRP Publication 27 (Pergamon Press, 1977)

(38) H. Smith and J.W. Stather, NRPB-R52 (1976)

(39) J. Tadmor, Hlth Phys, 30, 95-112 (1976)

(40) J.A. Martin Jnr. and C.B. Nelson, IAEA Proc. Symp. Physical Behaviour of Radioactive Contaminants in the atmosphere, IAEA-SM-181/32 (1974)

(41) J. Fitzpatrick, Ph.D. Thesis, Imperial College, London (1976)

(42) R.H. Clarke, J. Fitzpatrick, A.J.H. Goddard and M.J. Henning, J. Br. Nucl. Energy Soc., 15, 297-303 (1976)

(43) A.C. Chamberlain, AERE,HP/R 1261 (HMSO, 1953)

(44) Reactor Safety Study, WASH-1400, (1975, draft 1974)

(45) D.H. Slade (ed.), USAEC, "Meteorology and Atomic Energy - 1968" (1968)

(46) R.R. Draxler and W.P. Elliot, Atmosph.Environ., 11. 35-41 (1977)

(47) T.W. Horst, Atmosph. Environ., 11, 41-46 (1977)

(48) L.P. Prahm and R. Berkowicz, Nature, 271, 232-234 (1978)

(49) W.G.N. Slinn, Nucl. Safety, 19, 205-219 (errata 365)(1978)

(50) K.T. Whitby, Atmosph. Environ., 12, 135-159 (1978)

(51) G.A. Briggs quoted in (24)

(52) A.J. Russo, J.R. Wayland and L.T. Ritchie. "Influence of plume rise on the consequences of radioactive material releases" Sandia Labs., Albuquerque, New Mexico, Sand 76-0534(1977)

(53) J.R. Beattie and P.M. Bryant, UKAEA, AHSB(S) R135 (1970).

(54) Atomic Energy Off., "Accident at Windscale No.1 Pile on October, 1957" HMSO, Cmnd. 302 (1957)

(55) K.F. Baverstock and J. Vennart, Hlth PHys., 30, 339-344 (1976)

(56) P.E. McGrath, D.M. Ericson Jnr. and I.B. Wall, IAEA Symp. on the Handling of radiation accidents, IAEA-SM-215/23(1977)

(57) R.G. Jaeger (ed. in chief), Engineering Compendium on Radiation Shielding, Vol.I (pub. Springer Verlag, 1968)

(58) E.W. Sidebotham (quoted in (13))

(59) R.L. French, Hlth Phys, 11, 369-383 (1965)

(60) S.J. Strachan and A.J.H. Goddard, Annals of Nuclear Energy, 6, 91-102 (1979)

(61) H.F. Macdonald, P.J. Darley and R.H. Clarke, IAEA Symp. on Physical Behaviour of radioactive contaminants in the atmosphere. IAEA-SM-181/33,337-348 (1974)

(62) C.M. Huddleston, Q.C., Klingler, Z.G., Burzon and R.M. Kinkaid, Hlth Phys, 29, 537-548 (1965)

(63) J.O. Corbett, CEGB Report RD/B/N3865 (1977)

(64) C.E. Clifford (see section 4.5.1.5 of (57))

(65) P.M. Bryant, Hlth Phys, 12, 1393-1405 (1966)

(66) R.F. Griffiths, Atom, 314-325 (1978)

(67) Gale, Humphreys and Fisher (1963), quoted in (63).

(68) L.R. Anspaugh, J.H. Shinn, P.L. Phelps and N.C. Kennedy, Hlth Phys, 29, 571-582 (1975)

(69) H. Enge, "Introduction to Nuclear Physics" (Addison Wessley, 1966)

(70) W.G. Cross, Physics Med. Biol., 13, 611-618 (1968)

(71) L.V. Spencer, Phys. Rev., 98, 1597-1615 (1955)

(72) C.D. Zerby and F.L. Keller, Nucl. Sci. and Engineering, 27, 190-218 (1967)

(73) R. Loevinger, Radiology, 66, 55-62 (1956)

(74) W.G. Cross, Can. J. Phys, 45, 2021-2040 (1967)

(75) W.G. Cross, Can. J. Phys, 47, 75-83 (1969)

(76) R. Loevinger, E.M. Japha and G.L. Brownell in "Radiation Dosimetry", Chapt. 16 (eds. G.J. Hine and G.L. Brownell, Academic Press, 1956)

(77) S.M. Beynon (Mrs.) CEGB Report RD/B/N2633 (1973)

(78) R. Woollatt, N.I.I., Private communication (1978)

(79) J.J. Hillary and J.C. Taylor, UKAEA TRG report 2317(W) (1972)

(80) J.J. Hillary and J.C. Taylor, UKAEA TRG report 888(W) (1965)

(81) D.A. Collins, A.E. McIntosh, R. Taylor and W.D. Yuille, UKAEA TRG report 956 (W) (1965)

(82) J.J. Hillary and J.C. Taylor, UKAEA TRG Report 2433 (W) (1973)

(83) H.F. Macdonald, IAEA Symp. Rapid Methods for measuring radioactivity in the Environment, IAEA-SM-148/38 (1971)

(84) G.A. Harte,CEGB Report RD/B/N3564 (1976)

(85) I.S. Eve, Hlth Phys, 12, 131-161 (1966)

(86) E.E. Lewis, "Nuclear Power Reactor Safety", (Wiley, 1977)

(87) F.R. Charlesworth and W.S. Gronow, Proc. Symp., Containment and siting of Nuclear Power Plants, IAEA-SM-89/41, 143-170 (1967)

(88) M.J. Berger (see section 4.3.1.2A of ref (57))

(89) A.B. Chilton, Nucl. Sci. and Engineering, 27, 403-410 (1967)

(90) M.J. Berger, J. of Applied Physics, 28, 1502-1508 (1957)

(91) C.E. Clifford and G.D. Wait, Nucl. Sci. and Engineering, 27, 483-485 (1967)

(92) C.M. Lederer, J.M. Hollander and I. Perlman, "Table of Isotopes" (6th ed.) (J. Wiley, 1967)

(93) A. Tobias, CEGB Report RD/B/M2453 (1972)

(94) G.J. Schriber, H.R. Voelkle, H.H. Loosli, H. Oeshger, The ANS Transactions, 31, 444 (1979) (jointly pub. by ANS and ENS)

(95) F.O. Hoffman, Hlth Phys, 32, 437-441 (1977)

(96) L. Maisel, Probability, Statistics and Random Processes (pub. Simon and Schuster, 1971)

(97) H.F. Macdonald and J.H. Mairs, CEGB Report RD/B/N4440 (1978)

(98) BNES Conference proceedings, Radiation Protection in Nuclear Power Plants and the Fuel Cycle, (Bristol 1978, pub. 1979)

APPENDIX A

This appendix deals with the methods used to calculate the external gamma exposure rates from contamination on a smooth plane, which should be representative of deposits from plumes on the ground given appropriate corrections (see chapter 3.3).

Section A.1. Exposure from an infinite uniform deposit of gamma activity on a smooth plane.

This appendix describes the development of a numerical routine, in a form which could be incorporated into the WEERIE model, to estimate external gamma exposure rates from activity deposited from a plume of mixed fission products. The problem is initially represented by the source material located in an infinite homogeneous medium using build-up factors on the direct flux to be able to derive a total exposure rate. Corrections for the presence of the ground can then be applied, after which the detailed effects of different grid systems for the numerical calculation are considered. The conversion of the derived build-up factor exposure flux, in terms of source photon energies, to an overall exposure rate is discussed.

This provides a well documented problem which can be used to test the results derived by the model under development, so finally comparisons are made between the results of this routine and those from previously published work.

Section A1.1. Infinite medium build-up factors for point sources.

The exposure about one metre above a deposit of gamma

emitters can be taken as that relevant to potential irradiation of people. This defines the receptor point for the calculations which follow.

The intention of the method used here is that the deposited activity, in this case of infinite uniform extent, can be adequately represented by an array of point sources. Further it is assumed that the direct flux from each point source can be multiplied by an appropriate build-up factor, so that the exposure due to scattered photons is also included in the calculations.

The geometry of this particular problem can best be characterised in cylindrical polar coordinates (ρ,ϕ,z), where there is no dependence on the azimuthal angle (ϕ). Hence figure A.1 shows the basic relationship between the n^{th} point source on the ground $(\rho = \rho_n,\ z = 0)$ and the receptor at $(\rho = 0,\ z = 1\ m.)$. The direct path between these two points is: (A.1) $r_n = (\rho_n^2 + 1)^{\frac{1}{2}}$, where this distance is used to determine the direct flux (N^d) from geometric and attenuation considerations. It is assumed that the n^{th} point source has a strength S_n (dis per unit time), which is determined by the area it represents.

The number of photons crossing an area dS at the receptor, per unit time, having travelled directly from the n^{th} point source of strength S_n is, taking into account the solid angle subtended by dS from the point source, (A.2) $N_n^d dS = S_n \cdot \frac{dS}{4\pi r_n^2} \cdot e^{-\mu \cdot r_n}$,

FIGURE A.1

Diagram of a receptor above a smooth plane containing a point source.

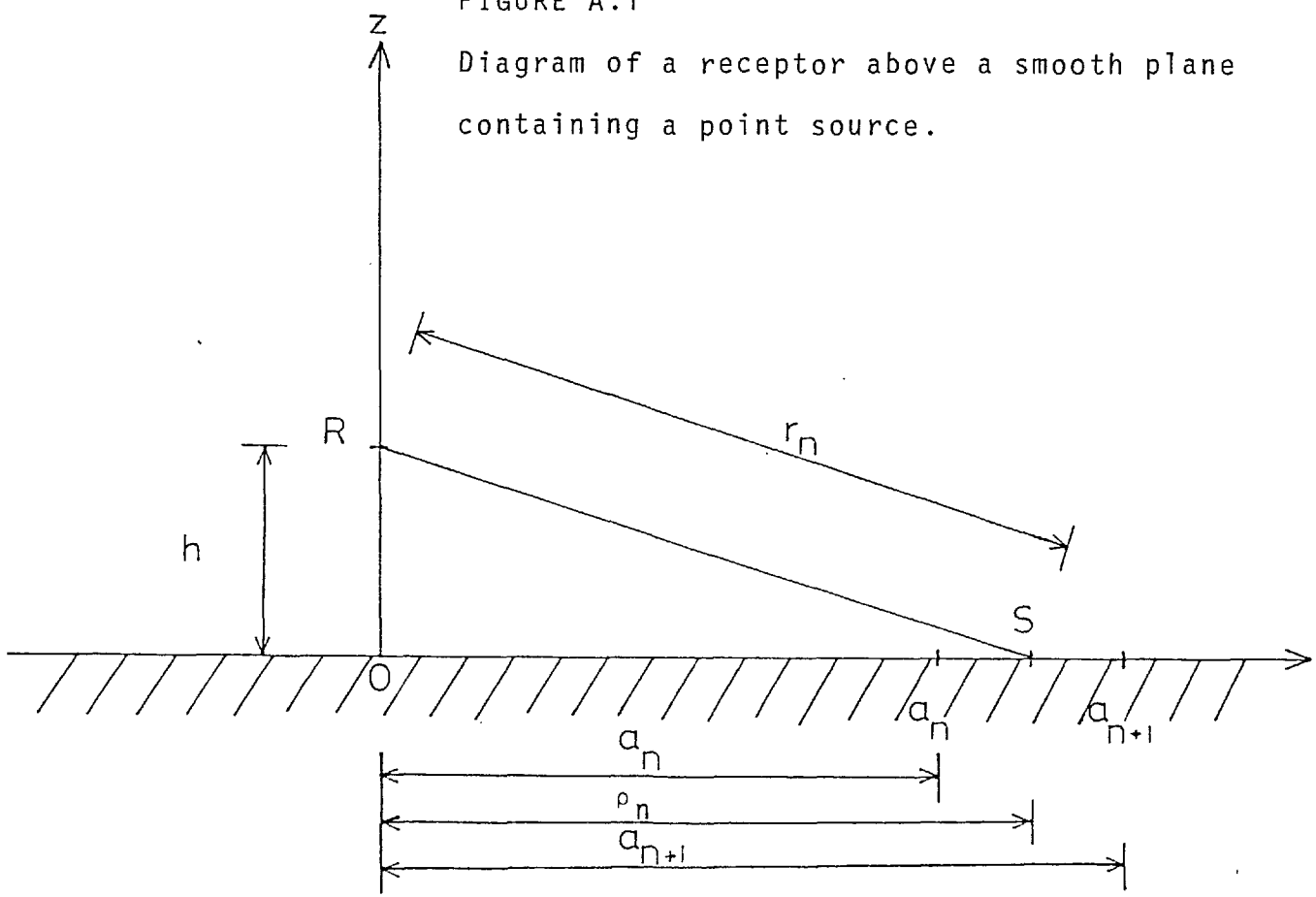

where μ is the linear attenuation coefficient in dry air. The source photons are assumed to be emitted isotropically, which should be the case for a mixed fission product deposit.

To calculate an exposure the direct flux of photons of energy E_o has to be converted by appropriate build-up factors ($B(\mu r_n, E_o)$). The build-up factors used in WEERIE, for cloud gamma estimates, are for energy deposition in an infinite air medium for point sources (Berger (88)). These factors were stored for twelve energy groups, as proposed by Sidebotham, where the energy deposition values should be equivalent to those for exposure in this type of calculation (Chpt. 4.3.1.2 (57))

Due to the closeness of the receptor point to the deposit special attention was paid to these build-up factors within the first mean free path, in this initial development. A quadratic formula was used to produce compatible build-up factors within this range (Chilton 1967(78)). These factors can be expected to allow the exposure to be estimated to an accuracy better than about 10%.

Hence the exposure flux at energy E, from the n^{th} point source (N_n^E) can be defined as (A.3) $N_n^E.dS = S_n N_n^d.B(\mu r_n, E).dS$, where $\mu = \mu(E)$. This has to be summed for all point source contributors on the infinite smooth plane to give the total exposure flux at this energy. (A.4) $N^E.dS = dS\Sigma_{n=1}^{\infty} N_n^E$.

Section A1.2. Introduction of ground correction factors

The problems involved in a gamma exposure calculation

where the receptor point is close to a smooth plane boundary of two semi-infinite homogeneous mediums have been intensively studied. Some of these results have been applied to the development of the required external gamma exposure routine.

The two media concerned in this calculation are soil and air, both of which are composed primarily of elements with low atomic numbers. The attenuation coefficients in a given medium are normally directly proportional to the density of that medium, particularly for low density materials such as air. Despite the large differences in density these two materials have similar scattering properties, when distances are expressed in units of mean free paths for gamma rays with initial energies well above that where photoelectric effects are important (i.e E>a few 10's of keV). This enables some simplifications to be made in both theoretical and experimentally derived results (Berger 1957(90), Clifford and Wait 1966(91)).

As a result of these studies ground correction factors ($K(\mu\rho,\mu r,h,E)$) have been derived for a point source in air at or very close to the ground surface (Chpt. 4.5.12 (57)). These are intended to correct the point source build-up factors derived for an infinite homogeneous medium for the effects of the scattering and absorption of the ground. Some general properties of these correction factors are described below.

When the receptor point is close to the ground and is well removed from the source, say $\mu\rho<1.5$, then the correction factor approaches one half. This represents the long range probability for photons travelling close to the boundary,

which go direct to the locality of the receptor, being in either the dense ground or much less dense air. Any photons which start travelling close to the surface in the dense medium are rapidly attenuated compared to those in the less dense medium, for one distance scale. Hence, given a source which emits uniformly in all directions, only those original photons travelling close to the surface in the less dense medium will reach a distant receptor near the ground.

In the case where the receptor and point source, on the ground, are very close another important effect has been observed. Within this region back-scattering of photons, initially emitted into the dense medium, can increase the exposure rate at the receptor. Detailed differences very near to the source can be caused by different theoretical and experimental devices to avoid problems of representing the surface and the finite size of real sources.

In the region within one tenth of a mean free path in air the ground correction factors (K) can be determined if the appropriate build-up factors and scattering factors (K_s) are known. The formula below is used:

(A.5) $$K(\mu\rho,\mu h,E) = ((B(\mu r,E)-1).K_s(\mu\rho,\mu h,E)+1)/B(\mu r,E),$$

which is derived by a consideration of the direct and scattered fluxs in this region (Chpt. 4.5.3.2 (57)). The dependence of these ground correction factors on the short range build-up factors is the reason why a quadratic formula was used at short distances in this development stage. The infinite medium

build-up factors are close to unity in this region, so the ground correction factors are quite sensitive to these values as the factors K_s become large very close to the source. Once these correction factors have been derived the build-up factors in WEERIE can be used for total exposure calculations.

Values of Ks have been derived for cobolt-60 and Cs-137 sources, which emit gamma rays at about 1.25 MeV and 0.66 MeV respectively (Chpt. 4.5.3.2. (57)). These values are of a similar form when referred to coordinate units of mean free paths in air for the appropriate gamma ray energy. In this region where the source is close to the receptor (say 1 metre which is about 0.01 m.f.p.) the derived values of the ground correction factor can rise to 1.2 or more. These short range values have to be matched to those for longer ranges taken directly from a graph for source photons of mean energy 1.25 MeV (i.e. Co^{60}) (Chpt. 4.5.1.3. (57)). Typically ground correction factors could be expected to be accurate to about 7% in the exposure estimates.

Hence the ground correction factors can be introduced into equation A.4 to formally define the final exposure flux N_g^E as,

$$(A.6) \quad N_g^E dS = dS \sum_{n=1}^{N} (S_n . B(\mu r_n, E) . K(\mu\rho, h, E) . \exp(-\mu rn)) / (4\pi r_n^2),$$

where N is a cut-off value to any numerical estimate.

Section A1.3. Defining a grid for numerical ground gamma exposure estimates.

Three considerations are important in the choice of a grid

to esimate numerically external ground gamma exposures. Firstly the grid cells have to represent reasonably well the gamma emitting deposit within their boundaries which can be defined either in plane polar or cartesian coordinate systems. Secondly the distance at which the numerical integration procedure is terminated has to be assessed for its effect on the overall accuracy of the method. Both these points will have to account for the finite dimensions of a plume in WEERIE and the resulting contamination patterns. Lastly the computing time taken by the numerical method must be minimised once a reasonable level of accuracy has been reached.

During the initial development and testing of the routine on the uniform infinite smooth plane deposit the point symmetry properties of this case could be used to most advantage by a grid of cells defined by concentric circles cutting radii emanating from a point in the plane which is immediately below the receptor. A cartesian grid would be more useful in the final form, so as to match the axial and crosswind characteristics of the deposit left by a plume dispersing in the atmosphere. Both these types of grids were used in the initial development of this routine.

The next step was to assess the properties of the exposure flux from the deposited material, as given in equation A.5. From the geometric solid angle and the expoential attenuation the function representing the main trend of the direct exposure flux is monotonically decreasing, which should present no pathological problems to the numerical integration over the smooth plane of uniform contamination.

These two terms in the flux can be evaluated immediately below the receptor and at some larger distances, with the results:

(A.6) $T(\mu r)=EXP(-\mu r)/(\mu r)^2$, (a) $T(0.01)=10^4$; (b) $T(0.1)=90$ and (c) $T(4)=2.0\ 10^{-3}$.

These values show the very rapid decrease of the direct gamma exposure with increasing source-receptor separation.

The build-up factors (B) only deviate slightly from unity within 1 m.f.p. of the source, but approach a value of order ten at greater distances so diminishing the rate of decrease of this exposure flux. This represents the increased component of scattered radiation (sky shine) produced at large distances from the source. The ground correction factors (K) tend to enhance the importance of short range contributions from the deposited activity, as these are greater than unity close to the source, and decrease to one half within a few m.f.p.'s, as described in the previous section. Hence the trend shown by the values in equation A.6 is not significantly altered by the application of both infinite medium build-up factors and appropriate ground correction factors.

This characteristic of part of equation A.5 has to be considered when deciding on the grid delimeters which define the point source strengths (S_n) in the form,

(A.7) $$S_n = A_n.w,$$

where w = uniform contamination level and A_n = area of the n^{th} grid cell. As each cell is represented by a point source the differences from the contributions at the extremes of a cell

should be averaged out by the position of the point source. This is particularly important close to the receptor where the function "T" is changing most rapidly. Hence the smallest grid cells were concentrated close to the receptor and a gradual progression to greater cell dimensions was made at larger source-receptor separations.

An annular grid was used initially to determine a set of radial delimeters, A and B in figure A.1, for the numerical integration, where the source was placed at the mid-radius of each annulus. The number of delimeters were increased so that the following conditions held: i. None of the m annuli contribute more than a fraction 2/m to the total exposure flux;

ii. The most distant annulus contributes less than 1% of the total exposure flux;

iii. No significant change in the total exposure flux is produced when each of the annuli is halved to produce a set of 2m annuli.

The first of the above conditions primarily limits the size of the grid cells immediately below the receptor. The third condition also has this effect but confirms that each point source reasonably represents an average contribution from the corresponding grid cell. This last condition helps to define the delimeters of source cell areas at all distances from the receptor.

The second of the above conditions deals with the termination of the numerical integration. This should be at a distance where the exposure flux arising from more distant sources if negligible compared to the error (ε) of the method (ie $\varepsilon < 10\%$)½ The outer radius of the uniform plane deposit defined by this method was four mean free paths in air (i.e. 400 m. for E = 0.6 MeV and about 1 km for photons in Sidebotham energy groups well above 2 MeV). These distances correspond roughly with some of the large areas, such as fields, typical of the UK, which is more critical than the effect of the curvature of the Earth.

Curtailing the numerical integration at this distance from the receptor one metre above the smooth plane of uniform contamination may have to be reviewed if a significantly higher exposure point was used. In this case the ground correction factors would have to be modified for the new height of the receptor above the deposit. The angular flux distribution would change, losing the sharp peak due to photons travelling horizontally which is a characteristic of a receptor close to the ground. Generally there would be larger contributions from more distant portions of the deposit for receptors well above this plane.

The point sources can be located either at the mid-point of the annuli or at the centroid where these horizontal distances (ρ_n) can be defined along with the source strengths as:

(A.8) (a) mid-point, $\rho_n^{mp} = (a_n + a_{n-1})/2$

(b) centroid, $\rho_n^{c} = (2/3).(a_n.a_{n-1} + a_n^2 + a_{n-1}^2)$

and

(A.9) $$S_n = \pi.(a_n^2 - a_{n-1}^2), \quad \text{where } a_0 = 0.$$

An inspection of these two sets of receptor-source distances shows that the centroid set are systematically greater than those of the mid-points for the same delimeters, as

(A.10) $$\rho_n^{mp} - \rho_n^{c} = \frac{-(a_{n-1}-a_n)^2}{6(a_n+a_{n-1})}.$$

This difference is larger for coarse grids, particularly close to the receptor where any differences most readily affect the exposure calculation.

Table A.1 shows values of the derived exposure flux, using equation A.5 out to 4 mfp's with a uniform contamination level of one photon per second per unit area. Both mid-point and centroid source locations are used in a coarse annular grid and a fine annular grid, produced by inserting an extra delimeter at the mid-point of every coarse annulus, so doubling the number of annuli. These values show that the centroid source points systematically underestimate the exposure flux relative to the value from the set of mid-point sources. As expected the finer grids are in closer agreement than the coarse grids. This suggests that the mid-point values are closer to a true estimate for the exposure flux from a plane

APPENDIX A

Table A.1 Exposure flux values for four plane polar sample grids

GRID (location of point source)	EXPOSURE FLUX (E=0.66 MeV, μ=9.4 $10^{-3}m^{-1}$)
MIDPOINT	
coarse	2.82
fine	2.79
CENTROID	
coarse	2.58
fine	2.72
.....	
mean of four	2.73

of uniform contamination, where the centroid set tends to be optimistic. Also the set of mid-point sources appears to satisfy the third convergence criterion better than the centroid set. The extreme difference between the numerically derived results in table A.1 is 10% which is roughly equal to the size of errors expected by using both build-up and ground correction factors, and the deviation about the mean is 3%. The mid-point grid sources may be slightly pessimistic, to about 3% above a more accurate mean estimate.

Next a cartesian grid was introduced to assess this flux from a uniform deposit emitting gamma rays. The delimeters are defined such that these boundary lines cross the x and y axes at the same points as the concentric circles used to define the plane polar grid, where this is shown in figure A.2. Hence the outer plane polar delimeter is a circle inscribed within the outer square delimeter of the cartesian grid. When a fine cartesian grid is produced the number of point sources is increased by a factor of four, which is directly reflected in computing costs. The horizontal source-receptor separations for the cartesian grid is given, for delimeters a_i and b_i along the x and y axes respectively, as below:

(A.11)
$$\rho_{i,j} = \begin{cases} \left(\left(\left(a_i+a_{i-1}\right)/2\right)^2+\left(\left(b_j+b_{j-1}\right)/2\right)^2\right)^{\frac{1}{2}} & i \neq j \\ \left(a_i+a_{i-1}\right)/(2)^{\frac{1}{2}} & i = j \end{cases}$$

The values of $\rho_{i,i}$ are a factor of $2^{\frac{1}{2}}$ greater than the set of values for the mid-point sources in the plane polar grid. This

FIGURE A.2 Diagram showing the sample points defined by a cartesian grid and a plane polar grid relative to a plume axis.

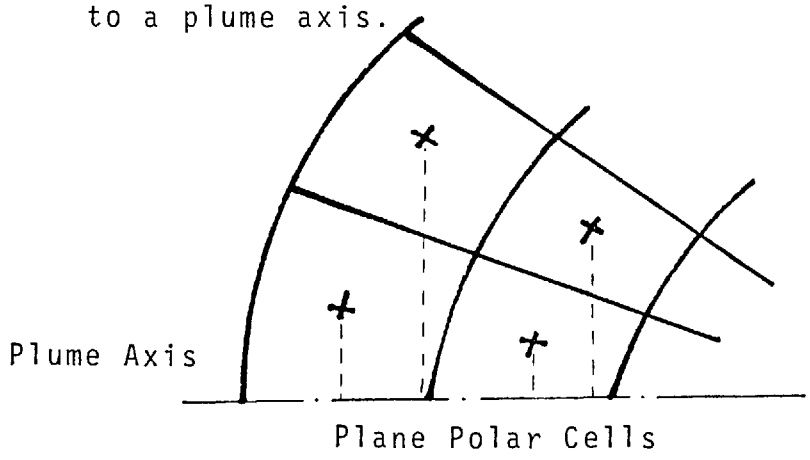

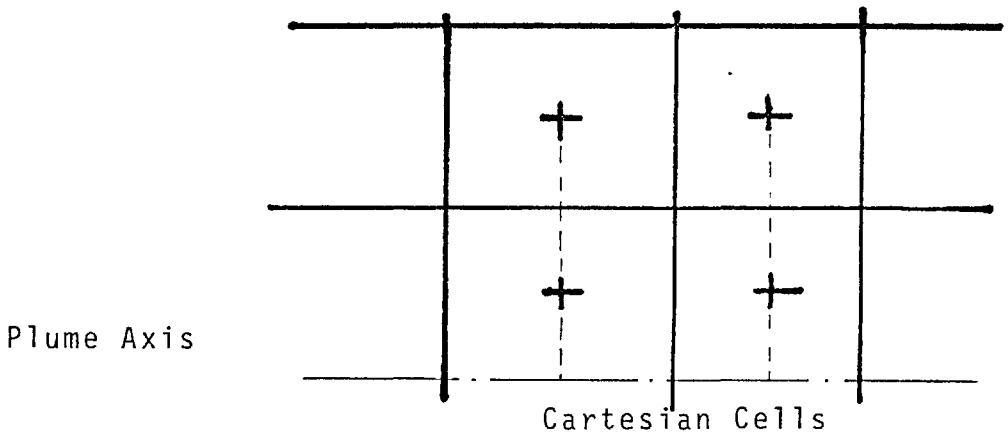

led to a second set of cartesian delimerers which were reduced by a factor of $2^{\frac{1}{2}}$ so necessitating more delimeters to be introduced to retain the same cut-off distance.

The resulting exposure fluxes from these cartesian grids are given in table A.2, again for a unit emission rate from a uniform infinite source on a smooth plane. These results are within a range of about 3% which shows good agreement. The scaling down modification to the coarse grid does not produce as great a difference as conversion to a fine cartesian grid, produced by halving the size of cells along both axes.

The seven results from tables A.1 and A.2 produce a mean deviation of about 2% which is well within the expected error band of the method. The coarse cartesian grid should be of sufficient accuracy for use in WEERIE, although it could cause a slight systematic underestimate as it is just below the mean exposure flux for this case of a receptor one metre above an infinite uniform smooth plane deposit of unit gamma activity.

The energy dependence of these results was investigated by considering source photons at 1.25 MeV and 0.66 MeV. These energies bracket 1 MeV which has been shown to be roughly the average gamma ray energy for a wide range of mixed fission products ((59), (13)). This entailed using different build-up factors at all mean free path distances. Minor adjustments were made for the ground correction factors at very short distances. The numerical integration was extended to four mean free paths in both cases, where the most distant point

APPENDIX A

Table A.2 Exposure flux values for three cartesian sample grids

GRID	EXPOSURE FLUX (E=0.66 MeV, $\mu = 9.4\ 10^{-3}\ m^{-1}$)
coarse	2.66
fine	2.75
scaled down	
coarse ($2^{-\frac{1}{2}}$)	2.68
mean of three	2.70

sources still contributedless than 1% of the total exposure flux.

As the ground correction factors in the numerical procedure are paramet-rised in distance units of mean free paths and they are of similar form at these two energies few differences were expected. The energy dependent build-up factors are different, but as the exposure flux is primarily due to sources within 0.5 mfp's of the receptor no significant changes are produced. The effect of using ground correction factors for the receptor 0.01 mfp off the ground, in this energy range, rather than one metre is also not significant.

The small changes in the exposure flux produced by using factors for 0.66 MeV and 1.25 MeV gamma rays are less than those produced by different grids for the numerical integration. This reflects the effects of a receptor point very close to the ground so that only sources with a small separation from the receptor are important to the overall exposure flux. The behaviour in this energy range should permit reasonable estimates of this quantity for mixed fission product deposits modelled in WEERIE.

Section A1.4. Conversion of the build-up factor flux results to exposure rates.

An exposure flux (N_g^E) has been calculated which has to be converted to an exposure rate in air under standard conditions.

The intention of this build-up factor method is to calculate a flux in terms of photons of source energy E which would give

the same exposure as that measured in practice. Compton scattering and, above 1.05 MeV, pair production degrade the energy of the photons which finally reach the receptor and deposit energy at this location. Absorption of photons along the path can also reduce the final exposure. Hence the actual flux consists of a spectrum of photons with energies not exceeding that of the photons leaving the source. The effectiveness of this scattered component in producing exposures is represented by the deviation from unity of the energy deposition point source build-up factors.

An exposure rate (G(E)) can be defined for this exposure flux by applying an energy dependent factor (F(E)), as below:

(A.12a) $$G(E) = F(E) \cdot N_g^E \text{ Roentgens/second}$$

where (A.12b) $$F(E) = \frac{E(\text{MeV/photon}) \cdot 1.6\ 10^{-6}\ \text{erg/MeV} \cdot \mu_a\ (\text{cm}^2/\text{g})}{98.7\ (\text{erg per (g.Roentgen)})}$$

In WEERIE twelve Sidebotam energy groups (See table A.3) are used so that only twelve values of the conversion factor are defined, one at each of the characteristic energies. These kernal energies were chosen as being "usefully representative of the major gamma emitting fission products". Inaccuracies due to this representation of the energy spectrum of the source photons is expected to be small for releases containing a wide selection of fission products.

These exposure rates can not be directly interpreted as dose rates for particular organs or tissues. If these detailed dose rates were required more specialised routines would be

APPENDIX A

Table A.3 Energy structure of Sidebotham's twelve groups for gamma rays emitted by fission products

Group Number	Photon Energy (MeV) of group		
	Lower bound	Upper bound	Group value
1	(0.0)	0.39	0.27
2	0.39	0.64	0.51
3	0.64	0.88	0.76
4	0.88	1.28	1.00
5	1.28	1.88	1.55
6	1.88	2.35	2.20
7	2.35	2.70	2.50
8	2.70	3.20	2.90
9	3.20	4.0	3.5
10	4.0	4.95	4.5
11	4.95	5.80	5.4
12	5.80	above 5.8	6.2

needed which dealt with the relationship between a "phantom", representing a standard man, and the particular activity released((33), (9)).

An exposure rate can now be calculated from numerical estimates of the exposure flux for a receptor one metre above an infinite uniform smooth plane of gamma emitting material.

Section A1.5. Comparison of exposures from an infinite uniform smooth plane deposit of gamma emitting activity.

A smooth infinite plane surface, with a uniform contamination of caesium-137, is a case which has been studied by several workers. This should enable the results of the routine described in the appendix to be compared to other published results.

The long lived Cs137 isotope ($t_{\frac{1}{2}}$=30 y) has a short lived daughter $Ba137^{m}$ ($t_{\frac{1}{2}}$=2.5 mins.), and the decay scheme is such that a gamma ray of energy 0.66 MeV is produced by this barium isotope in 84.5% of all Cs137 decays (Lederer 1967(92), Tobias 1972(93)). These properties are used to predict the level of ground contamination by Cs137 which would produce a dose one metre above the ground, of 0.5 rad in air during the first year after deposition. A time integration is made over the decaying exposure rate for this year to derive the total exposure, assuming there are no redistribution processes, such as weathering or decontamination, affecting the deposit. Ground roughness is not considered in this ideal case of a smooth plane. The flux to exposure rate factor for this particular

APPENDIX A

Table A.4 Level of uniform Caesium-137 contamination on a smooth plane delivering a given dose in air during the first year after deposition

REFERENCE	INITIAL GROUND CONTAMINATION (Micro Ci/m^2)
French (1965) (59)	5.96
Beattie and Bryant (1970) (53)	6.29
Slade (ed. 1968) (45)	6.05
Corbett (1977) (63)	6.39
present work	6.12

gamma ray energy was interpolated from the available data.

Table A.4 displays the initial Cs137 activity levels (micro Ci/m^2) derived from several publications alongside the results from an application of the routine developed in this work. All the results in this table refer to an exposure point one metre above the ground, except for that due to French (1965,(59)) who used a Monte Carlo method with a receptor three feet above the smooth infinite plane. The result due to Corbett (1977,(63)) has had the effects of ground roughness and weathering factors removed. The deviation of these results about the mean, 6.16 micro Ci/m^2, is less than 3% of this value, and the spread of the extreme results is less than 7%.

These results show that the routine developed represents reasonably the exposure one metre above an infinite uniform smooth plane deposit of long lived gamma emitting activity. This routine can be incorporated into WEERIE with appropriate modifications to allow for the two dimensional dependence of the patterns of deposited activity (see chapter 3).

APPENDIX B

External dose due to beta radiation from ground deposits using Loevingers formula

Experimental data was used by Loevinger to derive empirical formulae to describe the energy deposition in solids and gases for beta particles resulting from nuclear beta decay. Point sources were described in this manner and the results were then extended to a thin plane source by appropriate integration (see (73), (76)).

The dose rate for an infinite smooth plane source of short range beta particles is given below:

(B.1) (a) $\dot{D}_\beta\ (x,y,d) = K(E_o,\bar{E}_\beta).w(x,y).f(d,E_o,\bar{E}_\beta)$ rads/second;

(b) $w(x,y)$ = deposited activity in Ci/m^2;

(c) $$f(d,E_o,\bar{E}_\beta) = \begin{cases} c(1+\ln(c/d\nu)-EXP(1-d\nu/c)) + EXP(1-\nu d) & d<c/\nu \\ EXP\ (1-d\nu) \qquad \text{for } d>c/\nu \end{cases}$$

(d) $K(E_o,\bar{E}_\beta)=0.0297.\bar{E}_\beta.\alpha.\nu$ $((rads/sec.)/(Ci/m^2))$

(e) $\alpha=(c^2.(3-e)+e)^{-1}$

(f) $\nu = 18.6(2-\bar{E}_\beta/\bar{E}^*_\beta)/(E_o-0.036)^{1.37}\ cm^2g^{-1}$

(effective beta attenuation coefficient in air or soft tissue)

(g) d = depth of dry air between the dose point and the plane (g/cm^2), and E_o, $\bar{E}_\beta$ and $\bar{E}^*_\beta$ are, respectively, the peak, mean and theoretical mean, for allowed transitions, beta energies for

a given decay. As the apparent beta attenuation coefficient (ν) is assumed to be valid for air and soft tissue the above expression can be used for doses in either medium. The beta sources in WEERIE are such that conversion electrons, effectively releasing monoenergetic beta particles, and rarer transitions are neglected as not being of significance to total exposures from fission products and would need separate evaluation of these minor dose rates.

The value of α is derived from the integration and normalisation for this formula. The value of c was given as being energy dependent, where for a point source it had the form,

(B.2) $$c = 3.11.EXP(-0.55\ E_o);$$

where the maximum value is

(B.3) $$C = (e\ /\ (3-e))^{\frac{1}{2}} = 3.11.$$

For dosimetry purposes, in air or soft tissue, involving plane sources this can be adequately represented by the values in table B.1, as the dose rate is not very sensitive to this parameter. No explicit dependence on the properties of the medium are given for this parameter, where the presence of high Z material (Z>20) can be significant (70).

The given form of the effective beta attenuation coefficient (ν) is also restricted to air and soft tissue. This relies on the peak beta energy (E_o) and the deviation of the mean beta energy from that expected for an allowed beta transition. This ratio should be unity for an allowed transition, but for

APPENDIX B

Table B.1 Energy dependence of parameters in Loevinger's formula

Range of peak beta energies (MeV)		c	α
Upper limit	Lower Limit		
0.17	0.036	3	0.190
0.5	0.17	2	0.260
1.5	0.5	1.5	0.297
approx. 3	1.5	1	0.333

strontium-90 it is 1.17. Most of the beta decays exhibited by the fission products in WEERIE are allowed transitions (10), (13)) so $\bar{E}_\beta/\bar{E}^*_\beta$ has been taken as unity for all isotopes, which should not introduce excessive inaccuracies.

The relationship between the mean beta energy and the peak value has been given roughly as:

(B.4) $$\bar{E}_\beta = a.E_o$$

where a is in the range 0.3 to 0.45 for the energy range from 0.1 MeV to 3 MeV. ICRP-2 (29) has given a more definite formula for this relationship as:

(B.5) $$\bar{E}_\beta = 0.33E_o(1-E_o^{\frac{1}{2}}/4)(1-Z^{\frac{1}{2}}/50).$$

Only the mean beta energies are avilable in WEERIE, as used in the estimation of cloud beta exposures. These have been derived from the intensities (I_β) of all beta decay sequences which each fission product can exhibit i.e.

(B.6) $$\bar{E}_\beta \text{ (isotope j)} = \sum_{all\ i} \bar{E}_{\beta i} \cdot I_{\beta i}$$

To derive an approximate value of E_o for use in defining the attenuation coefficient (ν), the simple relationship,

(B.7) $$E_o = 3\bar{E}_\beta$$

was used. This is expected to reduce the accuracy of the final beta exposure rate, but should still provide a reasonable estimate from which the importance of external ground beta doses can be assessed.

Given the density of dry air at STP the depth (d) required in this application can be given as 0.129 g/cm^2. A few characteristics of equation B.1 can be discussed using this value of d. The ratio c/(dν) is unity at a peak beta energy of about 1.45 MeV, but as c reduces by a third above 1.5 MeV c/(dν) is unity again at 1.93 MeV. The term in the beta dose rate, $\nu f(E_o,\overline{E}_\beta,d)$ when d>c/ν, can be expected to have a maximum at a peak beta energy of 1.9 MeV, where the beta dose rate could have a maximum at slightly higher energies. Owing to the stepped form of the parameter c the form of these two functions become complicated. The complete function which holds all the energy dependencies in equation B.1 is shown in figure B.1, plotted against the peak beta decay energy, and shows a flat response between 2 MeV and 3 MeV compared to values below 0.8 MeV. The maximum close to a peak beta energy of 2 MeV in the function $\nu.f(E_o,\overline{E}_\beta,d)$ can be observed from the curve in figure B.2.

For very large beta decay energies the logarithmic term in the function f is dominant. In the region where

(B.8) $$\nu d/c=1-\varepsilon$$

and ε is small, the function f reduces to

(B.9) $$f(\nu d/c = 1-\varepsilon)=EX\ P(1-c(1-\varepsilon)) + c\sum_{n=3}^{\infty}(-1)^{n-1}.\varepsilon^{n}.((n-1)!-1)/n!.$$

Hence for small ε the condition at νd/c>1 still holds approximately, and due to the particular form of this relationship is still dominant for :E_o=3 MeV, c=1,νd/c=0.545 so that $c(1+\ln(c/(\nu d))-EXP(1-\nu d/c))/EXP(1-\nu d)=3.10^{-2}/1.5$. As the upper

FIGURE B.1 Dependence on peak beta decay energy of Loevinger's formula for energy deposition in air by beta rays one metre above a smooth plane of uniform contamination.

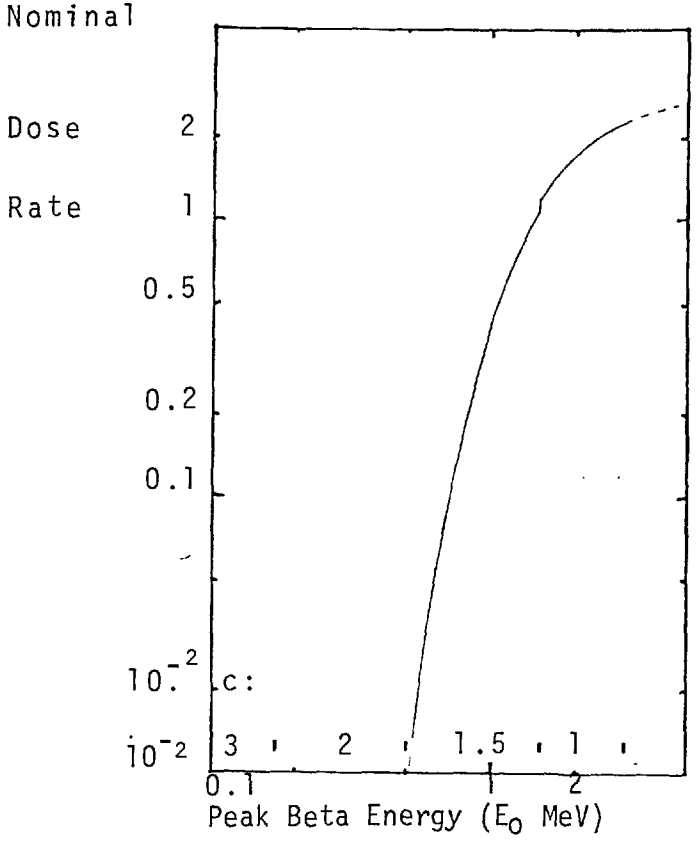

FIGURE B.2 Dependence on peak beta decay energy of Loevinger's prediction of beta energy deposition in air per unit of mean source beta energy one metre above a smooth plane of uniform contamination.

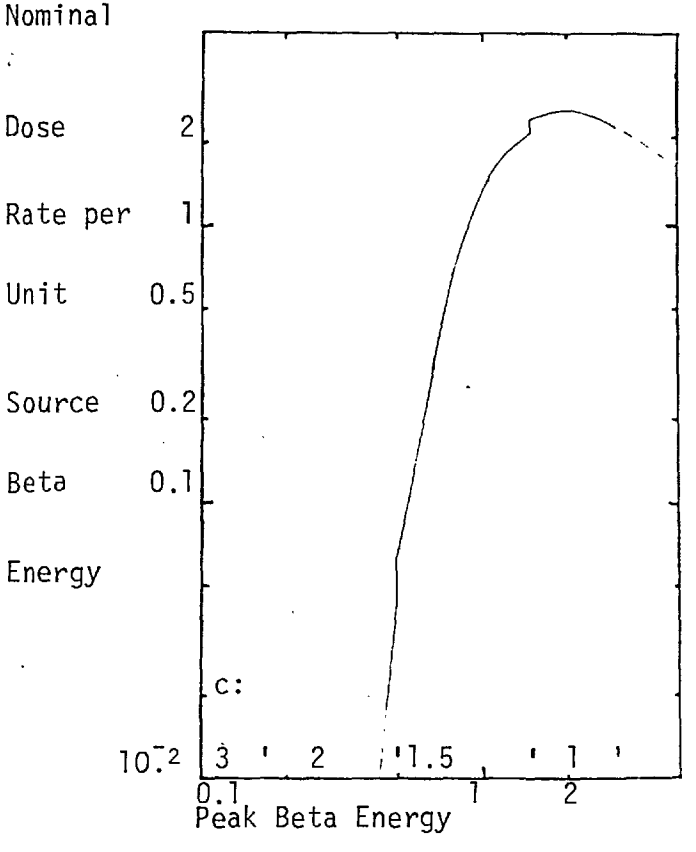

limit of this formula is for a peak beta decay energy of about 3 MeV, the logarithmic term is not dominant in the range considered. At low energies, and large ν, the dependence reverts to the simple exponential decrease. This represents very low energy beta emitters not giving any dose one metre from the plane source due to severe attenuation by the air, as shown in figure B.1.

The use of a single apparent attenuation coefficient (ν) for a complete beta spectrum is a gross approximation except for the energy range 5 MeV to 0.5 MeV in light media ($Z<13$) (70). The medium here, air, can be described as consisting of material of low atomic number ($Z(O/N) = 8/7$), so satisfying the latter condition. In WEERIE the peak beta decay energies for significant fission products are within the above range, where few exceed 3 MeV beyond which Loevinger's formula becomes progressively inaccurate (see chapter 3). All low energy beta emitters are effectively surpressed by one metre of air and would contribute very little to the total beta dose rate above a plane of mixed fission product beta activity.

The wide range of beta emitters which would be considered by this method in any estimate of a dose rate one metre above a plane deposit of mixed fission products should be adequately covered by this description of the dose delivered given its radiological significance. One additional source of uncertainty which has to be noted is that the atmospheric pressure and humidity varies, but the fixed value of the depth of air (d) used here should be representative of many dry conditions (Chpt. 7 of (45)).

APPENDIX C

	PAGE
1: (60)	332
2: (33)	344
3: Review article	345

Annals of Nuclear Energy, Vol. 6, pp. 91–102
0306-4549/79/0201-0091$02.00/0

CALCULATION OF THE DEPLETION OF A RADIOACTIVE PLUME IN THE ATMOSPHERE AND SUBSEQUENT EXPOSURE DUE TO DEPOSITED ACTIVITY

S. J. STRACHAN and A. J. H. GODDARD
Department of Mechanical Engineering, Nuclear Power Section, Imperial College of Science and Technology, South Kensington, London SW7 2BX

(*Received* 22 *September* 1978)

Abstract—An efficient method has been developed for calculating the depletion, by dry deposition and washout to the ground, from a plume of fission products in the atmosphere, and for determining the isotopic composition of resulting gamma and beta activities in the ground deposit at any selected point downwind. By integration over the pattern of material on the ground, gamma and beta exposure rates may be derived as a function of the ageing time of the deposit. Elements in the plume are assigned to one of up to four 'groups'; elements within each group being assigned a particular deposition velocity and washout coefficient.

Calculations have been performed, for a notional MAGNOX depressurization accident, which illustrate the sensitivity of ground gamma spectra and exposure rate to the use of isotope-dependent deposition velocities. Circumstances under which it may be necessary to perform a full two-dimensional integration over the pattern of material on the ground are discussed.

1. INTRODUCTION

In the safety assessment of nuclear installations it is necessary to be able to predict various properties of material deposited in a pattern on the ground following a hypothetical accidental release of radioactivity to the atmosphere. These properties would include near-ground gamma-ray spectral and total dose rates, and the activities of particular isotopes in the deposit as a function of ageing time. Estimated gamma dose commitments and isotope activities might be considered in relation to Derived Emergency Reference Levels which are intended to be guides to those responsible for initiating counter measures should an accidental release occur.

In this paper, modifications and extensions are described which have been made to the environmental assessment computer program WEERIE (Clarke, 1973a, b) to permit a more detailed treatment of a plume in the atmosphere and of the associated deposited material, with the main objective being to calculate gamma-ray exposure in the contaminated area. Improvements were necessary in the deposition and plume travel models incorporated in WEERIE, in order to obtain a more accurate description of deposited material, which is the source term for all ground gamma calculations. Element-dependent deposition has been incorporated into the plume depletion model and detailed allowance made for the effects of the production of isotopes by radioactive decay as the plume travels downwind. Washout by rain has also been included as a depletion process.

Gamma-ray exposure rates are calculated at 1 m above the deposit of mixed fission products, where the two-dimensional variations of the ground concentration pattern of gamma-ray sources is taken account of by energy dependent integration. Twelve groups (Sidebotham, 1971) are used to describe the gamma spectral exposure. Gross beta-ray exposure rates are calculated using local concentrations. The deposit may be aged to determine the time dependence of these exposure rates.

The significance of the refinements described here may be illustrated by the results of a representative calculation. A notional MAGNOX depressurization accident with single channel meltdown has been selected and used to illustrate the relative magnitudes of ground gamma and beta dose commitments compared with those incurred via other routes such as inhalation and cloud gamma. Two technical aspects of the present study are illustrated in detail using this example: firstly, the effect upon ground gamma spectral and total exposure rate of using isotope-dependent deposition velocities and the importance, in this respect, of the halogen release fraction. Secondly, conditions are discussed under which a full spatial integration over the pattern of deposited activity on the

ground may be necessary when calculating the ground gamma exposure rate, rather than relying upon the infinite plane approximation.

2. IMPROVED TRAVEL AND DEPLETION MODEL

2.1. *The WEERIE program*

The basic WEERIE program models a wide range of factors affecting the release to the atmosphere of fission products from reactors under normal or operating conditions; the most important of these factors are:

(i) Fuel fission product inventory for a particular fuel irradiation history, using the routine FISP (Clarke and Utting, 1970).

(ii) Element-dependent release from fuel and the time-dependence of the release to the containment.

(iii) Plate-out and re-suspension of isotopes within coolant circuit and containment.

(iv) Filtration and time-dependence of leakage from containment to the environment.

(v) Atmospheric dispersion, under particular conditions of wind speed and atmospheric stability, according to a Gaussian model.

(vi) Radioactive decay and transmutation during leakage and travel downwind.

(vii) Depletion of the plume by deposition as discussed below.

(viii) Time-integrated organ doses and cloud beta doses calculated from local concentrations at the point of interest.

(ix) Time-integrated cloud gamma exposure calculated by integrating numerically over the plume volume.

With a corresponding increase in computing time, the time period of the release from the fuel may be divided up and time-integrated doses for these subdivisions calculated separately.

As the initial aim was to estimate inhalation and cloud doses (Hoffman *et al.*, 1977; Clarke 1973a,b), deposition was considered solely as a factor depleting cloud concentrations, and only a single deposition velocity was applied to all isotopes in a single calculation. One overall deposition velocity cannot describe accurately the depletion of individual isotopes from the plume, especially when daughter products often have a different deposition rate from their parents, such as ^{88}Kr–^{88}Rb and ^{132}Te–^{132}I. In this latter case the use of an iodine isotope's deposition velocity, with no re-suspension, decreases ^{132}I ground concentrations at longer distances downwind by overestimating the deposition of the parent ^{132}Te isotope. The use of one deposition velocity typical of aerosols or chemically active material would lead to an underestimate of the plume concentrations of non-depositing inert gases and their daughter radionuclides.

The original WEERIE program applied the source depletion fraction $Q^*(x, 0)$ to all isotopes after decay due to travel from 0 to x m downwind. $Q^*(x, 0)$ is evaluated according to:

$$Q^*(x,0) = \exp\left[-\left(\frac{2}{\pi}\right)^{1/2} \cdot \frac{v_g}{u} \int_0^x \frac{\exp(-\frac{1}{2}(h/\sigma_z(p))^2)\,dp}{\sigma_z(p)} \right] \quad (1)$$

(Slade, 1968; Hosker, 1973), where $\sigma_z(x)$ is the vertical (Gaussian) dispersion parameter and h the effective height of release.

2.2. *Improvements in the model*

An improved treatment may be obtained if depletion and radioactive decay are more closely related in the calculation, allowing element-dependent deposition velocities to be used. This can be achieved by calculating the average distance (X_n) a daughter isotope travels, where this radionuclide at least reaches

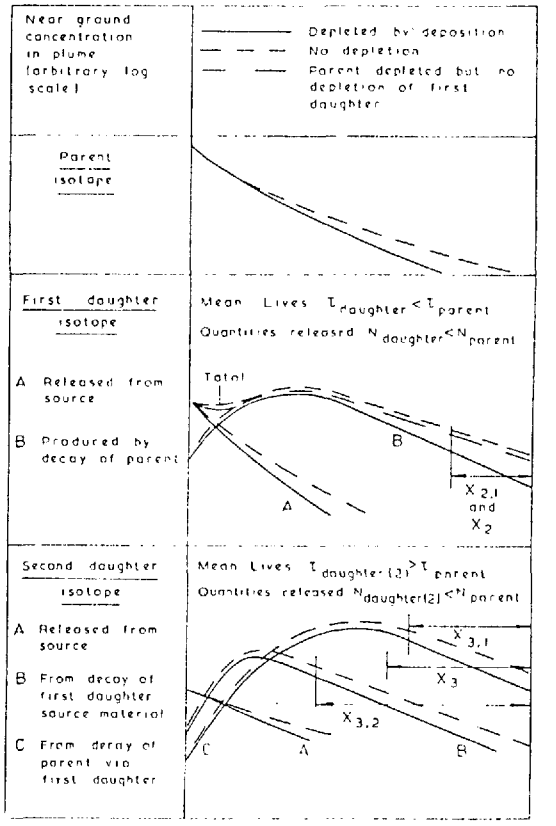

Fig. 1. Schematic representation of the downwind travel, subject to decay and deposition, of a parent isotope and two daughters showing also the mean travel distances $X_{n,m}$ and weighted mean distance X_n.

the downwind distance of interest (x m) after production in the plume.

Up to six isotopes can be present in a decay chain of the routine FISP which defines the isotopes used in WEERIE. The n-th isotope in a decay chain may have contributions to its atmospheric concentration from decays of the original released amounts of its $n-1$ precursors, as well as the amount of the n-th isotope released at the source of the plume. The average distance travelled, $X_{n,m}$, of that quantity of the n-th isotope produced within the plume before at least reaching a given distance x m downwind, will depend on the particular initiating precursor m. For example this mean distance $X_{n,1}$, travelled by atoms of the n-th isotope produced from material of the first isotope in the decay chain is expected to be different from the mean distance $X_{n,n-1}$ travelled by isotope n atoms generated from the released $(n-1)$-th isotopes' material. Figure 1 illustrates average distances travelled for a parent isotope and two daughters.

WEERIE generally uses analytical formulae for speed of calculation and the values $X_{n,m}$ are evaluated in this mode. The mean values $X_{n,m}$ have to be calculated for travel of the n-th isotope originating from the m-th isotope in the decay chain, and then a weighted mean value, X_n, found from the different source isotopes.

The probability of a single isotope reaching a distance x m downwind, allowing for radioactive decay, is $f(x, \lambda_i) = \exp(-\lambda_i \cdot x/u)$, where λ_i is the radioactive decay constant of the isotope and u m s^{-1} is the mean windspeed. The probability of this isotope having reached x m downwind then decaying within the next dx m is $F(x) = f(x, \lambda_i^*)\lambda_i^* \cdot \mathrm{d}x$, where $\lambda^* = \lambda/u$. Hence for a decay sequence originating in the m-th isotope the probability of the n-th isotope at least reaching a distance xm downwind is:

$$
\begin{aligned}
&P(x_m, x_{m+1}, \ldots, x_{n-1}, n, m) \cdot \mathrm{d}x_m, \mathrm{d}x_{m+1}, \ldots, \mathrm{d}x_{n-1} \\
&\quad = f(x_m, \lambda_m^*) \cdot \lambda_m^* \, \mathrm{d}x_m \\
&\qquad \times f(x_{m+1} - x_m, \lambda_{m+1}^*) \cdot \lambda_{m+1}^* \, \mathrm{d}x_{m+1} \cdots \\
&\qquad \times f(x_{n-1} - x_{n-2}, \lambda_{n-1}^*) \cdot \lambda_{n-1}^* \, \mathrm{d}x_{n-1} \\
&\qquad \times \exp(-\lambda_n^* \cdot (x - x_{n-1})) \\
&\quad = \exp(-x_m(\lambda_m^* - \lambda_{m+1}^*)) \\
&\qquad \times \exp(-x_{m+1}(\lambda_{m+1}^* - \lambda_{m+2}^*)) \cdots \\
&\qquad \times \exp(-x_{n-1} \cdot (\lambda_{n-1}^* - \lambda_n^*)) \\
&\qquad \times \exp(-\lambda_n^* x) \cdot \lambda_m^* \cdots \lambda_{n-1}^* \cdot \mathrm{d}x_m \cdots \mathrm{d}x_{n-1}.
\end{aligned}
$$

where the $(m+1)$-th isotope is formed when $x_m = x_{m+1}$ and decays when $x_{m+1} = x_{m+2}$. The mean value of the distance travelled by the n-th isotope originating from the m-th isotope is then given by equation (2).

$$
X_{n,m} = \frac{\displaystyle\int_{x_m}^{x_{m+1}} \int_{x_{m+1}}^{x_{m+2}} \cdots \int_{x_{n-1}}^{x} (x - x_{n-1}) P(x_m, x_{m+1} \ldots x_{n-1}, n, m) \, \mathrm{d}x_m, \mathrm{d}x_{m+1} \ldots \mathrm{d}x_{n-1}}{\displaystyle\int_{x_m}^{x_{m+1}} \int_{x_{m+1}}^{x_{m+2}} \cdots \int_{x_{n-1}}^{x} P(x_m, x_{m+1} \ldots x_{n-1}, n, m) \, \mathrm{d}x_m, \mathrm{d}x_{m+1} \ldots \mathrm{d}x_{n-1}} \qquad (2)
$$

A final value X_n can then be determined where $X_{n,m}$ are weighted in proportion to the quantity of isotope m released at the source. A cut off is used in practice, where the earliest precursor p which contributes at least 1 in 10^4 of the atoms of the n-th isotope and all subsequent precursors $p+1$ to $n-1$ are included in the weighting of the mean value of X_n.

The depletion fraction of this material produced in the plume is, on average, as given in equation (3), using K and F defined by equation (1).

$$
\begin{aligned}
Q^*(x, x - X_n) &= \exp\left(-K \int_{x - X_n}^{x} F(p) \, \mathrm{d}p \right) \\
&= \exp\left[-K \int_0^{x} F(p) \, \mathrm{d}p + K \int_0^{x - X_n} F(p) \, \mathrm{d}p \right] \\
&= Q^*(x, 0) \cdot Q^*(x - X_n, 0). \qquad (3)
\end{aligned}
$$

A set of $Q^*(x, 0)$ is calculated, then stored in grid form for different deposition velocities in the program, with an associated Lagrangian interpolation routine.

The analytical formulae derived from equation (2) rapidly become more complicated as n increases from 2 to 6. When all $\lambda_i^* x \ll 1$, $X_{n,m}$ is determined by terms of order $n-m$ in the series expansion of the exponentials in the relevant formulae, giving the limiting result $X_{n,m} = x/(n-m)$. The program has to test for these limiting cases owing to the finite word length of a digital computer.

With this improved travel model the element-dependent depletion of daughter material formed within the plume is allowed for as each decay chain is evaluated for travel from 0 to x m downwind; the original material released at the source having already been appropriately depleted.

In comparison, the program TIRION 2 (Kaiser, 1976), which also models the consequences of releases of radioactivity, produces time-integrated concentrations on consecutive grid points, allowing first for decay and then for depletion over each grid spacing. WEERIE can produce the time-integrated concentrations at any point in one step, but for execution speed in detailed numerical gamma exposure calculations, a grid of gamma-ray source strengths is estab-

lished. As time-integrated concentrations in air are calculated, the deposited activity at a given distance downwind is produced, after allowing for travel up to that point, by applying the appropriate deposition velocity.

An additional feature of this modified version of WEERIE is that the deposited material at any point within the plume boundaries can be aged, assuming no re-suspension. This allows a study of the time-dependence of ground gamma and beta exposure rates after the passage of the whole or a time segment of the plume generated by this version of WEERIE. The neglect of re-suspension is normally unlikely to lead to any serious underestimation of exposure in the vicinity of the initial deposit.

At present grouped element-dependent deposition is used where elements can be associated with one of, at most, four deposition velocities. This can represent the general range of deposition velocities for individual elements reported in the literature. Dry deposition velocities are not varied with distance, although any changes in the chemical and physical form of the isotopes could affect these depletion rates after release. In addition, element-dependent washout has been incorporated into this deposition model, using a depletion fraction given by $Q^*(t, 0) = \exp(-W \cdot t)$, where W is the washout coefficient (see, for example, Pasquill, 1974). This washout can be stopped after a given time of travel.

The methods described here assume that atmospheric dispersion, both laterally and vertically, may be described by Gaussian functions. Parameters describing this mean dispersion, for example those due to Pasquill (1961) or more recent parameters based upon a detailed description of the boundary layer due to Smith (1973) can be used in the WEERIE program. Building entrainment may be superimposed upon these dispersion coefficients; modelling entrainment at short distances by effective Gaussian coefficients ensures that plume material is fully accounted for in the model.

The source depletion model, defined in equation (1), implies that the assumed vertical form of the concentration distribution is unaffected by deposition even under stable category F conditions. Surface depletion models allow the vertical concentration profile to change owing to loss of material at the ground. A detailed model has been described by Scriven and Fisher (1975). Further comparisons between these two models are given by Horst (1977). Generally these models are in better agreement for lower deposition velocities and shorter travel times. For deposition velocities less than 1 cm/sec ground level concentrations agree to within 10% for at least 2 days' travel time (Draxler and Elliot, 1977). Appropriate modifications to the deposition velocity can be made to allow comparable results to be produced by source and surface depletion models.

Modelling of atmospheric dispersion could be improved by introducing time-dependent meteorology, so allowing dispersion characteristics to change during or after a release. The use of this approach for continuous, operational releases would be of particular interest. For ease of calculation, such a model could employ time-parameterization of all depletion processes. Investigations into the effects of transitory conditions would be necessary in exploring inherent limitations of a simple treatment involving the Gaussian model.

3. External Exposures from Deposited Material

Both ground gamma and beta exposure rates are calculated in this new version of WEERIE, to complement the cloud dose and exposure results. A routine has been written (Strachan, 1978) which yields the gamma exposure rate from a smooth plane deposit of the mixed fission products from the plume, which has a distribution varying downwind and crosswind and, of course, with age. A two-dimensional grid of weighted point sources is used to represent the smooth plane of gamma emitting activity. This grid of integration points is set in terms of gamma-ray mean free paths in air so that off-axis exposure rates can be evaluated. The routine has been suitably adapted for incorporation in WEERIE. The accuracy of off-axis exposure rates is diminished when the dispersion parameters are of a comparable size to the spacing of the integration grid, but this would occur only very close to a point source and at short downwind distances in stable conditions. Building entrainment may, however, broaden the plume (Slade, 1968) at these short distances and alleviate this effect.

Gamma-ray exposure build-up factors for an infinite air medium (Jaeger, 1968) are used in conjunction with correction factors (Jaeger, 1968), (Chilton, 1967) allowing for the scattering and absorbing properties of the ground. Twelve energy groups (Sidebotham, 1971) are employed to evaluate the spectral distribution of the exposure from deposited fission products, as used also in the existing WEERIE cloud gamma routine. The integration of exposure rates, in a given energy group, is stopped at large distances such that contributions from further terms would be negligible compared with the estimated errors in the build-up and ground correction factors.

A comparison of the results of this routine, with previously published results, is given in Table 1. Here

Table 1. Predicted deposited ^{137}Cs activity required to produce a given exposure in air 1 m above a smooth, uniform plane

Reference	^{137}Cs activity ($\mu Ci\ m^{-2}$) to give 0.5 rads in first year
French (3-ft dose point, table 5) (1965)	5.96
Beattie and Bryant (1970)	6.29
Slade (1968)	6.05
Corbett (1977)	6.39
Strachan (1978)	6.12

the initial ^{137}Cs deposited activities which give 0.5 rads in air, during the first year, at 1 m above a smooth infinite uniform plane source of this radionuclide are shown, 84.5% of decays from ^{137}Cs (Tobias, 1972; Lederer *et al.*, 1967) lead to a 0.66 MeV gamma ray from ^{137m}Ba. These results show agreement within the expected accuracies, allowing for some differences in the assumptions of the various calculations. The results of French's calculations (French, 1965), covering a wide energy range, are of a form suitable for use in the program to estimate the infinite deposit ground gamma exposure rates from the local activity. The results of the numerical routine are expected to be more accurate than those based upon an infinite deposit assumption for off-axis exposure points or when the plume dimensions are small compared with the gamma mean free paths in air, within the limits on accuracy discussed above.

Ground roughness can be readily allowed for by two methods:

(i) An overall reduction factor based upon observation.

(ii) The insertion of an extra medium between ground and exposure point in the above calculations, as discussed by Huddleston *et al.* (1965) and Anspaugh *et al.* (1975).

Weathering can be treated by allowing either of the above methods (i) or (ii) to vary with time. This process can be due to re-suspension of the deposited activity, or chemical absorption into the ground (Bryant, 1966) increasing the shielding effects of the ground. A more realistic description may be obtained by using a combination of the above methods.

Beta rays have a much shorter range in air than gamma rays so that knowledge of the local cloud or ground beta activity is sufficient to calculate beta exposures. The formula given by Loevinger (1956) and Loevinger *et al.* (1956) for the beta dose at a given height above a uniform infinite smooth plane deposit is used in this program. This formula may not be the best description of beta exposure but is of sufficient accuracy (Cross, 1967, 1968, 1969; Spencer, 1955) for gross beta calculations over several hundred fission products and their associated ranges of beta energies. Also, this formula can be easily programmed and rapidly executed.

Both the beta and gamma exposures are evaluated at a height of 1 m above the plane of deposited activity, enabling a gross beta/gamma ratio for the deposited material to be estimated. The 1 m of air absorbs much of the beta energy, especially below 0.5 MeV, so that only high energy beta rays penetrate to the exposure point while gamma rays are not strongly attenuated by air and gross beta gamma ratios therefore decrease rapidly with distance from a mixed fission product deposit.

4. APPLICATIONS TO A NOTATIONAL ACCIDENT

4.1. *Description of notional accident parameters*

To demonstrate the use of the methods described in Sections 2 and 3 and to permit a discussion of their importance, a notional MAGNOX depressurization accident has been modelled. The description of the accident must not be taken as definitive but has been derived from various published studies (Clarke, 1973a, b; Macdonald, 1971; Macdonald and Clarke, 1972; Macdonald, 1975). Through modelling the accident, the effect of using element-dependent deposition velocities rather than a single overall value may be studied, as may effects of the finite size of a plume upon ground gamma exposure rates.

It is assumed that 81.2 kg fuel are involved in the single channel (UKAEA, 1972). This has been irradiated at 5 MW/Te to a burn-up of 3500 MWd/Te and time-dependent fluxes and fission fractions have been employed in modelling fission product production (Fitzpatrick, 1976). Build up of isotopes by neutron capture, such as ^{134}Cs, not treated by FISP, can be allowed for by FISP 4 (Beynon, 1973) calculations supplementing this minor limitation in WEERIE's FISP routine. In this case the ^{134}Cs activity released is a tenth of that of ^{137}Cs. Most of the fuel is assumed to be involved within half an hour after reactor shutdown and the release is assumed to be complete after

Table 2. Assumed release fractions for notional MAGNOX depressurization accident (Macdonald, 1971)

Elements	Release fraction
Xe, Kr	1.0
I, Br (no channel blockage)[a]	0.1
Te, As, Ge, Cd, Rb, Se	0.1
Cs, Ga, Ru, Mo, Sn, Te, Zn	0.01
Sr, Zr, Ba, Ag, Nb, Y, La, Rh, Pd, Sb, Ce, Pr, Nd, Pm, Sm, Eu, Gd, Tb	0.001

[a] With a channel blockage this halogen release fraction is reduced to 0.01.

one hour. A leak rate from the gas circuit to the environment with a half-life of about 10 min is assumed (Macdonald, 1971). It has been pessimistically assumed that material escaping from the fuel is not subject to plate-out, re-suspension or filtration (Macdonald, 1971). Release fractions assumed in this study for fission product elements from the fuel are given in Table 2, after Abbott (cited by Macdonald, 1971 and Clarke, 1973a, b).

Meteorological conditions are described, using the Smith (1973) model, for a release at midday in spring or autumn, with significant cloud cover. A mean wind speed, at 10 m, of 5 m/sec is assumed which implies a weather category P = 2.6 (approximately Pasquill category C) and an inversion at about 1 km height. Building entrainment is assumed (Davies and Moore, 1964; Munn and Cole, 1967; Culkowski, 1967), where the dispersion coefficients used are modified such that the semi-ellipse of the Gaussian plume's 10% concentration limit, from a ground level release, immediately inscribes the downwind sides of a reactor building taken to be 40 m high and 60 m crosswind. A ground roughness coefficient of $z_0 = 30$ cm, typical of fairly flat English countryside of mixed fields, woods and villages is assumed. Effects of moving from a region of one roughness value to another are not considered. A sampling time of 1 hr was used to match the period of release.

Element-dependent deposition velocities used in this model are shown in Table 3. These values are typical of those expected in a release from a nuclear installation (Chamberlain, 1962; Gifford and Pack, 1962; Hoffman, 1977; USEAC, 1975; Weiss and Keller, 1977; Martin *et al.*, 1974, 5; Tadmor, 1973; Beattie and Bryant, 1970). Here inert gases are assumed not to be deposited (Tadmor, 1973) while halogen atoms are preferentially depleted from the plume. Most elements are assumed to be in the form of submicron sized particles, so that deposition relies on turbulence in the atmosphere. The weather conditions are such that the assumption of uniform instantaneous depletion from the whole plume, implicit in equation (1), is acceptable.

Table 3. Assumed group deposition velocities for element-dependent depletion

Element	Group deposition velocity (cm/sec)
Xe, Kr	0
I, Br	1.2
All other elements	0.3

One time step of the WEERIE program has been used to produce a source term accumulated over the period of release. Exposure rate calculations start at the end of the release when all the released activity has escaped. The use of this assumption will artificially increase ground exposure rates at short times after the release but will be negligible after about 10 hr. Total exposures from ground deposits, after the initial period, will be unaffected. Hence from 1 to 10 hr after the start of the release, in this example, the estimated exposure rates can be treated as upper limits to more probable exposure rates, which could be determined by a more detailed study.

4.2. *Doses and exposures from the notional accident*

In order that exposures resulting from deposited material may be seen in perspective, inhalation dose commitments and external exposures, resulting directly from the plume, have been calculated using the parameters described in Section 4.1, including element dependent deposition.

Inhalation dose commitments from this notional accident are shown in Fig. 2. The thyroid dose commitment is the largest for a single organ under these conditions; the particular ERL is unlikely to be exceeded beyond 0.3 km downwind. Figure 3 shows the downwind variation of the initial ^{131}I and ^{137}Cs deposited activities; a total of 1040 Ci of ^{131}I and 9 Ci of ^{137}Cs are released in this notional accident. The derived ERL's (Baverstock and Vennart, 1976) are shown in Table 4, for dose commitments via the grass–milk food chain. ^{137}Cs does not, in this case, pose any significant hazard via this route, owing to its low (1%) assumed release fraction. ^{131}I ground contamination falls below the adult and child DERL's at about 3 km and 20 km respectively, where the latter would represent a significant area of land over which short term restrictions on milk consumption could be necessary. In these weather conditions deposition has a small effect on plume concentrations.

Cloud beta and gamma exposures in air are shown in Fig. 4. The differences between the semi-infinite cloud gamma approximation and the numerical cloud

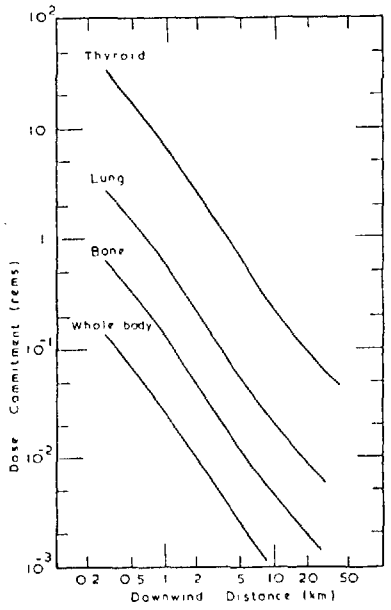

Fig. 2. Predicted downwind distance-dependence, on the plume axis, of selected mean inhalation dose commitments for the notional MAGNOX accident (see text for release and dispersion conditions).

gamma estimation, within about 5 km of the installation, are due to the spread of the plume being less than or comparable with the gamma mean free paths

Table 4. Derived ERL's for deposited activity giving dose commitments via the grass milk food chain (Baverstock and Vennart, 1976)

Isotope	DERL (μCi/m^2) Adult	Child (6-month old)
^{131}I (Thyroid)	27	1.8
^{137}Cs (Whole Body)	36	18.0

in air. Neither the mean cloud beta or gamma exposures are predicted to exceed ERL's under these conditions. In Figs 2-4 the effects of the inversion at 1 km height start to be seen after about 20 km, while building entrainment only exerts an influence within a few hundred metres of the release point.

Ground gamma and beta exposure rates at 1 km downwind are shown in Fig. 5 for times greater than 4 hr following the beginning of release from the fuel. Element-dependent deposition has been used as for the preceeding figures. Considering the ground gamma exposure rate in air 1 m above the ground, which as has been noted will be an upper limit at short times, this rate is expected to fall below 10 mR/hr within about 7 hr of the release. The ground beta exposure rate, at the same exposure point, is expected to fall below 10 mrad/hr only after about three days. The total beta exposure rate in air at this height above the ground is always greater than the

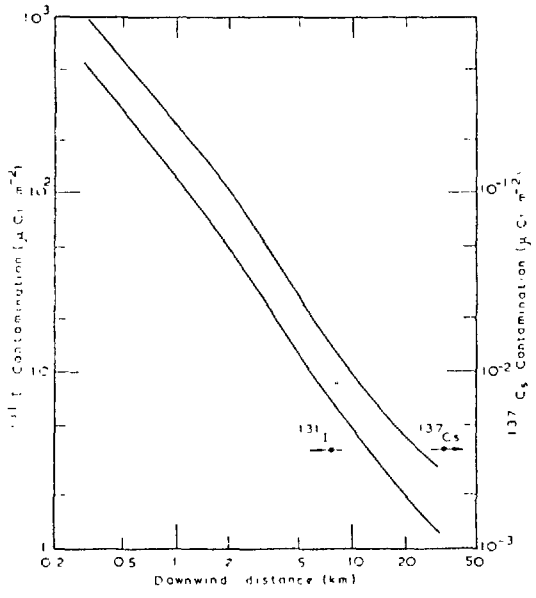

Fig. 3. Predicted downwind distance-dependence, on the plume axis, of the mean ^{131}I and ^{137}Cs ground contamination immediately following the release from the notional MAGNOX accident, using the three-group deposition model.

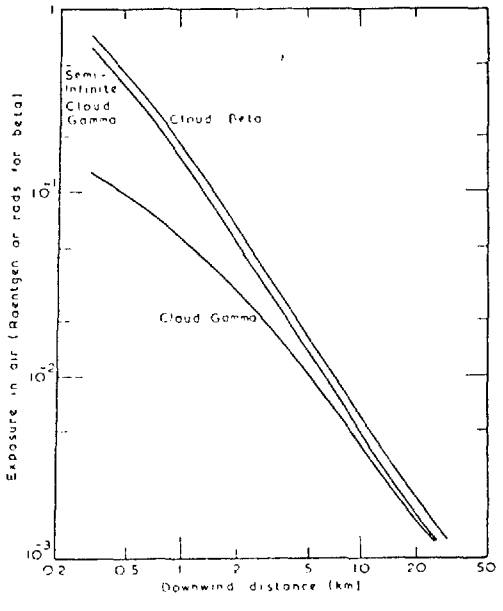

Fig. 4. Downwind distance-dependence of the mean on-axis gamma exposure in air and beta external dose, 1 m above ground, predicted for the notional MAGNOX accident. Gamma exposures for both finite and semi-infinite clouds are shown.

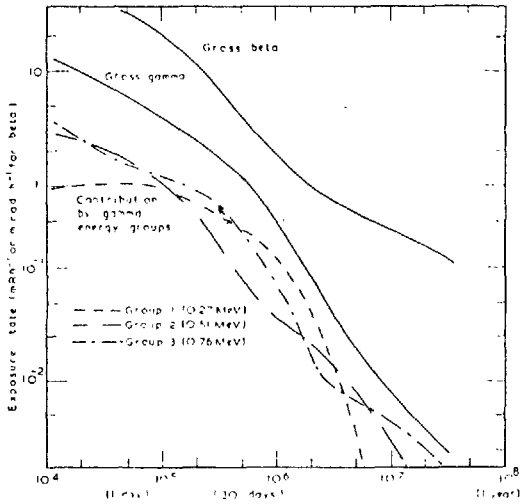

Fig. 5. Time-dependence of the rates of gamma exposure in air and beta external dose from ground contamination, 1 m above ground and 1 km downwind on the plume axis following the notional MAGNOX accident, predicted using the three-group deposition model. Contributions to the gamma exposure rate from three gamma energy groups are also shown.

corresponding ground gamma exposure rate within the limits of the plume; however the relatively lower radiological significance of external beta radiation must be borne in mind.

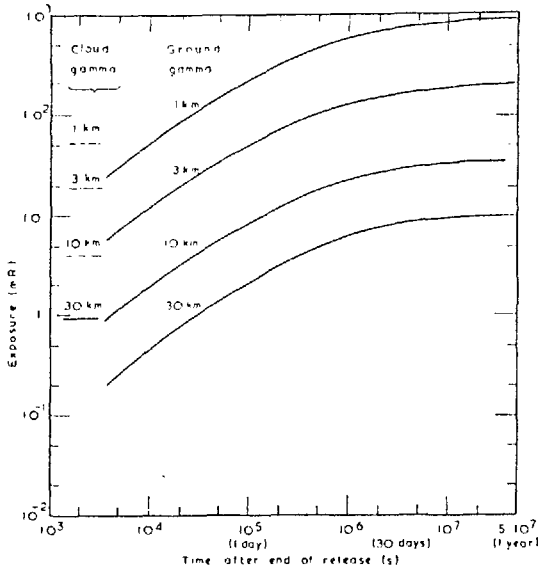

Fig. 6. Accumulation in time of mean ground gamma exposure in air at on-axis points, 1 m above ground, at several downwind distances, for the notional MAGNOX accident, using the three-group deposition model. Cloud gamma exposures at these points are shown for comparison.

The ground gamma rate is dominated, in this case, for the first month by iodine isotopes. For the next two months ^{95}Nb, ^{95}Zr and ^{103}Ru are the most prominent single contributors. Finally ^{137m}Ba, the short-lived daughter of ^{137}Cs, dominates the total gamma exposure spectrum after three months with a small contribution from ^{134}Cs. From such ground gamma exposure rates evaluated at several downwind distances the accumulation of this gamma exposure has been calculated during the first year after the release. These are shown in Fig. 6 with the cloud gamma exposures at the same points shown for comparison. The ground exposure exceeds that from the cloud within a day, but at shorter times closer to the point of release. This behaviour is of a similar character as that for a notional FBR accident considered by Kelly *et al.* (1977).

4.3. *Comparison of deposition models*

The use of a single overall deposition velocity as a model in calculating exposures from deposited material has been compared with the results from element-dependent deposition, for two different halogen release fractions, under the single weather condition described in Section 4.1.

The single overall deposition velocity chosen was 0.3 cm/sec; this is representative of the majority of released elements (Beattie and Bryant, 1970), especially those which determine the long term activity, i.e. Cs, Ru, Rh, Zr, Nb. Under the assumed dispersion conditions the depletion fraction Q^*, from equations (1) and (3) is approximately unity within several kilometers of the release point and does not change rapidly with downwind distance. For example, Q^* (20 km, v_g = 0.3 cm/sec) = 0.97, Q^*(20 km, v_g = 1.2 cm/sec) = 0.86. Hence the deposited activity is primarily determined by the deposition velocity and a consequence is that the use of the single deposition velocity reduces the iodine contamination by a factor of four, assuming little depletion of the plume has occurred. This reduces the range of ^{131}I contamination above DERL's to about 1 km and 7 km for adults and children respectively, so reducing the contaminated area by an order of magnitude. The ground exposure rates are affected not only by the reduced halogen deposition in the single deposition velocity model, but also by the inclusion of inert gases.

Considering the initial ground gamma exposure rate in more detail, in Figs 7(a) and (b) the two deposition models are compared with different halogen release fractions (10% and 1%) for an on-axis point 1 km downwind. The exposure rate is plotted in a cumulative manner as a function of gamma-ray energy, thus indicating spectral differences. There are

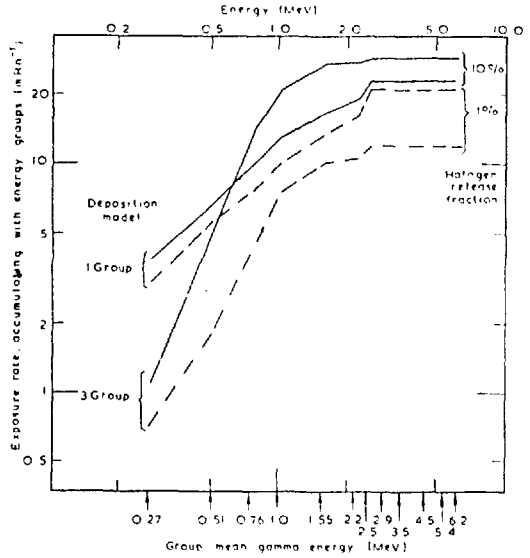

Fig. 7(a). Predicted on-axis exposure rate in air 1 m above ground and 1 km downwind immediately following the release from the notional accident. Exposure rates are shown, for various combinations of deposition model and halogen release fraction, accumulating with energy group. These short cooling time rates represents an upper limit (see text).

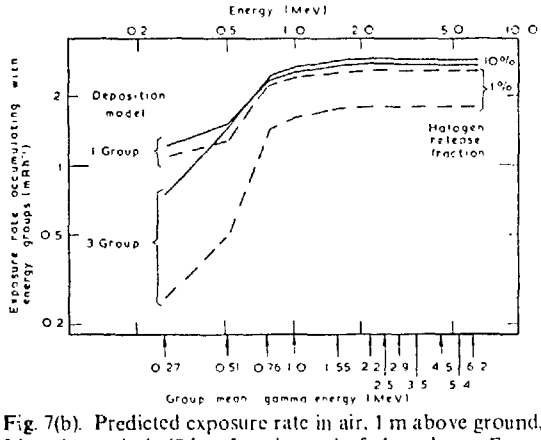

Fig. 7(b). Predicted exposure rate in air, 1 m above ground, 1 km downwind, 40 hr after the end of the release. Exposure rates are shown, as in Fig. 7(a), accumulating in gamma energy group and for various combinations of deposition model and halogen release fraction.

differences in the total exposure rates for each deposition model for a given halogen release fraction. The results for a single overall deposition velocity are not greatly dependent on the iodine content of the plume, when initially deposited. This is mainly due to the short-lived inert gases' contribution e.g. ^{88}Kr, ^{87}Kr, ^{133}Xe etc. The deposit formed by element-dependent depletion is much more dependent on iodine concentrations in the plume, when the contamination is initially formed. Also the exposure source spectrum is different, owing to the absence of any contribution from ^{133}Xe and associated isotopes in the lowest energy group and of ^{87}Kr and ^{88}Kr contributions at higher energies.

After ageing of the deposited material by 40 hr, as shown in Fig. 7(b), the single overall deposition model's exposure spectrum still retains the major low energy contribution from ^{133}Xe, compensating for the effect of the lower iodine deposition velocity. The major iodine isotope contributing to the ground gamma exposure rate at this time in all cases shown here is ^{132}I with a half-life of 2.3 hr. This is the short-lived daughter of ^{132}Te, half-life of 78 hr, so that most of the ^{132}I in the deposits has been formed by decay from deposited ^{132}Te, which is the same in both deposition models. The element-dependent case with 1% release fraction of iodine lies below the other cases, owing to the absence, as before, of inert gases. In the case of the 10% release, with the halogen deposition velocity of 1.2 cm/sec, other iodine isotopes are comparable in importance to ^{132}I, especially at short ageing times.

Table 5 gives the ratios, for the simple model relative to the element-dependent deposition model, of the total on-axis ground gamma and beta exposure rates in air at 1 m above the ground for various distances and ageing times, for the two halogen release fractions. Differences between the two models lie approximately within a factor of two and the gamma exposure rates show a tendency, for the two models, to approach the same value as the deposits age. Eventually the long-lived caesium isotope will dominate; it has the same deposition velocity in both models. The total beta exposure rate is more dependent on iodine deposition and shows somewhat more varied behaviour.

Deposition velocities quoted for iodine show variations depending on the circumstances of the release and the calculations with the element-dependent model have been repeated with the halogen deposition velocity increased to 2.0 cm/sec, which might represent a release of purely elemental iodine. In Table 6 the resulting gamma and beta exposure rates are given relative to the basic three-group model used in forming Table 5. Changes in exposure rates are less than those shown in Table 5 where the one-group model is considered, as might be expected by the greater similarity of the two deposition models.

While the possible limitations of the source depletion method (equation 1) under stable category F atmospheric conditions have been pointed out it is nevertheless worthwhile to perform equivalent calculations to those shown in Table 5 but with the Pas-

Table 5. Predicted ratios of exposure rates for one-group deposition model to those from the three-group deposition model (conditions as in Section 4.1)

Release fraction of halogens	Downwind Distance (km)	Cooling time (hr)	Ratios of one- to three-group models: Gamma exposure rates	Beta dose rates
1%	1	0	1.75	1.99
	1	40	1.42	0.93
	30	0	1.15	1.13
	30	40	1.43	0.94
10%	1	0	0.80	1.06
	1	40	0.95	0.57
	30	0	0.76	0.87
	30	40	1.01	0.63

Table 6. Predicted ratios of exposure rates for modified† three-group deposition model relative to three-group model of Table 3

Release fraction of halogens	Downwind distance (km)	Cooling time (hr)	Ratios modified basic: Gamma exposure rates	Beta dose rates
1%	1	0	1.21	1.12
	1	40	1.05	1.09
	30	0	1.30	1.16
	30	40	1.04	1.07
10%	1	0	1.49	1.39
	1	40	1.29	1.39
	30	0	1.37	1.26
	30	40	1.19	1.26

† The modified three-group deposition model assumes a r_d (halogens) = 2.0 cm/sec corresponding to purely elemental iodine in the release.

quill category F model used for both one- and three-group models. Under these conditions, from 0 to 30 km, depletion fractions Q^* for halogens in the three-group model would be 0.019 while for non-halogen, non-noble gas elements (and all elements in the one-group model) the fraction would be 0.37. The ratio of the calculated exposure rates for the two models are shown in Table 7. As in Tables 5 and 6, the ratios will depend upon the extent to which noble gases and iodine isotopes reach the exposure points according to the two models under the particular circumstances. Owing to this balancing of effects, the ratios in Table 7 do not differ greatly in variation or magnitude from those given in Table 5 for average

Table 7. Predicted ratios of exposure rates for one-group deposition model to those from the three-group deposition model (Pasquill category F weather conditions, ground level release without building entrainment)

Release fraction of halogens	Downwind distance (km)	Cooling time (hr)	Ratios of one- to three-group models: Gamma exposure rates	Beta dose rates
1%	1	0	1.84	1.83
	1	40	1.10	0.57
	30	0	1.49	1.01
	30	40	1.55	1.08
10%	1	0	1.24	1.40
	1	40	1.34	0.75
	30	0	1.24	0.84
	30	40	1.69	1.38

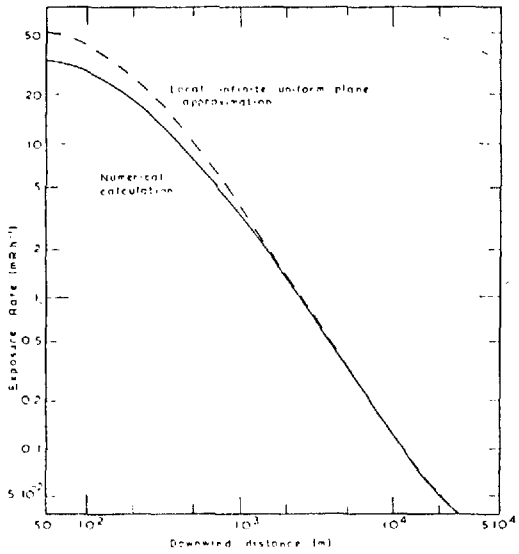

Fig. 8. On-axis exposure rate in air 1 m above ground after 40 hr cooling predicted for the notional MAGNOX accident and plotted against downwind distance. The deposit was formed using the three-group deposition model and results of numerical calculation and local infinite uniform plane approximation are compared. (See text for release and dispersion conditions).

weather conditions. It should be emphasized, however, that the predicted spatial extent of iodine deposition would differ greatly between the two models. This merits study with a model with improved representation of deposition under stable conditions.

4.4. *Effects of finite plume size on gamma exposures from deposited activity*

A brief discussion is given here of the spatial distribution of gamma exposure from the deposited activity arising from the notional accident.

The downwind distance-dependence of the on-axis ground gamma exposure rate, shown in Fig. 8, has a distance-dependence similar to that of the cloud gamma exposure. Building entrainment, within a few hundred metres, reduces the on-axis exposure rates by broadening the pattern of deposited activity; this effect also helps to avoid numerical difficulties with the routine for integrating over the ground deposit which would arise close to a point source. Results for the infinite uniform plane approximation are also shown in Fig. 8; it will be seen that, owing to the geometrical differences, finite and infinite deposit calculations converge more rapidly than do the corresponding results for cloud gamma exposure shown in Fig. 4.

The crosswind-dependence of the gamma exposure rate is shown in Fig. 9, at 1 km downwind after 40 hr cooling of the deposit. Both the results of the numerical calculation and the infinite uniform plane approximation are shown; the effect of the penetrating nature of gamma rays in air may be seen, the deposit acting approximately as a thick line source. When the exposure point is well beyond the 10% lateral concentration limit of the plume the beta exposure rate will be negligible compared with the gamma component, as the former follows the local deposited activity and therefore also the trend of the infinite plane approximation. There will be large changes in the gross beta/gamma ratio compared with that close to the centreline of the deposit.

5. CONCLUSIONS

The use of element-dependent deposition when calculating ground patterns of activity gives ground gamma and beta exposure rates which show detailed differences from those obtained using a single overall deposition velocity model. Major differences could however, be observed if the aim were to calculate the spatial extent of deposition of a single halogen isotope. Ground gamma spectra, which depend upon the isotopic composition of the deposit, also show signifi-

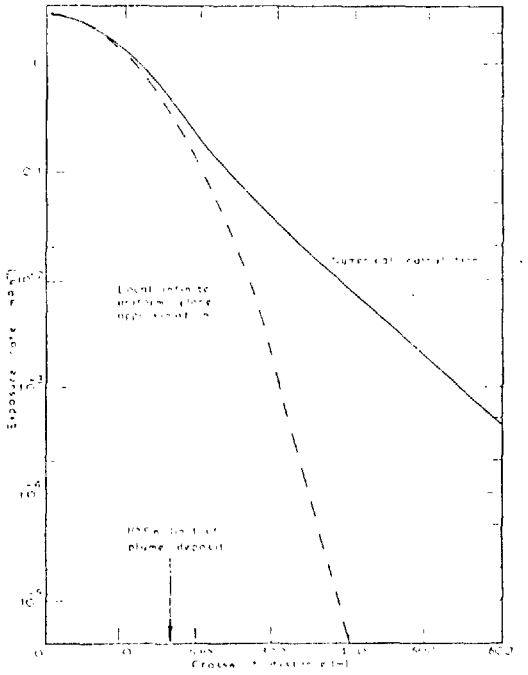

Fig. 9. Predicted crosswind-dependence of the exposure rate in air 1 m above ground at 1 km downwind, after 40 hr cooling of the deposit from the notional MAGNOX release, formed using the three-group deposition model. Results for the numerical calculation and local infinite uniform plane approximation are compared. (See text for release and dispersion conditions).

cant differences when these two deposition models are used. Further work should be undertaken to assess the ability of Gaussian dispersion models to predict ground deposition patterns under stable conditions for strongly depositing nuclides.

For the notional accident that has been used as an example in this study, estimated ground gamma and beta exposures exceed corresponding exposures due to the cloud itself after an ageing of the deposit of about one day. The role of ground roughness and weathering in reducing the ground component of exposure merits further study. Modelling a change of meteorological conditions affecting a release would further extend the scope of this environmental analysis code.

Acknowledgements—The authors wish to acknowledge the support of the Nuclear Installations Inspectorate, Health and Safety Executive, although the views expressed are not necessarily those of the Nuclear Installations Inspectorate. Discussions with Dr H. M. ApSimon are gratefully acknowledged.

REFERENCES

Anspaugh L. R., Shinn J. H. Phelps P. L. and Kennedy N. C. (1975) *Hlth Phys.* **29**, 571–582.
Baverstock K. F., and Vennart J. (1976) *Hlth Phys.* **30**, 339–344.
Beattie J. R. and Bryant P. M. (1970) UKAEA Report, *AHSB(S) R*135.
Beynon S. M. (1973) CEGB Report *RD/B/N* 2633.
Bryant P. M. (1966) *Hlth Phys.* 12, 1393–1405.
Chamberlain A. C. (1962) UKAEA Report *AERE-M*1122.
Chilton A. B. (1967) *Nucl. Sci. Engng* **27**, 403–410.
Clarke R. H. (1973a) *Hlth Phys.* **25**(3), 267–280.
Clarke R. H. (1973b) PhD Thesis, CEGB, Berkeley Nuclear Laboratories.
Clarke R. H. and Utting R. E. (1970) CEGB Report *RD/B/N* 1737.
Corbett J. O. (1977) CEGB Report *RD/B/N* 3865.
Cross W. G. (1967) *Can. J. Phys.* **45**, 2021–2040.
Cross W. G. (1968) *Physics Med. Biol.* **13**, 611–618.
Cross W. G. (1969) *Can. J. Phys.* **47**, 75–83.
Culkowski W. M. (1967) *Nucl. Saf.* **8**, 257–259.
Davies P. O. A. L. and Moore D. J. (1964) *Int. J. Air Wat. Pollut.* **8**, 515–523.
Draxler R. R. and Elliot W. P. (1977) *Atmosph. Environ.* **11**, 35–41.
Fitzpatrick J. (1976) Private communication, Imperial College.
French R. L. (1965) *Hlth Phys.* **11**, 369–383.
Gifford F. A. and Pack D. H. (1962) *Nucl. Saf.* 3(4), 76–80.
Hoffman F. O. (1977) *Hlth Phys.* **32**, 437–441.
Hoffman F. O., Miller C. W., Shaeffer D. L. and Garten C. T., Jr. (1977) *Nucl. Saf.* **18**, 343–354.
Horst T. W. (1977) *Atmosph. Environ.* **11**, 41–46.
Hosker R. P., Jr. (1974) *Proc. Symp. Physical Behaviour of Radioactive Contaminants in the Atmosphere*, Vienna (*IAEA-SM*-181/19).
Huddleston C. M., Klingler Q. C., Burson Z. G. and Kindaid R. M. (1965) *Hlth Phys.* **11**, 537–548.
Jaeger R. G. (Ed.) (1968) *Engineering Compendium on Radiation Shielding*, Chapter 4.3 Chilton A. B.; Chapter 4.5 Clifford C. F. and Clarke E. T., Springer Verlag.
Kaiser G. D. (1976) UKAEA Report *SRD R*63.
Kelly G. N., Jones J. A. and Hunt B. W. (1977) NRPB Report *NRPB-R*53.
Lederer C. M., Hollander J. M. and Perlman I. (1967) *Table of Isotopes*, (6th Edn) John Wiley, New York.
Loevinger R. (1956) *Radiology* 66, 55–62.
Loevinger R., Japha E. M. and Brownell G. L. (1956) in *Radiation Dosimetry* (Eds Hine G. J. and Brownell G. L.), Chapter 16, Academic Press, New York.
Macdonald H. F. (1971) *Proc. Int. Symp. Rapid Methods for Measuring Radioactivity in the Environment*, *IAEA-SM*-148/38.
Macdonald H. F. and Clarke R. H. (1972) *Proc. 6th Int. Congress of the SFRP*, Paper VI, SFRP/15.
Macdonald H. F. (1975) *Ann. nucl. Energy* **2**, 625–635.
Martin J. A., Jr., Nelson C. B. and Cuny P. A. (1974/5) A Computer Code for Calculating Doses, Population Dose, and Ground Deposition Due to Atmospheric Emission of Radionuclides, USEPA Office of Radiation Programs.
Munn R. E. and Cole A. F. W. (1967) *Nucl. Saf.* **8**, 257–259.
Pasquill F. (1961) *Met. Mag., Land.* 90, 1063, 33–49.
Pasquill F. (1974) *Atmospheric Dispersion*, (2nd Edn), Ellis Horwood, Chichester.
Scriven R. A. and Fisher B. E. A. (1975) *Atmosph. Environ.* **9**, 49–59.
Sidebotham E. N. (1971) *Proc. BNES Conference, Chemical Nuclear Data Measurements and Application*, Canterbury.
Slade D. H. (Ed.) (1968) *Meteorology and Atomic Energy*, Chapter 4.4 Ishtzer N. F. and Slade D. H.; Chapter 7.4, 7.5 Henley J. W., USAEC.
Smith F. B. (1973) Internal Meteorological Office Note TDN 40 (Met. 0.14). Also in *Atmospheric Diffusion* (Pasquill, F.) pp. 373–377, Ellis Horwood Chichester, (1974).
Spencer L. V. (1955) *Phys. Rev.* **98**, 1597–1615.
Strachan S. J. (1978) Private communication, Imperial College.
Tadmor J. (1973) *Hlth Phys.* **24**, 43–52.
Tobias A. (1972) CEGB Report *RD/BM*2453.
UKAEA (1972), *Reactors UK*, (5th Edn) August.
U.S. Atomic Energy Commission Reactor Safety Study (1975) *WASH*-1400, Appendix 6.
Weiss B. H. and Keller J. H. (1977) *Proc. IVth Int. Congress of the IRPA*, Paris.

3. Recent Developments in Calculating Doses Incurred from Deposited Activity and from Cloud Activity Following an Accidental Release of Radioactivity in the Atmosphere, *A. J. H. Goddard, G. Gouvras, S. J. Strachan (Imperial College-UK)*

In this paper, work that has had as its objective improvements in two aspects of the calculation of doses following an accidental release of radioactivity into the atmosphere is described. These are, first, estimation of the spatial, temporal, and isotopic variations of the deposited activity on the ground and the corresponding exposures in air immediately above the ground, and second, improved calculations of the external gamma-ray exposure in air, the photon flux and corresponding organ doses arising from the passing plume of release material. These improvements have been carried out within the framework of the environmental assessment computer program WEERIE, which was originally prepared at the CEGB, Berkeley Nuclear Laboratories by Clarke. To illustrate these two improved aspects of the calculation, a notional MAGNOX depressurization has been simulated with involvement of the fission products released from a single channel of fuel.

The problem of depleting a plume of radioactive material, including all radiologically significant isotopes, by allowing for simultaneous depletion and radioactive decay, has been approached by assigning the deposition velocity of each element to one of up to four grouped values, where each group represents a different range of depletion rate. Element-dependent washout can also be included along with the effects of elemental dry deposition. The restrictions on the depletion model used are discussed briefly. To allow for the succession of parents and daughters in radioactive decay where these elements may have different deposition velocities, analytical relationships have been developed to represent the mean distances traveled in the atmosphere by each isotope in a decay chain. From these calculations the isotopic composition of the resulting beta and gamma activities on the ground may be determined at any selected point downwind or crosswind. This also represents an improvement in modeling air concentrations and subsequent inhalation dose commitments and external cloud exposures.

Previous estimates of the cloud gamma doses to individuals have been expressed in terms of exposure in air. It is of interest to explore the validity of this approach when calculating human organ doses and this has led to the development of a routine for calculating gamma energy spectra for any stack height or weather category; spectra may be calculated both on the plume axis or at off-axis points. By this means, the degradation of the scattered photon spectrum may be explored away from the plume. The method is based on the point-source moments method where the particular points considered are the integration points that are normally used within the WEERIE program to establish the cloud gamma exposure in air near the ground. The concentrations of activity at each sampled (integration) point in the plume are first computed for the type of release considered and the scattered photon spectrum is subsequently calculated using the moments method for infinite homogeneous air; the scattering or absorbing effects of the ground are then taken into account, depending on the point-source height and horizontal distance from the dose point. Monte Carlo calculations and experimental data from the open literature are combined in analytical expressions of the ground correction factors, which modify the radiation pattern established from the infinite-medium calculations. The routine is provided with an in-built facility to select between various grid configurations for the actual plume so that a desired degree of accuracy is achieved within certain time limitations. On the basis of existing work elsewhere on photons irradiated by both isotopic and beam environments of photons, data files have been created using computational interpolation and extrapolation techniques; these files contain values of doses per incident photon on the surface of the phantom, for the entire energy region covered by the degraded fission product photons, and are stored for a variety of organs and other parts of the body of the standard adult hermaphrodite MIRD phantoms. The cloud spectra incident on the phantoms, weighted by the dose fractions mentioned above, yield the values of dose from the plume.

To illustrate the use of these methods, a notional MAGNOX depressurization accident has been modeled, the description of this accident has been taken from various published studies. Various meteorological dispersion conditions, together with building entrainment, have been employed in examining a range of consequences from the single hypothetical release. The sensitivity of consequences, particularly the area of ground deposition, to the magnitude of deposition velocities is demonstrated, while the time dependencies of the external ground and cloud exposures are compared, including at short times while the notional accident is in progress. It is shown that external exposure from the ground exceeds that from the cloud within about one day and eventually becomes many times greater. By considering both an early and a late phase of the release and applying the moments method mentioned above to the cloud gamma calculation, cloud gamma spectra and organ doses are presented for both on-axis and off-axis points near the ground.

In conclusion, methods for linking these methods with stored population (census) data are reviewed.

4. Plume Diffusion over Hilly Terrain,* *G. J. Schriber (Muehleberg Nucl Power Station-Switzerland), H. R. Voelkle (Swiss Federal Radioactivity Surveillance Commission-Switzerland), H. H. Loosli, H. Oeschger (Univ Bern-Switzerland)*

The commonly used model of local atmospheric transport is the Gaussian plume, which calculates the atmospheric concentration $X(x,y,z)$ of a pollutant by the following expression[1]:

$$X(x,y,z) = \frac{Q}{2\pi u \sigma_y \sigma_z} \exp\left(\frac{-y^2}{2\sigma_y^2}\right) \left\{ \exp\left[-\frac{(z-H)^2}{2\sigma_z^2}\right] + \exp\left[-\frac{(z+H)^2}{2\sigma_z^2}\right] \right\},$$

where x, y, and z are the Cartesian coordinates (downwind, crosswind, and vertical), Q is the source strength, H the effective release height (stack height plus plume rise), and u the mean downwind velocity. σ_y and σ_z are the crosswind and vertical plume standard deviations. Since this model has only been tested in flat regions, its application for hilly terrain still remains in question.[1] Therefore, diffusion experiments were carried out around the Muehleberg Nuclear Power Plant, situated near Bern (Switzerland) in a very irregular terrain, to check the validity of the Gaussian plume model at that site and, if necessary, to point out the possibilities to adapt this model.

*The authors wish to thank the Swiss Meteorological Institute, Air Pollution Section, Payerne, and the Federal Office of Energy Economy, Nuclear Safety Division, Wuerenlingen, for their collaboration.

Vol. 20 No. 1—J. Inst. Nuc. Eng.

A Review of Deposition and other processes affecting the consequences of unplanned Atmospheric Releases from Nuclear Installations

by S. J. STRACHAN*

This paper is based upon a paper in the postgraduate award section of the 1978 Nuclear Educationalists' Meeting with additional background material.

1. INTRODUCTION

The nuclear power industry relies on high technology and strict design and engineering standards. Long term reliability of individual components and systems are prerequisites for safety. The systems employed often have built-in redundancies, particularly those which automatically monitor the state of a reactor core. Maintenance and operating practices have been developed to match these high engineering standards.

In the unlikely event of a fault in one component or system a parallel or back-up system can generally be used, so minimising the chances of a sequence of events which could lead to fuel damage and escape of active material. Mechanisms are provided for shutting down a reactor under fault conditions, so further reducing any chance of an unplanned release. The overall design of reactors helps to contain and reduce any possible releases. Nevertheless sequences of events, of extremely low probability, can be envisaged which could allow active material to escape to the atmosphere. The consequences and risks of this possibility have to be evaluated for public safety.[1] The discussion in this paper will deal with some aspects of the required assessment process, particularly those affecting deposition.

The nature and extent of deposition in an unplanned release will depend on the type of installation which is the source of escaped radioactivity. Three categories of sources can be immediately identified:

(i) Reactors,
(ii) Fuel reprocessing and fabrication plants,
(iii) Transportation.

Discussion here is limited to those types of unplanned events which allow radioactivity to disperse in the atmosphere.

The materials in each type of installation have different ranges of physical and chemical properties. Most attention will be given to any possible releases from the first of the three source categories listed above. The importance of deposition will depend on many factors, including:

(i) The source inventory,
(ii) The source conditions,
(iii) Special conditions producing releases to the atmosphere,
(iv) Meteorological conditions for dispersion,
(v) Radioactive, chemical and physical transformations in the air,
(vi) Conditions and utilisation of surfaces where deposition may occur.

Initially the different sources will be discussed. Secondly an assessment of the results of release mechanisms on the escape of radioisotopes will be made. This is followed by a review of the material's behaviour in the environment. Any material suspended in the atmosphere can be deposited on surfaces by several different mechanisms, which are often grouped as:

(i) Gravitational settling,
(ii) Dry (turbulent) deposition,
(iii) Washout,
(iv) Rain-out.

Chemical transformations of the airborne material will also affect its deposition.

The effects of deposition in the atmosphere are then discussed with respect to the pathways which can produce dose commitments and exposures:

(i) Inhalation dose commitments from the cloud,
(ii) External cloud exposures,
(iii) External exposures from deposited material,
(iv) Dose commitments from ingestion of contaminated food and water,
(v) Doses from resuspension of deposited material.

2. SOURCES AND TYPES OF RELEASES

Radioactive material associated with nuclear power can be considered in three groups, consisting of fission products, actinides and activation products. The chemical and physical forms isotopes take within the reactor under normal and accident conditions not only determine the release from the fuel but also affect deposition within the containment and later in the atmosphere.

The production of the radioactivity in question starts by irradiating fuel in a reactor. Subsequent stages involve its removal, transportation and finally its reprocessing. The types of situations which can lead to atmospheric releases and their effects on materials' deposition properties are considered in the above order.

2.1 Reactors

For most reactor types an accident leading to an unplanned release of activity to the atmosphere will involve the coolant. It is these possible releases that will be discussed in most detail. Other escape routes could occur during fuel handling.

Fission products are the radionuclides most likely to be released, while only in extreme circumstances could actinides escape in significant quantity. Activation products are generally less abundant but if associated with the coolant could become a hazard in unplanned releases. Some factors affecting the production and release of each of these types of activity from reactors are mentioned briefly below.

2.1.1 Source Inventory

The irradiation history of fuel within a reactor defines the quantities of fission products and actinides

*Nuclear Power Section, Mechanical Engineering Department, Imperial College

J. Inst. Nuc. Eng.—Vol. 20 No. 1

TABLE 1 Source Inventories

Total Activity (10^8 Ci) of Radio-isotopes considered in study

	WASH-1400[6] PWR, 1000 MV(e)	FBR[7] 1300 MW(e)
Fission Products	39.1	59.1
Actinides	$1.1.10^{-3}$*	19.42†
Activation Products		0.71‡

*$Pu^{238,239}$ only

†Includes Np^{239}, Pu^{241} etc

‡Na^{24} only

present at any given time. Many computer routines have been written to predict these activities, such as FISPIN[2], RICE[3], FISP[4] and HYACINTH[5], for reactor physics and fuel management requirements as well as hazard calculations. The relative sources of activities can be seen for a typical LWR and FBR in Table 1.[6,7]

2.1.1.1 Fission Products

The total radioactive fission product inventory increases with in-core irradiation. The species vary with time during the irradiation.

Most short lived isotopes (e.g. Kr88, Rb88, Te132, I132) have a steady state concentration which is mainly determined by the recent irradiation history. Long lived isotopes (e.g. Cs137, Sr90) can accumulate over the whole of the fuel's life. The formation of longer lived and stable isotopes allows production of isotopes by neutron capture, where some may not be produced as abundantly by direct fission, such as Cs134. Also the fractions of fission events from different fissile isotopes can change with irradiation and subsequent production of new fissioning isotopes, such as plutonium in thermal uranium fuelled reactors. This can alter the yields of different isotopes from the fission process.

2.1.1.2 Actinides

Initially the actinides in the fuel are restricted to a few fissile and fertile isotopes of uranium in most thermal reactors, and include some plutonium isotopes in fast reactors. During irradiation these decay along normal decay chains but neutron capture events (and more exotic reactions) can build up higher actinides, including isotopes of plutonium, americium, curium, etc. The range of actinides in the fuel is significantly increased as burnup proceeds. Radon is the only gaseous heavy element, where Rn222 is the longest lived isotope with a half life of 3.8 days. The production of higher actinides is particularly dependent on the reactor and fuel types.

2.1.1.3 Activation products

Neutron losses outside of the fuel lead to most of the activation products in a reactor core and its surrounding biological shield. The core is usually constructed of materials minimising these neutron losses, so reducing problems associated with activation.

The moderator and fuel cladding should both be of material with low neutron capture cross-sections. Under high temperature operating conditions physical strength may be required at the cost of extra neutron absorption. In these cases, e.g. AGR, FBR, steel cladding may be used where there can be activation products including Co60 and other transition elements' isotopes. The coolant is another source of activation products, which are often short lived. Exceptions to this include the production of Na24 in liquid sodium cooled fast reactors and tritium in water reactors where boron poisons are present. Breeder regions could also be classed as areas where activation occurs, but under purposely designed conditions.

2.1.2 Fuel behaviour and releases to the coolant

In this section most attention will be given to the interactions of fission products which affect their release and subsequent behaviour. Conditions within the fuel pin are a major influence and can be quite different in various reactor types. Many fields of study are involved with different aspects of pellet-cladding interactions and their results are of wide interest.

2.1.2.1 Internal behaviour of the fuel and associated cladding

Under normal operational conditions some gaseous and volatile fission products diffuse out of the fuel's crystal lattice and are trapped by the fuel cladding. This process tends to preferentially generate 'free' isotopes with relatively long half lives, as these have more probability of diffusing through the fuel than short lived isotopes[8].

These 'free' isotopes can also be released by cracking of the fuel, which additionally reduces the diffusion distance required for escape. Other temperature dependent effects enhancing releases include sweeping by grain boundary movements and crystal lattice phase changes, where the latter is of importance for metallic Uranium fuel as in early MAGNOX stations[9]. These 'free' isotopes can affect the fuel's temperature by altering the conductance across any fuel-cladding gap. The cladding can absorb various elements, such as Iodine, Tellurium and metallic solutions of Caesium and Cadmium with Zircalloy cladding, so altering its physical properties. Chemical 'getters' can impose some control on the action of these 'free' isotopes. These internal contaminants can reduce the integrity of the cladding as the initial containment of fission products by weakening of the cladding and inducing greater stresses, strains and corrosion on the cladding. Stringent temperature control mechanisms can be required to minimise these effects and so prolong the economically useful and safe life of the fuel[9]. The effects of high irradiation

and possible corrosion by the coolant may be more important in fast rather then thermal reactors[10,11].

Cracks in the cladding can lead to ingress of the coolant into the fuel pin. This will affect the chemical nature of the 'free' isotopes. Coolants such as carbon dioxide and water may produce oxides and salts, while liquid Sodium could reduce any oxides formed within ceramic oxide fuel. Under normal conditions this can lead to slow operational releases of fission products to the coolant, or possibly a few 'burst' releases if coolant is heated to high temperatures within a faulty fuel pin during start-up and refuelling[10,11]. With transient accident conditions bursts of 'free' fission product activity could be released from fuel pins followed by further releases if circumstances led to prolonged high temperatures. Ceramic oxide fuel can retain most of its fission products until temperatures in the region of 1500-1700°C and melts at about 2500°C.

The cladding of the fuel can be important in the type of elements and chemical species released. The elements Barium and Strontium tend to be released more readily than their oxides, whereas the oxides of Ruthenium are more readily released than its elemental form. Zirealloy has an affinity for Oxygen so can reduce the rate at which releases from the fuel are oxidised[13]. Steel has less affinity with oxygen so allowing a more oxidising environment within damaged fuel. These factors can lead to greater Strontium releases from Zircalloy clad fuel than steel clad fuel with an oxidising coolant[13], where air could enter the coolant under accident conditions. Allowing oxidising atmospheres to reach the fuel may increase overall releases by exothermic reactions raising fuel temperatures and removing fuel surfaces. This effect could release actinides at high temperatures where the fuel is almost molten, although radon gas may be released at lower temperatures. Oxidisation of graphite moderators could produce carbon monoxide and less oxidising environment in the coolant[14].

Vaporised MAGNOX cladding can reduce the releases of halogens relative to other elements such as alkali metals[15]. Carbon coated particle fuel may have significantly different release patterns, as metallic diffusion through porous carbon by elements including Caesium and Strontium, can be of importance through this first coating[16]. These particle fuels are usually bonded within a carbon matrix which would also affect releases.

Activation products in structural members of the reactor core would only become involved in the improbable event of major melting in the core. Actinide releases could increase in relative importance in these circumstances.

2.1.3 Escape through containments and to the atmosphere

The effects of the coolant circuit and other processes changing the deposition behaviour of the constituents of a release are discussed in this section. Also possible releases from fuel handling are briefly discussed.

Plate-out of material in the coolant circuit is an important effect. For most chemical forms release from the fuel the plate-out rate is typically within the range of 10^{-2} s^{-1} to 10^{-4} s^{-1}[17,18]. Non-reactive materials, such as inert gases and organic halides (eg methyl iodide), have much lower plate-out rates. Actinides, except Radon, have displayed rapid plate-out in test rigs[19,20]. High temperatures may allow greater releases and less condensation of elements such as Caesium and Tellurium, due to their relatively large vapour pressures[13]. Resuspension of plated out material can occur after radioactive decay or scouring by coolant borne particles, but each depends on the structure of the deposits. This can be a factor determining the size spectrum of aerosol particles.

The coolant may continue to react with the released material within the coolant circuit while it is escaping. Activation products in the coolant also follow the same escape path. Other effects can include coating of particles, where this affects the accretion of aerosols and hence their deposition behaviour. Plutonium oxide can be prevented from forming large branched aerosols with poor transportation properties by Sodium coolants which coat the initially small particles[21].

Filtration within an intact coolant system can reduce releases, particularly of chemically active material. Collection efficiencies for relatively inert material on the filters may not be as good as for less penetrating species[22]. Coolant flow patterns within different reactor cores under accident configurations can have significant effects on releases, especially if periods of stagnation occur[23,13].

Behaviour of material outside of the reactor building are discussed in a later section: the case of coolant leaking directly to the atmosphere will not be discussed further at present. Many reactor types, including PWR, BWR, AGR and LMFBR, have at least one internal containment building around the whole core and coolant circuit. These designs, including pre-stressed concrete pressure vessels for some LWR's and AGR's, can reduce releases, although the containments may have leak rates of a few per cent each day. Further oxidation can occur in any containment with an ordinary atmosphere. This may be of importance in LMFBR where the coolant can react to form many compounds, such as oxides, peroxides, hydroxides, carbonates and bicarbonates[24].

Leaks from the containment can be reduced by keeping the internal air pressure during an accident below that of the atmosphere, by pumping air through filters to the environment. A gas coolant may also be treated by this method. The final release would then contain only those chemicals which could penetrate the filters, usually consisting of inert non-depositing material.

Within a containment natural deposition on surfaces can occur, where gravitational settling could remove the largest particles, especially for dense elements like actinides. Deposition of smaller aerosol particles could be enhanced by specially designed paint and water spray systems, provided this is compatible with the coolant. These deposition processes within the containment act as a variable efficiency filtration on the different components of the release. Hence deposition rates of material penetraling the containment walls, where this loss might occur at greater than operational rates under accident conditions, would tend to decrease with time[13].

Other unplanned releases to the atmosphere might occur during fuel handling at the reactor. Here any of the old fuel with weakened cladding and insufficient cooling could overheat due to fission product decay heat, so producing a 'burst' release of volatile material, but at lower temperatures than in the core. This

material would then behave in the containment as discussed above but without the influence of the reactors' coolant. Fast reactor fuel handling has been designed to be done within the coolant to avoid this overheating effect which is particularly important for high burn-up fuels. Often the fuel is stored at the reactor before transportation, so the radioactive hazard reduces but is in the form of the intermediate and long lived isotopes.

2.2 Transportation

It is common practice to have one reprocessing or storage installation servicing many reactors in one region, so imposing the risks of transporting radioactive materials.

Fuel transportation flasks are designed to withstand major impacts without allowing any leakage of the active material. The low temperatures of the fuel, which has decayed for a period of several months or more, would lessen any activity which could escape, primarily to gases, in the event of a serious accident. The use of transportation should be secure and kept to a minimum[1].

2.3 Reprocessing

The basic stages within a reprocessing plant involve removal of cladding from the fuel, dissolution of fuel and then separation and treatment of the actinides and fission products. Design of each stage in this process can minimise the amount of activity which could escape to the atmosphere. Efficient filtration systems, cold traps and scrubbing systems have to be used which are of high reliability.

In the first stage, when the cladding is removed, inert gases and volatile elements are released. The fuel is also prepared for dissolution, usually as a fine dust so releasing most of the fission products. This includes Tritium produced within the fuel rods. Radon is usually of low importance in reprocessing plants as it has short lived isotopes which have decayed to low steady state activities within its natural decay chains. Other short lived fission products, generally at the start of decay sequences, will also have decayed during storage and transport before reprocessing. Thus longer lived penetrating isotopes, with any short lived daughter products will make up any release, for example I131, $Xe131^{m}$, Kr85, I129 and H3. Fuel can also be stored for a period at the reprocessing plant, so allowing the fuel activity, particularly that of I131, to fall even lower. The preparatory stage, such as sintering, will affect the form of fission products released. Failure of the filtration system at this first stage could lead to release of long lived isotopes of Caesium, Tellurium, Selenium, Antimony and Ruthenium (and associated Rhodium)[26] compounds. Possibly rare earths, such as Cerium-144, could be released under extreme failure conditions which would also allow escape of activation products from any cladding, such as steel, at this stage.

At later stages the active material is generally in solution and the fission product inventory has already been reduced, so gaseous releases are less likely. The remnants of the noble gases in the fuel will be released from the dissolver along with some iodine. Further stages can also release iodine including preparing the final storage of separated fission product waste. Actinide waste contains fewer volatile elements so is less likely to produce releases to the atmosphere during reprocessing and final disposal.

Long term disposal of all radioactive waste has to be in a secure form minimising the chance of any releases.

3 DEPOSITION AND ITS MODELLING

Dry deposition velocities are discussed initially followed by a discussion of their use in modelling the depletion of airborne concentrations from plumes.

3.1 Deposition velocities

Aerosols which do not have a significant gravitational settling velocity can produce high levels of ground concentrations above the level expected if gravitational settling was the only deposition process. A general deposition velocity, as defined below in equation 1[27], can quantify the gross results of all deposition processes acting or the material, but does not describe any detailed effects.

$$\text{Deposition Velocity} \left(\frac{\text{m}}{\text{sec}}\right) = \frac{\text{W Ground contamination } (\text{Ci}/\text{m}^2)}{\text{X Ground level air concentration } (\text{Ci.s.m}^{-3})} \quad (1)$$

Generally processes involving airborne water on deposition are treated separately.

An atmospheric release from a nuclear installation will probably contain a large range of elements, each of which will be in several chemical forms. Results of experiments to measure the deposition velocity over a range of elements have been published. Many experiments have concentrated on elemental Iodine[28,29,30,31], which has isotopes giving one of the most immediate hazards from reactor releases. A wide scatter of results has been produced, not only between different experiments, but also within single studies, as in Table 2. No simple reasons have been given for this scatter, usually of at least a factor of three from minimum to maximum (see Table 2). Variations in the atmospheric dispersion conditions can not always explain the differences. Humidity can be a factor, as reported by Weiss and Kelter[32], where damp surfaces could produce much greater deposition velocities. Also the type of calculations required can determine the magnitude of the deposition velocity used (Hoffman[23]). Food contamination studies would generally require the amount of activity deposited on vegetation, while external exposure estimates would need information of deposits on all surfaces. Hence deposition velocities depend on many parameters. Deposition models often only deal with a limited range of these parameters so are approximations to the real situation.

One approximation is that all the released material of one element can be described by a single deposition velocity. Variation of this value could occur as the release proceeded, as noted in the previous sections. This implicitly requires averaging over the properties of the different chemical species involved, for example with halogens including Iodine

$$v(\text{mean Iodine}) = \frac{v(\text{elemental}).X(\text{elemental}) + v(\text{aerosol}).X(\text{aerosol}) + v(\text{organic}).X(\text{organic})}{X(\text{elemental} + X\,\text{aerosol}) + X(\text{organic})}$$

Generally elemental halogens deposit more rapidly than aerosols, while organic halides do not readily

TABLE 2 Isotopes—Deposition Velocities on Different Surfaces

DEPOSITION VELOCITY cm s^{-1} ON GIVEN SURFACES (MEAN VALUES IF NO RANGE IS QUOTED)

ISOTOPE	WATER	SOIL	GRASS	STICKY PAPER	REFERENCE
I^{131}	1.4-2.3	0.5-1.4	1.2-2.1	0.1-1.1	from (27)
Cs^{137}	0.9	0.04	0.2	0.2	from (27)
Ru^{103}	2.3	0.4	0.6	0.4	from (27)
Stable I_2	—	—	0.31-6.3	—	from (33)

deposit. Hence the mean halogen deposition velocity could be expected to decrease with travel as the airborne elemental halogen concentrations, and to a lesser extent the aerosol component, are rapidly depleted. This is a similar effect in distance to what could occur, in time, to releases which are held up by containments so producing a decrease in the airborne highly depositing material. Over comparatively short distances, depending on the dispersion conditions, this decrease might not be of significance with respect to the measured variation in the deposition velocities. A constant deposition velocity for each element could be used in a study where consequences were to be predicted within a restricted range.

Radioactive decay can influence the deposition velocity of isotopes of one element or of similar elements. For example with iodine-132, which is a quite short lived daughter of Tellurium-132, after several kilometres downwind travel most of the I-132 in the plume could be due to decays from Te-132, where the latter is normally produced in greater quantities by fission reactors. This I-132 would tend to be in the same form as its Tellurium parent, which could be predominately as small aerosol particles. This would mean I-132 could have a significantly different deposition velocity from other Iodine isotopes. Possibly 50% of an I-131 release, with a half life of eight days, could be in elemental form. Another example of short lived isotopes having their deposition behaviour affected by production in the atmosphere by decay of their longer lived parents are those of Rubidium. These, especially Rb-88 are formed after decay of Krypton isotopes which would mostly be released as free gases. These daughter products would be initially produced as single ions presumably forming neutral single atoms with a new deposition rate. Agglomeration and chemical reactions might then start to alter the deposition velocity to that of other alkali metals such as Caesium. The Cs-137 isotope is long lived, with a half life of about 30 years, and has little contribution to its cloud concentration from decay of Xenon-137, so is more likely to retain its initial form on release to the atmosphere.

Chemical changes during exposure to the atmosphere can affect deposition of radioisotopes. This would be or importance primarily for the more reactive components of a possible release, such as elemental Iodine and Sodium oxides. If released, activated Sodium, Na-24, would probably reach the atmosphere as particles or coatings on other aerosols. Sodium oxides react with water vapour to produce the hydroxide and other compounds, with different deposition properties as mentioned in an earlier section.

In other fields of environmental pollution studies, the chemical transformations of sulphur dioxide in the atmosphere pose similar problems. Combined, or closely related releases, such as from a blowdown stack and a water cooling tower, can have interactions altering the release properties[34].

The expected composition of a release and the required detail of calculation would determine the importance of the accurate use of deposition velocities. The changes in the deposition character of the isotopes of Te-I-Xe and Kr-Rb-Sr are those of most radiological significance which have to be modelled when dealing with fission product releases.

3.2 Depletion Models

The properties of two general methods of modelling dry deposition are discussed here. The simpler model is to allow for depletion by reducing a release's source strength and not affecting the assumed distribution of airborne material. The other method deals in more detail with the vertical profile of airborne contamination and assumes only the material from the vicinity of the surface layer is deposited.

One advantage of the source depletion method is its easy implementation, where the depletion fraction for travel from 0 to x metres downwind is given by equation 2[27], for measurements at the ground.

$$\frac{Q^*}{Q} = \exp\left[-\left(\frac{2}{\pi}\right)^{1/2} \frac{v}{\bar{u}} \cdot \int_0^x \frac{\exp\left\langle -\frac{1}{2}\cdot\left(\frac{h}{\sigma_z(p)}\right)^2\right\rangle dp}{\sigma_z(P)}\right] \quad (2)$$

v = deposition velocity (assuming gravitational settling is negligible)

$\bar{u}$ = mean windspeed

h = effective height of release

$\sigma_z(x)$ = vertical (Gaussian) dispersion coefficient

This is applied to the concentration profile, which remains the same as in the case with no depletion. It is assumed that the whole plume has good vertical mixing, as in unstable conditions. Under neutral and stable conditions this model is more accurate when $v/\bar{u}$ is low, where this ratio has to be lower in more stable weather to retain accuracy. The problem of resuspension of material has to be modelled, which involves time delays and other difficulties for any simple model. The above formula has to be modified

if reflections from an inversion layer are included after long travel times. When isotopes are produced within the plume their deposition, which may be at a different rate from their parent isotopes, has to be included. Allowing for changes of deposition velocity could become cumbersome. A simplification would be to use a few groups to cover the appropriate range of elemental deposition velocities, where the mean values are separated by statistically significant differences. The integration in equation (2) can be done for each distance separately or by an accumulation of small steps[35].

Surface depletion models are usually more complicated[36,37], as they calculate a vertical distribution profile rather than assume a fixed distribution. These also model the surface layer in the atmosphere which tends to have a smaller turbulent diffusivity than higher air in the main body of the mixing layer (see Figure 1).[38] For long travel times more of the material with a surface depletion model is at a greater height than that predicted by a source depletion model with the same low level release height. Under these conditions a source depletion model tends to overestimate the ground level air concentration and so overestimates the short range contamination. This can become a significant spurious depletion of plumes beyond a distance, typically where the vertical distribution profile is not expected to change significantly further downwind.

These two methods can agree to within 10% in the ground level concentration for up to periods of 6h, 2d and more than 10d for deposition velocities of 3, 1 and 0.3 cm s^{-1} under neutral conditions.[36] Various correction factors[36,38] can be applied to the deposition velocity for use in the source depletion model compensating for this long distance deficiency.

Single weather conditions generally last for periods shorter than 6h[39], so that the two depletion methods are both valid under stable conditions provided excessively large deposition velocities for the given conditions are not used with source depletion. One plume can be used to estimate consequences out to 100 km by the source depletion model without significant discrepencies provided the conditions implicit in equation 2 are reasonably satisfied.

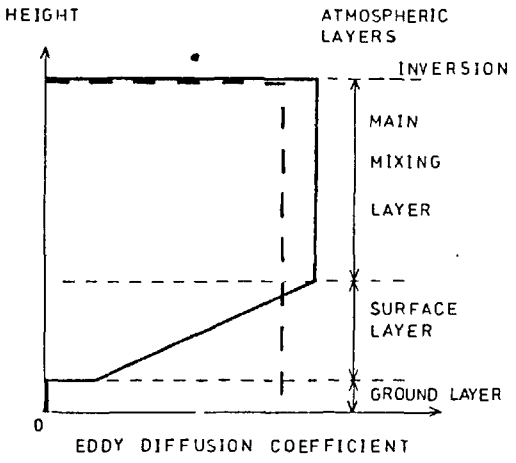

Figure 1 Two qualitative Forms of the Turbulent Eddy Diffusivity in the Atmospheric Boundary Layer {..... (39), —— (38)}

In some circumstances changes of dispersion conditions can have an important effect on the deposition of released material, such as dawn and sunset.[10] Another factor which affects deposition is the roughness length of the surface.[11] Rough land, such as forests rather than pasture, increases deposition rates, although the material is more dispersed due to more vertical mixing. Transition between different land types could also affect deposition behaviour of aerosols in the atmosphere.[12]

3.3 Other forms of plume depletion

Wet processes in the atmosphere can increase deposition rates[27] of airborne material released from a nuclear installation. Other effects altering the air concentrations include leakage through an inversion layer[13] and changes in the height of the mixing layer.

Plumes can be depleted by two main types of wet processes. One is where the precipitation falls through the whole height of the plume, which is termed as wash-out. Typically raindrops collect aerosol particles by processes including impaction, electrostatic effects, reaction rates with water, solubility in water and relative sizes of aernsol and precipitation particles. Rainfall which consists of many small droplets tends to be a more efficient scavenger than rainfall consisting of large raindrops.

Fog can be a very efficient scavenging mechanism which can be regarded as a form of wash-out in stable conditions[12]. Gases can also dissolve in these water droplets and be washed out[27].

The depletion rate Λ for wash-out, sec^{-1}, is assumed to deplete the plume by the fraction $Q^*/Q = e^{-\Lambda t}$[39,27], where t is the time wash-out has been acting on the plume. Equations using Gaussian dispersion formulae to predict time-averaged cloud concentrations and ground contaminations are given in many references[27], where the plume is assumed not to lean through the effects of wind direction shear with elevation (Ekmann layer[27,46]).

Values of the instantaneous wash-out rate are typically about 10^{-4} sec^{-1} for a rainfall rate of 1 mm/h, where rain structure and time sampling can produce large variations[41]. The variation of Λ with rainfall rate depends on the size and density of the airborne particles, but generally increases with rainfall rate. Wash-out of very small particles, and that due to light rainfall, may be due to different effects than wash-out of larger particles and heavier precipitation rates. Gases can be washed out by rainfall, where molecular diffusion, solubility and reaction rates all affect the wash-out coefficient. Bromine gas reacts fairly rapidly with water, unlike fodine, so can have an appreciable wash-out coefficient[27]. The chemical form of gases is important in this respect, where organic forms are often less efficiently precipitated. Evaporation of water droplets can have profound effects on wash-out, and other wet depletion processes.

Another depletion process by precipitation, often referred to as rain out, is when the released material is included within small water droplets which later coagulate to form raindrops and so are precipitated under gravity. This would most often occur when the release was associated with a large release of water

vapour, from an adjacent cooling tower or in an accident situation from the water coolant itself for LWR's. Nucleation, accretion and evaporation processes of droplets is a complicated problem where a simple treatment cannot be accurate in all cases, and is often omitted from atmospheric models of environmental codes[49]. One major effect after the end of precipitation is the wet surfaces remaining, where these can greatly increase normal deposition by surface elements[32].

Other effects which can affect the ground level concentrations of a plume involve any inversion and the top of the mixing layer. Material can be transported at low rates through an inversion, so depleting the main bulk of airborne material[30]. Later the inversion can break up so allowing material to remix with the lower layers, which may have been severely depleted by effects at the ground. A more common effect is the 'fumigation' of releases which have travelled overnight. Nightfall and the downward movement of the mixing layer could isolate material at levels above the night-time inversion. The material next to the ground could be greatly depleted during travel throughout the night under quite stable conditions. At dawn the mixing layer again rises so allowing the undepleted upper air to mix with the low concentrations at ground level increasing these concentrations. Similar effects can be found at coastlines after a plume has travelled over a large water surface[49], although the stable air, often found over water, may reduce effective deposition velocities.

4. THE DEPLETED PLUME AND ITS CONSEQUENCES

A distinction can be made between doses and exposures from a cloud of radioactive material and from the fraction which is deposited on the ground. The airborne material is only present at an exposure point for a short period as it passes downwind, whereas deposited material can remain in one position giving exposures for a long time. The differences between the periods of exposure to the cloud and ground activity produce different calculational requirements, as reflectec by the different dose paths. The consequences of depletion of the plume and the resultant ground contamination will be discussed in the next two sections, respectively.

4.1 The depleted cloud

Usually time integrated concentrations (Ci sec/m^{-3}) are employed to calculate inhalation dose commitments and external exposures from the cloud of radioactive material. The effects on prediction of possible doses after allowing for depletion will be discussed.

The downwind range of interest and the period over which a release is assumed to occur affect the importance of deposition processes. For short downwind distances, of up to a few kilometres, depletion of the plume under most conditions is generally not very important for air concentrations, except with material of high deposition velocity (eg $V_{depo} > 5$ cm/sec). At larger distances the differences in elemental deposition rates could start to affect the relative importance of inhalation dose commitments. Figure 2 shows the source depletion fractions for various conditions. For example if Iodine isotopes deposit more

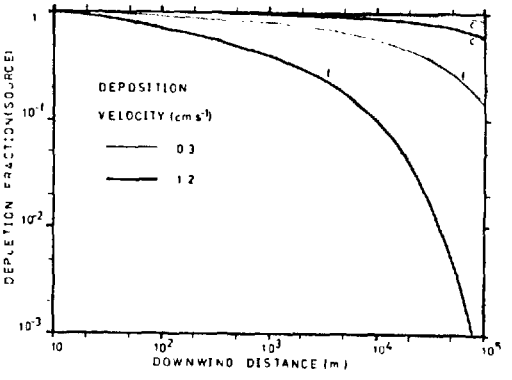

Figure 2 Source Depletion Fractions (as in Equation 2) for Pasquill Weather Categories F and C with Dry Deposition Velocities of 1.2 cm s^{-1} and 0.3 cm s^{-1}

rapidly in elemental form than metallic aerosols the thyroid dose commitments could be reduced, so possibly making other organ dose commitments more critical at distances of say 10 km to 30 km by reducing iodine air concentrations. At greater distances, of say up to 100 km, deposition can greatly affect the cloud concentrations. Particular elements and isotopes can be left in the cloud due to their own or their parents' non-depositing behaviour. In this respect inhalation doses may be of less importance than whole body exposure from the surrounding airborne activity.

The organ dose commitments produced by the concentration of activity in the air may be more dependent on the deposition properties of the material than the concentration alone. Aerosols and other material which do not deposit very rapidly would tend not to be readily deposited ir some parts of the lung, so possibly reducing doses. Also this material, which is fairly inert or of a form which is not easily transportable, may not be readily incorporated in the blood stream or the alimentary canal. This would alter the type of internal dose pattern. Some isotopes may not reach their critical organs so reducing dose equivalents, although lung doses may increase in this case if inhaled radioisotopes are not removed.

4.2 Ground contamination

The activity deposited on the ground is generally only a small fraction of the activity which passes close to the ground at any given position, due to the nature of depletion, as is shown by the typically low ratios of V(deposition)/$\bar{u}$. Consequences of ground contamination are of a longer time duration than cloud doses, which means that redistribution of the deposited activity can have significant effects. These effects will be discussed after the types of exposure pathways.

4.2.1 Exposure and dose pathways

The immediate problems with radioactive contamination are external beta and gamma exposures. Beta rays are quite rapidly attenuated in air, where for energies less than 0.5 MeV they have a range in dry air of less than 1 m, although straggling at the end of the range can occur[50,51,52].

The local deposit will determine the ground beta exposure, where significant shielding may be produced by ground roughness. When deciding on a method to calculate external beta doses their relatively low radiological significance has also to be considered. Gamma rays are more penetrating than beta particles, so their external exposure will come from a greater range of the deposit, which requires appropriate calculations[53,54,55]. The geometry of an exposure point close to the ground limits the contributions from large distances more than occurs with cloud gamma exposures. Ground roughness[56] also plays a role in the gamma ray flux and total exposure.

Significant external exposures would be limited to short downwind distances, although for most releases external exposures from deposited activity exceed the corresponding cloud exposures after about only one day[24,6]. The effects of building entrainment on releases from low levels or through leaks in the final containment have to be considered at these short downwind distances[39]. For large releases this ground exposure can become important during the period of the release[6,57]. At short times a wide range of deposition behaviour has to be considered to produce an adequate representation of the situation.

The lower exposure rates at larger distances would produce an increase in the background radiation level, which is eventually determined by the release and behaviour of long lived active isotopes, such as Cs137, Sr90 and to a lesser extent I129 and H3, as well as any actinides escaping. This may have to be considered if one site is going to be used for several reactors over an extended period of many decades, where operational emission limits might be chosen to allow for rare accidental releases of activity. To study these ground exposures a deposition model would have to be chosen which enabled predictions to be reasonably accurate and avoid problems of material depositing too rapidly and restricting, spuriously, the downwind extent of deposition.

This last problem particularly applies to the estimations of contamination as a first step in the prediction of doses through food chains. Much interest has been paid to thyroid dose commitments from I131 incurred through the air-grass-cow-milk food chain, where many deposition velocity measurements are directly relevant to this situation. The youth of the person receiving this dose is of importance (MRC)[50,59,60]. Other food chains can also be investigated[1], where the deposition velocity for the relevant surface and chemical form has to be used. This may impose requirements on the deposition model to cope with different depletion rates for each isotope within one decay chain, so as to obtain the most accurate results. One of the problems which has to be overcome is that the more radiologically significant isotopes also occur where deposition behaviour changes most rapidly between elements, eg Te-I-Xe-Cs and Se-Br-Kr-Rb.

4.2.2 Effect of redistribution of contamination

There are some dose pathways produced by movement of ground contamination in addition to those mentioned in the preceding section. Redistribution of deposited activity can also affect these doses. Rainfall and subsequent runoff from surfaces can immediately relocate precipitated material.

Resuspension of material[61] into the air can pose the risks of inhalation doses. Radioactive decay from deposited material can resuspend some activity, especially from the surfaces of particles. Inert gases formed within deposited particles may have to diffuse through its structure, which may vary greatly between particles formed during different parts of the release. Soil erosion[61,62] can also resuspend the finest particles and move the less transportable particles, although this would tend to occur more on bare dry soils which could have a lower initial deposit than land with vegetation cover. Physical resuspension by human activity could also occur during efforts to clean a contaminated area. All these processes have different time dependencies where resuspension would occur under differing weather conditions and wind directions.

Many competing factors could prevent resuspension, including absorption by vegetation (both leaves and roots), fixation in the soil and effects of ground water. It has been noted that Caesium can become fixed in soils within two years[63], so releases of Cs137 may produce unacceptable long term gamma exposures from its short lived daughter $Ba137^{M}$.

This briefly displays the extent of the problems involved in attempting to deal with ground contamination. To do detailed calculations on this whole problem would require the formulation of a complicated model and the compilation of many data sets. This additional complexity represents the extension of the problem from just a simple atmospheric model to one of the whole environment.

The area of interest could extend beyond the limits of the plume originally released and depend greatly on local conditions. Generally further dispersion would reduce the magnitude of the doses from all pathways, but there could be localised concentrating factors such as water movements and the local topography[62]. The effect of activity being redistributed within the soil and plants would alter the shielding effects already produced by ground roughness. Seasonal variations, such as rainfall, could be important during the ageing of the deposit, particularly while it is comparatively new. Empirical time-dependent weathering factors have been given which reduce activities[64] in the original deposit but do not give detailed information about the lost material.

5. CONCLUSION

A fuller understanding of deposition can lead to a more complete description of unplanned releases and their consequences. This could enable further investigations to be made attempting to find measurable factors which could categorise these releases.

REFERENCES

(1) Royal Commission on Environmental Pollution (chairman Sir Brian Flowers) 6th report Nucl. Pow. and Environ. HMSO Cmnd 6618 (1976).
(2) Richardson, B. L. UKAEA TRG (memo) 6907 (R) (1976).
(3) Nair, S. and Henning, M. J. CEGB report RD/B/N4079 (1978).
(4) Beynon, S. M. (Mrs.) CEGB report RD/B/N2633 (1973).
(5) Harte, G. A. CEGB report RD/B/N3564 (1976).
(6) Reactor Safety Study. WASH-1400 (1975).
(7) Kelly, G. N., Jones, J. A. and Hunt, B. W. NRPB-R53 (1977).

(8) Macdonald, H. F., Darley, P. J. and Clarke, R. H. Proc. Symp. Phys. Behav. Radioact. Contams. in the Atmosphere 337-348 (1974).
(9) Poulter, D. R. (ed.) The design of gas-cooled graphite moderated reactors (OUP, 1963).
(10) BNES review of SMiRT 4 and ANS Topical Meeting, *Nucl. Energy* 17 (3) 185-255 (1978).
(11) Laithwaite, J. M. UKAEA Reactor Safety course lecture No. 52 (1975).
(12) Hillary, J. J. and Taylor, J. C. UKAEA TRG report TRG 2433 (w) (1973).
(13) Reactor Safety Study, WASH 1400, Appendix 7 (1975).
(14) UKAEA Reactor Safety course, lecture 6 (1975).
(15) Abbott, D. G. CEGB report RD/B/M1664 (1970).
(16) Simon, S. UKAEA Reactor Safety Course, lecture 32 (1975).
(17) Clarke, R. H. *Hlth. Phys.* 25 267-280 (1973).
(18) Macdonald, H. F. IAEA Symp. on Rapid Methods for Measurement of Radioactivity in the Environment. IAEA/SM-148/38 43-54 (1971).
(19) Collins, D. A., McIntosh, A. E., Taylor, R. and Yuille, W. D. UKAEA report TRG 956 (W) (1965).
(20) Hillary, J. J. and Taylor, J. C. UKAEA TRG 2317 (W) (1972).
(21) Allen, M. D., Briant, J. K., Kaune, W. T. and Craig, D. K. *Hlth. Phys.* 34 539-547 (1978).
(22) Hillary, J. J. and Taylor, J. C. UKAEA TRG 888 (W) (1965).
(23) Wall, W. A. J. UKAEA Reactor Safety Course, lecture 30 (1975).
(24) Kelly, G. N., Jones, J. A. and Hunt, B. W. NRPB-R53 (1977).
(25) Laser, M., Beaujean, H., Fliss, P., Merz, F. and Vygen, H. Proc. Symp. Phys. Behav. Radioact. Contam. in the Atmos. 99-107 (1974).
(26) Scharwz, G., Bonka, H., Brussermann, K. and Brenk, D. Proc. Symp. IAEA Comb. Eff. Radioact., Chem. Therm. Releases Environ. 193-207 (1975).
(27) Slade, D. H. (ed.) Meteorology and Atomic Energy -1968 (USAEC, 1968).
(28) Chamberlain, A. C. and Chadwick, R. C. *Nucleonics* 11 (8) 22 (1953).
(29) Chamberlain, A. C. *Int. J. Air Pollut.* 3 63 (1960).
(30) Bunch, D. F. (ed.) Controlled Environmental Radioiodine Tests Progress Rep. 3/IDO-120 63 (1968).
(31) Fields, R. E. (ed.) Convair Report FZM 1985 (1960).
(32) Weiss, B. H. and Keller, J. H. IRPA 4th Int. Congress, Paris, Session SO 2 paper 184 (1977).
(33) Hoffman, F. O. *Hlth. Phys.* 32 437-441 (1977).
(34) Hubschmann, W. G., Nestor, K. and Wilheim, J. G. IAEA Proc. Symp. Comb. Eff. Radioact., Chem. Therm. Releases Environ. 233-242 (1975).
(35) Kaiser, G. D. UKAEA-SRD-R-63 (1976).
(36) Draxler, R. R. and Elliott, W. P. *Atmos. Environ.* 11 35-41 (1977).
(37) Horst, T. W. *Atmos. Environ.* 11 41-46 (1977).
(38) Scriven, R. A. and Fisher, B. E. A. *Atmos. Environ.* 9 49 (1975).
(39) Pasquill, F. Atmospheric Dispersion. 2nd Edition (Ellis Horwood, 1974).
(40) ApSimon, H. M. and A. J. H. Goddard. Proc. IV Int. Congress IRPA, Paris (1977).
(41) Konig, L. A., Nester, K., Schuttelkopf, H. and Winter, M. IAEA Proc. Symp. Behav. of Radioactive Contaminants in the Atmosphere 67-90 (1974).
(42) Michael, P., Raynor, G. S. and Brown, R. M. IAEA Proc. Symp. Phys. Behav. Radioact. Contaminants in the Atmosphere. 91-97 (1974).
(43) Maul, P. R. CEGB report SSD/MID/R28/75 (1975).
(44) Slinn, W. G. N. *Nucl. Saf.* 19 205-219 (1978).
(45) Vogt, K. J. Proc. Symp. Phys. Behav. of Radioact. Contaminants in the Atmos., 3-34 (1974).
(46) Seinfeld, J. H. Air Pollution (McGraw Hill, (1975).
(47) Beattie, J. R. and Bryant, P. M. UKAEA AHSB(S) R135 (1970).
(48) Hoffman, F. O., Miller, C. W., Shaeffer, D. L. and Garten, C. T. Jnr., *Nucl. Saf.* 18 343-354 (1974).
(49) ApSimon, H. M. Private Communication (1978).
(50) Spencer, L. V. *Phys. Rev.* 98 1597-1615 (1955).
(51) Loevinger, R. *Radiology* 66 55-62 (1956).
(52) Cross, W. G. *Can. J. Phys.* 47 75-83 (1969).
(53) Chilton, A. B. *Nucl. Sci. Engng.* 27 403-410 (1967).
(54) Jaeger, R. G. (ed. in chief) Engng Compendium on radiation shielding (Springer-Verlag, 1968).
(55) French, R. L. *Hlth. Phys.* 11 369-383 (1965).
(56) Huddleston, C. M., Klinger, Q. C., Burson, Z. G. and Kindaid, R. M. *Hlth. Phys.* 11 537-548 (1965).
(57) McGrath, P. E., Ericson, D. M. Jnr. and Wall, I. B. IAEA Symp. on the handling of radiation accidents. IAEA-SM-215/23 (1977).
(58) Baverstock, K. F. and Vennart, J. *Hlth. Phys.* 30 339-344 (1976).
(59) Charlesworth, F. R. and Gronow, W. S. Proc. Symp., Vienna Containment and Siting of Nucl. Power plants 143-170 (1967).
(60) Shaw, J. and Palabrica, R. J. *Annls. Nucl. Sci. Engng.* 1 241-254 (1974).
(61) Anspaugh, L. R., Shinn, J. H., Phelps, P. L. and Kennedy, N. C. *Hlth. Phys.* 29 571-582 (1975).
(62) Ritchie, L. T., Brown, W. D. and Wayland, J. R. *Nucl. Saf.* 19 220-238 (1978).
(63) Bryant, P. M. *Hlth. Phys.* 12 1393 (1966).
(64) Corbett, J. O. CEGB report BD/B/N3865 (1977).

CORRECTIONS TO TEXT (insertions have been underlined)

Contents

(section) 7.2 Suggestions for future work 294

Chapter 1

page 9 line 10 Delete second close bracket: (17),Martin

page 10 line 9 Hyphenate long-term

line 31 To read : food chain doses

page 11 line 29 Replace pessimistic by certain

page 15 line 10 Replace were by was

Chapter 2

page 22 line 37 Delete : details of the

line 38 Insert commas about phrase: and associated routines

page 25 line 23 Delete : 0.3

page 30 line 11 to read as : Kr88/Rb88, Te132/I132 and I135/Xe135^{m}.

page 30 equation 2.14(b) Replace p,n by p,x

page 31 Single deposition model second row entries column 1
Replace $v_g^I = v_g^{Te}$ by $v_g^1 = v_g^{Te}$
and last row column 1 , Replace : (v_g^T by (v_g^I

page 34 equation 2.23 , end of upper line of integral
to read as : $dt_m \ldots dt_{n-1}$

page 35 equation 2.25(a) Insert open bracket immediately to right
of equals sign : $=((t.D_{n,n-1})/$

page 39 line 11 Add apostrophe : isotopes'

page 41 Rename equation 2.37 as 2.38

page 42 line 1 equation 2.41 right hand side of equation to
read as : $a.R^{\alpha}$

page 52 line 4 replace 30 by 30 km

line 38 Change second comma to colon to read as
deposition: they

page 54 line 3 Replace 2.37 by 2.38

Chapter 3

page 64 line 5 Replace provded by provided

page 75 last line add extra close bracket:(6))) and

page 80 line 10 To read as exposure rate

CORRECTIONS(CONTINUED)

Chapter 4

page 93 equation 4.4 Insert superscript j to upper limit of summation over $j = 1$ to N^j

page 96 line 3 Replace full stop by comma to read as (dx_j, dy_j)

page 97 line 1 Replace Z by 2 in equation 4.15

page 99 line 4 To read as : means

page 103 line 33 To read as (Grønow and Gausden (2))

page 105 equation 4.38 Replace dr_i by dr_j

page 108 line 19 Replace W by $\bar{W}$

Chapter 5

page 125 see amended page with added qualifying statements

page 129 line 11 Replace possible by possibly

page 130 lines 26 and 27 replace pessimistic by inaccurate

page 130 line 35 Close bracket to read as : (breast)

page 132 line 3 To be read as suppressed

page 139 line 24 Geometric mean intended , so replace $-\frac{1}{2}$ by $+\frac{1}{2}$

page 141 penultimate line To be read as long lived

page 157 Figure 5.1 Order of curves from top of figure to be read in the same order as Figure 5.5 labels i.e. labels in order:Thyroid,Lung,Thyroid,Lung.

page 184 Figure 5.24 Vertical axis to read from top as: 2,1,0.5,0.2,0.1,0.05,0.02,0.01

page 192 line 33 Insert after :of the release; the phrase: (similar to figure 5.32)

page 218 line 13 Insertion to read as : proportionately larger high

page 220 line 22 Replace 3.1 by 3.2

line 24 Replace 3.2 by 3.1

page 225 Table 5.24 4^{th} row , column 2 Replace F by C'

CORRECTIONS (CONTINUED)

Chapter 6

page 228 line 2 Replace designed by delivered

page 238 see amended page with extra qualifying statements.

page 247 line 37 Replace $3.10^{-y}\ r^{-1}$ by $3.10^{-4}\ yr^{-1}$

page 260 see amended page with extra qualifier

page 269 line 15 Replace extent by extend

page 279 line 19 (continued from previous line) Replace mith by mity ie proximity)

Chapter 7

page titled as 294 to be read as page 295

page titled as 295 to be read as page 294

Appendix A

page 307 equation A.6 replace $(-\sqrt{\mu}rn)$ by $(-\sqrt{\mu}r_n)$ (i.e. subscript n)

page 311 line 4 Replace if by is

line 5 Replace $\frac{1}{2}$ by .

page 319 equation A.12b Denominator on right to be replaced by 87.7

Appendix B

page 327 line 2 Insert second open bracket i.e. ((10),

page 328 line 10 Replace become by becomes